NASA TECHNICAL TRANSLATION

NASA TT F-477

NASA TT F-477

N68-22462
(ACCESSION NUMBER)
(THRU)
317
(PAGES)
1
(CODE)
(NASA CR OR TMX OR AD NUMBER)
13
(CATEGORY)
FACILITY FORM 602

SCATTERING OF LIGHT IN A TURBID MEDIUM

by K. S. Shifrin

Gosudarstvennoye Izdatel'stvo Tekhniko-Teoreticheskoy Literatury
Moscow-Leningrad, 1951

GPO PRICE $ _____

CFSTI PRICE(S) $ _____

Hard copy (HC) _____

Microfiche (MF) _____

ff 653 July 65

NATIONAL AERONAUTICS AND SPACE ADMINISTRATION • WASHINGTON, D. C. • APRIL 1968

NASA TT F-477

SCATTERING OF LIGHT IN A TURBID MEDIUM

By K. S. Shifrin

Translation of "Rasseyaniye Sveta v Mutnoy Srede."
Gosudarstvennoye Izdatel'stvo Tekhniko-Teoreticheskoy Literatury,
Moscow-Leningrad, 1951.

NATIONAL AERONAUTICS AND SPACE ADMINISTRATION

For sale by the Clearinghouse for Federal Scientific and Technical Information
Springfield, Virginia 22151 – CFSTI price $3.00

TABLE OF CONTENTS

	Page
Introduction	1
CHAPTER I GENERAL CHARACTERISTICS OF THE PROBLEM	
1. Introduction	3
2. Fundamental Equations and Boundary Conditions	7
3. Linear Characteristics	11
4. Optical Constants	17
CHAPTER II FUNDAMENTAL FORMULAS	
1. Potentials	25
2. Solution of Equations for the Potentials	29
3. Diffracted Fields and Intensities	33
4. Coefficients of Scattering and Attenuation	37
CHAPTER III PARTIAL WAVES	
1. Amplitudes of Partial Waves	41
2. Angular Functions. Convergence	47
3. Two Methods for Writing the Fundamental Formulas	51
4. One Error in the Formulas for Intensities	56
CHAPTER IV SMALL PARTICLES	
1. Rayleigh Formula	58
2. Absolutely Reflecting Particle	64
3. Resonance. Eigen Oscillations	67
CHAPTER V LARGE PARTICLES	
1. Derivatives of Rays	71
2. Reflected and Refracted Light	74
3. Light Undergoing Internal Reflections. Rainbows	79
4. Energy Distribution Between Different Fluxes	85
5. Scattering Indicatrix and Degree of Polarization for Scattered Light	88
6. Nontransparent Particles	97
CHAPTER VI ABSORBING AND FULLY REFLECTING PARTICLES HAVING ANY DIMENSIONS	
1. Coefficients of Attenuation and Scattering	99
2. Asymptotic Value of the Attenuation Coefficient for Large Particles	104
3. Scattering Indicatrix	114
4. Radiation	120
CHAPTER VII TRANSPARENT PARTICLES HAVING ANY DIMENSIONS	
1. Attenuation Coefficient	124
2. Geometric Optics of a Sphere as the Limiting Case of Diffraction.	134
3. Scattering Indicatrix	146
CHAPTER VIII PARTICLES WITH ELECTRICAL PROPERTIES DEVIATING SLIGHTLY FROM THE SURROUNDING MEDIUM PROPERTIES	
1. Fundamental Equation	166
2. First Approximation for the Sphere	171
3. Second Approximation for a Sphere Whose Dimensions are Comparable with the Wavelength	179

PRECEDING PAGE BLANK NOT FILMED.

4. Nonspherical Particles 185
5. Scattering Coherence 196
CONCLUSION 203
APPENDIX 205

SCATTERING OF LIGHT IN A TURBID MEDIUM

K. S. Shifrin

Introduction /5*

This book is devoted to a systematic discussion of the theory of scattering and absorption of plane electromagnetic waves by particles of a turbid medium. This problem, which lies at the basis of the optics of turbid media in general, almost exhausts the optics of translucent bodies -- i.e., those bodies in which scattering is infrequent.

The problem of multiple scattering is not discussed in this book.

Investigations of a wide class of atmospheric-optical phenomena, optics of the sea, colloid solutions and aerosols, as well as several meteorological, astrophysical, and applied problems represent different aspects and areas of application for the theory presented below.

There has been a formal solution of the classical problem of scattering of electromagnetic waves by particles having a spherical form for many years. However, we cannot be satisfied with a solution which is written in the form of an infinite series. The compilation of survey formulas, graphs, and tables is of great importance. We have attempted to direct our main attention to this second aspect of the matter.

Interference between fields scattered by individual particles may also be of importance in certain cases, concurrently with single scattering. A general analysis of the problem for translucent bodies is contained in the book.

In addition to the theory, the book briefly presents experimental data.

We shall briefly discuss the contents of each chapter.

The perturbation introduced by a particle into a field may be determined as the deviation of the particle's electrical properties from the properties of the surrounding medium, as well as its dimensions. A dimensionless parameter corresponds to each of these situations. When distinguishing between particular areas of the problem, we must indicate the region in which both parameters change.[1]

Therefore, in the first chapter we describe both the linear dimensions of /6 the particles, and their electrical characteristics, along with a general formulation of the problem.

* Numbers in the margin indicate pagination in the original foreign text.

(1) The following, frequently encountered statement illustrates the fact that this assumption is outdated: "A small particle has a Rayleigh scattering indicatrix". In Chapter IV we show that this statement is erroneous when applied to substances with a large refractive index.

The difficulties encountered by the researcher who might wish to apply the formulas for the scattering theory to specific problems are related to a significant extent with the confusion existing in the literature on this problem. The authors of different studies frequently employ formulas which differ from each other. Sometimes these are actually different formulas, and in other cases they differ only in terms of the notation. Many authors have written the basic formulas, employing the notation of special functions of the problem introduced by Mie. Other authors employ present-day notation. Numerous mistakes and errors are encountered in different authors when they derive the basic formulas and analyze them. In 1946 we realized the necessity of a systematic discussion of the problem and subsequent derivation of the basic formulas. This derivation comprises the second chapter.

The third chapter is an auxiliary chapter. It contains several relationships which are necessary for practical computations in terms of general formulas. In this chapter we also present a correction of one general error which is assumed in the formulas for intensity.

Chapter IV is devoted to extremely small particles (macroscopic globules whose radii are considerably less than the scattered wave lengths).

The transition from one limiting case to another which we have studied is of great interest, along with an analysis of the two limiting cases describing the scattering by small particles. We have thus discovered quite interesting resonance phenomena.

Chapter V is devoted to extremely large particles.

In contrast to Chapters IV, VI, VII, where the analysis of different particular cases is introduced as viewed from the general formulas given in Chapter II, for the sake of clarity we shall resort directly to the formulas of Fresnel and the laws of geometrical optics. In Chapter VII, however, we present /7 a strict derivation of the formulas of geometrical optics of a sphere, directly from the general diffraction formulas.

We give the numerical data for scattering of visible light by drops of water.

Chapters VI and VII pertain to particles having any dimensions.

Chapter VI investigates the results derived from tabulating the precise formulas for absorbed and completely reflected particles. The fact that we have eliminated confusion with the limiting value of the attenuation factor and that we have strictly analyzed the physical causes for the "duplication" of this factor is of great importance. In our opinion, the consideration of diffraction phenomena in thermal radiation of small particles and a simple approximation method for computing the indicatrix of enormous opaque particles are of interest.

Chapter VII is devoted to transparent particles.

The results derived from tabulating the precise formulas are analyzed,

and the experimental data for the geophysical problems are investigated. An approximation method which we developed for calculating the scattering indicatrix of enormous transparent particles is of importance. The complex computational problem of the indicatrix of a large transparent sphere is thus practically solved.

Chapter VIII presents a method for analyzing the problem. In principle, this method differs from the method of curvilinear coordinates presented in Chapter II. The simplicity of the formulas obtained represents an important feature of the method which we developed. It enables us to examine ellipsoids, along with spheres whose dimensions are comparable to the wave length. In addition, in Chapter VIII we investigate the principal problem of coherent scattering by a system of particles.

A table of angular functions which we compiled is presented at the end of the book. The use of this table significantly facilitates the work of the reader in tabulating the precise indicatrixes in the entire "middle" region of the dimensions where simple formulas for small and large particles, which are presented in the book, cannot be employed. Thus, the entire spectrum of particle dimensions is encompassed.

This enumeration does not exhaust the contents of the book and, in addition, does not exhaust the circle of problems pertaining to the problem under con- /8
sideration, which could be found on the pages of our book. The limitation of space has compelled us to omit these problems and to discuss others in an excessively curtailed form. A certain justification for these drawbacks, it seems to us, is the fact that this book represents the first systematic discussion of the problem both in Soviet literature, and in foreign literature. We have called particular attention to the work of Soviet authors, whose role is usually inadequately presented.

The selection of the material was dictated by an attempt to present a picture which is as clear and well-ordered as possible. In our opinion, an analysis of the different contradictions, which was performed by developing several points and by new computations, has made it possible to approach the solution of this problem.

The author is indebted to associate member of the Academy of Sciences, Professor Ya. I. Frenkel'; associate member, Professor T. P. Kravts; academician V. V. Shuleykin; Professor A. A. Gershun, and professor M. I. Yudin for discussing individual problems.

CHAPTER I

GENERAL CHARACTERISTICS OF THE PROBLEM

§ 1. Introduction

The propagation of electromagnetic waves in a real body is accompanied /9
by their scattering and absorption.

The optical inhomogenity of a body is the reason for the scattering of light. This basic assumption was established by L. I. Mandel'shtamn in 1907 (Ref. 1).

We should point out that we are discussing bodies whose optical inhomogenities are distributed at random. These locally inhomogeneous bodies, particularly those which show light scattering, are called turbid bodies.[1]

Different factors may cause optical inhomogeniety. For example, these factors may be fluctuations of density caused by thermal motion, or extraneous macroscopic particles located in the body, etc.

This book is devoted to an examination of the theory of phenomena caused by the presence of extraneous macroscopic particles in the body. The book does not investigate phenomena accompanying the propagation of light in optically homogeneous bodies (absorption in molecules, etc.) as well as other phenomena produced by density fluctuations. The reader will find the theory and description of these phenomena, for example, in the course of G. S. Landsberg (Ref. 2), and in greater detail in his articles (Ref. 3, 4).

The scattering of light leads to side scattering of light. This may be caused by photoluminescence. An article by S. I. Vavilov (Ref. 5) is devoted to analyzing the relationship between both types of phenomena.

An analysis of single scattering lies at the basis of the theory of light scattering in turbid media. However, in certain cases multiple scattering may also be of importance along with single scattering. This factor leads us to divide all turbid bodies into two classes: strongly turbid bodies, whose theory requires allowance for multiple scattering, and weakly turbid bodies, or translucent bodies, whose theory does not necessitate allowance for multiple scattering.

This book is primarily devoted to analyzing single scattering. This problem practically exhausts the theory of translucent bodies, and lies at the basis of the optics of strongly turbid bodies.

The scattering theory developed below has a wide range of application.

The optics of clouds, fogs, rain, air aerosol, and many other practical problems are closely related to these problems (visibility, theory of photographing far-removed objects, etc.) and comprise the meteorological aspect of the problem.

---

(1) Locally homogeneous bodies, i.e., bodies with constant or slowly changing optical properties, do not scatter light. In the theory of refraction and mirages, for example, air whose inhomogeneous density distribution causes the curvature of light rays is regarded as such a body. We might add that we will discuss the concept of turbidity in § 3 of this chapter.

This thus pertains to the problem of determining optical indications of a change in the weather, i.e., the problem of establishing quantitative relationships between optical and thermodynamic characteristics. These indications now consist of selecting empirical rules in the majority of cases.

We shall not discuss these rules here. The reader will find a great amount of information on this subject in the book by P. I. Brounov (Ref. 6), and in the works of N. N. Kalitin [see, for example, (Ref. 7) and others].[1]

The theory developed below for optical methods of probing the atmosphere is of significant importance (Ref. 28, 29).

The propagation of light in the depths of the sea, optical methods of studying sea water, and other problems determine the interest in a scattering theory for optics of the sea.

The problem of the concealed photographic image, optical methods for investigating colloid systems and aerosols, and the problems of intrastellar particles and zodiacal light in astrophysics are related to this theory. /11

The problems enumerated above are far from exhausting the list of problems and studies related to scattering of light by particles. For example, this problem is of great importance for determining the efficient operational regime of the Wilson Chamber [see (Ref. 9) and others], for the optical properties of granular metallic films[2], for studying fine powders, colloid light filters, etc.

We shall now present certain historical facts.

Important results have been obtained by Soviet scientists in developing the problem discussed in this book.

Even before the Great October Socialist Revolution, we had the studies of O. D. Khvol'son on multiple scattering of light by particles, the studies of L. I. Mandel'shtam on the causes of light scattering in general, and the studies of T. P. Kravts on the scattering of light in solutions.

In particular, important results were obtained in the Soviet period.

V. V. Shuleykin studied the scattering of light by particles. Along with tabulating precise formulas, he investigated the transition from small particles to extremely large particles, and extensively applied the results of this study toward explaining the optical phenomena in the sea and the atmosphere.

---

(1) The old observation of Cornu (Ref. 8) is also of interest. He established the fact that rapid changes in the polarization of celestial light precede a sharp change in the weather. These phenomena occur much earlier than any other indication of a change in the weather.

(2) These films were first studied by the Kiev physicist I. I. Kosonogov (Ref. 10) and provide an example of two-dimensional sol. The track in the Wilson chamber may be regarded as a one-dimensional sol.

G. I. Pokrovskiy performed numerous laboratory studies dealing with different problems on the optics of turbid media. N. N. Kalitin performed numerous observations on the distribution of the brightness of the sky. He related the results derived from these observations to the scattering of light by particles. T. P. Kravets and M. V. Savost'yanova performed numerous studies on the scattering and absorption of light by small metallic particles. The results of these studies lie at the basis of the theory on the nature of the concealed photographic image. A. A. Lebedev performed important studies on the transmittance of fogs. I. A. Khvostikov studied the scattering of light in fogs. These /12 investigations led to the important hypothesis regarding the existence of "submicroscopic" particles. The method developed by I. A. Khvostikov for probing the atmosphere by means of a projected beam is also of importance. A. A. Gershun performed important investigations on light scattering in sea water, on multiple scattering, and on the theory of the light field. On the basis of these studies, A. A. Gershun obtained important results in solving many practical problems. The investigations by V. G. Fesenkov provided interesting applications for the theory of light scattering to the analysis of many astrophysical problems. New methods of studying multiple scattering and important results in this area were obtained by V. A. Ambartsumian, Ye. S. Kuznetsov, and V. V. Sobolev.

V. V. Sharonov, N. G. Boldyrev, V. A. Berezkin, and V. A. Faas significantly developed and advanced the problem of visibility -- a problem which is important in practice and which is closely related to the scattering theory. The book by V. V. Sharonov (Ref. 27) discussed the problems of visibility in relation to the theory of scattering.

Methods, which were new in principle, dealing with the problem of diffraction in a sphere were developed recently by V. A. Fok (Ref. 11, 12). The earlier work of V. A. Fok is also of importance, along with these studies. In this work , he provides a new asymptotic representation for Bessel functions. The formulas of V. A. Fok and their application to our problem will be found by the reader in Chapters III and VII.

Our presentation is far from exhaustive. In certain sections of the book, we have discussed in detail the works of some of the authors mentioned above, and have also turned to the studies of other Soviet authors.

We would like to point out that, along with the specific problems of the optics of turbid media, important results have been obtained in our country which may explain those fundamental physical assumptions which lie at the basis of our concepts of light scattering in general. This fact was noted in 1940 by academician S. I. Vavilov.

"... the problem of scattering is one of the chapters of optics in which very important advances have been definitely made, particularly due to the work of Soviet physicists." I would like to point out that the basic assumption of /13 present day science regarding molecular scattering of light states that any volume filled with a substance must scatter light due to fluctuations. This assumption developed from the position maintained by L. I. Mandel'shtam in his controversy with Planck at the beginning of the century. The fluctuation theory of molecular scattering of Smolukhovskiy and Einstein arose from this

controversy. I would also like to mention the long systematic interchange of the outstanding studies by L. I. Mandel'shtam, G. S. Landsberg and their students on the problem of scattering. These studies brought a new interpretation of the problem and led to the discovery of the so-called Raman scattering. It is sufficient to mention the important studies of deceased O. D. Khvol'son" (from an address on October 19, 1940, at the conference on visibility at the State Optical Institute [Ref. 13]).

§ 2. Fundamental Equations and Boundary Conditions

The Maxwell equations for electric and magnetic fields and induction lie at the basis of the investigation:

$$\left.\begin{aligned} \operatorname{rot}\mathbf{H} &= \frac{4\pi}{c}\mathbf{j} + \frac{1}{c}\frac{\partial \mathbf{D}}{\partial t}, \\ \operatorname{rot}\mathbf{E} &= -\frac{1}{c}\frac{\partial \mathbf{B}}{\partial t}, \\ \operatorname{div}\mathbf{D} &= 4\pi\rho, \\ \operatorname{div}\mathbf{B} &= 0. \end{aligned}\right\} \qquad (1.1)^1$$

Here **E** and **H** are the electric and magnetic fields, **D** and **B** -- electric and magnetic induction, **j** -- density of the ohmic current, ρ -- charge density, c -- speed of light in a vacuum.

Let us introduce in the customary manner the linear relationships between /14 the fields and the inductions, the current density, and the electric field:

$$\mathbf{D} = \varepsilon\,\mathbf{E}; \quad \mathbf{B} = \mu\,\mathbf{H}; \quad \mathbf{j} = \sigma\,\mathbf{E}. \qquad (1.2)$$

The macroscopic constants s, μ and σ are the physical characteristics of matter: the dielectric constant, magnetic permeability, and electroconductivity. They depend essentially on the electromagnetic field frequency. We shall discuss this dependence at a later point.

The utilization of macroscopic equations and constants assumes that we are disregarding the atomic structure of matter. This fact determines the lower boundary of the particle dimensions to which the calculations performed later on pertain. It signifies that the dimensions of all the bodies under consideration must be considerably greater than the atomic dimensions.

We may define this boundary more precisely in many cases. For example,

---

(1) The formulas in the book are indicated by two numbers in parentheses: the first number designates the chapter number, and the second designates the formula number in the chapter.

References to the literature are given in brackets. We have not attempted to compile a complete bibliography, but have referred primarily to the most important studies. A bibliography of articles on this problem before 1940 is given in the survey by I. A. Khvostikov (Ref. 14).

References in the text are sometimes given in the following form: see: IV, 3. This means see Chapter IV, § 3.

we should recall that the electroconductivity of metal σ is proportional to the mean free path of electrons in it, ℓ.

In a large fragment, the mean free path is determined by scattering by thermal waves. In a particle whose linear dimensions a will be considerably less than the quantity ℓ for a large fragment, the mean free path will be determined by the particle dimensions. In this case, the electroconductivity will be proportional to the particle dimensions ($\sigma \sim a$). When the particle dimensions increase, for a on the order of ℓ, the linear behavior of σ with a is disturbed, and σ changes into a constant value in the case $a \gg \ell$ -- the electroconductivity of a massive fragment.[1]

In contrast to the initial theory of Drude-Lorentz, the present-day theory of metals assumes that ℓ is one hundred times greater than the lattice constant. Thus, for example, ℓ is on the order of 500 Å for silver at room temperatures. Consequently, this value indicates the limit of the particle dimensions for which we may employ the macroscopic value of σ in the given case.

We shall assume that ε, μ and σ are not dependent on time. With respect to their dependence upon the coordinates, we shall assume that they are constant /15 within a body and change in a jump-like manner when changing from one body to another. Consequently, the body surfaces will be discontinuity surfaces of ε, μ, σ. This represents an essential limitation of the theory. Thus, all scattering characteristics which are related to the internal optical inhomogeniety of particles are omitted from our investigation. They may be of importance when studying scattering by condensation nuclei covered with a water envelope, by hail stones, and also by snow and ice granules having a composite structure. The demand for mathematical simplicity, on the one hand, and the limited present-day knowledge of particle internal structure, on the other hand, compel us to conform with this limitation.

In every problem which we shall discuss below, we shall assume that the following three characteristics hold:

(a) There are no free charges in any of the bodies under consideration;

(b) The magnetic permeabilities equal unity ($\mu = 1$);

(c) The electric and magnetic fields are purely periodic functions of time, i.e., their dependence on time is determined by the factor $e^{i\omega t}$ (where ω is the field frequency).

These assumptions enable us to avoid unnecessarily cumbersome formulas which would limit their generality in practice (for the group of problems in which we are interested).

---

(1) Our discussion on the dependence of σ upon the dimensions is similar to the discussion performed during an analysis of transport phenomena in ultrarefied gases. For particles whose dimensions are considerably less than ℓ, an electron gas is ultrararefied .

Actually, the fact that particles in the atmosphere or in colloid solutions are usually charged simply indicates that the particle will also have a constant electric field, along with a diffracted field. This constant electric field will be combined with the diffracted field. It will have no influence upon the diffracted field (i.e., upon scattered light), and therefore it cannot be taken into account. Charged and uncharged particles scatter light in absolutely the same manner.

With respect to the magnetic permeability μ, experience has shown that for all substances it practically equals unity in the visible and infrared regions. This pertains not only to dielectrics, but also to ferromagnetic substances (iron, nickel, etc.) for which μ assumes enormous values in the static case.

One reason for this is magnetization inertia, making it impossible to trace the rapid field oscillations in a light wave.

The transition to static values of μ occurs in the region of ultra-short /16 waves. This transition was studied experimentally by V. K. Arkad'yev (Ref. 15) in 1913. Observing reflection and absorption of waves in wires he found, for example, that μ changes smoothly from $\mu = 80$ in the case $\lambda = 72.7$ cm to $\mu = 4.5$ in the case $\lambda = 1.31$ cm for iron.

With respect to the latter assumption (point c), this means that we are dealing with scattering of monochromatic light. In those cases when we are investigating scattering of a composite bundle, the latter may be regarded as a superposition of monochromatic bundles. Therefore, the latter limitation is also unimportant.

When the three factors (a, b, c) indicated above are taken into consideration along with relationships (1.2), the system of equations (1.1) for internal regions (outside of the discontinuity surface of ε and σ) may be rewritten as follows

$$\operatorname{rot} \mathbf{H} = \left(\frac{4\pi\sigma}{c} + i\frac{\omega\varepsilon}{c}\right)\mathbf{E}; \tag{1.3}$$

$$\operatorname{rot} \mathbf{E} = -\frac{i\omega}{c}\mathbf{H}; \tag{1.3*}$$

$$\operatorname{div} \mathbf{E} = 0; \quad \operatorname{div} \mathbf{H} = 0.$$

It may be readily seen that the two last equations are the result of the two first equations in the system which we obtained. Therefore, they will be omitted from future discussion. Omitting **H** and **E**, respectively, from equations (1.3) and (1.3*), we obtain

$$\Delta \mathbf{E} + k^2 \mathbf{E} = 0; \quad \Delta \mathbf{H} + k^2 \mathbf{H} = 0. \tag{1.4}$$

Here Δ is the Laplace operator, and

$$k^2 = \frac{\omega^2\varepsilon - i4\pi\omega\sigma}{c^2}. \tag{1.5}$$

Thus, the fields **E** and **H** must satisfy the oscillatory equations with a complex wave number. If k_0 is the wave number for a vacuum ($k_0 = \frac{\omega}{c}$), we then

have

$$k = k_0 m; \quad m = \sqrt{\varepsilon - i\frac{4\pi\sigma}{\omega}}. \tag{1.6}$$

Here m is the complex refractive index.

In addition to the equations (1.4), the fields **E** and **H** must satisfy /17
certain boundary conditions. On the discontinuity surfaces they may be reduced to the requirement that the Maxwell equations be satisfied within the regions encompassing sections of these surfaces. It is well known that this is equivalent to the reqirement that the tangential components of the electric and magnetic fields be continuous. Thus, since each of the field vectors is broken down in the tangent plane into two independent (mutually perpendicular) components, the boundary conditions on the dividing surface lead to four scalar equations. In addition to the conditions on the discontinuity surface, the solution of the oscillatory equation must also satisfy conditions at infinity. They may be formulated in the so-called radiation principle.

The essence of this is as follows.

In order to obtain an unequivocal solution, it is necessary that the diffracted section of the field represent a wave which diverges from the diffraction source, along with the natural requirement that the diffracted (perturbed) section of the field decrease rapidly at infinity. The fact of the matter is that, in formal terms, converging waves traveling from infinity to the diffraction source satisfy the oscillatory equation, along with diverging waves. The radiation principle naturally requires that waves of the latter type be omitted. In electrodynamics this fact corresponds to rejection of the advanced potentials [see (Ref. 16), page 153].[1]

Let us now turn to the formula for light intensity. We should recall that the magnitude (averaged over time) of the radiation energy flux vector is called light intensity. This victor may be computed per unit area, normal to /18
the direction of propagation. We shall call it the Umov-Poynting vector.[2]

---

(1) V. D. Kupradze (Ref. 17) has provided strict proof for the radiation principle.

The necessity of deriving a radiation principle in order to solve the system of Maxwell equations definitively in an infinite region should not be regarded as a drawback of this system. This is related to the fact that we have imposed a stationary solution, which is periodic in time, upon the system. This means that the stationary solution of the wave equation, which is periodic in time, is not equivalent to the solution of this equation with correctly formulated initial conditions. Strictly speaking, only the latter method of solution is correct. Thus, no "parasite" waves, traveling from infinity to the source, are produced, and there is no necessity of omitting them, i.e., in the radiation principle.

(2) The concept of the motion of energy was first introduced into science by N. A. Umov, as applied to propagation of elastic deformation energy. Ten years later, Poynting formulated a theorem regarding the flux of (continued)

Since our fields are complex, the mean value of the Umov-Poynting vector may be determined by the following formula [see, for example, (Ref. 19), page 91]:

$$\Pi = \frac{c}{8\pi} \operatorname{Re} [\mathbf{E}, \mathbf{H}^*]. \tag{1.7}$$

Our final problem is to calculate the vector Π by means of $\mathbf{E}$ and $\mathbf{H}$ and certain integrals containing Π, since observations and measurements are usually reduced to measuring intensity. We should note that a similar situation occurs in other wave phenomena -- for example, in wave mechanics. The problem may be formulated in mathematical terms for linear quantities (fields, ψ-functions), while the squares of the quantities are those which are customarily measured.

§ 3. Linear Characteristics

The general formulation of the problem in the theory of light scattering in a turbid body does not differ from the formulation of diffraction problems in electrodynamics. This formulation is as follows. For a certain outer "illumination" -- or, more precisely, for a certain value of the unperturbed electromagnetic field (or the frequency distribution of quantities characterizing the field, in the case of non-monochromatic radiation) -- and for a certain spatial distribution of electromagnetic properties of the turbid body, the field must be determined at a certain point outside of, or within, the body (or the frequency distribution of field elements).[1]

This problem may be broken down into two parts. First, we may formulate the problem of determining the electric field scattered by an individual element of the turbid body, assuming that the outer field in which the "turbid element" is located is known. This outer field represents a superposition of the field irradiating the body, and the field produced (where the "turbid element" is located) by all remaining elements of the body under consideration. Second, the influence of all elements (particles) of the body must be summed. /19

Since the field acting upon a given "particle" is determined by all the "particles" (including itself), the division of the problem into two sections is not valid, generally speaking, and we have a single problem. However, in actuality in the majority of real turbid media this division is reasonable, and essentially different methods may be applied for analyzing both parts of the general problem. This is determined by the fact that the structure of the "turbid particle" and the structure of the turbid macrovolume are entirely different, with respect to the natural scale of the length included in our problem -- the wave length of incident radiation λ. The distance between molecules comprising the "turbid particle" d is usually $\ll \lambda$ -- in other words, we may regard the "turbid particle" as continuous, whereas the distance between different "turbid particles" in the macrovolume ℓ is usually $\gg \lambda$. Since individual "turbid particles" have a random distribution in the macrovolume or, in any case, their

---

(2) (continued) electromagnetic energy. An article by T. P. Kravts (Ref. 18) discusses the interesting history of the development of modern opinions on energy and its motion.

(1) The difference from the usual diffraction problem lies in the distribution of electric properties within the body.

mutual arrangement changes in a period of time which is comparable with the observational time, the turbid macrovolume may be regarded as a collection of incoherent emitters, and their intensities may be combined, but not the fields. As regards the "particle", the fields must be combined in view of the fact that their mutual arrangement does not change. In the first case (the problem of the macrovolume), the problem may be formulated in the form of a certain integrodifferential equation for multiple scattering. In the second case (the problem of the particle) the problem may be reduced to a wave equation with boundary and initial conditions, or to an integrodifferential equation which is equivalent to it. In the general case, along with the wave length λ, the following quantities having the dimensionality of length are included in our problem: d -- distance between elements within the particle; a -- particle dimensions; ℓ -- mean distance between particle centers in a turbid medium; R -- dimensions of the turbid volume.

Thus, we have the following four dimensionless parameters for the characteristics of the problem: /20

$x_1 = \frac{d}{\lambda}$ characterizes the particle structure;

$x_2 = \frac{a}{\lambda}$ characterizes the particle scattering properties;

$x_3 = \frac{\ell}{\lambda}$ characterizes the medium structure;

$x_4 = \frac{R}{\lambda}$ characterizes the scattering properties of the volume as whole.

In addition to the apparent inequalities

$$x_1 < x_2 < x_3 < x_4, \tag{1.8}$$

the following relationships also customarily hold:

$$x_1 \ll 1;\ x_4 \gg 1.$$

With respect to x_2 and x_3, they can assume any values coinciding with the general inequality (1.8). The limiting cases may be studied most simply of all when x_2 and x_3 are either very large, or are very small.

These cases are as follows:

a) $x_3 \gg 1;\quad x_2 \ll 1,$

b) $x_3 \gg 1;\quad x_2 \gg 1,$

c) $x_3 \ll 1;\quad x_2 \ll 1.$

The first two cases are usually investigated. With respect to case (c), it is usually omitted, although it is important for several problems of the optics of turbid media.[1] In this case, the division of the problem into two independent sections, which was indicated above, will not be valid: an analysis of the elementary scattering, and allowance for multiple scattering.

(1) In the case of light scattering by particles which themselves are aggregates of extremely small particles. For example, emulsions of this type were studied by L. M. Moroz, and Ya. I. Frenkel' (Ref. 20).

In actuality, in the cases (a) and (b) the distance between the particles is considerably greater than the wave length. This means that the particles may be regarded as incoherent emitters. The random distribution of particles /21 (which frequently changes during a period of time which is comparable to the observation time) leads to such a sharp change in the phase of the fields scattered by individual particles that interference phenomena are not observed. (This is approximately the same reason why it is impossible to observe interference phenomena in thick plates). In this case, the light field may be described by light technology methods. The customary equation of multiple scattering in a turbid medium belongs to this region. A different situation occurs, if the distances between the particles are comparable to, or greater than, the wave length. Interference of light which is scattered by individual particles plays an important role here. In physical terms, this means that we must combine the fields, and not the radiation intensity, with allowance for the corresponding phases. The intensities are always combined, whereas the fields can be computed if their phases are opposed. For example, it is apparent that if the distance between the particles is considerably less than λ, we must deal with the problem of wave reflection from a solid body.

This interesting and important problem will be discussed in VIII, 5 in greater detail. In all the remaining sections, we shall only discuss elementary scattering [cases (a) and (b)].

We should also point out that we can divide the general problem into two independent sections if $a \sim \ell$ [and the general inequality (1.8) loses any meaning]. The interaction of particles upon each other occurs here (see VIII, 5).

The parameters x_i are the main linear characteristics of the problem. Their magnitudes and the relationships between them determine the nature of any specific problem. For example, in the case $x_3 \gg 1$ when, consequently, we may employ the equation of multiple scattering, the following parameter is of significance :

$$\tau \sim \frac{a^2 R}{l^3} = \frac{x_2^2 x_4}{x_3^3}.$$

This quantity is called the optical thickness of a turbid medium, and characterizes the degree of multiple scattering.

The condition $\tau \lesssim 1$ indicates that we may disregard multiple scattering. This condition does not follow from all the preceding limitations of the problem.

Due to the fact that the purpose of this book is to study translucent /22 media, we shall also assume that this condition holds.

We should note that all the linear characteristics of the problem are not exhausted with the quantities x_i. For example, the quantities characterizing the form of the particles or the macrovolume, etc. can hold here. However, the parameters x_i are of decisive importance for studying the entire problem.

Let us investigate what values the parameters x_2 and x_3 assume for different problems in the atmosphere.

In a so-called pure atmosphere, admixtures are of the main importance, particularly in their lower layers.[1] This pertains to particles having a radius of approximately 0.1μ: drops of water or solutions of acids, salts, and bases, and also crystals of ice and dust having a mineral or organic origin. Primarily NaCl, HCl, $MgCl_2$, $MgSO_4$, $CaSO_4$, etc. are encountered. These extremely small drops and particles form the so-called atmospheric mist.

The thermodynamic stability of such small drops is caused by the high concentrations of substances dissolved in them. Drops with intermediate dimensions (between drops of mist and cloud drops) are unstable. These drops exist for a very short period of time in the initial stages of cloud formation.

The number of particles fluctuates from several hundreds per cubic centimeter in pure mountain air up to hundreds of thousands in the cities. The diurnal and yearly pattern of this number provides the periodicity of the transmittance and other optical phenomena caused by the admixtures.

In meteorology, we are primarily dealing with two radiation fluxes -- solar radiation with a energy maximum in the case of $\lambda = 0.5\mu$, and terrestrial radiation and gases of the air, with a maximum in the case of $\lambda = 10\mu$. For admixtures, the quantity $x_2 \lesssim 1$ and $x_3 >> 1$. The large value of x_3 indicates that we may apply the customary summation rules for intensities. On the other hand, for the case $\lambda = 10\mu$ in very dusty air x_3 is about 5-10. Allowance for /23 interference between scattering centers may be of importance.

Since x_2 does not exceed unity, an analysis of elementary scattering does not entail any difficulties, if it is assumed that the particles are spherical. However, it is significant that crystals of ice and other dust particles preferably take the form of discs or rods. We shall investigate the scattering of light by such particles in VIII, 4.

Let us now discuss the situation during the propagation of light in clouds, rain, and fogs.

(a). Clouds. Studies of cloud elements have been performed by many authors [see, for example, the studies of Ye. S. Selezneva (Ref. 21), A. M. Borovikov (Ref. 22), etc.]. A. M. Borovikov gives a curve, which we have shown in Figure 1, for the distribution by size of cloud drops. This is the result

---

(1) This may be readily established if we compare the visual range of visibility in a Rayleigh atmosphere with the real range. In the case t = 0°C and p = 760 mm Hg, the Rayleigh range is about 350 km, while the real range is considerably less (∿ 20 km).

of averaging observations of different types of clouds.

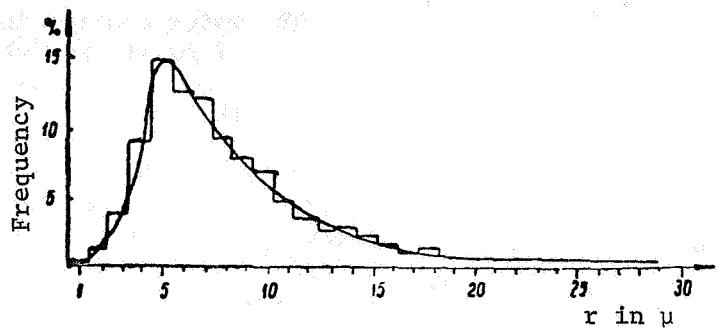

Figure 1. Curve Showing the Distribution of Drops by Size in Clouds

The frequency in percents is plotted along the ordinate axis, and the radius of drops in microns is plotted along the abscissa axis. It may be seen in Figure 1 that the cloud consists mainly of drops having a radius of 5-7μ. The proportion of these drops amounts to 50% of the entire number of drops. Drops with r = 5μ display the greatest frequency. The average size of the drops $\bar{r} = \left(\frac{\Sigma n_i r_i}{\Sigma n_i}\right)$ is somewhat greater: $\bar{r}$ = 8.3μ. Along with the first maximum close to 5-10μ, in certain cases (quite rarely) there is a second maximum at 15-25μ [according to Selzneva (Ref. 21), Figure 2].

Table 1 presents more detailed data on the distribution of drops in clouds. /24

TABLE 1

Form of Clouds	Radius In μ				Water Content in Relative Units	Mean Distance Between Drops in mm
	Mean	Greatest Frequency	Max.	Min.		
St	6.8	5	29	1	8	1.09
Ac	7.1	6	16	4	5	1.15
Sc	8.0	5-7	40	2	12	1.29
N_3	9.7	7	72	3	34	1.57

The mean radius of the drops in a cloud increases with altitude. We have advanced (1949) the following explanation for this important fact.

A decrease in the temperature with altitude leads to a decrease in the amount of water vapor which may be found in a unit of air mass. Since the total reserve of water does not change, the content of liquid water must increase with altitude. This means that the dimensions of the drops will increase

with altitude (their number per unit of mass will not change).

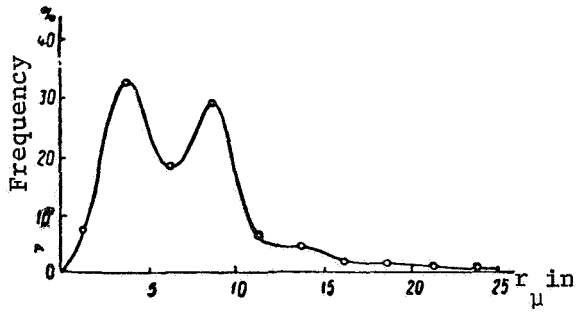

Figure 2. "Two-Humped" Distribution Curve

The water content in the cloud increases from its periphery to the center. The greatest water content is found in the center, close to the upper edge. The absolute water content values in the clouds change from 0.01 g/m^3 to several g/m^3 (in Cumulanimbus). On the average, the water content is not above /25 0.2 g/m^3 for the usual clouds, whereas it is about 1 g/m^3 for different forms. The mean distances between particles are shown in Table 1 for a water content of 1 g/m^3.

I. A. Khvostikov (Ref. 23) has studied the transmittance of fogs and clouds, as well as the degree of scattered light polarization. This study led him to the important conclusion that a large group of "submicroscopic" particles, with a radius of about 0.1μ, exists in clouds, along with the drops indicated above (∿ 5-10μ).[1] Thus, although the number of these particles is large, the water content which they introduce into the cloud is on the order of several percents. Unfortunately, as of the present no final clarification has been provided for this important problem (see VIII, 1).

(b) Fogs and Rain.

Table 2 presents certain data regarding fogs and rain. The data on rain intensity presented in the last column represent a quantitative determination of different types of rain. The data on water content indicate the water content in the liquid phase.

TABLE 2

Type of Formation	Drop Diameter in mm	Mean Distance Between Drops in mm	Water Content in g/m^3	Rain Intensity in mm/hr
Fog	0.01	4.3	$6 \cdot 10^{-3}$	Traces
Thick Fog	0.10	21	$57 \cdot 10^{-3}$	0.05
Fine Rain	0.20	36	$93 \cdot 10^{-3}$	0.25
Light Rain	0.45	70	0.14	1.00
Moderate Rain	1.00	123	0.28	4.00
Strong Rain	1.50	130	0.83	15.00
Very Strong Rain	2.10	138	1.8	40.00
Showers	3-5	137	5.4	100.0

(1) The customary methods of determining drops in clouds do not record such small particles.

In addition to the hydrometeors, the atmosphere also includes snow, snow grains, snow and ice pellets and hail. The theory developed for rain may be applied to these cases, if it is approximately assumed that these particles are /26 spheres with a certain effective radius and with effective electric properties. This approximation is rather rough, and may only be applied for qualitative discussions.

Assuming that drops in the clouds have a radius of about 5 μ, we find that x_2 will be about 10 in the visible region. It may be assumed that this value is large. The quantity $x_3 (\sim 10^3)$ is also large here. Both parameters have even larger values in the case of fog and rain.

Consequently, the basic problem which now confronts us is to study scattering by an enormous transparent drop. We will discuss this problem in detail at a later point.

Table 3 shows the values for the parameters x_2 and x_3 in the infrared region.

TABLE 3

	x_2	x_3
Clouds	0.5	100
Fogs	1	430
Thick Fogs	10	2100
Rain	20	3600

We thus have two different problems: the first problem is for the case of clouds and fine fogs; the second is for the case of thick fogs and rain. In the first case, we may assume that the particles are comparable with the wave lengths; in the second case, we may assume that they are larger. In both cases, it is not possible to take into account interference between particles ($x_3 \gg 1$).

We may see that the geophysical problems require an investigation of any values for the ratio a/λ. The situation is the same in problems of colloid physics and astrophysics. Metallic and semiconductor particles also are of importance, along with dielectric, transparent or absorbing particles. Therefore, we shall make a general analysis of the problem later, confining ourselves neither to particle dimensions nor to the nature of the particles. We shall always assume (except for VIII, 4) that the particles are spheres.

§ 4. Optical Constants /27

The physical properties of scattering particles are of significant importance in the problem under consideration, along with the linear characteristics which were summarized above. In accordance with (1.6), all of the optical properties of matter in which we are interested may be described by one complex

number m -- the complex refractive index.

In several cases, it is advantageous to draw a distinction between the real and imaginary part in the complex refractive index m. For this purpose, m is usually written in one of the two following forms:

$$\left.\begin{aligned} m &= n(1 - i\chi) \\ m &= n - i\varkappa. \end{aligned}\right\} \tag{1.9}$$

or

Here n is the refractive index; χ -- absorption index; $\varkappa$ -- absorption coefficient:

$$\varkappa = n\chi. \tag{1.10}$$

The dielectric constant ε in the general case is also a complex quantity. It may be written as follows:

$$\varepsilon = \varepsilon' - i\varepsilon'',$$

where ε' and ε'' are the real and imaginary parts, respectively of ε.

Thus, for m^2 we have:

$$m^2 = \varepsilon' - i\left(\varepsilon'' + \frac{4\pi\sigma}{\omega}\right) \tag{1.11}$$

and

$$\left.\begin{aligned} \varepsilon' &= n^2(1 - \chi^2) = n^2 - \varkappa^2, \\ \varepsilon'' + \frac{4\pi\sigma}{\omega} &= 2n^2\chi = 2n\varkappa. \end{aligned}\right\} \tag{1.12}$$

We should recall the physical meaning of the quantities n and $\varkappa$.

Equations for the fields (1.4) may be satisfied by a solution of the following type

$$e^{i(\omega t - ky)} = e^{i(\omega t - k_0 m y)}.$$

An infinite plane wave, having the frequency ω and (in a vacuum) the wave vector k_0, propagated along the axis Y, corresponds to this solution.

Replacing m by n and x, we obtain:

$$e^{i(\omega t - k_0 n y)} \cdot e^{-k_0 \varkappa y}.$$

Thus, we obtain a plane wave having the length $\lambda' = \frac{2\pi}{k_0 n}$. The wave /28
amplitude decreases by the quantity $e^{-\alpha' y}$, where $\alpha' = \frac{\varkappa 2\pi}{\lambda}$ in the case of displacement by y of unit of length. With respect to the light intensity which is determined by means of the square of the fields, it also decreases according to the law $c^{-\alpha y}$, but twice as rapidly ($\alpha = 2\alpha'$).

A plane wave undergoes significant changes when penetrating an absorbing body: the wave becomes heterogeneous. This means that planes of constant phase do not coincide with planes of constant amplitude.[1] In addition, in its

(1) In contrast to the case indicated above, where both planes coincide (The XOZ-plane).

customary form the refraction law does not hold. The ratio between the sine of the angle of this incidence and the sine of the angle formed by the wave normal and the perpendicular to the dividing surface at the point of incidence depends on the angle of incidence. Thus, the rate at which the wave is propagated depends on the angle of incidence.

For example, cases are possible in which, along with a zero angle of incidence, there is one angle at which light which penetrates the dividing boundary does not undergo refraction. Thus, for gold this angle is about 76° in the visible region.

We shall assume that the quantities n and × are given from this point on. They essentially depend on the frequency, and their values must be found experimentally from experiments with radiation of different wave lengths. These experiments usually consist of determining × (directly, based on light attenuation after it has penetrated a film having a definite thickness) and of the simultaneous determination of n (depending on the reflection coefficient). Very frequently, particularly when determining the optical constants of metals, only the polarization ratios are studied in reflected light.[1]

These measurements were performed for a large class of different substances, and their results may be found in, for example, (Ref. 24) or in other handbooks. We cannot discuss the data pertaining to different specific substances here. /29

We shall only dwell somewhat in detail on optical constants of metals and liquid water, since the former is of importance in colloid optics, and the latter is of importance in geophysics.

The optical constants have a pronounced, and in general odd, behavior in the ultraviolet, optical, and close infrared regions which encompass the absorption bands of electrons in a metal. For all metals in this region, n and × are approximately of the same order and have values of about 0.5 - 3.

In Table 4 we present, for example, the optical data for gold, which were employed in the calculations of Mie. These data were obtained experimentally.

TABLE 4

λ in μ	m	λ in μ	m
0,420	$1{,}70 - i\,1{,}70$	0,550	$0{,}57 - i\,2{,}45$
0,450	$1{,}73 - i\,1{,}72$	0,600	$0{,}38 - i\,2{,}96$
0,500	$1{,}10 - i\,2{,}02$	0,650	$0{,}41 - i\,3{,}54$
0,525	$0{,}79 - i\,2{,}23$		

(1) It should be noted that the determination of n and × for metals is a rather complex experimental problem. Polarization experiments are complicated by factors introduced by the metal surface layers, thus confusing the picture. In view of the large absorption of metals, experiments on penetration through a film require very thin films. Exact measurement of the thickness of these films must be done independently.

The diverse change in n and $\varkappa$ in the visible region is the reason for the different coloration of different metals. This coloration is supplementary to the color of penetrating rays. Thus, for example, thin gold films appear green in transmitted light. The situation is different for bodies with small absorption, in which the color is caused by scattering and selective absorption of light by turbidity elements. In this case, the coloration in the reflected and transmitted light is one and the same (for example, colored paper, etc.).

All the metals have a very similar picture in the infrared region, approximately after λ equals 1 - 2 μ, behind the absorption bands of individual substances. Both optical constants increase with an increase in λ, and become increasingly identical. This important fact was established experimentally in 1903 in the studies of Gagen and Rubens. Their result can be readily understood, if we note that the term $4\pi\sigma/\omega$ becomes very large in the formula for m in the case of sufficiently small ω. /30

This means that we approximately have

$$m=\sqrt{-i\frac{4\pi\sigma}{\omega}}=\sqrt{\frac{4\pi\sigma}{\omega}}\left(\frac{\sqrt{2}}{2}-i\frac{\sqrt{2}}{2}\right). \tag{1.13}$$

This approximate relationship holds, beginning with $\lambda = 5\mu$.

Thus, in actuality we have $n = \varkappa = \sqrt{\frac{2\pi\sigma}{\omega}}$.

According to the Fresnel formulas, the reflection coefficient in the case of normal incidence will be

$$R=\left|\frac{m-1}{m+1}\right|^2=\frac{(n-1)^2+\varkappa^2}{(n+1)^2+\varkappa^2}. \tag{1.14}$$

Since n and $\varkappa$ in our case are large ($\sim$ 10), for R we obtain

$$R=1-\frac{2}{\sqrt{\frac{2\pi\sigma}{\omega}}}. \tag{1.15}$$

With an increase in the wave length , the reflection coefficient of metals strives to unity.

Formula (1.15) was substantiated with a large amount of experimental material. It is even more interesting to note that it contains no arbitrary constants.

Let us now turn to water. Let us investigate the manner in which its optical constants change as the wave length increases.

The refractive index of water decreases with an increase in λ in the ultraviolet and visible regions. We present the corresponding data (in the case of t = 20°C) in Table 5 and Figure 3 ($\Delta = n - 1.300$ is given in Figure 3).

Absorption in this region is very small. In Table 6 we present the data for the absorption coefficient α in $\frac{1}{cm}$ pertaining to intensity attenuation of transmitted light: /31

$$I(l) = I_0 e^{-\alpha l}. \tag{1.16}$$

TABLE 5

λ in μ	n	λ in μ	n	λin μ	n
0,214	1,4032	0,509	1,3360	0,768	1,3289
0,303	1,3581	0,589	1,3330	1,028	1,3245
0,405	1,3428	0,671	1,3308	1,256	1,3210
0,486	1,3371				

This same table presents the data for ×:

$$x = \frac{\alpha\lambda}{4\pi}.^{1} \tag{1.17}$$

The absorption has a minimum at 0.5 μ. For attenuation by a factor of e, water thickness of 67 m is necessary. With an increase in λ, the absorption at first increases slowly, and then very rapidly. The absorption band of water lies at λ = 0.944 μ.

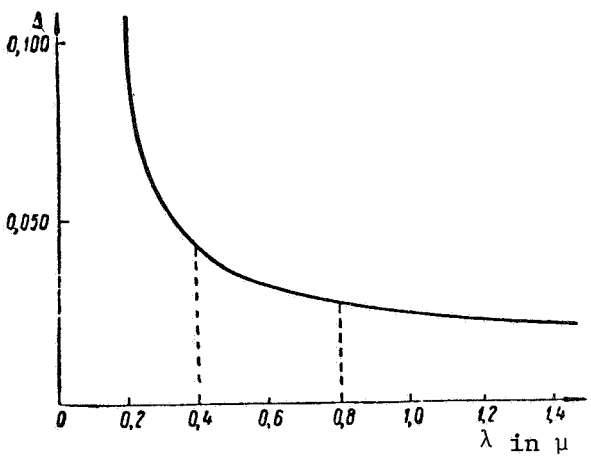

Figure 3. Refractive Index of Water (Δ = n - 1.300; the Dashed Lines Separate the Interval of Visible Radiation).

In addition to this band, water has an entire series of bands in the infrared region. They are located at the following wave lengths (in μ): /32

1,128—1,480	6,56— 8,99	58
1,843—1,985	9,74—17,33	66
3,194	31,0	79
4,98 —6,49	50,0	103

The band at 3.2 μ has the strongest absorption, then there is a wide interval of strong absorption located after 11 μ. Absorption in the band at 6.1 μ is weaker than in the two sections of λ indicated above.

A large portion of the liquid water bands represents water vapor bands (shifted toward large λ). Consequently, they must be attributed to absorption in a free molecule. However, certain bands are characteristic for liquid water, and their occurrence is caused by a change in the energy levels of the molecule H_2O in the condensed state under the influence of neighbors. The bands overlap each other, causing strong absorption in the entire infrared region. The situation

---

(1) We would like to call the attention of the reader to the fact that the absorptive power of a substance may be described by three different quantities: the absorption index χ, the refractive index ×, and the absorption coefficient α. These quantities may be determined by the relationships (1.9), (1.10), (1.16) and (1.17).

The quantities α, χ and × may be usually calculated by means of α, experimentally.

TABLE 6

λ in μ	α in $\frac{1}{см}$	$\varkappa \cdot 10^8$	λ in μ	α in $\frac{1}{см}$	$\varkappa \cdot 10^8$
0,200	0,090	4,3	0,800	0,0204	13,0
0,300	0,015	3,58	0,900	0,161	115
0,415	0,00035	0,115	0,995	0,472	373
0,500	0,00015	0,0596	1,05	0,368	299
0,600	0,00107	0,511	1,21	1,30	1252
0,700	0,0030	1,67			

is characterized in Table 7, where we employ α and the reflection coefficient for normal incidence R (in %).

When compiling this table, we employed not only the old data of Ladenburg and Rubens, but also several new studies. In this connection, we would like to point out the careful research by Veyngerov (Ref. 25), who determined R for water in the region 11 - 18 μ. He was able to eliminate several experimental errors of previous studies. The results which he obtained primarily coincide with the results of previous authors.

We should point out that an interesting survey of data on dispersion and /33 absorption of radiation in water was compiled in his time by the Kazan physicist D. A. Gol'dgammer (Ref. 26).

In accordance with (1.14), the reflection maxima are related to the absorption bands. They are shifted somewhat toward large λ. "Metallic reflection" (R → 1 in the case $\varkappa \to \infty$) will hold at the absorption maxima. A change in α and R to λ = 27 μ is shown in Figure 4, and the behavior of R in the 25-300 μ interval is shown in Figure 5. The quantity R increases after λ ∿ 24 μ, reaching 15% in the case λ = 300 μ.

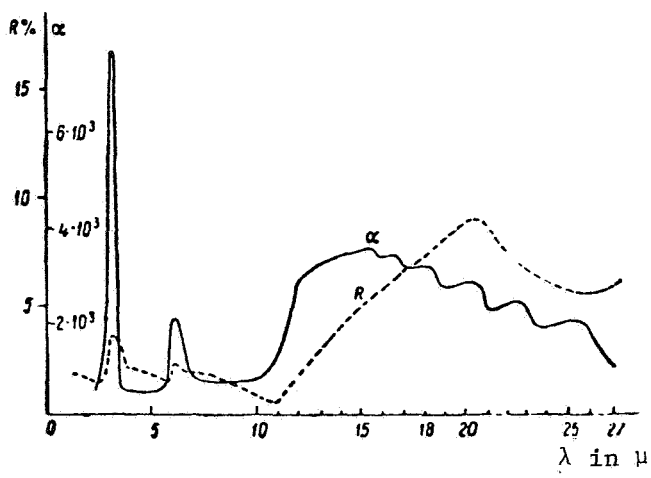

Figure 4. Coefficients of Reflection R and Absorption α of Radiation by Water.

In Table 7 we present the optical constants of water which we computed according to α and R. The quantity n may be determined according to the following formula

$$n = \frac{1+R}{1-R} + \sqrt{\left(\frac{1+R}{1-R}\right)^2 - 1 - \varkappa^2} \doteq \doteq 1 + 2R + \sqrt{4R - \varkappa^2}, \quad (1.18)$$

which directly follows from (1.14).

With a further increase in λ, /34 we enter the region of centimeter waves. Water also has strong dispersion here, which is caused by inertia of dipoles when they rotate in the external field. "Friction", related to this rotation, leads to strong absorption. The dispersion

theory in this region closely coincides with numerous measurements.

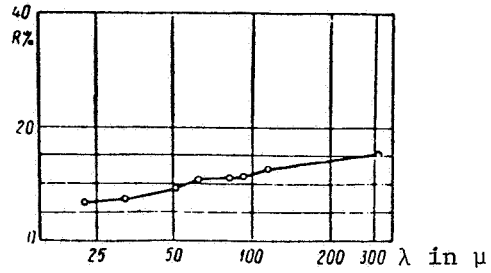

Figure 5. Coefficient for Reflection of Long Thermal Waves by Water.

A change in the electric properties of water with a change in λ in the centimeter region [real (ε') and imaginary (ε") portions of the dielectric constant] is shown in Figure 6.

We should note that n and ×, computed theoretically, do not change directly into the n and × indicated at the end of Table 7. The reason for this is that the eigen absorption bands, which do not allow for the theory of rotational dispersion, lying in this region are of significant importance for $\lambda \leqq 1$ cm.

In the region of meter waves, the dielectric constant acquires statistical value ($n = 9$, $\varepsilon = 81$).

In connection with the "metallic" reflection in absorption bands mentioned here, in conclusion let us discuss one prevalent error. This error is related to the concept of the "blackness" degree of a given body in a certain spectral interval.

Strictly speaking, in order to approximate an absolutely black body, it is necessary to take a substance with a very large absorption coefficient. In other words, it is assumed that the body is "black" in those spectral regions where strong absorption occurs. This opinion is erroneous. By way of an /35
example, we may point to metals. They strongly absorb visible radiation; however, they are very far from a black body.

The degree of blackness of a given body -- i.e., the extent to which it approximates an absolutely black body -- may naturally be determined from the absorptive power of the body a. For an absolutely black body $a = 1$; for any real body $a < 1$. If the body thickness (in the direction of refracted rays) is ℓ, and the reflection coefficient is R, we obtain the following for a:

$$a = (1 - R)\left(1 - e^{-\frac{4\pi}{\lambda}\varkappa l}\right).$$

The first parenthesis gives the portion of the flux penetrating the body. The second parenthesis indicates the portion of the flux penetrating the body which is absorbed by the body.

An absolutely black body may be characterized by two features: (1) the /36
reflection R equals zero; (2) the transmission $e^{-\frac{4\varkappa}{\lambda}\varkappa\ell}$ equals zero.

The first property depends on the behavior of the substance in a given spectral region, and upon the radiation angle of incidence. The second property depends in addition on the body thickness. It may be readily seen that, if we compare the degree of "blackness" of the body in different spectral intervals

TABLE 7

λ in μ	α in $\frac{1}{см}$	R in %	$\varkappa$	n
1,50	2,64	1,95	$0,314 \cdot 10^{-4}$	1,323
2,00	70	1,74	$0,111 \cdot 10^{-2}$	1,304
3,00	7330	3,40	0,1747	1,409
3,20	6640	4,10	0,169	1,473
3,40	1440	3,25	0,0389	1,438
4,5	447	2,14	0,0160	1,342
5,47	335	1,68	0,0146	1,297
6,00	2140	2,00	0,101	1,311
7,00	810	1,95	0,0451	1,327
8,00	755	1,67	0,0480	1,292
9,00	700	1,44	0,0501	1,268
10,00	705	0,95	0,0560	1,208
11,00	1200	0,75	0,105	1,154
12,00	2590	2,00	0,247	1,190
13,00	2890	3,10	0,298	1,270
15,00	3570	5,30	0,426	1,346
18,00	2990	6,70	0,427	1,497
52	1160	9,30	0,480	1,554
63	1020	10,74	0,512	1,768
83	710	11,75	0,469	1,885
100	460	12,28	0,366	1,991
117	360	12,8	0,335	2,044
152	320	13,4	0,387	2,059
314	242	15,1	0,605	2,041

when the thickness remains unchanged, the degree of blackness for the body a will be at a maximum for a certain absorption coefficient $\varkappa$. For very small $\varkappa$ and very large $\varkappa$, a will be close to zero.

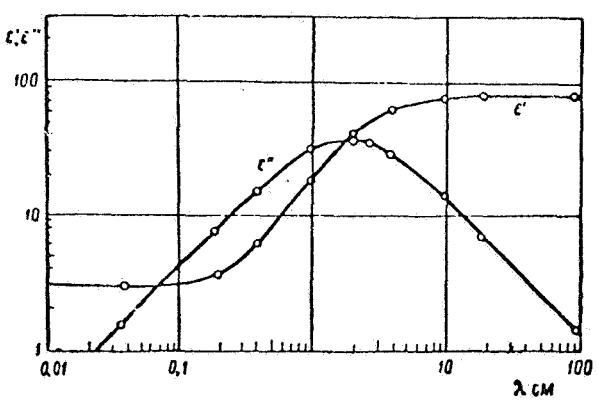

Figure 6. Real and Imaginary Sections of the Water Dielectric Constant in the Centimeter Region.

Similarly to this, the degree of blackness for the body will change when there is a change in the angle (if the body is a plane layer) of incidence of rays on the body. It will equal zero in the case of tangential incidence (R = 1) and will be small in the case of normal incidence (ℓ is at a minimum).

If both "blackness" characteristics interest us separately, we must derive two different criteria of "blackness".

We should point out that the requirements for absolute "blackness" with respect to both features at once are mutually exclusive. At the point where the body is "blacker" in terms of the first characteristic, it will be less "black" in terms of the second characteristic.

It is well known that in electrodynamics a black body cannot be determined by a suitable selection of boundary conditions. In formal terms, in the diffraction theory, in order to obtain a black body one resorts to mathematical /37

Riemann space of infinite shortness [(Ref. 30), page 853]. It is equivalent to "a hole in a vacuum".

In electrodynamics the physical method for obtaining an ideally black body is as follows. A substance with $n = 1$ and $\varkappa \to 0$ is selected, and a layer of this substance must have a thickness ℓ such that

$$\frac{4\pi}{\lambda}\varkappa l \to \infty.$$

Thus, if the body thickness is large enough, it will be closest to a black body in those spectral regions where the substance is the most transparent, i.e., at that point where $|m - 1| \ll 1$. For example, a deep reservoir will be blacker in the visible region, where the water is transparent, than it will be in the infrared region.

CHAPTER II

FUNDAMENTAL FORMULAS /38

Let us present a precise solution for the problem of diffraction of electromagnetic waves in a sphere [see (Ref. 31-35, 14, 36-39)].

In the case under consideration, the surface of the sphere will be the surface of discontinuity. Therefore, we may conveniently consider the problem in spherical coordinates.

We shall show that the problem of finding the six unknown functions (**E** and **H**) may be reduced to the problem of finding two functions -- of the electric and magnetic potentials (U_1 and U_2). The field components may be computed by simple differentiation from these potentials. The potentials U_1 and U_2 represent solutions of the oscillatory equation. We may obtain them by employing the Fourier method in the form of infinite sums of special solutions with indefinite coefficients. The coefficients may be determined by "joining" the values within and outside the sphere.

Thus, the desired solution process will consist of the following parts:

(1) Reduction of the system of equations and boundary conditions for the field components to equations and conditions for the potentials;

(2) Solution of the equation for the potentials;

(3) Reversion back to the fields (derivation of the formulas for the fields from the potentials) and determination of formulas for intensities;

(4) Derivation of formulas for coefficients of scattering and attenuation.

§ 1. Potentials

Let us select the origin in the center of the sphere, and let us draw the axis as is shown in Figure 7. We will employ a to designate the radius of the sphere. Let a plane wave which is polarized linearly fall upon a particle in the

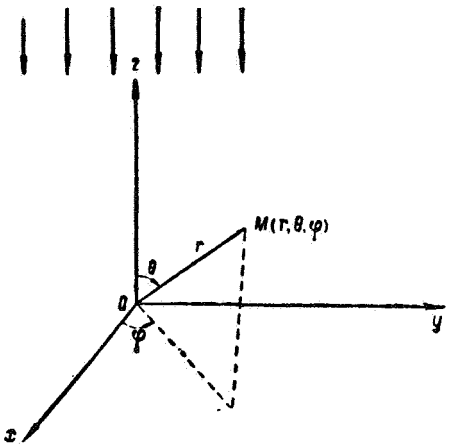

Figure 7. Arrangement of Axes when Deriving the Fundamental Formulas.

negative direction on the Z-axis. The X-axis is the direction of electric oscillations, and the Y-axis is the direction of magnetic oscillations. The electric and magnetic fields in the incident wave may be described by the following formulas: /39

$$\left.\begin{aligned} \mathbf{E}^0 &= \mathbf{E}_0 e^{ik_\alpha z}, \quad E_{0x} = E_0, \quad E_{0y} = E_{0z} = 0, \\ \mathbf{H}^0 &= \mathbf{H}_0 e^{ik_\alpha z}, \quad H_{0y} = -m_\alpha E_0, \quad H_{0x} = H_{0z} = 0. \end{aligned}\right\} \quad (2.1)$$

Here $k_\alpha = m_\alpha k_0$ is the magnitude of the wave vector of the incident radiation in the outer sphere (in which our sphere is immersed); $k_0 = \frac{\omega}{c}$ -- radiation wave vector in a vacuum[1].

For simplicity of notation, from this point on we shall omit the factor E_0 in the intermediate formulas. It will be necessary to introduce this factor in the expression for the fields in the final formulas.

In the spherical coordinate system (see Figure 7), the Maxwell equations (1.3) may be written as follows: /40

$$im^2 k_0 E_r = \frac{1}{r\sin\theta}\left\{\frac{\partial}{\partial\theta}(\sin\theta H_\varphi) - \frac{\partial}{\partial\varphi}H_\theta\right\}; \quad (2.2)$$

$$im^2 k_0 E_\theta = \frac{1}{r\sin\theta}\left\{\frac{\partial}{\partial\varphi}H_r - \frac{\partial}{\partial r}(r\sin\theta H_\varphi)\right\}; \quad (2.3)$$

$$im^2 k_0 E_\varphi = \frac{1}{r}\left\{\frac{\partial}{\partial r}(rH_\theta) - \frac{\partial}{\partial\theta}H_r\right\}; \quad (2.4)$$

$$-ik_0 H_r = \frac{1}{r\sin\theta}\left\{\frac{\partial}{\partial\theta}(\sin\theta E_\varphi) - \frac{\partial}{\partial\varphi}E_\theta\right\}; \quad (2.5)$$

$$-ik_0 H_\theta = \frac{1}{r\sin\theta}\left\{\frac{\partial}{\partial\varphi}E_r - \frac{\partial}{\partial r}(r\sin\theta E_\varphi)\right\}; \quad (2.6)$$

$$-ik_0 H_\varphi = \frac{1}{r}\left\{\frac{\partial}{\partial r}(rE_\theta) - \frac{\partial}{\partial\theta}E_r\right\}. \quad (2.7)$$

---

(1) We should note that in the article of Wolfson in Handbuch der Physik (Ref. 39), an error is included which then leads to invalid final formulas. Wolfson selects the amplitudes of the fields $\mathbf{E}^0$ and $\mathbf{H}^0$ in the following way:

$$E_{0x} = E_0 \qquad E_{0y} = E_{0z} = 0$$
$$H_{0y} = -E_0 \qquad H_{0x} = H_{0z} = 0.$$

It may be readily seen that these fields ($m_\alpha \neq 1$) do not satisfy the Maxwell equations. This error slipped into the book of V. D. Kupradze [see (Ref. 87), equation (18) on page 16].

The incident field excites the inner field in the sphere. The outer and inner fields must satisfy the conditions of continuity of the tangential components on the surface of the sphere:

$$E_\theta^a = E_\theta^i; \quad H_\theta^a = H_\theta^i, \tag{2.8}$$

$$E_\varphi^a = E_\varphi^i; \quad H_\varphi^a = H_\varphi^i. \tag{2.9}$$

The index i designates the quantities pertaining to the sphere, and the index a - k pertains to the outer medium. It is known that a system of boundary conditions (2.8) and (2.9) cannot be satisfied, if it is not assumed that there is a certain diffracting field E in outer space, along with the incident field E^0. Thus, the outer field $E^\alpha = E^0 + E$. In addition, since conditions (2.8) - (2.9) must hold in every moment of time, this means that all the fields -- incident, diffracting, and excited in the sphere (inner) -- must have one and the same time dependence. This is possible if all three fields have one and the same frequency.

Thus, in contrast to Raman scattering, for example, the scattering under consideration here must occur without a change in frequency.

We shall represent an arbitrary electromagnetic field as the superposition of two types of oscillations.

We shall call the first type electric oscillations, and we shall assume /41 that the radial magnetic field component in these oscillations equals zero at every point:

$$H_r = 0; \quad E_r \neq 0. \tag{2.10}$$

The second type is magnetic oscillations. The radial component of the magnetic field in magnetic oscillations differs from zero, and the electric component equals zero everywhere:

$$E_r = 0; \quad H_r \neq 0. \tag{2.11}$$

In the case of electric oscillations, we obtain the following from equation (2.5):

$$\frac{\partial}{\partial\theta}(\sin\theta E_\varphi) = \frac{\partial}{\partial\varphi} E_\theta.$$

This relationship will be satisfied, if it is assumed that $\sin\theta E_\phi$ and E_θ are derivatives of a certain third function Φ: the first with respect to ϕ, and the second with respect to θ:

$$\sin\theta E_\varphi = \frac{\partial\Phi}{\partial\varphi}, \quad E_\theta = \frac{\partial\Phi}{\partial\theta}.$$

Substituting these relationships in formulas (2.3) and (2.4), we obtain

$$im^2k_0\frac{\partial\Phi}{\partial\theta} = -\frac{1}{r}\frac{\partial}{\partial r}(rH_\varphi), \quad im^2k_0\frac{\partial\Phi}{\partial\varphi} = \frac{\sin\theta}{r}\frac{\partial}{\partial r}(rH_\theta).$$

We may satisfy these relationships, if we assume that $\Phi = \frac{1}{r}\frac{\partial\psi}{\partial r}$, where ψ is a certain new function. We then obtain

$$H_\varphi = -\frac{im^2k_0}{r}\frac{\partial\psi}{\partial\theta}; \quad H_\theta = \frac{im^2k_0}{r\sin\theta}\frac{\partial\psi}{\partial\varphi}.$$

Substituting this in formulas (2.2), (2.6) and (2.7), we note that if we introduce the function $U_1 = \frac{\psi}{r}$ -- instead of the function ψ -- the formula (2.2) assumes the following form

$$E_r = \frac{1}{r\sin\theta}\left\{\frac{\partial}{\partial\theta}\left(-\sin\theta\frac{\partial U_1}{\partial\theta}\right) - \frac{\partial}{\partial\varphi}\left(\frac{1}{\sin\theta}\frac{\partial U_1}{\partial\varphi}\right)\right\} \tag{2.12}$$

since both latter formulas lead to one and the same equation -- the wave equation for the function $U_1(r, \theta, \phi)$:

$$\frac{1}{r}\frac{\partial^2}{\partial r^2}(rU_1) + \frac{1}{r^2\sin\theta}\frac{\partial}{\partial\theta}\left(\sin\theta\frac{\partial U_1}{\partial\theta}\right) + \frac{1}{r^2\sin^2\theta}\frac{\partial^2 U_1}{\partial\varphi^2} + k^2U_1 = \Delta U_1 + k^2U_1 = 0. \tag{2.13}$$

Employing the relationships indicated above and substituting the derivatives with respect to θ and ϕ by the derivatives with respect to r from equation (2.13) in the expression for E_r, we obtain the following relationships: /42

$$\left.\begin{aligned} &E_r = \frac{\partial^2}{\partial r^2}(rU_1) + k^2rU_1;\\ &E_\theta = \frac{1}{r}\frac{\partial^2(rU_1)}{\partial r\,\partial\theta};\quad E_\varphi = \frac{1}{r\sin\theta}\frac{\partial^2(rU_1)}{\partial r\,\partial\varphi};\\ &H_r = 0;\quad H_\theta = -\frac{im^2k_0}{r}\frac{\partial}{\partial\theta}(rU_1);\\ &H_\varphi = \frac{im^2k_0}{r\sin\theta}\frac{\partial}{\partial\varphi}(rU_1). \end{aligned}\right\} \tag{2.14}$$

They express all the field components for the case $H_r = 0$ by means of one function $U_1(r, \theta, \phi)$ -- the potential of electric oscillations.

If we substitute these expressions in equations (2.2) - (2.7), it may be readily seen that equations (2.14) form a solution of the system of Maxwell equations, if U_1 is a solution of the wave equation.

The situation is the same for magnetic oscillations. Here all the field components may be expressed by means of a certain function $U_2(r, \theta, \phi)$ -- the potential of magnetic oscillations.

In the general case, oscillations of both types will exist in the field. We thus obtain the following expressions for the field components:

$$\left.\begin{aligned} &E_r = \frac{\partial^2(rU_1)}{\partial r^2} + k^2rU_1;\\ &E_\theta = \frac{1}{r}\frac{\partial^2(rU_1)}{\partial r\,\partial\theta} - \frac{ik_0}{r\sin\theta}\frac{\partial}{\partial\varphi}(rU_2);\\ &E_\varphi = \frac{1}{r\sin\theta}\frac{\partial^2(rU_1)}{\partial r\,\partial\varphi} + \frac{ik_0}{r}\frac{\partial}{\partial\theta}(rU_2);\\ &H_r = \frac{\partial^2(rU_2)}{\partial r^2} + k^2rU_2;\\ &H_\theta = \frac{1}{r}\frac{\partial^2(rU_2)}{\partial r\,\partial\theta} + \frac{im^2k_0}{r\sin\theta}\frac{\partial}{\partial\varphi}(rU_1);\\ &H_\varphi = \frac{1}{r\sin\theta}\frac{\partial^2(rU_2)}{\partial r\,\partial\varphi} - \frac{im^2k_0}{r}\frac{\partial}{\partial\theta}(rU_1). \end{aligned}\right\} \tag{2.15}$$

The functions U_1 and U_2 are solutions of the wave equation

$$\Delta U_j + k^2 U_j = 0, \quad j = 1,2. \tag{2.16}$$

The boundary conditions for the potentials U_1 and U_2 on the sphere may be /43 obtained from the continuity requirement of the tangential (θ and ϕ) components of the fields. We may see from equations (2.15) that for this purpose it is necessary that the following four quantities be continuous on the surface of the sphere:

$$\left.\begin{aligned} m^2 r U_1;\quad & \frac{\partial}{\partial r}(rU_1); \\ rU_2;\quad & \frac{\partial}{\partial r}(rU_2). \end{aligned}\right\} \tag{2.17}$$

It is important that the boundary conditions are not mixed -- i.e., are separate for U_1 and U_2. This indicates the mutual independence of electric and magnetic oscillations. In view of this independence, the electric oscillations in an incident wave are responsible for the electric oscillations in diffracted and refracted waves, and the magnetic oscillations in the incident wave are responsible for the magnetic oscillations in excited waves. We cannot treat the solution of only one type of oscillations, since both types occur in a plane wave falling on a sphere.

At infinity, the functions U_1 and U_2 must satisfy the radiation principle. Thus, our problem consists of finding two independent solutions of the wave equation with independent boundary conditions.

§ 2. Solution of Equations for the Potentials

We shall solve the equations for the potentials U_1 and U_2 (2.16) by employing the Fourier method. We may set the following as a special solution:

$$U = f(r)\,Y(\theta, \varphi).^{1}$$

Dividing the variables, we obtain the following equations for f and Y:

$$\frac{1}{r}\frac{d^2(rf)}{dr^2} + \left(k^2 - \frac{\lambda}{r^2}\right) f = 0; \tag{2.18}$$

$$\frac{1}{\sin\theta}\left\{\frac{\partial}{\partial\theta}\left(\sin\theta\frac{\partial Y}{\partial\theta}\right) + \frac{1}{\sin\theta}\frac{\partial^2 Y}{\partial\varphi^2}\right\} + \lambda Y = 0. \tag{2.19}$$

The equation for Y is the well known equation for spherical functions. /44

It has a single-valued and continuous solution over the entire sphere only for $\lambda = n \cdot (n + 1)$, where $n = 0, 1, 2, \ldots$

In this case, the following spherical functions represent its solution [(Ref. 40), page 606]:

$$Y_n(\theta,\varphi) = a_0 P_n(\cos\theta) + \sum_{m=1}^{\infty}(a_m \cos m\varphi + b_m \sin m\varphi)\,P_n^{(m)}(\cos\theta).$$

---

(1) Since the equations for both potentials are the same, we shall not write the index for U. The index appears when we satisfy the boundary conditions, which are different for U_1 and U_2.

Here $P_n(\cos\theta)$ is the Legendre polynomial:

$$P_n(\cos\theta)=\frac{1}{2^n}\sum_{k=0}^{\left[\frac{n}{2}\right]}(-1)^k\frac{(2n-2k)!\cos^{n-2k}\theta}{(n-k)!(n-2k)!}. \tag{2.20}$$

The functions $P_n^{(m)}(\cos\theta)$ are related with $P_n(\cos\theta)$ by means of the following formula:

$$P_n^{(m)}(\cos\theta)=(\sin\theta)^m\frac{d^m P_n(\cos\theta)}{d\cos\theta^m}. \tag{2.21}$$

We may make the following substitution in equation (2.18)

$$f_n(r)=\frac{R_n(kr)}{\sqrt{kr}}.$$

We now obtain the following equation ($x = kr$) for $R_n(x)$:

$$\frac{d^2R_n(x)}{dx^2}+\frac{1}{x}\frac{dR_n(x)}{dx}+\left[1-\frac{\left(n+\frac{1}{2}\right)^2}{x^2}\right]R_n(x)=0.$$

This is the Bessel equation, and its solution is represented by cylindrical functions with half-integral index:

$$R_n(x)=Z_{n+\frac{1}{2}}(x).$$

[Here we employ $Z_{n+\frac{1}{2}}$ to designate the general solution of the equation for $R_n(x)$]. Thus, the $n^{\underline{th}}$ special solution of equation (2.16) will be:

$$U_n(r,\theta,\varphi)=(kr)^{-\frac{1}{2}}Z_{n+\frac{1}{2}}(kr)Y_n(\theta,\varphi). \tag{2.22}$$

Of all the cylindrical functions, only functions of the first type $J_{n+\frac{1}{2}}$ /45 are finite at zero. Therefore, they are the only ones which may be utilized for the solution within the sphere. Outside of the sphere, in accordance with the radiation principle, the solution must have the nature of a diverging wave.

Since we chose the time factor in the form $e^{+i\omega t}$, only the Hankel function of the second type gives us a wave diverging from the diffraction source ($e^{i(\omega t-kr)}$) [see the asymptotic expressions of cylindrical functions in the case $x > n$ in III, 1]. Consequently, only this function can be employed to compile the solution outside of the sphere. We shall employ the following notation:[1]

$$\left.\begin{aligned}\sqrt{\frac{\pi x}{2}}\,J_{n+\frac{1}{2}}(x)&=\psi_n(x);\\ \sqrt{\frac{\pi x}{2}}\,H^{(2)}_{n+\frac{1}{2}}(x)&=\zeta_n(x).\end{aligned}\right\} \tag{2.23}$$

---

(1) In order to avoid confusion, we should note that in certain cases the same notations ψ_n and ζ_n are introduced for the functions differing from ours by the factor $1/x$ [see (Ref. 30), page 894].

The functions ψ_n and ζ_n are two independent solutions of the following equation

$$\frac{d^2F_n}{dx^2}+\left(1-\frac{n(n+1)}{x^2}\right)F_n=0. \tag{2.24}$$

The special solution (2.22) within the sphere will be of the type $\frac{\psi n(kr)}{kr} Y_n$, and outside of the sphere it will be of the type $\frac{\zeta_n(kr)}{kr} Y_n$.

The total solution must be represented in the form of the superposition of special solutions with indefinite coefficients. These indefinite constants may be computed from the boundary conditions.

The incident wave participates in the boundary conditions (2.8), (2.9) in the outer field, along with the diffracted wave. Therefore, we must first compute the electric and magnetic potentials of the incident wave, which also must be represented in the form of series with respect to $Z_{n+\frac{1}{2}} Y_n$. This may /46 be readily done, if we employ the well known expansion of a plane wave in terms of Legendre polynomials:

$$e^{ik_a r\cos\theta}=\sum_{l=0}^{\infty} i^l(2l+1)\frac{\psi_l(k_a r)}{k_a r}P_l(\cos\theta). \tag{2.25}$$

The exciting field is a plane wave, polarized along the X-axis and moving along the Z-axis in the region of negative Z. In accordance with the Cartesian components of its fields (2.1), the spherical field components will be

$$\left.\begin{aligned}
E_r^0&=e^{ik_a r\cos\theta}\cos\varphi\cdot\sin\theta;\\
E_\theta^0&=e^{ik_a r\cos\theta}\cos\varphi\cdot\cos\theta;\\
E_\varphi^0&=-e^{ik_a r\cos\theta}\sin\varphi;\\
H_r^0&=-m_a e^{ik_a r\cos\theta}\sin\varphi\cdot\sin\theta;\\
H_\theta^0&=-m_a e^{ik_a r\cos\theta}\sin\varphi\cos\theta;\\
H_\varphi^0&=-m_a e^{ik_a r\cos\theta}\cos\varphi.
\end{aligned}\right\} \tag{2.26}$$

Differentiating the right and left hand sides of equation (2.25) with respect to θ and multiplying by $\frac{\cos\phi}{ik_a r}$ and $\frac{\sin\phi}{ik_a r} m_a$, we readily obtain

$$\left.\begin{aligned}
E_r^0&=\sum_{l=1}^{\infty} i^{l-1}(2l+1)\frac{\psi_l(k_a r)}{(k_a r)^2}P_l^{(1)}(\cos\theta)\cos\varphi;\\
H_r^0&=\sum_{l=1}^{\infty} i^{l+1}(2l+1)\frac{\psi_l(k_a r)}{(k_a r)^2}P_l^{(1)}(\cos\theta)\sin\varphi.
\end{aligned}\right\} \tag{2.27}$$

The zero terms in the sums vanish, since $\frac{dP_0}{d\theta}=0$. Comparing the formulas for E_r^0 and H_r^0 with the formulas (2.15) which determine the fields in terms of the potentials corresponding to them, we readily find that the electric and magnetic

potentials in the incident wave will be

$$\left.\begin{aligned} U_1^0 &= \frac{1}{k_a^2 r}\sum_{l=1}^{\infty} i^{l-1}\frac{(2l+1)}{l(l+1)}\psi_l(k_a r)P_l^{(1)}(\cos\theta)\cos\varphi; \\ U_2^0 &= \frac{-m_a}{k_a^2 r}\sum_{l=1}^{\infty} i^{l-1}\frac{(2l+1)}{l(l+1)}\psi_l(k_a r)P_l^{(1)}(\cos\theta)\sin\varphi. \end{aligned}\right\} \tag{2.28}$$

In accordance with (2.17), the following relationships must hold on the surface/47 of the sphere:

$$\left.\begin{aligned} m_a^2\{r(U_1^0+U_1^a)\}_{r=a} &= m_i^2\{rU_1^i\}_{r=a}, \\ \frac{\partial}{\partial r}\{r(U_1^0+U_1^a)\}_{r=a} &= \frac{\partial}{\partial r}\{rU_1^i\}_{r=a}; \end{aligned}\right\} \tag{2.29}$$

$$\left.\begin{aligned} \{r(U_2^0+U_2^a)\}_{r=a} &= \{rU_2^i\}_{r=a}, \\ \frac{\partial}{\partial r}\{r(U_2^0+U_2^a)\}_{r=a} &= \frac{\partial}{\partial r}\{rU_2^i\}_{r=a}. \end{aligned}\right\} \tag{2.30}$$

Here U^a is the potential of the diffracted field, and U^i is the potential of the internal field.[1] In view of the fact that these linear relationships must hold at every point of the sphere, the potentials U^a and U^i can have only the same angular dependence as the potentials of incident radiation. Thus, only the following spherical functions are included in our solution:

$Y_l(\theta, \varphi) = P_l^{(1)}(\cos\theta)\cos\varphi$ – for the electric potential,

$Y_l(\theta, \varphi) = P_l^{(1)}(\cos\theta)\sin\varphi$ – for the magnetic potential.

With allowance for this factor, the general expressions for the potentials U_1^a, U_2^a, U_1^i, U_2^i may be written as follows, by analogy with the potentials of incident radiation:

$$\left.\begin{aligned} U_1^a &= \frac{1}{k_a^2 r}\sum_{l=1}^{\infty} C_l\zeta_l(k_a r)P_l^{(1)}(\cos\theta)\cos\varphi, \\ U_2^a &= -\frac{m_a}{k_a^2 r}\sum_{l=1}^{\infty} B_l\zeta_l(k_a r)P_l^{(1)}(\cos\theta)\sin\varphi; \end{aligned}\right\} \tag{2.31}$$

$$\left.\begin{aligned} U_1^i &= \frac{1}{k_i^2 r}\sum_{l=1}^{\infty} C_l^*\psi_l(k_i r)P_l^{(1)}(\cos\theta)\cos\varphi, \\ U_2^i &= \frac{-m_i}{k_i^2 r}\sum_{l=1}^{\infty} B_l^*\psi_l(k_i r)P_l^{(1)}(\cos\theta)\sin\varphi. \end{aligned}\right\} \tag{2.32}$$

We should recall that both spherical functions satisfy the equation (2.19)/48 [$\lambda = \ell(\ell + 1)$]. It thus follows that $P_\ell^{(1)}(\cos\theta)$ satisfies the following equation

---

(1) We shall designate the diffracted fields by the index a. We shall omit this index in subsequent chapters.

$$\frac{d}{d\theta}\left(\sin\theta\,\frac{dP_l^{(1)}}{d\theta}\right)-\frac{P_l^{(1)}}{\sin\theta}+l(l+1)\sin\theta P_l^{(1)}=0. \tag{2.33}$$

The coefficients C_ℓ, B_ℓ, C_ℓ^*, B_ℓ^* must be determined so that the conditions (2.29)-(2.30) hold. These conditions produce (with respect to the pairs of coefficients C_ℓ, C_ℓ^* and B_ℓ, B_ℓ^* with the given index ℓ) two independent systems of two linear equations each. We may write them, by introducing the following notation:

$$\frac{2\pi a}{\lambda}=k_0a=\rho_0;\quad \frac{2\pi a}{\lambda}m_a=\rho_0\cdot m_a=k_a\cdot a=\rho. \tag{2.34}$$

where $\frac{m_i}{m_a}=\frac{k_i}{k_a}=m$ is the relative (complex) refractive index.

For C_ℓ and C_ℓ^*, we have:

$$\left.\begin{aligned}\zeta_l(\rho)C_l-\psi_l(m\rho)C_l^*&=i^{l+1}\frac{2l+1}{l(l+1)}\psi_l(\rho),\\ m\zeta_l'(\rho)C_l-\psi_l'(m\rho)C_l^*&=i^{l+1}\frac{2l+1}{l(l+1)}m\psi_l'(\rho).\end{aligned}\right\} \tag{2.35}$$

A similar system is obtained for B_ℓ and B_ℓ^*:

$$\left.\begin{aligned}m\zeta_l(\rho)B_l-\psi_l(m\rho)B_l^*&=i^{l+1}\frac{2l+1}{l(l+1)}m\psi_l(\rho),\\ \zeta_l'(\rho)B_l-\psi_l'(m\rho)B_l^*&=i^{l+1}\frac{2l+1}{l(l+1)}\psi_l'(\rho).\end{aligned}\right\} \tag{2.36}$$

The systems (2.35) and (2.36) definitely determine the coefficients in the potentials, within an accuracy of all numerical factors. Solving them with respect to C_ℓ and B_ℓ, we obtain

$$\left.\begin{aligned}C_l&=i^{l+1}\frac{2l+1}{l(l+1)}\frac{\psi_l(\rho)\psi_l'(m\rho)-m\psi_l'(\rho)\psi_l(m\rho)}{\zeta_l(\rho)\psi_l'(m\rho)-m\zeta_l'(\rho)\psi_l(m\rho)},\\ B_l&=i^{l+1}\frac{2l+1}{l(l+1)}\frac{\psi_l'(\rho)\psi_l(m\rho)-m\psi_l(\rho)\psi_l'(m\rho)}{\zeta_l'(\rho)\psi_l(m\rho)-m\zeta_l(\rho)\psi_l'(m\rho)}.\end{aligned}\right\} \tag{2.37}$$

Similar expressions are obtained for C_ℓ^* and B_ℓ^*, which we shall not write down due to lack of space.

Substituting these expressions in (2.31) and (2.32), we obtain a unique solution of the equations for the potentials satisfying all of the boundary conditions. /49

§ 3. Diffracted Fields and Intensities

In accordance with (2.15), we may obtain the expressions for the components of both the internal and diffracted fields from the potentials. Since we shall be interested in a diffracted field, we shall only write its components here. Thus, we may introduce the factor E_0 omitted previously.

$$E_r^a=\frac{E_0}{k_a^2r^2}\sum_{l=1}^{\infty}C_l l(l+1)\zeta_l(k_ar)P_l^{(1)}(\cos\theta)\cos\varphi, \tag{2.38}$$

$$
\left.
\begin{aligned}
E_\theta^a &= -\frac{\cos\varphi E_0}{k_a r}\sum_{l=1}^{\infty}\left\{C_l\zeta_l'(k_a r)P_l^{(1)\prime}(\cos\theta)\sin\theta - \right.\\
&\quad \left. - iB_l\zeta_l(k_a r)\frac{P_l^{(1)}(\cos\theta)}{\sin\theta}\right\},\\
E_\varphi^a &= -\frac{\sin\varphi E_0}{k_a r}\sum_{l=1}^{\infty}\left\{C_l\zeta_l'(k_a r)\frac{P_l^{(1)}(\cos\theta)}{\sin\theta} - \right.\\
&\quad \left. - iB_l\zeta_l(k_a r)P_l^{(1)\prime}(\cos\theta)\sin\theta\right\},\\
H_r^a &= \frac{-E_0}{k_0 k_a r^2}\sum_{l=1}^{\infty}B_l l(l+1)\zeta_l(k_a r)P_l^{(1)}(\cos\theta)\sin\varphi,\\
H_\theta^a &= -\frac{l\sin\varphi E_0}{k_0 r}\sum_{l=1}^{\infty}\left\{C_l\zeta_l(k_a r)\frac{P_l^{(1)}(\cos\theta)}{\sin\theta} + \right.\\
&\quad \left. + iB_l\zeta_l'(k_a r)P_l^{(1)\prime}(\cos\theta)\sin\theta\right\},\\
H_\varphi^a &= \frac{l\cos\varphi E_0}{k_0 r}\sum_{l=1}^{\infty}\left\{C_l\zeta_l(k_a r)P_l^{(1)\prime}(\cos\theta)\sin\theta + \right.\\
&\quad \left. + iB_l\zeta_l'(k_a r)\frac{P_l^{(1)}(\cos\theta)}{\sin\theta}\right\}.
\end{aligned}
\right\} \tag{2.38}
$$

The primes designate the derivatives with respect to the argument indicated under the index of the function ($k_a r$ and $\cos\theta$). At a sufficiently large distance from the particle, in the so-called wave zone, we may disregard the components E_r and H_r as compared with the θ and ϕ components. The diffracted field will be a transverse wave which is propagated from the diffraction source. /50

Let us introduce the following notation:

$$c_l = i^l C_l, \quad b_l = -i^l B_l; \tag{2.39}$$

$$Q_l(\theta) = \frac{P_l^{(1)}(\cos\theta)}{\sin\theta}, \quad S_l(\theta) = -P_l^{(1)\prime}(\cos\theta)\sin\theta. \tag{2.40}$$

Employing asymptotic expressions for the functions $\zeta_\ell(k_a r)$ ($k_a r \gg \ell$: see III, 1), we readily obtain

$$
\left.
\begin{aligned}
E_\varphi^a &= -\frac{\sin\varphi E_0}{k_a}\cdot\frac{e^{-ik_a r}}{r}\sum_{l=1}^{\infty}(c_l Q_l + b_l S_l),\\
E_\theta^a &= \frac{\cos\varphi E_0}{k_a}\cdot\frac{e^{-ik_a r}}{r}\sum_{l=1}^{\infty}(c_l S_l + b_l Q_l),\\
H_\varphi^a &= \frac{\cos\varphi E_0}{k_0}\cdot\frac{e^{-ik_a r}}{r}\sum_{l=1}^{\infty}(c_l S_l + b_l Q_l),\\
H_\theta^a &= \frac{\sin\varphi E_0}{k_0}\cdot\frac{e^{-ik_a r}}{r}\sum_{l=1}^{\infty}(c_l Q_l + b_l S_l).
\end{aligned}
\right\} \tag{2.41}
$$

According to these formulas, the diffracted field may be represented in the form of sums of individual partial waves. The excitation intensity of the ℓth partial wave may be determined by the numbers c_ℓ and b_ℓ, which depend essentially on ρ and m.

For small ρ (see Chapter IV), only the coefficients c_ℓ and b_ℓ with small numbers are of significant importance. The field related with the coefficient c_1 corresponds to the so-called Rayleigh scattering.

We shall show later on that the excitation intensity of subsequent partial waves increases when the particle dimensions increase. All the farther removed partial electric and magnetic waves begin to come into play, and the intensity /51 of waves with small numbers oscillates. With an increase in ℓ, the oscillation amplitude decreases approximately as $1/\ell$. For large particles, the number of partial waves which must be taken into account is of the order ρ (III, 1). The excitation intensity of subsequent waves rapidly decreases, so that the number ρ determines the order of the number at which we can truncate our infinite series. The latter fact makes it possible to estimate the distances r at which we may employ formula (2.41) instead of the general formulas (2.38). Since the asymptotic representations which we have employed are valid in the case $x \gg \ell$ (III, 1), this means that we can employ formulas (2.41) in the case $r \gg a$, since $\ell \sim \rho$. In the problems in which we are interested, this condition always holds.

The following is readily apparent from the formulas (2.41) for electric and magnetic fields in a scattered wave:

$$\frac{1}{m_a} H_\varphi^a = E_\theta^a; \quad \frac{1}{m_a} H_\theta^a = -E_\varphi^a.$$

These equations hold not only for complete fields, but also for fields of individual partial oscillation, just as for its electric and magnetic portion. We find from the subsequent equations that both for magnetic and electric portions of individual partial oscillations, the following formula holds

$$E_\varphi^a H_\varphi^a + E_\theta^a H_\theta^a = 0.$$

This designates the mutually perpendicular nature of the electric and magnetic fields for the electric and magnetic portion of each partial wave. It is apparent that complete fields have the same property.

The sums included in the formulas for E_θ^a and E_ϕ^a (just as for H_θ and H_ϕ) are complex expressions which, generally speaking, have different phases in the given direction (θ, ϕ). This means that scattered light will be polarized elliptically (incident light which is linearly polarized), and this polarization will be different in different directions. If, on the other hand, we confine ourselves to examining only Rayleigh scattering, elliptical polarization vanishes (see IV, 1). The first electric partial wave is polarized linearly. The linear polarization will occur in the directions $\phi = 0$ and $\phi = \frac{\pi}{2}$ in the /52 general case. This important conclusion from the Mie theory has been repeatedly substantiated in experiments on colloid solutions. The essential amount of scattered light is polarized, in general, as is predicted by theory. In several

cases, however, there is a large portion of unpolarized light. This cannot be regarded as representing an error in the theory. It simply means that under the conditions of the corresponding experiment those assumptions which underlie our discussions do not hold. Most frequently, this means that colloid particles cannot be regarded as spheres [see, for example, the experiments of Steibing (Ref. 41) on colloid solutions of gold]. Sometimes this may be caused by a high concentration of particles, so that there is a large portion of multiply scattered light in the scattered bundle. In this case, the conclusion derived from the theory presented above is not valid.

Let us now calculate the intensities in scattered light.

We obtain the following from (1.7) on the basis of formulas (2.1) for the fields E^0 and H^0 for the intensity of incident radiation I_0, when there is no absorption:

$$I_0 = \frac{c m_a E_0^2}{8\pi}. \tag{2.42}$$

We obtain ($E_\theta = H_\phi = 0$) for the intensity ϕ of the component of scattered light, i.e., for the intensity of that portion of scattered light which passes through the polarizer with the axis parallel to the curvilinear axis of ϕ, on the basis of (1.7) and (2.41):

$$I_\varphi = I_0 \frac{\sin^2\varphi}{k_a^2 r^2} \left| \sum_{l=1}^{\infty} (c_l Q_l + b_l S_l) \right|^2. \tag{2.43}$$

Similarly, we have the following for the θ-component of ($E_\phi = H_\theta = 0$) from (1.7) and (2.41):

$$I_\theta = I_0 \frac{\cos^2\varphi}{k_a^2 r^2} \left| \sum_{l=1}^{\infty} (c_l S_l + b_l Q_l) \right|^2. \tag{2.44}$$

The formulas (2.43) and (2.44) are very important. They give the intensity of scattered light for the case when the incident bundle is polarized linearly. We should recall that ϕ is the angle between the direction of the electric vector in the incident wave and the projection of the scattering direction on the plane which is perpendicular to the direction in which the incident wave is propagated. /53

We customarily deal with nonpolarized light, in which the direction of the electric vector continuously rotates in space. Consequently, the formulas for the quantities I_ϕ and I_θ may be obtained in this case by averaging the formulas indicated above over the angle ϕ. Since $\overline{\cos^2\phi} = \overline{\sin^2\phi} = \frac{1}{2}$, for natural light, we have

$$\left.\begin{aligned} I_\varphi &= \frac{I_0}{2k_a^2 r^2} \left| \sum\nolimits_\varphi \right|^2 = \frac{I_0}{2k_a^2 r^2} i_1 = \frac{I_0}{2} \frac{a^2}{r^2} \cdot \frac{i_1}{\rho^2}, \\ I_\theta &= \frac{I_0}{2k_a^2 r^2} \left| \sum\nolimits_\theta \right|^2 = \frac{I_0}{2k_a^2 r^2} i_2 = \frac{I_0}{2} \frac{a^2}{r^2} \cdot \frac{i_2}{\rho^2}. \end{aligned}\right\} \tag{2.45}$$

For purposes of brevity, we shall designate the sum contained in I_ϕ by means of Σ_ϕ, and shall designate the sum in I_θ by Σ_θ. We shall designate the squares of the moduli of these sums by i_1 and i_2. Many studies have been devoted to calculating the intensities I_ϕ and I_θ (we shall also designate them by I_1 and I_2 or by I_s and I_p) for different specific cases. The authors usually did not start with the formulas given here, but with the formulas which may be extracted directly from the study of Mie. The formulas thus obtained give values which are twice as large. We shall discuss this problem below.

§ 4. Coefficients of Scattering and Attenuation

The scattering process consists of two, essentially different portions: the initial, non-stationary portion of the process, and the stationary portion. We are only interested in the second portion. In the stationary process, the algebraic value of the energy flux through any closed surface must equal zero, if there are no sources or discharges of the electromagnetic field within the surface. The efficiency of the sources must be determined when the latter are present. Our absorbing particle represents a discharge for the electromagnetic field. Therefore, when taken with an inverse index, the complete energy flux per unit of time through a large sphere, whose center coincides with the /54 center of our particle (radius of the sphere $r \gg \lambda$), must equal the amount of energy absorbed by the particle per unit of time. We shall designate this quantity, referred to intensity of the incident flux, by k_a, and shall call it the absorption coefficient of the particle. It has the dimensionality of area, and is sometimes called the effective diameter for absorption. We may determine the scattering coefficient k_s in a similar way. This is the total flux of electromagnetic energy scattered by a particle in all directions, also referred to a unit of incident flux intensity. The total flux attenuation, resulting from the particle penetrating it, will be comprised of the scattering and the absorption. We thus have the following for the attenuation coefficient k:

$$k = k_a + k_s \tag{2.46}$$

The field outside of the particle (**E**, **H**) is a superposition of the incident field ($\mathbf{E}^0$, $\mathbf{H}^0$) and the diffracted field ($\mathbf{E}^a$, $\mathbf{H}^a$):

$$\mathbf{E} = \mathbf{E}^0 + \mathbf{E}^a; \quad \mathbf{H} = \mathbf{H}^0 + \mathbf{H}^a. \tag{2.47}$$

The mean vector of the energy flux Π is determined by the formula (1.7). In view of (2.47), it may be represented in the following form

$$\mathbf{\Pi} = \mathbf{\Pi}^0 + \mathbf{\Pi}^a + \mathbf{\Pi}',$$

where Π^0 is the flux of the incident field; Π^a --diffracted field; and Π' -- the flux produced by interference of incident and scattered radiation. The total flux, directed outwards through the large sphere, will be the integral of the radial component Π with respect to the sphere. In accordance with the statements presented previously regarding the coefficients of absorption and scattering, we have

$$I_0 k_a = -\int \Pi_r r^2 \, d\Omega; \quad I_0 k_p = \int \Pi_r^0 r^2 \, d\Omega. \tag{2.48}$$

Here I_0 is the intensity of incident radiation; $d\Omega$ -- element of the solid angle $d\Omega = \sin\theta \, d\theta \, d\phi$, a $r^2 d\Omega$ -- element of cross section on the sphere. All of the integrals are taken over the sphere.

The flux of incident radiation is constant with respect to direction. Therefore, its integral over the sphere equals zero:

$$\int \Pi_r^0 r^2 \, d\Omega = 0.$$

For k_s and $k = k_s + k_a$, we thus obtain /55

$$k_s = \frac{1}{I_0} \mathrm{Re} \int \frac{c}{8\pi} [\mathbf{E}^a, \mathbf{H}^{a*}]_r r^2 \, d\Omega, \tag{2.49}$$

$$-k = \frac{1}{I_0} \mathrm{Re} \int \frac{c}{8\pi} \{ [\mathbf{E}^0, \mathbf{H}^{a*}]_r + [\mathbf{E}^a, \mathbf{H}^{0*}]_r \} r^2 \, d\Omega. \tag{2.50}$$

Let us investigate the integral for k_s. We have:

$$[\mathbf{E}^a, \mathbf{H}^{a*}]_r = E_\theta^a H_\varphi^{a*} - E_\varphi^a H_\theta^{a*}.$$

Substituting the expressions for the fields (2.41), performing integration over ϕ, and grouping the terms in an appropriate way, we obtain the double sum of the following three types of expressions:

$$\text{a)} \ (c_l b_m^* + b_l c_m^*) \int_0^\pi \left(\frac{dP_l^{(1)}}{d\theta} \frac{P_m^{(1)}}{\sin\theta} + \frac{dP_m^{(1)}}{d\theta} \frac{P_l^{(1)}}{\sin\theta} \right) \cdot \sin\theta \, d\theta;$$

$$\text{b)} \ (c_l c_m^* + b_l b_m^*) \times$$

$$\times \int_0^\pi \left(\frac{dP_l^{(1)}(\cos\theta)}{d\theta} \frac{dP_m^{(1)}(\cos\theta)}{d\theta} + \frac{P_l^{(1)}}{\sin\theta} \frac{P_m^{(1)}}{\sin\theta} \right) \sin\theta \, d\theta.$$

The sums will have a common factor

$$\frac{1}{I_0} \frac{cE_0^2}{8m_a k_0^2} = \frac{\pi}{k_a^2}.$$

Both integrals may be readily calculated. Integral (a) equals zero, since its integrand is $d(P_\ell^{(1)} P_m^{(1)})$, and the function $P_\ell^{(1)} P_m^{(1)}$ equals zero in the case $\theta = 0, \pi$. In the integral (b) we may transform the first component integrating it by parts:

$$\int_0^\pi \frac{dP_l^{(1)}}{d\theta} \frac{dP_m^{(1)}}{d\theta} \sin\theta \, d\theta =$$

$$= \sin\theta \frac{dP_l^{(1)}}{d\theta} P_m^{(1)} \Big|_0^\pi - \int_0 \frac{d}{d\theta} \left(\sin\theta \frac{dP_l^{(1)}}{d\theta} \right) P_m^{(1)} \, d\theta.$$

The term outside of the integral equals zero. By means of equation /56
(2.33) for conjugate Legendre polynomials, the latter integral may be rewritten as follows:

$$\int_0^\pi \left\{ l(l+1)\sin\theta P_l^{(1)} - \frac{P_l^{(1)}}{\sin\theta} \right\} \frac{P_m^{(1)}}{\sin\theta} \sin\theta \, d\theta.$$

Substituting the expression obtained in the integral (b), it may be readily seen that it is now reduced to the integral over the sphere of the product of two different spherical functions.

Based on the theorem regarding orthogonality of these functions [see (Ref. 40)], we find that the integral (b) equals zero in the case $\ell \neq m$ and $\frac{2\ell^2(\ell+1)^2}{2\ell+1}$ in the case $\ell = m$.

Thus, our double sum with respect to m and ℓ degenerates into an ordinary sum with respect to ℓ.

If we take into account the common factor indicated above, which is located in front of the sum, we finally obtain

$$k_S = \frac{2\pi}{k_a^2} \sum_{l=1}^{\infty} \frac{l^2(l+1)^2}{2l+1} (|c_l|^2 + |b_l|^2). \tag{2.51}$$

Let us now calculate the attentuation coefficient. In accordance with (2.50), we have:

$$-k = \frac{1}{I_0} \operatorname{Re} \int \frac{c}{8\pi} \{E_\theta^0 H_\varphi^{a*} - E_\varphi^0 H_\theta^{a*} + E_\theta^a H_\varphi^{0*} - E_\varphi^a H_\theta^{0*}\} \, r^2 \, d\Omega.$$

In order to calculate this integral, we must have the expressions E_ϕ^0, E_θ^0, H_ϕ^0, H_θ^0 expanded in the same series as the diffracted fields. By means of the potentials U_1^0 and U_2^0 of the plane wave and formulas (2.15), we obtain the following (we introduce E_0, which was omitted previously, into the formulas):

$$E_\theta^0 = \cos\varphi \sum_{l=1}^{\infty} q_l (\psi_l' S_l + i\psi_l Q_l),$$

$$E_\varphi^0 = -\sin\varphi \sum_{l=1}^{\infty} q_l (\psi_l' Q_l + i\psi_l S_l),$$

$$H_\theta^0 = -im_a \sin\varphi \sum_{l=1}^{\infty} q_l (\psi_l Q_l - i\psi_l' S_l),$$

$$H_\varphi^0 = -im_a \cos\varphi \sum_{l=1}^{\infty} q_l (\psi_l S_l - i\psi_l' Q_l).$$

For purposes of brevity, the following notation is introduced here: /57

$$q_l = i^{l-1} \frac{2l+1}{l(l+1)} \cdot \frac{E_0}{k_a r}.$$

Employing the formulas for the fields and the integrals indicated above of the angular functions we readily obtain

$$\int (E_\theta^0 H_\varphi^{a*} - E_\varphi^0 H_\theta^{a*}) \, r^2 \, d\Omega =$$

$$= \frac{2\pi E_0^2 e^{ik_a r}}{k_a k_0} \sum_{l=1}^{\infty} l(l+1) i^{l-1} (c_l^* \psi_l' + ib_l^* \psi_l).$$

$$\int (E_\theta^a H_\varphi^{0*} - E_\varphi^a H_\theta^{0*})\, r^2\, d\Omega =$$
$$= \frac{2\pi E_0^2 e^{-ik_a r}}{k_a k_0} \sum_{l=1}^{\infty} l(l+1)\, i^{-(l+1)} (i c_l \psi_l - b_l \psi_l').$$

Replacing the functions ψ_ℓ and ψ'_ℓ by their asymptotic expressions (see III, 1)

$$\psi_l(x) = \frac{1}{2i}\left\{e^{i\left(x - l\frac{\pi}{2}\right)} - e^{-i\left(x - l\frac{\pi}{2}\right)}\right\};$$
$$\psi_l'(x) = \frac{1}{2}\left\{e^{i\left(x - l\frac{\pi}{2}\right)} + e^{-i\left(x - l\frac{\pi}{2}\right)}\right\}$$

and recalling the formula for I_0, we obtain

$$-k = \frac{2\pi}{k_a^2} \operatorname{Re} \sum_{l=1}^{\infty} \frac{l(l+1)}{2} \{e^{ik_a r} i^{l-1} [c_l^* (e^{ik_a r} i^{-l} + e^{-ik_a r} i^l) +$$
$$+ b_l^* (e^{ik_a r} i^{-l} - e^{-ik_a r} i^l)] + e^{-ik_a r} i^{-l+1} [c_l (e^{ik_a r} i^{-l} -$$
$$- e^{-ik_a r} i^l) - b_l (e^{ik_a r} i^{-l} + e^{-ik_a r} i^l)]\}.$$

Let us now introduce two sets of complex numbers into the discussion:

$$z_{1,l} = i(-1)^l (c_l - b_l);$$
$$z_{2,l} = i e^{-2ik_a r} (c_l - b_l).$$

It may be readily seen that the expression in the parentheses is /58

$$z_{2,l}^* + z_{1,l}^* + z_{1,l} - z_{2,l} = 2 \operatorname{Re} z_{1,l} - 2i \operatorname{Im} z_{2,l}.$$

When this expression is substituted in the formula for (-k), the term with $z_{2,\ell}$ drops out, since it is an imaginary number.

Thus, we obtain the following for -k:

$$-k = \frac{2\pi}{k_a^2} \operatorname{Re} \sum_{l=1}^{\infty} ll(l+1)(-1)^l (c_l - b_l),$$

or

$$k = \frac{2\pi}{k_a^2} \operatorname{Im} \sum_{l=1}^{\infty} l(l+1)(-1)^l (c_l - b_l). \qquad (2.52)$$

CHAPTER III /59

PARTIAL WAVES

In accordance with the fundamental formulas (2.41), the calculation of diffracted fields may be reduced to summation of the fields of partial waves. The purpose of this chapter is to indicate the formulas which are necessary for practical computations of partial waves and intensities. These formulas represent a compulsory intermediate link between the general relationships of

Chapter II and different specific formulas, which we derived and analyzed in Chapters IV - VII.

In addition, this chapter will also be devoted to different systems for writing the fundamental formulas, and we shall point out one general error which is usually permissible in formulas for intensities.

§ 1. Amplitudes of Partial Waves

We shall call the coefficients c_ℓ and b_ℓ amplitudes of partial waves. These coefficients may be determined by means of cylindrical functions with half-integer indices. We shall present some properties of these functions again, which we feel will be necessary at a later point.

Along with the functions ψ_ℓ and ζ_ℓ introduced previously, we would also like to point out two other functions $\chi_\ell(z)$ and $\eta_\ell(z)$. All of these functions may be determined by the following equations

$$\left.\begin{aligned}
&\psi_l(z)=\sqrt{\frac{\pi z}{2}}\,J_{l+\frac{1}{2}}(z),\\
&\chi_l(z)=(-1)^l\sqrt{\frac{\pi z}{2}}\,J_{-\left(l+\frac{1}{2}\right)}(z)=\\
&\qquad\qquad=-\sqrt{\frac{\pi z}{2}}\,Y_{l+\frac{1}{2}}(z),\\
&\zeta_l(z)=\sqrt{\frac{\pi z}{2}}\,H^{(2)}_{l+\frac{1}{2}}(z);\quad \eta_l(z)=\sqrt{\frac{\pi z}{2}}\,H^{(1)}_{l+\frac{1}{2}}(z).
\end{aligned}\right\}\tag{3.1}$$

The following relationships hold between these four functions: /60

$$\left.\begin{aligned}
&\zeta_l(z)=\psi_l(z)+i\chi_l(z);\quad \psi_l(z)=\frac{1}{2}\left[\zeta_l(z)+\eta_l(z)\right];\\
&\eta_l(z)=\psi_l(z)-i\chi_l(z);\quad \chi_l(z)=\frac{1}{2i}\left[\zeta_l(z)-\eta_l(z)\right].
\end{aligned}\right\}\tag{3.2}$$

We should also note that the Wronskian of the functions ψ_ℓ and ζ_ℓ equals i, i.e., the following formula holds:

$$\zeta_l\psi_l'-\zeta_l'\psi_l=i\tag{3.3}$$

for any ℓ. The first three functions ψ_ℓ, χ_ℓ and ζ_ℓ, and also the general expression of these functions, are as follows:

$$\left.\begin{aligned}
&\psi_0(z)=\sin z;\quad \psi_1(z)=\frac{\sin z}{z}-\cos z,\\
&\psi_2(z)=\left(\frac{3}{z^2}-1\right)\sin z-\frac{3}{z}\cos z,\\
&\psi_l(z)=\sum_{r=0}^{l}\sin\left(z-\frac{(l-r)\pi}{2}\right)\frac{(l+r)!}{(l-r)!\,r!\,2^r z^r}.
\end{aligned}\right\}\tag{3.4}$$

$$\left.\begin{aligned}
&\zeta_0(z)=ie^{-iz};\quad \zeta_1(z)=-e^{-iz}\left(1-\frac{i}{z}\right),\\
&\zeta_2(z)=-ie^{-iz}\left(1-\frac{3i}{z}-\frac{3}{z^2}\right),\\
&\zeta_l(z)=i^{l+1}e^{-iz}\left[1-\frac{i}{2z}\frac{l(l+1)}{1!}-\right.\\
&\left.-\frac{(l-1)}{(2z)^2}\frac{l(l+1)(l+2)}{2!}+\ldots+(-i)^l\frac{(2l)!}{(2z)^l\,l!}\right].
\end{aligned}\right\}\tag{3.5}$$

$$\left.\begin{aligned}
&\chi_0(z)=\cos z,\quad \chi_1(z)=\sin z+\frac{\cos z}{z};\\
&\chi_2(z)=\left(\frac{3}{z^2}-1\right)\cos z+\frac{3}{z}\sin z,\\
&\chi_l(z)=\sum_{r=0}^{l}\cos\left(z-\frac{(l-r)\pi}{2}\right)\frac{(l+r)!}{(l-r)!\,r!\,2^r z^r}.
\end{aligned}\right\}\tag{3.6}$$

The expressions for $\eta_\ell(z)$ may be obtained from the formulas for $\zeta_\ell(z)$ by replacing the sign before i.

All four functions satisfy recursion formulas of the following form: /61

$$\psi_{l+1}(z)=\frac{2l+1}{z}\psi_l(z)-\psi_{l-1}(z).\tag{3.7}$$

This expression must be employed in our problem when calculating cylindrical functions of high orders. The derivatives of all four functions may be expressed in terms of the functions themselves. The following formula holds for all the functions:

$$\psi_l'(z)=\psi_{l-1}(z)-\frac{l}{z}\psi_l(z).\tag{3.8}$$

The function $\psi_\ell(z)$ and also $\psi_\ell'(z)$ may be expanded in power series with respect to z:

$$\left.\begin{aligned}
&\psi_l(z)=\frac{z^{l+1}}{1\cdot3\ldots(2l+1)}\left\{1-\frac{1}{(2l+3)}\frac{z^2}{2}+\right.\\
&+\frac{1}{2!(2l+3)(2l+5)}\left(\frac{z^2}{2}\right)^2+\ldots+\frac{(-1)^k}{k!}\left(\frac{z^2}{2}\right)^k\times\\
&\left.\times\frac{1}{(2l+3)\ldots(2l+2k+1)}+\ldots\right\},\\
&\psi_l'(z)=\frac{(l+1)z^l}{1\cdot3\ldots(2l+1)}\left\{1-\frac{l+3}{l+1}\cdot\frac{1}{(2l+3)}\frac{z^2}{2}+\ldots+\right.\\
&\left.+\frac{(-1)^k(l+2k+1)}{k!\cdot(l+1)}\left(\frac{z^2}{2}\right)^k\frac{1}{(2l+3)\ldots(2l+2k+1)}+\ldots\right\}.
\end{aligned}\right\}\tag{3.9}$$

Although these expressions represent the function and its derivative with respect to the entire plane of the complex variable z, they are only suitable in practice in the case $z \ll \ell$. In this case, we may confine ourselves to only the first term in the sums. We thus obtain:

$$\psi_l(z)=\frac{z^{l+1}}{(2l+1)!!};\quad \psi_l'(z)=\frac{(l+1)z^l}{(2l+1)!!}.\tag{3.10}$$

In a similar way, we have

$$\left.\begin{aligned}\zeta_l(z) &= 1\cdot 3\ldots(2l-1)\frac{l}{z^l}e^{-iz};\\ \zeta_l'(z) &= -1\cdot 3\ldots(2l-1)l\cdot i\frac{e^{-iz}}{z^{l+1}}.\end{aligned}\right\} \tag{3.11}$$

We should also point out the formulas for $\chi_\ell(z)$ and $\chi_\ell'(z)$:

$$\chi_l(z) = \frac{1\cdot 3\ldots(2l-1)}{z^l};\quad \chi_l'(z) = -\frac{1\cdot 3\ldots(2l-1)\cdot l}{z^{l+1}}. \tag{3.12}$$

In the opposite case $z \gg \ell$, the following approximate formulas which are /62 directly obtained from (3.4) - (3.6) hold:

$$\left.\begin{aligned}&\zeta_l(z) = i^{l+1}e^{-iz};\quad \eta_l(z) = (-i)^{l+1}e^{iz},\\ &\psi_l(z) = \sin\left(z-\frac{l\pi}{2}\right);\quad \chi_l(z) = \cos\left(z-\frac{l\pi}{2}\right)\end{aligned}\right\}. \tag{3.13}$$

Let us now turn to the amplitudes of partial waves.

Let us investigate the case of small spheres ($\rho < 1$). We shall also assume that the complex refractive index m is small, so that $|m\rho|$ is also smaller than unity. By means of formulas (3.5) and (3.9), in this case we readily obtain

$$\left.\begin{aligned}c_l &= \frac{(-1)^{l+1}\rho^{2l+1}e^{i\rho}}{l^2[(2l-1)!!]^2}\,\frac{m^2r-q}{m^2p+\frac{l+1}{l}t},\\ b_l &= \frac{(-1)^l\rho^{2l+1}e^{i\rho}}{l^2[(2l-1)!!]^2}\,\frac{r-q}{p+i\frac{l+1}{l}}.\end{aligned}\right\} \tag{3.14}$$

Here r, q, p and t are the following series:

$$\left.\begin{aligned}r &= 1-\frac{\rho^2}{2(2l+3)}\left[m^2+\frac{l+3}{l+1}\right]+\ldots\\ q &= 1-\frac{\rho^2}{2(2l+3)}\left[1+m^2\frac{l+3}{l+1}\right]+\ldots\\ p &= 1+i\rho-\rho^2\left[\frac{1}{l}+\frac{(l-1)(l-2)}{l(2l-1)}+\frac{m^2}{2(2l+3)}\right]+\ldots\\ t &= 1+i\rho-\rho^2\left[\frac{l-1}{2l-1}+m^2\frac{(l+3)}{2(2l+3)(l+1)}\right]+\ldots\end{aligned}\right\} \tag{3.15}$$

For small ρ, replacing $e^{i\rho}$, r, q, p and t by 1, we have

$$c_l = (-1)^{l+1}\frac{\rho^{2l+1}}{l^2[(2l-1)!!]^2}\,\frac{m^2-1}{m^2+\frac{l+1}{l}}. \tag{3.16}$$

When computing b_ℓ, we must take the fact into account that

$$r-q = \frac{\rho^2(m^2-1)}{(2l+3)(l+1)}\left\{1+\rho^2\frac{m^2+1}{2(2l+5)}-\ldots\right\}.$$

We thus obtain

$$b_l = (-1)^l\frac{\rho^{2l+3}}{(l+1)(2l+1)(2l+3)[(2l-1)!!]^2}\cdot(m^2-1). \tag{3.17}$$

In the case of small ρ, c_1 -- the amplitude of the first electric partial /63 oscillation -- plays the main role. The scattering of light caused by this first oscillation was studied by Rayleigh. It is called Rayleigh scattering. We shall discuss this at a later point. We would also like to point out that, in view of the fact that the first two expansion terms $e^{i\rho}$ coincide with the

first two expansion terms p and t, the correction terms to the formulas (3.16) and (3.17) have the order ρ^2.

We shall now indicate the formulas for the amplitudes of partial waves in the case of large particles ($\rho \gg 1$). We shall employ formulas (3.13). Substituting them in c_ℓ and b_ℓ, we obtain the expressions for the amplitudes which are valid in the case $\rho \gg \ell$:

$$
\begin{aligned}
c_l &= i^l \frac{2l+1}{l(l+1)} \times \\
&\times e^{i\rho} \frac{\sin\left(\rho - l\frac{\pi}{2}\right)\cos\left(m\rho - l\frac{\pi}{2}\right) - m\cos\left(\rho - l\frac{\pi}{2}\right)\sin\left(m\rho - l\frac{\pi}{2}\right)}{\cos\left(m\rho - l\frac{\pi}{2}\right) + lm\sin\left(m\rho - l\frac{\pi}{2}\right)}, \\
b_l &= i^l \frac{2l+1}{l(l+1)} \times \\
&\times e^{i\rho} \frac{\cos\left(\rho - l\frac{\pi}{2}\right)\sin\left(m\rho - l\frac{\pi}{2}\right) - m\sin\left(\rho - l\frac{\pi}{2}\right)\cos\left(m\rho - l\frac{\pi}{2}\right)}{l\sin\left(m\rho - l\frac{\pi}{2}\right) + m\cos\left(m\rho - l\frac{\pi}{2}\right)}.
\end{aligned}
\tag{3.18}
$$

It must be noted that the coefficients c_ℓ and b_ℓ oscillate with an increase in ℓ, and their modulus is thus less than $\frac{2(\ell+1)}{\ell(\ell+1)}\left|\frac{m+1}{m-1}\right|$.

For large ℓ, the oscillation amplitude decreases as $1/\ell$. Up to what numbers does this occur? The answer to this question cannot be obtained from formulas (3.18), since they are only valid up to $\ell \ll \rho$. More general formulas for the coefficients can be obtained if we employ the asymptotic formulas of Debye [see (Ref. 33)] for cylindrical functions. These formulas have a different form, depending on which of the following inequalities holds

$$\text{a) } l + \frac{1}{2} < \rho \text{ or (b) } l + \frac{1}{2} > \rho.$$

We should note that, if these inequalities are replaced by strong inequalities, the Debye formulas change into the customary asymptotic formulas. /64

In case (a) we have:

$$
\left.
\begin{aligned}
\zeta_l(\rho) &= \frac{e^{-i\left(\rho f_0 - \frac{\pi}{4}\right)}}{(\sin\tau_0)^{1/2}}; \qquad \psi_l(\rho) = \frac{\cos\left(\rho f_0 - \frac{\pi}{4}\right)}{(\sin\tau_0)^{1/2}}, \\
\zeta_l'(\rho) &= e^{-i\left(\rho f_0 + \frac{\pi}{4}\right)}(\sin\tau_0)^{1/2}; \\
&\qquad \psi_l'(\rho) = \cos\left(\rho f_0 - \frac{\pi}{4}\right)(\sin\tau_0)^{1/2}.
\end{aligned}
\right\}
\tag{3.19}
$$

The following notation is employed here:

$$f_0 = \sin\tau_0 - \tau_0\cos\tau_0; \quad \cos\tau_0 = \frac{l+\frac{1}{2}}{\rho}. \tag{3.20}$$

In view of the fact that $\frac{\ell + \frac{1}{2}}{\rho} < 1$, the latter equation determines τ_0 as a real angle lying between 0 and $\frac{\pi}{2}$.

In the case (b):

$$\left.\begin{aligned} \zeta_\ell(\rho) &= i\frac{e^{-i\rho\tau_0}}{(i\sin\tau_0)^{1/2}}; & \psi_\ell(\rho) &= \frac{1}{2}\frac{e^{i\rho\tau_0}}{(i\sin\tau_0)^{1/2}}, \\ \zeta'_\ell(\rho) &= -ie^{-i\rho\tau_0}(i\sin\tau_0)^{1/2}; & \psi'_\ell(\rho) &= \frac{1}{2}e^{i\rho\tau_0}(i\sin\tau_0)^{1/2}. \end{aligned}\right\} \tag{3.21}$$

Here τ_0 is the negative imaginary root of the equation

$$\cos\tau_0 = \frac{\ell + \frac{1}{2}}{\rho}. \tag{3.22}$$

This means that $\tau_0 = -i\theta$, where $\theta = \operatorname{arch}\left(\frac{\ell + \frac{1}{2}}{\rho}\right) > 0$ (with respect to the positive root of the function arch χ).

The intermediate region, when $(\ell + \frac{1}{2})$ is on the order of ρ, may be omitted/65 in the first approximation[1].

Let us now turn to the formulas for amplitudes. The case of real m is of basic interest, since the case of large transparent spheres entails the greatest difficulty when being studied. In this case (which we are discussing here), both arguments of the cylindrical functions are real.

It is advantageous to divide the entire region in which ℓ changes into the following three groups:

1) $\ell + \frac{1}{2} < \rho < m\rho$,

2) $\rho < \ell + \frac{1}{2} < m\rho$,

3) $\rho < m\rho < \ell + \frac{1}{2}$.

---

(1) In case (b), our formulas for ψ_ℓ and ψ'_ℓ differ from the corresponding Debye formulas by the factor $1/2$. This $1/2$ was omitted erroneously by Debye.

In Chapter VII, we present the asymptotic formulas of V. A. Fok for cylindrical functions. The essential advantage of the Fok formulas consists of the fact that they are valid in the intermediate region ($\ell \sim \rho$), where formulas (3.19) and (3.21) do not apply. In case (b) an asymptotic analysis of the Fok formulas leads to formulas (3.21), and not to those indicated by Debye.

Let us introduce the two angles τ_0 and τ_1 by means of the following equations:

$$\cos\tau_0 = \frac{l+\frac{1}{2}}{\rho}; \quad \cos\tau_1 = \frac{l+\frac{1}{2}}{m\rho}. \tag{3.23}$$

In the first group, both angles are real; in the third group, both angles are imaginary and negative. In the second group, τ_0 is imaginary negative, and τ_1 is real.

We shall also employ the following notation

$$f_0 = \sin\tau_0 - \tau_0\cos\tau_0; \quad f_1 = \sin\tau_1 - \tau_1\cos\tau_1. \tag{3.24}$$

Substituting the Debye expressions for cylindrical functions in the formula for c_ℓ, we obtain the three following formulas for c_ℓ in different regions [the /66
factor $(-1)^\ell i \frac{2\ell+1}{\ell(\ell+1)}$ is omitted temporarily]:

$$1)\quad c_l = \frac{\sin\tau_1\cos\left(\rho f_0 - \frac{\pi}{4}\right)\cos\left(m\rho f_1 + \frac{\pi}{4}\right) -}{e^{-i\left(\rho f_0 - \frac{\pi}{4}\right)}\sin\tau_1\cdot\cos\left(m\rho f_1 + \frac{\pi}{4}\right) -} \longrightarrow$$

$$\longrightarrow \frac{-m\sin\tau_0\cos\left(\rho f_0 + \frac{\pi}{4}\right)\cos\left(m\rho f_1 - \frac{\pi}{4}\right)}{-m\sin\tau_0 e^{-i\left(\rho f_0 + \frac{\pi}{4}\right)}\cos\left(m\rho f_1 - \frac{\pi}{4}\right)};$$

$$2)\quad c_l = -\frac{i}{2}e^{3i\rho f_0}\frac{\sin\tau_1\cos\left(m\rho f_1 + \frac{\pi}{4}\right) -}{\sin\tau_1\cos\left(m\rho f_1 + \frac{\pi}{4}\right) +} \longrightarrow$$

$$\longrightarrow \frac{-im\sin\tau_0\cos\left(m\rho f_1 - \frac{\pi}{4}\right)}{+im\sin\tau_0\cos\left(m\rho f_1 - \frac{\pi}{4}\right)};$$

$$3)\quad c_l = -\frac{i}{2}e^{3i\rho f_0}\frac{\sin\tau_1 - m\sin\tau_0}{\sin\tau_1 + m\sin\tau_0}.$$

Similar expressions are obtained for b_ℓ. In view of the fact that τ_0 and τ_1 and, consequently, f_0 and f_1 are real in the first group, the amplitudes in the first group are finite and are approximately on the order of $\frac{2\ell+1}{\ell(\ell+1)}$. In the second group, we have

$$\cos\tau_0 = \operatorname{ch}\theta; \quad \sin\tau_0 = -i\operatorname{sh}\theta;$$
$$if_0 = -\operatorname{ch}\theta(\theta - \operatorname{th}\theta) = -\eta < 0.$$

Thus, in the second group the amplitudes contain an exponentially decreasing factor $e^{2i\rho f_0} = e^{-\rho\eta}$ and, consequently, they are vanishingly small ($\rho \gg 1$). The situation is the same in the third group. We thus arrive at the following important conclusion: for large ρ the number of terms which must be retained in the sum of Chapter II have the order of magnitude ρ. The terms with $\ell + \frac{1}{2} > \rho$ are negligibly small.

Therefore, in the future in the case of asymptotic calculations we shall only investigate terms included in the first group of numbers.

The formula given above for c_ℓ (and the similar formula for b_ℓ) may be suitably transformed, if we change everywhere from trigonometric functions (containing ρ) to exponential functions. /67

Let us introduce the following notation

$$\varepsilon_2 = \frac{m \sin \tau_0 - \sin \tau_1}{m \sin \tau_0 + \sin \tau_1}; \quad \varepsilon_1 = \frac{\sin \tau_0 - m \sin \tau_1}{\sin \tau_0 + m \sin \tau_1}. \tag{3.25}$$

In this case, we obtain

$$\left.\begin{aligned} c_l &= (-1)^l i \frac{2l+1}{l(l+1)} \times \\ &\quad \times \frac{1}{2}\left\{1 - e^{2i\rho(f_0 - mf_1)} \frac{1 - i\varepsilon_2 e^{2im\rho f_1}}{1 + i\varepsilon_2 e^{-2im\rho f_1}}\right\}; \\ b_l &= -(-1)^l i \frac{2l+1}{l(l+1)} \times \\ &\quad \times \frac{1}{2}\left\{1 - e^{2i\rho(f_0 - mf_1)} \frac{1 - i\varepsilon_1 e^{2im\rho f_1}}{1 + i\varepsilon_1 e^{-2im\rho f_1}}\right\}. \end{aligned}\right\} \tag{3.26}$$

These formulas are quite suitable for amplitudes in the case $\rho \gg 1$.

We shall analyze them at a later point. We would like to point out here that for large ρ the expression within the parentheses is the sum of unity and a rapidly oscillating term.

These formulas acquire a particularly simple form in the case $m \to \infty$ (absolutely reflecting particles). Here $\varepsilon_1 = -1$, $\varepsilon_2 = 1$, and c_ℓ and b_ℓ will be:

$$\left.\begin{aligned} c_l &= (-1)^l i \frac{2l+1}{l(l+1)} \frac{1}{2}\{1 + ie^{2i\rho f_0}\}; \\ b_l &= -(-1)^l i \frac{2l+1}{l(l+1)} \frac{1}{2}\{1 - ie^{2i\rho f_0}\}. \end{aligned}\right\} \tag{3.27}$$

§ 2. Angular Functions. Convergence

The spatial distribution of scattered light is determined by the angular functions $Q_\ell(\theta)$ and $S_\ell(\theta)$. We should recall that these functions are ($x = \cos\theta$):

$$\left.\begin{aligned} Q_l(\theta) &= \frac{P_l^{(1)}(\cos\theta)}{\sin\theta} = \frac{dP_l(x)}{dx}; \\ S_l(\theta) &= -P_l^{(1)\prime}(\cos\theta)\sin\theta = \frac{d}{d\theta} P_l^{(1)}(\cos\theta) = \\ &= -\sqrt{1-x^2}\,\frac{dP_l^{(1)}(x)}{dx}. \end{aligned}\right\} \tag{3.28}$$

We would like to point certain properties of these functions. All of these properties follow directly from the Legendre polynomial properties and the properties of the associated polynomials [see (Ref. 40)]. /68

The first few functions Q_ℓ and S_ℓ will be

$$\left.\begin{aligned} &Q_1=1;\quad Q_2=3x;\\ &Q_3=\frac{15}{2}x^2-\frac{3}{2};\quad Q_4=\frac{35}{2}x^3-\frac{15}{2}x.\end{aligned}\right\} \tag{3.29}$$

$$\left.\begin{aligned} &S_1=x;\quad S_2=6x^2-3;\\ &S_3=\frac{45}{2}x^3-\frac{33}{2}x;\quad S_4=70x^4-\frac{135}{2}x^2+\frac{15}{2}.\end{aligned}\right\} \tag{3.30}$$

When the sign for x is changed, the functions $Q_\ell(x)$ and $S_\ell(x)$ also change signs according to the following formulas

$$Q_l(-x)=(-1)^{l-1}Q_l(x);\quad S_l(-x)=(-1)^l S_l(x). \tag{3.31}$$

The following recursion relationship holds for the function $Q_\ell(x)$:

$$Q_l(x)=\frac{2l-1}{l-1}xQ_{l-1}-\frac{l}{l-1}Q_{l-2}. \tag{3.32}$$

In the computations, it is important that all the functions Q_ℓ are known (for a given angle) for different ℓ from $\ell = 1$ to ℓ of the order ρ.

By means of relationship (3.32), we may successively calculate all the functions $Q_\ell(x)$ with any number ℓ for given x, if the first few functions are known. Functions with small numbers may be computed directly according to formulas (3.29). As for the functions $S_\ell(x)$, they may be expressed in terms of $Q_\ell(x)$. The following formula holds:

$$S_l(x)=\frac{l^2}{2l+1}Q_{l+1}(x)-\frac{(l+1)^2}{2l+1}Q_{l-1}(x). \tag{3.33}$$

According to this formula, after all the requisite Q_ℓ are computed, all S_ℓ may be computed. The angular functions for the angles $\theta = 0$ and $\theta = \frac{\pi}{2}$ assume a particularly simple form.

We may obtain the expression $Q_\ell(1)$ if we recall that the Legendre polynomials represent the solution of the following differential equation: /69

$$(1-x^2)y''-2xy'+l(l+1)y=0.$$

In the case x = 1, we obtain

$$y'=\frac{l(l+1)}{2}y.$$

Since y(1) = 1, for $y' = Q_\ell$ we shall have

$$Q_l(1)=\frac{l(l+1)}{2}.$$

We obtain the following from formula (3.33) for S_ℓ:

$$S_l(1)=\frac{l(l+1)}{2}=Q_l(1). \tag{3.34}$$

The expression for $Q_\ell(0)$ may be readily found from the general expressions for the Legendre polynomials (2.20):

$$Q_{2l}(0)=0; \quad Q_{2l+1}(0)=(-1)^l \frac{(2l+1)!!}{2^l l!}. \tag{3.35}$$

In order to perform the calculations, it is advantageous to keep the fact in mind that

$$Q_{l+1}(0)=-\frac{l+1}{l} Q_{l-1}(0), \tag{3.36}$$

and the first $Q_\ell(0)$ may be computed directly according to (3.29). With respect to $S_\ell(0)$, they may be calculated most simply according to the following formula

$$S_l(0)=-(l+1) Q_{l-1}(0). \tag{3.37}$$

All the functions with odd numbers equal zero.

In the case of large ℓ, for Q_ℓ and S_ℓ we may find the asymptotic formulas, employing the customary asymptotic formulas for Legendre polynomials. However, these formulas are not very suitable, since they lose any meaning in the case $\theta = 0$ or π. An asymptotic formula which is much more suitable for Legendre polynomials was given by V. A. Fok (Ref. 42):

$$P_l(\cos\theta)=\sqrt{\frac{\theta}{\sin\theta}} J_0\left(\left(l+\frac{1}{2}\right)\theta\right) \tag{3.38}$$

(J_0 -- zero Bessel function).

This formula holds for all $0 \leqq \theta \leqq \frac{\pi}{2}$. We may readily obtain the following asymptotic expression from (3.38) for $Q_\ell(\theta)$ and $S_\ell(\theta)$: /70

$$Q_l(\theta)=\left(\frac{\theta}{\sin^3\theta}\right)^{1/2}\left(l+\frac{1}{2}\right) J_1(y). \tag{3.39}$$

Here J_1 is the first Bessel function, and $y = (\ell + \frac{1}{2})\theta$:

$$S_l=\left(l+\frac{1}{2}\right)^2\left(\frac{\theta}{\sin\theta}\right)^{1/2}\left\{J_0(y)-\frac{J_1(y)}{y}\right\}. \tag{3.40}$$

When the Bessel functions are replaced by their asymptotic expressions, we shall have the same expressions which are obtained from the customary asymptotic formulas for Legendre polynomials.

One important fact must be stressed here. In the case of large ℓ (and large y) Q_ℓ has the order $\ell^{1/2}$, and S_ℓ is one order of magnitude higher, i.e., $\ell^{3/2}$. This means that we may disregard Q_ℓ as compared with S_ℓ in the case of asymptotic calculations.

Employing the recursion formulas and rules indicated above, we compiled a table of angular functions Q_ℓ for thirteen angles: θ = 0, 1, 2, 5, 10, and every 10 to 90 for ℓ from 1 to 80. We shall give this table in the appendix. It

considerably facilitates the computation of the scattering index for any particles with $\rho \gtrsim 80$.

A calculation based on the recursion formulas is practically impossible if the "reference system" of values is not first computed based on any formula which is not a recursion formula. For this purpose, we employed formula (3.39). The values of Q_ℓ were computed according to the recursion formula and were compared with the "reference" values. The functions S_ℓ were computed in terms of the Q_ℓ according to formula (3.33).

Formulas (3.31) make it possible to rewrite the fundamental formulas for the fields E_θ and E_ϕ in a more advantageous form. Let us introduce the scattering angle β into the discussion. This angle, which may be read off from the direction in which light is propagated, and not from the direction toward the light source, as θ, is related with θ by the following relationship

$$\beta = 180^\circ - \theta. \tag{3.41}$$

Let us also introduce the amplitudes c_ℓ^* and b_ℓ^* which were determined as follows:

$$\left.\begin{aligned} c_l^* &= i(-1)^{l+1} c_l = \frac{2l+1}{l(l+1)} \frac{\psi_l(\rho)\,\psi_l'(m\rho) - m\psi_l'(\rho)\,\psi_l(m\rho)}{\zeta_l(\rho)\,\psi_l'(m\rho) - m\zeta_l'(\rho)\,\psi_l(m\rho)}; \\ b_l^* &= i(-1)^l b_l = \frac{2l+1}{l(l+1)} \frac{\psi_l'(\rho)\,\psi_l(m\rho) - m\psi_l(\rho)\,\psi_l'(m\rho)}{\zeta_l'(\rho)\,\psi_l(m\rho) - m\zeta_l(\rho)\,\psi_l'(m\rho)}. \end{aligned}\right\} \tag{3.42}$$

We should point out that the change from the angle θ to the angle β /71
indicates a reversal in the unit vector in the spherical coordinate system ($i_\theta = -i_\beta$). In order that there may not be a change in the coordinate system (from right to left), we must also change the direction in which the angle ϕ($i_\phi = -i_{\phi'}$) is measured. This also means a change in the signs in the projections of the fields ($E_\beta = -E_\theta$, $E_{\phi'} = -E_\phi$).

Designating the angular functions of β by an asterisk, we obtain

$$\left.\begin{aligned} E_\beta &= -i\frac{\cos\varphi E_0}{k_a}\frac{e^{-ik_a r}}{r}\sum_{l=1}^{\infty}(c_l^* S_l^* + b_l^* Q_l^*); \\ E_{\varphi'} &= -i\frac{\sin\varphi E_0}{k_a}\frac{e^{-ik_a r}}{r}\sum_{l=1}^{\infty}(c_l^* Q_l^* + b_l^* S_l^*). \end{aligned}\right\} \tag{3.43}$$

The angle β is more suitable than θ, and we shall frequently replace it by θ according to (3.41). As for the angle ϕ'($\phi' = 360 - \phi$), its substitution by ϕ is unimportant. Therefore, we shall usually omit the primes.

We should also recall that $H_{\phi'} = m_a E_\beta$ and $H_\beta = -m_a E_{\phi'}$.

Our solution of (2.38) and (2.41) may be represented in the form of an infinite series in terms of the elementary solution of an oscillatory equation.

Consequently, the important problem of the convergence of these series confronts us. It may be shown that all of our series are absolutely and uniformly convergent. We shall illustrate the absolute convergence of the series.

The convergence of a series of elementary solutions in the case of very slow oscillations ($k = 0$), which provide a solution of the Laplace equation, may be readily shown, if we take the fact into account that these series differ to an insignificant extent from the series for the generating function of the Legendre polynomials [see (Ref. 40), page 612].

The convergence of our series may be determined by estimating the terms in this series which have extremely high numbers. We shall assume that these numbers are much greater than the arguments of all the cylindrical functions contained in the solution, and we shall employ the formulas given in § 1 and 2 to determine these functions.

In analyzing the convergence of the solution, we must start with the fundamental formulas for the fields (or potentials). We cannot employ formulas (2.41), since they were obtained upon the assumption that $k_a r \gg \ell$, whereas we /72 are now dealing with an inverse inequality.

For example, let us investigate θ -- the magnetic field component -- and let us determine the term containing the ℓth partial electric wave in it.

We saw previously that for any θ

$$|Q_l| \leqslant \frac{l(l+1)}{2},$$

and from § 1 we have:

$$|C_l| \leqslant \frac{\rho^{2l+1}}{l(l+1)[(2l-1)!!]^2}\left|\frac{m^2-1}{m^2+1}\right|; \quad |\zeta_l(k_a r)| \leqslant \frac{(2l-1)!!}{(k_a r)^l}.$$

Consequently, it may be stated that the series converges for electric oscillations in H_θ just like a power series of the following type

$$\frac{\alpha^l}{1\cdot 3\ldots(2l+1)},$$

where

$$\alpha = \frac{\rho^2}{k_a r} = \frac{k_a a^2}{r}.$$

The situation is similar in other cases.

§ 3. Two Methods for Writing the Fundamental Formulas

In different studies on light scattering, the authors have frequently employed different methods for writing the fundamental formulas. Since the formulas are quite cumbersome, and contain a large number of intermediate notations, this fact frequently complicates the use of the investigation results. We shall now discuss this problem.

Basically, two systems of notation for the special functions of the problem

are employed: the special notation introduced by Mie, and the customary notation.[1] We have employed the latter.

The angles designating the direction from the center of the particle to the observation point are also selected in a different way. The angles selected for this purpose by Mie are not suitable, since the spherical field components, according to Mie, are not components across and along the plane of vision. In order to make a comparison with experiment, it is usually necessary to know these components exactly. In the coordinate system θ and ϕ which we selected, the requisite field components are obtained directly. /73

For purposes of orientation in literature on the problem, we shall indicate the formulas for transition between both notation methods [for greater detail, see (Ref. 43)].

We shall start with the formulas for θ and ϕ -- the electric field components (in the diffracted wave) obtained by Mie.

At a sufficiently large distance from the particle, these formulas may be written as follows (Ref. 32), formulas (52) and (19):

$$\left.\begin{aligned} E_{\varphi'} &= \frac{\lambda'}{2\pi}\frac{e^{-\frac{i2\pi r}{\lambda'}}}{r}\sum_{\nu=1}^{\infty}\left\{\frac{a_\nu}{\nu(\nu+1)}\frac{1}{\sin\theta'}\frac{\partial P_\nu}{\partial\varphi'}-\frac{p_\nu}{\nu(\nu+1)}\frac{\partial R_\nu}{\partial\theta'}\right\};\\ E_{\theta'} &= \frac{\lambda'}{2\pi}\frac{e^{-\frac{i2\pi r}{\lambda'}}}{r}\sum_{\nu=1}^{\infty}\left\{\frac{a_\nu}{\nu(\nu+1)}\frac{\partial P_\nu}{\partial\theta'}+\frac{p_\nu}{\nu(\nu+1)}\frac{1}{\sin\theta'}\frac{\partial R_\nu}{\partial\varphi'}\right\}.\end{aligned}\right\} \quad (3.44)$$

Thus, in order to avoid confusion when making a comparison with our notation, we have used primes to designate the angles θ and ϕ used by Mie.[2]

The quantities contained in the formulas (3.44) have the following meaning: ν -- number of the partial wave, $\lambda' = \frac{2\pi}{k_a}$ -- wave length of incident light in the external medium.

The coefficients α_ν and p_ν characterize the excitation intensity of the

---

(1) It is sometimes stated that Mie first provided the solution of the problem for any ρ. However, in 1899 the complete solution of the problem was published by Love [he assumed that $\sigma = 0$ (Ref. 31)]. The brevity of the discussion and the lack of physical assumptions in his study are apparently the reasons why this study is comparatively little known. For $m = \infty$, the problem was completely solved in 1893 by Thomson (Ref. 49). This case is significantly simpler than the case examined by Love and Mie.

(2) The formulas which we have written differ from the similar formulas in the study by Mie [formulas (77) on page 409] by the factor (- i). It may be readily seen, however, that formula (77) of Mie is inaccurate by making a comparison with the initial formulas (52).

corresponding partial wave. They may be expressed by means of the special functions $I_\nu(x)$ and $K_\nu(x)$ introduced by Mie (the formulas (53), (54) and (55) /74 of Mie):

$$\left.\begin{aligned} a_\nu &= (2\nu+1)\, i^\nu \frac{mI'_\nu(\rho)\, I_\nu(m\rho) - I'_\nu(m\rho)\, I_\nu(\rho)}{mK'_\nu(-\rho)\, I_\nu(m\rho) - I'_\nu(m\rho)\, K_\nu(-\rho)}; \\ p_\nu &= -(2\nu+1)\, i^\nu \frac{mI_\nu(\rho)\, I'_\nu(m\rho) - I_\nu(m\rho)\, I'_\nu(\rho)}{mK_\nu(-\rho)\, I'_\nu(m\rho) - I_\nu(m\rho)\, K'_\nu(-\rho)}. \end{aligned}\right\} \tag{3.45}$$

We have replaced the notation of Mie for $\frac{2\pi m_a a}{\lambda} = k_a a$ by our notation ρ, $\frac{m_i}{m_a}$ -- by m, and $k_i a$ -- by means of $m\rho$. If we compare the series for the functions $I_\nu(x)$ and $K_\nu(x)$ of Mie [formulas (27) and (29)] with the corresponding expressions for cylindrical functions with a half-integral index (see § 1), we may readily see that

$$\left.\begin{aligned} I_\nu(x) &= \sqrt{\frac{\pi x}{2}}\, J_{\nu+\frac{1}{2}}(x) = \psi_\nu(x); \\ K_\nu(-x) &= \sqrt{\frac{\pi x}{2}}\, (-i)^{\nu+1} H^{(2)}_{\nu+\frac{1}{2}} = (-i)^{\nu+1} \zeta_\nu(x). \end{aligned}\right\} \tag{3.45*}$$

Substituting relationships (3.45*) in the formulas for a_ν and p_ν, and comparing the expressions thus obtained with the formulas for c_ν and b_ν, we readily obtain

$$\left.\begin{aligned} a_\nu &= \nu(\nu+1)\, i^\nu C_\nu = \nu(\nu+1)\, c_\nu; \\ p_\nu &= -\nu(\nu+1)\, i^\nu B_\nu = \nu(\nu+1)\, b_\nu. \end{aligned}\right\} \tag{3.46}$$

In order to establish the relationship between the angles of Mie θ' and ϕ' and our angles θ and ϕ, let us turn to Figure 8. We selected the axes x, y, z (1, 2, 3) in the same way as Mie [see Figure 1 in (Ref. 32)], namely: a scattered wave is directed along the negative axis 3 and is polarized in the direction of the axis 1. Let us introduce the notation

$$v = \cos\theta = -\cos\beta.$$

It may be readily seen that the following formulas hold

$$\cos\theta = \sin\theta' \sin\varphi' = v;$$
$$\sin\theta \cos\varphi = \cos\theta';$$
$$\sin\theta \sin\varphi = \sin\theta' \cos\varphi'.$$

The functions P_ν and R_ν, whose derivatives with respect to the angles are /75 contained in formulas (3.44), are as follows:

$$P_\nu(\theta, \varphi') = \Pi_\nu(v) \cos\theta';$$
$$R_\nu(\theta', \varphi') = \Pi_\nu(v) \sin\theta' \cos\varphi'.$$

The quantity $\Pi_\nu(x)$ is the special function introduced by Mie. Comparing the differential equation for the functions $\Pi_\nu(x)$, and also the explicit form of these functions of Mie [formulas (34) and (38) in (Ref. 32)], with the

equation and the explicit expressions for the Legendre polynomials $P_\nu(x)$, we readily obtain:

$$\Pi_\nu(x) = \frac{d}{dx} P_\nu(x).$$

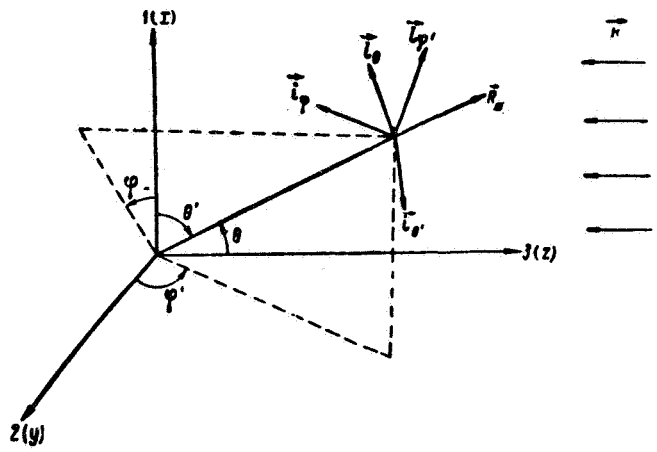

Figure 8. Relationship Between Angles Selected by Mie and our Angles

The relationships given above provide the meaning of all the quantities contained in the formulas of Mie for the fields [formulas (3.44)].

In view of the method selected by Mie to measure the angles ϕ' and θ', the components $E_{\phi'}$ and $E_{\theta'}$ are not components across (E_ϕ) and around (E_θ) of the plane of vision. However, these components can be determined by means of $E_{\phi'}$ and $E_{\theta'}$.

In actuality, let i_ϕ and $i_{\theta'}$ be /76 the unit vectors with respect to the curvilinear axes ϕ' and θ' at the observation point. In addition, let i_ϕ and i_θ be the unit vectors across and along the plane of vision at this same point, and let i_x, i_y and i_z be the unit vectors along the x, y, z axes.

Since we have

$$\mathbf{E} = E_{\varphi'} \mathbf{i}_{\varphi'} + E_{\theta'} \mathbf{i}_{\theta'},$$

we then have

$$E_\varphi = (\mathbf{E}, \mathbf{i}_\varphi) = E_{\varphi'} (\mathbf{i}_{\varphi'}, \mathbf{i}_\varphi) + E_{\theta'} (\mathbf{i}_{\theta'}, \mathbf{i}_\varphi),$$

$$E_\theta = (\mathbf{E}, \mathbf{i}_\theta) = E_{\varphi'} (\mathbf{i}_{\varphi'}, \mathbf{i}_\theta) + E_{\theta'} (\mathbf{i}_{\theta'}, \mathbf{i}_\theta).$$

The vectors i_θ and i_ϕ may be readily determined from the following considerations. Let $\mathbf{R}_0$ be the unit vector in the direction of the observation point. The vector i_θ lies in the plane ($\mathbf{R}_0$, i_z). In addition, it may be readily shown that

$$\mathbf{i}_\theta = -\frac{1}{\sin\theta} \mathbf{i}_z + \operatorname{ctg}\theta \cdot \mathbf{R}_0;$$

$$\mathbf{i}_\varphi = [\mathbf{R}_0, \mathbf{i}_\theta] = -[\mathbf{R}_0, \mathbf{i}_z] \frac{1}{\sin\theta}.$$

If we write out the rectangular components of the vectors $i_{\phi'}$, $i_{\theta'}$, i_ϕ, i_θ, we obtain the following formulas

$$(\mathbf{l}_{\varphi'}, \mathbf{l}_\theta) = -\frac{\cos\varphi'}{\sin\theta}; \quad (\mathbf{l}_{\theta'}, \mathbf{l}_\theta) = -\frac{\cos\theta'\sin\varphi'}{\sin\theta};$$
$$(\mathbf{l}_{\varphi'}, \mathbf{l}_\varphi) = -\frac{\sin\varphi'\cos\theta'}{\sin\theta};$$
$$(\mathbf{l}_{\theta'}, \mathbf{l}_\varphi) = -\frac{\cos\varphi'}{\sin\theta}.$$

Employing these relationships, expanding the angular functions in formulas (3.44), and replacing the angles θ' and ϕ' by the angles θ and ϕ, we obtain the following formula for E_θ:

$$E_\theta = \frac{\lambda'}{2\pi}\frac{e^{-\frac{2\pi i r}{\lambda'}}}{r}\cos\varphi \times \\ \times \sum_{\nu=1}^{\infty}\left\{\frac{a_\nu}{\nu(\nu+1)}(\cos\theta\Pi_\nu - \sin^2\theta\Pi'_\nu) + \frac{p_\nu}{\nu(\nu+1)}\Pi_\nu\right\}. \tag{3.47}$$

In precisely the same way, we obtain the expression for E_ϕ: /77

$$E_\varphi = -\frac{\lambda'}{2\Pi}\frac{e^{-\frac{2\pi i r}{\lambda'}}}{r}\sin\varphi \times \\ \times \sum_{\nu=1}^{\infty}\left\{\frac{a_\nu}{\nu(\nu+1)}\Pi_\nu + \frac{p_\nu}{\nu(\nu+1)}(\cos\theta\Pi_\nu - \sin^2\theta\Pi'_\nu)\right\}. \tag{3.48}$$

Formulas (3.47) and (3.48) give the field components along and across the plane of vision. If we now note that

$$\left.\begin{aligned} \Pi_\nu(\cos\theta) &= \frac{P_\nu^{(1)}(\cos\theta)}{\sin\theta} = Q_\nu(\theta); \\ \cos\theta\Pi_\nu - \sin^2\theta\,\Pi'_\nu &= -P_\nu^{(1)\prime}(\cos\theta)\sin\theta = S_\nu(\theta), \end{aligned}\right\} \tag{3.49}$$

we find that the expressions for E_θ and E_ϕ which we obtained from the formulas of Mie coincide exactly with the formulas for E_θ and E_ϕ indicated by us previously [formulas (2.41)].

Employing formulas (3.46), we may now write the expressions for the coefficients of scattering and absorption according to Mie. In accordance with the formula (2.51), for k_p we obtain:

$$k_p = \frac{2\pi}{k_a^2}\sum_{\nu=1}^{\infty}\frac{|a_\nu|^2 + |p_\nu|^2}{2\nu+1}. \tag{3.50}$$

For k we obtain the following, in accordance with (2.52):

$$k = \frac{2\pi}{k_a}\operatorname{Im}\left(\sum_{\nu=1}^{\infty}(-1)^\nu(a_\nu - p_\nu)\right). \tag{3.51}$$

We have already noted previously that the complete solution of the problem for any ρ (for $\sigma = 0$) was given by Love nine years before Mie. His solution was then employed by Rayleigh (Ref. 34), who tabulated the intensities I_s and I_p for $m = 1.5$ and $\rho = 1; 1.5; 1.75; 2.0; 2.25$. The Love-Rayleigh formulas were also employed by Ray (Ref. 44) ($\rho = 12$; $m = 1.33$). We shall indicate the relationship between our notation and the notation of Rayleigh. The following /78 relationships hold:

$$\left.\begin{aligned} a = R, \quad \rho = \eta, \quad m = \sqrt{K}, \\ c_l = \frac{2l+1}{l(l+1)} N_l; \quad E_\varphi = Y, \\ b_l = \frac{2l+1}{l(l+1)} M_l; \quad E_\theta = \frac{yZ - zY}{r}. \end{aligned}\right\} \tag{3.52}$$

§ 4. One Error in the Formulas for Intensities[1]

When the intensities are tabulated, one usually starts with the formulas of I_1 and I_2 indicated by Mie [see (Ref. 32), page 427]:

$$\left.\begin{aligned} I_1 = \frac{\lambda'^2}{4\pi^2 r^2} \left| \sum_{\nu=1}^{\infty} \left\{ \frac{a_\nu}{\nu(\nu+1)} \Pi_\nu + \right.\right. \\ \left.\left. + \frac{p_\nu}{\nu(\nu+1)} [v\Pi_\nu - (1 - v^2)\Pi'_\nu] \right\} \right|^2; \\ I_2 = \frac{\lambda'^2}{4\pi^2 r^2} \left| \sum_{\nu=1}^{\infty} \left\{ \frac{a_\nu}{\nu(\nu+1)} [v\Pi_\nu - (1 - v^2)\Pi'_\nu] + \right.\right. \\ \left.\left. + \frac{p_\nu}{\nu(\nu+1)} \Pi_\nu \right\} \right|^2. \end{aligned}\right\} \tag{3.53}$$

These formulas give the intensities I_1 and I_2 for a scattered bundle, under the assumption that a bundle of natural (unpolarized) light falls on a particle; the intensity of this light equals unity. The meaning of the quantities thus included and their relationship with our notation is given in § 3.

The error, which we mentioned, consists of the fact that formulas (3.53) are invalid -- the factor $^1/2$ is omitted in them. We should note that this leads to incorrect values for $I(\beta)$, but the form of the scattering indacitrix does not change (all the radius vectors are extended by a factor of two). This error has no influence upon the degree of polarization of scattered light. However, it is important, for example, when making an absolute comparison of the results derived from tabulating the intensities with experiment, or for computing the scattering coefficient based on the tabulated intensities.

The inaccuracy of formulas (3.53) may be shown by the following three /79 independent methods.

(a) The formulas (3.53) for intensity during scattering of natural light were obtained by Mie from the formulas for scattering intensity of linearly polarized light [formulas (78) on page 410 in (Ref. 32)]. Changing from linearly polarized light to natural light, Mie did not average over the different

[1]We shall follow our studies here (Ref. 43), 1946, and (Ref. 46).

orientations of the electric vector. He simply assumed that natural light may be represented as the combination of two linearly polarized (perpendicularly to each other) components. Combining the intensities I_1 and I_2 for each of the components, Mie obtained the formulas (3.53) for the quantities I_1 and I_2 for the entire bundle. Since the initial formulas of Mie correspond to the case when each of the linearly polarized components has an intensity equalling unity, the total intensity of the incident bundle equals two. When making a conversion to unit intensity of the incident bundle, we must thus divide the intensities obtained from formulas (3.53) by 2.

(b) The other method for demonstrating the inaccuracy of formulas (3.53) is as follows. One changes from the formulas of Mie, obtained for the fields E_θ and E_ϕ when linearly polarized light is scattered, to the scattering of natural light, by averaging over the polarization directions.

We calculated these formulas above [see formulas (3.47) - (3.48)]. Changing from the fields to the intensities (we shall designate them here by primes), we obtain

$$I_1' = \sin^2\varphi I_1; \quad I_2' = \cos^2\varphi I_2.$$

If we now wish to change to natural light, we must average over all possible directions of the electric vector, i.e., over the angle ϕ. Since $\sin^2\phi = \cos^2\phi = \frac{1}{2}$, we then have

$$I_1' = \frac{1}{2} I_1; \quad I_2' = \frac{1}{2} I_2.$$

(c) The simplest method of demonstrating the incorrectness of formulas (3.53) consists of comparing the numerical values obtained by these formulas for the case of small particles with the numerical values which are given by the /80 theory for extremely small particles (the case of Rayleigh).

For example, let us turn to the numerical values which are obtained according to formulas (3.53) for the quantities $i_{1,2} = \frac{4\pi^2 r^2}{\lambda'^2} I_{1,2}$ in the case $n = 1.25$ and $\rho = 0.4$. These values were obtained by Blümer [see (Ref. 56)]. Let us investigate the case of foward scattering ($\beta = 0$). According to the Rayleigh formula, we obtain

$$i_1 = i_2 = 51{,}06 \cdot 10^{-6},$$

while the following is contained in the Blümer table:

$$i_1 = i_2 = 107 \cdot 10^{-6},$$

i.e., the quantity is approximately twice as large. The deviation of half of the Blümer value from the Rayleigh by 5% is due to the fact that the particle cannot be regarded as small in the case $\rho = 0.4$.

We would like to mention that the error mentioned here was also assumed in the book by M. Born (Ref. 38). Born changes from the formulas for scattering of linearly polarized light to natural light, regarding it as the combination

of two mutually perpendicular components each of which has unit intensity. The quantities I_1 and I_2 thus obtained are the doubled intensities of the transverse and longitudinal components in a scattered bundle, as we mentioned above, and not the intensities written incorrectly by Born.

In conclusion, we would like to add that the error investigated here was assumed in the new book by G. Gertner (Ref. 45). The formulas for intensities, which he writes out on pages 27-28, are incorrect.

CHAPTER IV /81

SMALL PARTICLES

§ 1. Rayleigh Formula

The well-known Rayleigh formula [see (Ref. 47)] is obtained from the general formulas of Chapter II under the following two assumptions:

(a) The particle must be small compared with the wave length $\rho \ll 1$.

(b) The refractive index of its substance must be small, so that $|m|\rho$ must be less than unity.

This second factor is usually forgotten, and it is stated that the scattering of a small sphere is described by the Rayleigh formula. This statement is erroneous. In this chapter, we shall only discuss scattering by small spheres. However, the reader will see (§ 2 and 3) that both the scattering indicatrix and all the remaining quantities describing the scattering will differ essentially from the Rayleigh quantities, if condition (b) is not satisfied. If both conditions hold, and this is the case in the majority of cases in the visible region (since usually $|m|$ does not exceed two here), we can turn to formulas (3.16) - (3.17) to compute c_ℓ and b_ℓ. In the case of very small particles, we have

$$c_1=\rho^3\frac{m^2-1}{m^2+2};\quad c_2=-\frac{\rho^5}{18}\left(\frac{m^2-1}{2m^2+3}\right);\quad b_1=-\frac{\rho^5}{30}(m^2-1). \tag{4.1}$$

The coefficient c_1 is significantly greater than all the remaining values. Taking into account only this first term and noting that $Q_1(\theta) = 1$, and $S_1(\theta) = -\cos\theta$, we obtain

$$\left.\begin{aligned} E_\varphi &= -\frac{\sin\varphi E_0 e^{-ik_a r}}{r}k_a^2a^3\left(\frac{m^2-1}{m^2+2}\right);\\ E_\theta &= \frac{\cos\varphi\cos\theta E_0 e^{-ik_a r}}{r}k_a^2a^3\left(\frac{m^2-1}{m^2+2}\right).\end{aligned}\right\} \tag{4.2}$$

We shall show that the field obtained coincides exactly with the field of the /82
oscillating dipole at a large distance from it (in the wave zone). This dipole is excited in the sphere by a constant (along the sphere) field, whose

magnitude changes periodically with frequency ω.

We should recall that a sphere placed in a constant field E_0 acquires a dipole moment in it

$$\mathbf{P} = a^3\left(\frac{m^2-1}{m^2+2}\right)\mathbf{E}_0, \tag{4.3}$$

where a is the sphere radius, and m is the complex refractive index of the substance of the sphere. The field of the oscillating dipole will be as follows at a large distance from it, as is known

$$\mathbf{E} = \frac{(\ddot{\mathbf{P}}, \mathbf{R}_0)\mathbf{R}_0 - \ddot{\mathbf{P}}}{c_a^2 r}, \tag{4.4}$$

We must thus substitute the dipole moment not at the moment of time t under consideration, but at the time $t' = t - \frac{r}{c_a}$ (allowance for delay). Here $\mathbf{R}_0$ is the unit vector from the center of the dipole to the observation point, and r is the distance from the center of the dipole to the observation point.

Substituting (4.3) in (4.4) and noting that $\ddot{\mathbf{P}} = -\omega^2\mathbf{P}$, and $\frac{\omega^2}{c_a^2} = k_a^2$, we obtain:

$$\mathbf{E} = -\frac{k_a^2 a^3}{r}\left(\frac{m^2-1}{m^2+2}\right)e^{-ik_a r}\left[(\mathbf{E}_0\mathbf{R}_0)\mathbf{R}_0 - \mathbf{E}_0\right]. \tag{4.5}$$

The projections of the expression in the brackets upon the spherical axes will be: zero on the axis $\mathbf{R}_0$, + sin ϕ -- on the axis ϕ, and cos ϕ cos θ on the axis θ. Consequently, the components E_ϕ and E_θ exactly coincide with those indicated in formulas (4.2).

When there is an increase in the size of the particle, along with the electric dipole radiation, allowance must be made for the dipole magnetic radiation, quadrupole electric radiation, etc.

Mie gave the distribution of the electric force lines for the first eight partial waves (Ref. 32). They are also given in the book by Born (Ref. 38). For purposes of illustration, we shall present the electric force lines for only the electric 1 and the magnetic 2 dipoles (Figure 9).

In 1946, Ya. I. Frenkel' advanced the following clear explanation of these pictures of the force lines. /83

If a << λ, the field is practically constant over the particle length, and changes only in time. This leads to a picture of the force lines which is shown in Figure 9 (1). When the particle dimensions increase, it cannot be assumed that the field is constant in terms of magnitude along the particle, but at each moment of time it may be regarded as a superposition of the constant field and the supplementary field, as is shown in Figure 10. The constant field is designated by the heavy line, and the supplementary field is designated by

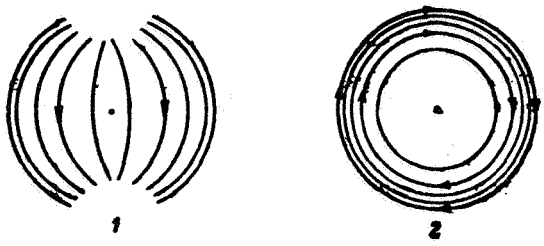

Figure 9. Electric Force Lines of the First Two Partial Waves

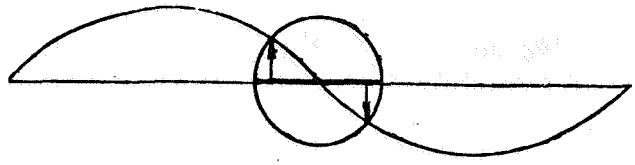

Figure 10. Diagram Showing the Appearance of the Second Partial Wave

the arrows. The constant field may be reduced to the picture shown in Figure 9 (1), and the supplementary field produces a ring current (magnetic dipole). Its electric force lines will be those shown in Figure 9 (2).

Let us now examine the scattering indicatrixes. For scattering of linearly polarized light, we obtain the following from (4.2)

$$I(\beta, \varphi) = I_0 \frac{16\pi^4 a^6}{\lambda_a^4 r^2} \left| \frac{m^2-1}{m^2+2} \right|^2 (1 - \sin^2\beta \cos^2\varphi). \tag{4.6}$$

The following distribution of scattered light in different planes corresponds /84 to this formula:

(1) In the plane perpendicular to the direction of the incident ray, i.e., in the case $\beta = 90°$:

$$I \sim \sin^2\varphi;$$

(2) In the plane produced by the incident ray and the magnetic vector, i.e., in the case $\phi = 90°$:

$$I \sim \text{const} - \text{periphery}$$

(3) In the plane produced by the incident ray and the electric vector ($\phi = 0$ or π):

$$I \sim \cos^2\theta.$$

We may obtain the scattering indicatrix of natural light from (4.6) by averaging over ϕ. Performing this averaging, we obtain the following

$$\left.\begin{aligned} I_1 &= I_0 \frac{9\pi^2 v^2}{\lambda_a^4 r^2} \left| \frac{m^2-1}{m^2+2} \right|^2 \frac{1}{2}; \\ I_2 &= I_0 \frac{9\pi^2 v^2}{\lambda_a^4 r^2} \left| \frac{m^2-1}{m^2+2} \right|^2 \frac{\cos^2\beta}{2}. \end{aligned}\right\} \tag{4.7}$$

We have here changed from the radius of the sphere a to its volume v.

The total indicatrix will be:

$$I(\beta) = I_0 \frac{9\pi^2 v^2}{\lambda_a^4 r^2} \left| \frac{m^2-1}{m^2+2} \right|^2 \left(\frac{1+\cos^2\beta}{2}\right). \tag{4.8}$$

We may call the formula (4.8) the Rayleigh formula. Following are its

characteristic features:

(a) Intensity of scattering $\sim \frac{1}{\lambda^4}$,[1]

(b) Scattering intensity is proportional to the square of the particle volume,

(c) Scattering in front and behind is the same.

Figure 11 shows this scattering indicatrix for an extremely small particle. /85 The inner curve expresses the function $I_2 = I_2(\beta)$, i.e., the indicatrix for the component of scattered light which is parallel to the plane of vision.

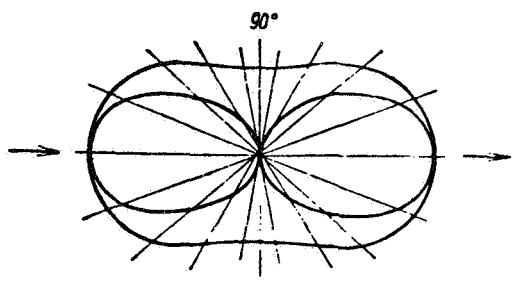

Figure 11. Indicatrix for Small ρ and Small m (Rayleigh Indicatrix)

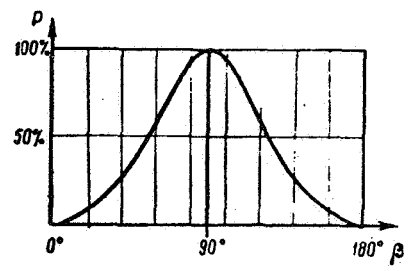

Figure 12. Polarization for Small ρ and Small m (Rayleigh Polarization)

We obtain the following from formulas (4.7) for the degree of polarization:

$$p = \frac{I_1 - I_2}{I_1 + I_2} = \frac{\sin^2\beta}{1 + \cos^2\beta}. \tag{4.9}$$

The graph for this function is shown in Figure 12. The degree of polarization is positive for all angles. It has a maximum equal to unity in the case $\beta = 90°$.

Let us now turn to the formulas for the coefficients of scattering and absorption for the case under consideration. In the general formulas (2.51) and (2.52), if we substitute the expressions for the coefficients c_ℓ and b_ℓ /86 in our case, then we obtain the following for the main terms:

$$k_p = \frac{24\pi^3}{\lambda_a^4} v^2 \left| \frac{m^2 - 1}{m^2 + 2} \right|^2; \tag{4.10}$$

---

(1) If it is assumed that m does not depend on λ. If m changes considerably with λ, the dependence of I on λ will be more complex. For example, let us assume that $\frac{4\pi\sigma}{\omega} \sim 1$ and $\varepsilon^2 - 1 \ll \frac{4\pi\sigma}{\omega}$, and then $\left|\frac{m^2 - 1}{m^2 + 2}\right|^2 \sim \lambda^2$. In this case, both the intensities and the scattering coefficient will be $\sim \frac{1}{\lambda^2}$, and not $\frac{1}{\lambda^4}$.

$$k = \frac{4\pi}{k_a^2} \operatorname{Im}(-c_1) = \frac{6\pi}{\lambda_a} v \operatorname{Im}\left(\frac{1-m^2}{m^2+2}\right). \tag{4.11}$$

Here v is the particle volume.

Formula (4.10) determines the so-called Rayleigh scattering coefficient.

Assuming that $\varepsilon_a = 1$, and $\sigma_a = 0$ and introducing the indices of refraction and absorption of the particle, we obtain

$$k = \frac{36\pi n\varkappa}{|m^2+2|^2} \frac{v}{\lambda_a}. \tag{4.12}$$

For small ρ, these formulas must closely describe the phenomena, since the correction terms for them, as follows from III, 1, have the order ρ^2.

Two important facts must be pointed out here: (1) when there is no dispersion, i.e., for constant x and n, with an increase in λ the attenuation coefficient for a small particle decreases as $\frac{1}{\lambda}$, instead of as $\frac{1}{\lambda^4}$ according to Rayleigh; (2) the attenuation coefficient for a small particle is proportional to its volume, and not the square of the volume, as is stated by Rayleigh.

This means that, when light passes through a layer of turbid medium, the attenuation of the bundle will be simply proportional to the amount of substance on the path of the ray. This also means that, since $\rho^3 \gg \rho^6$ (we should recall that $\rho \ll 1$), the attenuation coefficient for a small particle significantly exceeds the scattering coefficient.

Thus, for small particles the absorption, if it occurs, usually considerably exceeds the scattering.

We should also note that, according to formulas (4.10) - (4.12), we must obtain a decrease in k_p and k with an increase in λ. In some cases, when the dependence of n and $\varkappa$ upon λ is taken into account (and also when allowance is made for the second and third terms in the expansion with respect to ρ) $k_p(\lambda)$ and $k(\lambda)$ have maxima.

This maximum was calculated by Mie for k_p, for example, for particles of gold (see Figure 13; 1 and 2 -- dipole-electric scattering for Au and $m = \infty$, /87
3 -- dipole-electric + magnetic scattering for $m = \infty$). It is interesting to note that the scattering capability of gold particles is thus greater than that of absolutely conductive particles having the same dimensions.

The position of the radiation maximum is determined, in a certain sense, by the resonance between the eigen electromagnetic oscillations of the sphere and the external field.

There is one misunderstanding related to formulas (4.10) and (4.11), which sometimes leads to confusion. The attenuation coefficient must change into the

scattering coefficient when the absorption of light, in the proper meaning of the word, is absent. However, if we assume that m is real in formula (4.11) for k, we then obtain k = 0, while we should have obtained $k = k_p$.

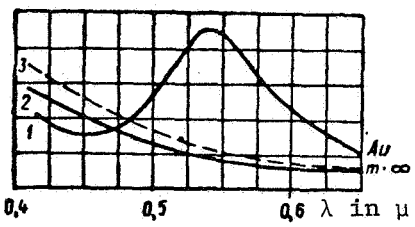

Figure 13. Coefficient of Scattering by Small Particles

(1) - gold particles; 2, 3 - particles with m = ∞.

In addition, if, for example, the imaginary part of m, which first equals zero, increases by an infinitesimal amount, the attenuation coefficient must also change by an infinitesimal amount. According to our formulas, it follows that k_p must suddenly change to k, which has an entirely different value.

In order to explain these ambiguities, we should note that formula (4.1), with which we obtain the expressions for k and k_p, contains only the first term in the expansion of the coefficient c_1 in series with respect to ρ. We may show that, if allowance is made for the subsequent terms in the expansion with respect to ρ, we may obtain the general formula for the attenuation coefficient, which changes into the formula for the Rayleigh scattering coefficient in the case of a small imaginary part of m. In the case of a large imaginary /88 part, it changes into formula (4.11).

In acuality, substituting the expressions for r, q, p and t given in III, 1 in the formula for c_1, and collecting the terms of one order with respect to ρ, we obtain

$$c_1 = \rho^3\left(\frac{m^2-1}{m^2+2}\right)\left\{1+\frac{3}{5}\rho^2\frac{m^2-2}{m^2+2} - i\frac{2\rho^3}{3}\frac{m^2-1}{m^2+2}+\cdots\right\}. \tag{4.13}$$

Substituting the expression (4.13) for c_1 and the expressions for c_2 and b_1 according to formula (4.1) (the subsequent terms will be of a higher order with respect to ρ) in the formula for k, we obtain:

$$k = \frac{2\pi}{k_0^2}\operatorname{Im}\left\{-2\rho^3\left(\frac{m^2-1}{m^2+2}\right)\left[1+\frac{3}{5}\rho^2\frac{m^2-1}{m^2+2} - i\frac{2\rho^3}{3}\left(\frac{m^2-1}{m^2+2}\right)+\right.\right.$$
$$\left.\left.+\cdots\right]+\frac{\rho^5}{15}(m^2-1)-\frac{\rho^5}{3}\left(\frac{m^2-1}{2m^2+3}\right)+\cdots\right\}. \tag{4.14}$$

This is the general formula for k as a function of ρ and m for small particles (within an accuracy of terms whose order is higher than ρ^6).

If the imaginary part of m is sufficiently large, we then obtain the formula (4.11), and if it is small, we obtain

$$k = \frac{128\pi^5 a^6}{3\lambda_0^4}\left|\frac{m^2-1}{m^2+2}\right|^2.$$

This accurately coincides with the Rayleigh scattering coefficient.

If the imaginary part is comparable with ρ^3, then the attenuation coefficient must be calculated according to the general formula (4.14).

We should add that for small conductive particles in the region within which the Gagen-Rubens law applies (1.13) ($\lambda > 5\mu$), we have

$$|m^2+2|^2 \simeq 4n^2x^2 = 4\left(\frac{2\pi\sigma}{\omega}\right)^2.$$

We have

$$k = \frac{9\pi c}{m_a \sigma} \cdot \frac{v}{\lambda_a^2}.$$

Thus, the attenuation coefficient is $\sim \frac{1}{\lambda^2}$.

The region of values of ρ, where it is valid to employ the simple formulas given in this section, may be determined both by the value of m (more precisely/89 m - 1), and by the accuracy which we require from the formulas. It will be different for different formulas. For example, for the indicatrix in the case of drops of water in the visible region (m = 1.33), the Rayleigh formula (4.8) in the case $\rho = 0.3$ yields an error of 5%. If it is assumed that an error of 2-3% is permissible, then the region of applicability for (4.8) will be $\rho \leq 0.25$.

§ 2. Absolutely Reflecting Particle

If the complex refractive index of a substance is very large (as compared with unity), the electromagnetic field will barely penetrate the substance. In formal terms, this follows from the fact that in this case the reflection coefficient, which is determined by the Fresnel formulas, will be close to unity for any angle of incidence, whereas the penetration coefficient indicating the intensity of the field penetrating the substance will be close to zero.[1] The physical factors causing the phenomena will be different, depending on what causes the large values of the modulus m -- whether its imaginary or real part is larger.

In the first case, the field does not penetrate the body, due to its absorption in the substance. We obtain a heterogeneous wave which is propagated along the dividing surface and which is rapidly weakened within the substance.

In the second case, the external field is attenuated by polarization of the substance. For any angle of incidence, the refraction angle will be very small ($\sim \frac{1}{|m|}$), and the penetration coefficient, which is correspondingly small, will be proportional to it. This is the behavior of water in the meter region.

An approximation of large $|m|$ may be employed in radio technology when investigating processes at the boundary dividing the earth and air.

---

(1) The reader may find the formulas for the coefficients of reflection and penetration in Chapter V [formulas (5.1) and (5.2)].

The case under consideration here pertains to metals in the infrared region ($\lambda > 5\mu$) where, as we have already indicated, both the real and the imaginary parts of m will be large.

Ferroelectrics or ferromagnets, particularly barium titanate, whose ferroelectric properties were recently discovered by B. M. Bul and I. M. Gol'dman, provide the best approximation to the limiting case under consideration. As /90 studies have shown (Ref. 48), the dielectric constant of this substance is on the order of 1500 for $\lambda = 18$ cm at room temperatures.

In this region of wave lengths, considerable dispersion in ε is initiated, but in the case of $\lambda = 3$ cm ε has a value of about 300, and in the $\lambda = 1$ cm, it has a value of about 126.

We shall investigate here the limiting case $|m| \to \infty$ and small ρ. The approximation formulas (3.14) are inapplicable, since they were obtained under the assumption that $|m\rho|$ is small. In our case, $|m|\rho \to \infty$, and we shall start directly from the fundamental formulas (2.39). Assuming $m \to \infty$ in these formulas, we obtain:

$$c_l = (-1)^l i \frac{2l+1}{l(l+1)} \frac{\psi_l'(\rho)}{\zeta_l'(\rho)}; \quad b_l = -(-1)^l i \frac{2l+1}{l(l+1)} \frac{\psi_l(\rho)}{\zeta_l(\rho)}. \tag{4.15}$$

If we replace the function ζ_ℓ in the denominators by ψ_ℓ and χ_ℓ, according to formulas (3.2), we find that

$$\frac{\psi_l'(\rho)}{\zeta_l'(\rho)} = \frac{\psi_l'^2 - i\chi_l'\psi_l'}{\psi_l'^2 + \chi_l'^2}; \quad \frac{\psi_l(\rho)}{\zeta_l(\rho)} = \frac{\psi_l^2 - i\chi_l\psi_l}{\psi_l^2 + \chi_l^2}.$$

We thus have

$$\operatorname{Re} \frac{\psi_l'}{\zeta_l'} = \left| \frac{\psi_l'}{\zeta_l'} \right|^2.$$

This means that

$$\operatorname{Im} l(l+1)(-1)^l c_l = \frac{l^2(l+1)^2}{2l+1} |c_l|^2. \tag{4.16}$$

A similar relationship holds for b_ℓ. In accordance with formulas (2.52) and (2.51), this means that for an absolutely reflecting particle the attenuation coefficient k coincides with the scattering coefficient k_p (the external field does not penetrate within the particle).

Let us now employ the formulas for cylindrical functions for small ρ given in III, 1. Substituting the first terms of the series with respect to ρ in (4.15), we readily obtain

$$\begin{aligned} c_l &= (-1)^{l+1} \frac{\rho^{2l+1}}{l^2[(2l-1)!!]^2}; \\ b_l &= (-1)^{l+1} \frac{\rho^{2l+1}}{l(l+1)[(2l-1)!!]^2}. \end{aligned} \tag{4.17}$$

The significant difference from the preceding case is immediately apparent: /91 the amplitudes of the electric and magnetic partial waves for one and the same ℓ are of one order of magnitude.

We should note that the amplitudes of the electric oscillations indicated in III, 1 [formula (3.16)] continuously change into the amplitudes (4.17) when m increases, which does not occur for the magnetic oscillations. The reason for this may be found in the following section.

The quantities c_1 and b_1 have the largest value:

$$c_1 = \rho^3; \quad b_1 = \frac{\rho^2}{2}. \tag{4.18}$$

Recalling that $Q_1 = 1$ and $S_1 = \cos\theta = -\cos\beta$ for the intensity of scattered light, we obtain (natural light decreases):

$$\left.\begin{aligned} I_1 &= \frac{I_0}{2r^2}\alpha\left(1-\frac{\cos\beta}{2}\right)^2, \\ I_2 &= \frac{I_0}{2r^2}\alpha\left(\frac{1}{2}-\cos\beta\right)^2, \qquad \left(\alpha = \frac{16\pi^4 a^6}{\lambda_a^4}\right) \\ I &= \frac{I_0}{2r^2}\frac{5}{4}\alpha\left(1-\frac{8}{5}\cos\beta+\cos^2\beta\right). \end{aligned}\right\} \tag{4.19}$$

The scattering intensity here, just as in the formula of Rayleigh, is inversely proportional to λ^4 and proportional to v^2. The Rayleigh symmetry is sharply disturbed. Primarily all of the scattered light is directed forward. The ratio of light scattered forward to light scattered backwards will be $1/9$, instead of unity in the Rayleigh case.

Figure 14 presents the scattering indicatrix of natural light by a small sphere which reflects completely (outer curve I, inner curve I_2). As we may see, it differs considerably from the Rayleigh indicatrix. We have also noted this fact in the forward.

There is also a significant difference in the polarization of scattered light. The degree of polarization may be determined by the formula

$$p = \frac{3(1-\cos^2\beta)}{5-8\cos\beta+5\cos^2\beta}. \tag{4.20}$$

At every angle $I_\phi > I_\theta$, i.e., the polarization is positive. At an angle of 90°, the degree of polarization will be $8/5$. The maximum polarization will /92 occur at the angle 60°, where I_θ vanishes. Here p equals unity. We thus see that for small spheres, when m increases, the polarization maximum moves forward from 90° for small m to 60° for large m. The curve showing the dependence of p on β is shown in Figure 15.

Substituting the expression (4.17) in the general formula for k_p, we readily obtain

$$k_p = \frac{30\pi^3 v^2}{\lambda_a^4}\left(1+\frac{6}{25}\rho^2+\cdots\right). \tag{4.21}$$

In accordance with the statements indicated previously, the fact does not surprise us that the Rayleigh scattering coefficient does not change into the coefficient for infinitely large m in the case $m \to \infty$. It is larger by a /93 factor of $5/4$.

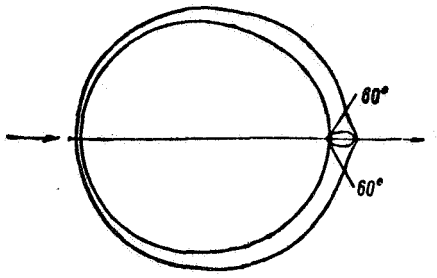

Figure 14. Indicatrix of a Small, Completely Reflecting Particle

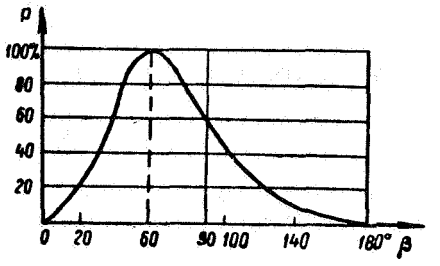

Figure 15. Polarization of Light Scattered by a Small, Completely Reflecting Particle

The formulas for the fields and the displacement of the polarization maximum to $\beta = 60°$ for small spheres, for the limiting case studied in this section, were established by Thomson (Ref. 49).[1]

§ 3. Resonance. Eigen Oscillations

The limiting case investigated in the preceding section is far from being a mathematical idealization. In actuality, the case of large, but not infinitely large, m is of great interest. It is also interesting to study the change from the Rayleigh limiting case to the Thomson case. We shall do this in this section. We shall assume, just as previously, that $\rho \ll 1$. With respect to the quantity $m\rho$, which we shall designate here by q, it may have any values.

Substituting the series given in III, 1 in the general formulas for the coefficients (2.39), we obtain the following general formulas for the amplitudes c_ℓ and b_ℓ in the case we are considering:

$$\left.\begin{aligned} c_l &= \frac{(-1)^l \rho^{2l+1}}{l(l+1)[(2l-1)!!]^2} \frac{\rho^2\psi_l'(q) - (l+1)q\psi_l(q)}{\rho^2\psi_l'(q) + lq\psi_l(q)} = \\ &= \frac{(-1)^{l+1}\rho^{2l+1}}{l^2[(2l-1)!!]^2}; \\ b_l &= \frac{(-1)^l \rho^{2l+1}}{l(l+1)[(2l-1)!!]^4} \frac{(l+1)\psi_l(q) - q\psi_l'(q)}{l\psi_l(q) + q\psi_l'(q)}. \end{aligned}\right\} \tag{4.22}$$

We may see that in the case under consideration the electric oscillation amplitudes change precisely into the expressions given previously. As for the magnetic oscillation amplitudes, this will only be the case for $q \to \infty$.

Only the first electric and the first magnetic oscillations are of importance. We obtain the following for them:

(1) We should also note that this problem was studied by Schwarzschild (Ref. 50) in relation to the problem of light pressure.

$$c_1 = \rho^3; \quad b_1 = -\frac{\rho^3}{2}\frac{2\psi_1(q) - q\psi_1'(q)}{\psi_1(q) + q\psi_1'(q)} = \frac{\rho^3}{2}\gamma(q). \tag{4.23}$$

Employing the explicit form of the function ψ_1 for $\gamma(q)$, we obtain /94

$$\gamma(q) = 1 + \frac{3}{q}\operatorname{ctg} q - \frac{3}{q^2}. \tag{4.24}$$

Let us study the manner in which the magnetic oscillation amplitude changes with a change in q. For small q, we have

$$\gamma(q) = -\frac{q^2}{15} - \frac{2q^4}{315} - \dots \tag{4.25}$$

This holds for $b_1 = -\frac{\rho^5 m^2}{30}$ in accordance with the formula (4.1) given in § 1. In this case $b_1 \ll c_1$, and we obtain Rayleigh scattering.

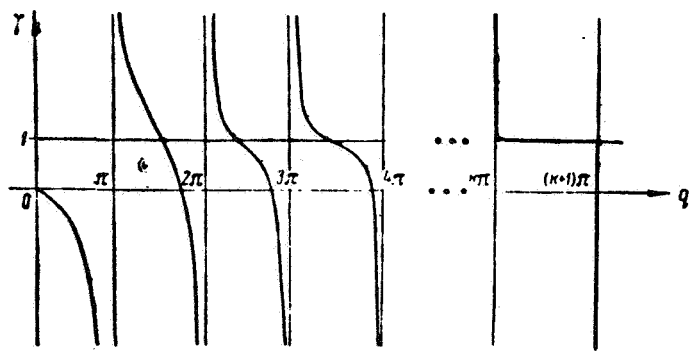

Figure 16. Curves for Resonance (the Curves are Deformed as m Increases, Striving to the Limiting Curve; the Curve Given on the Right is for a Completely Reflecting Particle).

With an increase in q, the function $\gamma(q)$ decreases, and for $q = \pi$ it becomes minus infinity. Resonance occurs here. Then γ becomes positive ($+\infty$), and in the case $q = 2\pi$ again strives to minus infinity. The resonance phenomena occur, in general, for $q = m\rho = k\pi$, where k is a whole number (see Figure 16).

The wave lengths at which resonance occurs may be determined by the following formula:

$$\lambda = \frac{2am}{k}, \qquad k = 1, 2, 3, \dots \tag{4.26}$$

The intensities of scattered light may be determined by the following formulas /95

$$\left.\begin{aligned} I_\varphi &= \frac{I_0}{2r^2}\alpha\left(1 - \frac{\gamma}{2}\cos\beta\right)^2 \\ I_\theta &= \frac{I_0}{2r^2}\alpha\left(\frac{\gamma}{2} - \cos\beta\right)^2 \end{aligned} \quad \left(\alpha = \frac{16\pi^4 a^6}{\lambda_a^4}\right). \right\} \tag{4.27}$$

In the case of resonance, the scattering intensities become infinite.

For small q, the scattering indicatrix will be a Rayleigh indicatrix. As q increases, the indicatrix will be deformed. When $\gamma = 1$, we obtain the indicatrix of an absolutely reflecting particle. With a further increase in q and as resonance is approached, the indicatrix again becomes a Rayleigh indicatrix, but the absolute intensity values will be very large. In Figure 17 we give the scattering indicatrixes for the cases 1) $\gamma = 0.5$, 2) $\gamma = 1$, 3) $\gamma = 5$, 4) $\gamma = 10$. This figure illustrates the change in the indicatrix when resonance is approached. (Curves 1 and 2 have the same scale; 3 is two times smaller, and 4 is 10 times smaller).

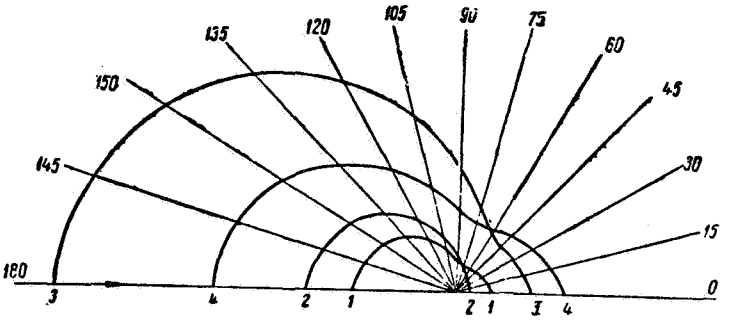

Figure 17. Indicatrixes of a Small, Very Refractive Particle. (As Resonance is Approached, the Indicatrix Strives to a Rayleigh Indicatrix).

With an increase in q, the branches of the curve $\gamma(q)$ will gradually be deformed. For large q, the curves will differ very little from the limiting curve shown on the right in Figure 16. Here $\gamma(q)$ will equal unity for all q, except $q = k\pi$. We thus obtain the transition to the case investigated in the preceding section ($m = \infty$).

The scattering coefficient in the case under consideration will be: /96

$$k_p = \frac{24\pi^3 v^2}{\lambda_a^4}\left(1 + \frac{\gamma^2}{4}\right). \tag{4.28}$$

As resonance is approached, k_p increases indefinitely.

Just as in the customary resonance problems, the scattering intensities can be kept from becoming infinite by allowing for the subsequent expansion terms which were omitted previously.

In the amplitude of the magnetic dipole oscillation, which only resonates once in our case, let us take into account the following terms in the expansion with respect to ρ. For γ we obtain:

$$\gamma(q) = \frac{q\psi_1'(q) - 2\psi_1(q)}{\left(1 - \frac{\rho^2}{2}\right)\psi_1(q) - \left(1 + \frac{\rho^2}{2}\right) q\psi_1'(q)}$$

We have only written here those supplementary terms which appear in the denominator $\gamma(q)$, since resonance is related to the vanishing of the denominator. Substituting $q = k\pi$ and noting that

$$\psi_1(k\pi) = (-1)^{k+1}, \text{ and } k\pi\psi_1'(k\pi) = (-1)^k,$$

we obtain

$$\gamma(k\pi) = \frac{3}{\rho^2} \text{ and } b_1(k\pi) = \frac{3}{2}\rho.$$

In resonance, we now have

$$I_\varphi = \frac{I_0}{2}\cdot\frac{a^2}{r^2}\cdot\frac{9}{4}\cos^2\beta; \quad I_\theta = \frac{I_0}{2}\cdot\frac{a^2}{r^2}\cdot\frac{9}{4}. \tag{4.29}$$

We have obtained the Rayleigh scattering indicatrix, but with scattering intensities which are larger by a factor of $\frac{9}{4\rho^4}$. The scattering coefficient in resonance will be

$$k = 6\pi a^2. \tag{4.30}$$

Thus, the resonating particle scatters a flux which is 6 times larger than that which arrives on its geometric cross section. This coefficient is also $\frac{9}{4\rho^4}$ times larger than the Rayleigh coefficient. For example, this means /97 that the scattering of a ferroelectric ball made of barium titanate with a = 1cm and with m = 39 will be 53,000 times larger for the first resonance peak than far from it.

The problem of the eigen electromagnetic oscillations of a sphere is closely related to the problem which we are investigating of dipole-magnetic resonance. This problem was studied by Debye (Ref. 33).

The selection of the possible eigen oscillations is determined in precisely the same way as the selection of the eigen elastic oscillations of any elastic system. In order to determine the amplitudes of partial waves producing the free electromagnetic oscillations of space outside of the sphere, in the non-homogeneous system of equations (2.35) - (2.36), determining the amplitudes of forced oscillations, we must set the free terms (forced field) equal to zero. We thus obtain a homogeneous system whose solution condition is that the corresponding determinant equal zero. In order to determine the eigen electric oscillations, we thus arrive at the following equation:

$$\frac{\zeta_l'(\rho)}{\zeta_l(\rho)} = \frac{1}{m}\frac{\psi_l'(m\rho)}{\psi_l(m\rho)} \tag{4.31}$$

and for the magnetic oscillations we arrive at the following equation

$$\frac{\zeta_l(\rho)}{\zeta_l'(\rho)} = \frac{1}{m}\frac{\psi_l(m\rho)}{\psi_l'(m\rho)}. \tag{4.32}$$

For each ℓ, this yields an infinite row of roots, and a complete selection of the system roots forms an infinite, two-dimensional array.

Two such arrays are included in our problem -- one for electric oscillations, and the other for magnetic oscillations.

For absolutely reflecting particles ($m = \infty$), we simply obtain

$$\left.\begin{array}{l}\zeta_l'(\rho)=0 \text{ for electric oscillations} \\ \zeta_l(\rho)=0 \text{ for magnetic oscillations}\end{array}\right\} \qquad (4.33)$$

We readily see from formulas (3.5) that in the case under consideration the infinite rows in each of the arrays degenerate into finite rows. The array/98 of "electric" eigen roots contains (ℓ + 1) in a row, and the array of "magnetic" roots contains $-\ell$ terms in a row.

The determinants of a homogeneous system are the denominators in amplitudes of partial waves of forced oscillations. The fact that they vanish designates the fact that the amplitude becomes infinite, if the numerators of the amplitudes also vanish.

However, it may be shown that all the roots are complex. This means that for any real ρ it is impossible for the amplitude to become infinite. One exception is the case of small ρ and large m, which is investigated in this section. As follows from formulas (4.22), we here have

$$\left.\begin{array}{l}\psi_l(q)=0 \text{ for electric oscillations.} \\ \dfrac{\psi_l'(q)}{\psi_l(q)}=-\dfrac{q}{l} \text{ for magnetic oscillations.}\end{array}\right\} \qquad (4.34)$$

Each of these equations has a countless number of real roots.

The electric eigen oscillations do not lead to resonance, since in the case of eigen frequencies the numerator in the amplitudes of the induced waves also vanishes. With respect to magnetic oscillations, they produce resonance in the case of eigen frequencies. In view of $\rho \ll 1$, the dipole resonance which we alone have studied is of great importance.

The complexity of the roots is caused by the damping of eigen oscillations. The reason for the damping is the radiation of energy. The oscillations are damped particularly strongly, if the refractive index of the sphere is close to the refractive index of the external medium.

We should also note that for an absorbing sphere the damping, in addition to the radiation, is connected with absorption.

CHAPTER V

LARGE PARTICLES

§ 1. Derivatives of Rays

We investigated the scattering of light by small particles ($\rho \ll 1$) above.

Let us now turn to another limiting case, the case of $\rho \gg 1$. It is very complex to obtain the precise numerical results according to the formulas given in Chapter II. We have already indicated previously that for $\rho \gg 1$ all amplitudes of partial waves up to $\ell \sim \rho$, approximately, are of the same order and, consequently, attention must be given to all of them. For example, this

means that for a drop of cloud with $a = 10\ \mu$ we must retain 120 - 150 terms in the sums (in the visible region), and for a drop of rain with $a = 100\ \mu$ we must retain 1200 terms! The calculations become practically impossible. It is apparent that we must search for some approximation methods to study this limiting case.

Drops of rain, from the viewpoint in which we are interested, differ in no way from small spherical lenses. The computations for them may successively employ the methods of geometric optics. It is natural to try and apply these methods for analyzing the scattering of light by spheres with $\rho \gg 1$. We shall show that, in actuality, in the limiting case of rather large particles the formulas given in Chapter II may be transformed to the formulas of geometric optics. Strictly speaking, this statement is not correct, and in the case $p \to \infty$ the limiting case will not hold, for example, for small angles near the forward direction ($\beta \sim \frac{1}{\rho}$). The scattering intensity within these small angles will be very large ($\sim \rho^2$). We shall investigate all these problems in greater detail later on. In this chapter we shall investigate the results which are produced by applying the elementary laws of geometric optics to our problem.

Several authors have applied geometric optics to the problem of scattering. /100 In the article by I. A. Khvostikov (Ref. 14) the reader will find references to the results of individual authors.

This problem was discussed in the greatest detail in our work (Ref. 53), which we shall follow here.

We have started with the work of academician V. V. Shuleykin (Ref. 51), (52), or (35), who studied the indicatrix of scattering by a large transparent sphere by employing the methods of geometric optics. However, unfortunately the very beginning section of his work included an error, so that certain conclusions which he indicated are incorrect.

We shall first investigate the case of a transparent, but not absorbing, sphere. We shall then turn to absorbing and absolutely reflecting particles.

In courses on meteorology, the theory of light scattering is usually studied separately from the theory of coronas and rainbows. This separation tacitly suggests to the reader that we are dealing with different problems. This point of view is incorrect. In actuality, the theory of rainbows, with all of its details, the theory of coronas, and all other phenomena related to drops or crystals are contained in the general theory of scattering. We shall establish the relationship between the scattering theory and the rainbow theory within the framework of the limiting case under consideration here. ($\frac{1}{\rho} = 0$).

Let us turn to the geometric optics of a transparent sphere. The formulas of Fresnel for the coefficients of reflection r and penetration d of light rays lie at the basis of our study. We shall divide rays with the following direction of the electric vector (direction of oscillations): (a) lying in the plane of incidence, and (b) perpendicular to the plane of incidence. We shall designate the former by p, and the latter by s.

As is well known:

$$r_s = \frac{\sin^2(\varphi - \psi)}{\sin^2(\varphi + \psi)}, \quad r_p = \frac{\mathrm{tg}^2(\varphi - \psi)}{\mathrm{tg}^2(\varphi + \psi)}; \tag{5.1}$$

$$d_s = \frac{\sin 2\varphi \cdot \sin 2\psi}{\sin^2(\varphi + \psi)}, \quad d_p = \frac{\sin 2\varphi \cdot \sin 2\psi}{\sin^2(\varphi + \psi)\cos^2(\varphi - \psi)}; \tag{5.2}$$

$$r_s + d_s = 1, \quad r_p + d_p = 1, \quad \frac{\sin\varphi}{\sin\psi} = n. \tag{5.3}$$

Here ϕ is the angle of incidence, ψ -- angle of refraction, and n -- relative refraction index. /101

For all calculations in § 2, 3, 4, we shall disregard light absorption in a drop, and shall assume that n = 1.33000. This approximately corresponds to the refractive index in water for the red line $\lambda_c = 0.656$ μ in the case ρ = 20°C.

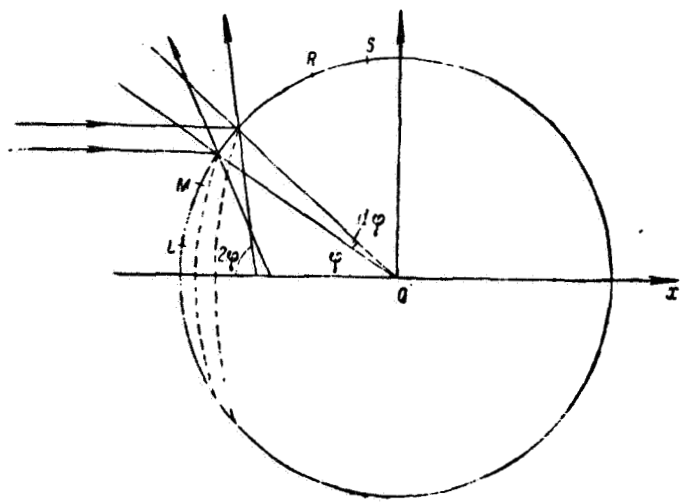

Figure 18. Incidence of a Plane Bundle of Rays on a Drop.

Let us investigate a spherical drop, on which a parallel bundle of natural light falls in the direction OX (Figure 18).

Let us separate some of the planes passing through the center of the drop and containing the direction OX. We shall call all the rays leaving the drop derivatives of the ray which first falls on the drop. The reflected ray will be the first derivative, the ray which is refracted twice will be the second derivative, etc.

Let us enumerate the apparent properties of the derivatives of the rays.

1. All the derivatives of the ray which lies in our plane initially will lie in the same plane. Therefore, we shall confine ourselves to studying the manner in which the scattered light is distributed over the scattering angles in the plane which we have selected.

The OX direction is the axis of the cylindrical symmetry of the problem. /102
We should note that if we are discussing the scattering of linearly polarized light, just as previously the problem would become a plane problem, but the cylindrical symmetry would naturally be absent. The s and p components in the incident bundle would be different. If the plane under consideration formed the angle ϕ with the direction of oscillations in the incident bundle, we would then obtain

$$I_s^0 = I^0 \sin^2 \varphi; \quad I_p^0 = I^0 \cos^2 \varphi.$$

Here I^0 is the intensity of incident light, I_s^0 and I_p^0 -- intensities of the s and p components in it.

In natural light, the angle ϕ changes continuously, and the mean values I_s^0 and I_p^0 are the same and equal $\frac{1}{2} I^0$.

2. All derivatives of a p-ray are p-rays; all derivatives of a s-ray are s-rays.

3. All derivatives of a ray falling on a drop at the angle ϕ leave the drop at the same angle ϕ.

4. Let the incident ray intersect the surface of the drop at a point whose polar angle is θ (the angles are read off from the direction OX counterclockwise). If $\theta > \pi$, i.e., if the ray intersects the drop in its lower part, its subsequent derivatives begin from the points with polar angles θ, $\theta + \mu$, $\theta + 2\mu$,.. If $\theta < \pi$, i.e., if the initial ray intersects the drop in its upper part, then its subsequent derivatives begin from the points with the polar angles θ, $\theta - \mu$, $\theta - 2\mu$, ... Here $\mu = \pi - 2\psi$.

Thus, the point at which the derivatives of the lower ray begin moves along the circumference counterclockwise, and the point at which the derivatives of the upper section begin moves clockwise. It may be readily seen that the angle of turn of a ray of the kth order may be determined according to the following general formula:

$$\beta^{(k)} = (k-2)\pi + 2[\varphi - (k-1)\psi].^{1} \tag{5.4}$$

5. All the derivatives of this ray have the same "thickness" as the /103
incident ray. Consequently, the following equation holds

$$I^0 = I^{(1)} + I^{(2)} + I^{(3)} + \ldots$$

Here I^0 is the intensity of the initial ray, and $I^{(k)}$ -- the intensity of its kth derivative.

§ 2. Reflected and Refracted Light

Let us investigate the three-dimensional distribution of reflected ray

(1) The angle of turn for derivatives of the lower rays are read off from these rays counterclockwise, and the angles of turn for the derivatives of the upper rays are read off clockwise, i.e., in those directions in which these derivatives actually turn ($k \neq 1$).

intensities. The scattering angle β for the reflected ray is related to the angle of incidence ϕ by the following relationship

$$\beta^{(1)} = \pi - 2\varphi. \tag{5.5}$$

We should note that essentially different results are obtained, depending on where we study the scattered light intensity -- immediately next to the drop, i.e., in the case $R - a \ll a$, or far from the drop -- i.e., in the case $R \gg a$ (R -- distance from the center of the drop to the observer).

In the first case, we can regard the drop as a plane drop. It may be readily seen that in this case the intensity of light reflected by different illuminated sections of the drop will not depend on their intensity at all, and will equal the product of the incident light intensity and the reflection coefficient. The intensity of light on the shady side will equal zero.

In actuality, a different amount of energy will naturally fall on similar areas which are distributed in an identical manner at different latitudes -- for example, LM and RS (see Figure 18). This is simply due to the fact that the width of the corresponding bundles will be different. However, since the bundle width does not change during reflection, then -- for example, in the polar regions (RS) where very narrow bundles fall -- all the reflected energy will also be transmitted in very narrow bundles, so that the intensity of scattered light will not depend on $\cos\phi$, and will change proportionally to r:

$$I^{(1)} = rI^{0}.\ ^{1}$$

Let us now investigate the intensity distribution of scattered light at large distances from the drop ($R \gg a$). /104

We may draw a concentric sphere with the radius R around the drop.

In addition, let us investigate a circular band on our drop which has the angular width $d\phi$ (Figure 18).

The area of this band is $dS_0 = 2\pi a^2 \sin\phi\, d\phi$. The flux of light falling on this band will be

$$dF^{(0)} = I^{(0)} \cos\varphi\, dS_0.$$

The flux reflected from this band will be

$$dF^{(1)} = r\, dF^{(0)} = rI^{(0)} 2\pi a^2 \cos\varphi \sin\varphi\, d\varphi.$$

This entire flux will be scattered (reflected) into the solid angle $d\Omega$ located between the scattering angles $\beta(1)$ and $\beta(1) + d\beta(1)$.

The magnitude of this solid angle will be: $2\pi \sin\beta(1)\, d\beta(1)$. In view of (5.6), we have $d\beta(1) = -2d\phi$ and, consequently,

$$|d\Omega| = 8\pi \cos\varphi \sin\varphi\, d\varphi.$$

---

(1) Therefore, the introduction of the factor $\cos\phi$ into the corresponding formulas in (Ref. 35) is erroneous.

On the observational sphere (its radius is R), this solid angle defines a band with the area $dS = R^2|d\Omega|$, on which light falls which is reflected by the band on the drop. Consequently, the scattered light intensity at the observation point will be

$$I^{(1)} = \frac{dF^{(1)}}{dS} = \frac{a^2}{4R^2} I^{(0)} \cdot r. \tag{5.6}$$

The latter formula provides the solution of the formulated problem.

The intensity of light reflected by a drop in a certain direction is proportional to the square of the drop radius and the reflection coefficient, and does not depend directly upon cos ϕ.

The quantity $4R^2/a^2$ characterizes the geometric turn of the initial plane bundle. The smaller the drop, the smaller the amount of light it turns into the same solid angle, and the smaller the scattering intensity per unit of solid angle $(I^{(1)}R^2)$. This demonstrates the physical meaning of the dependence of I upon the size of the drop a^2.

For the scattering indicatrix of s, p-rays $(\gamma_{s,p})$, we obtain:

$$\gamma^{(1)}_{s,p} = I^{(1)}_{s,p} R^2 = \frac{a^2}{4} I^{(0)}_{s,p} r_{s,p}. \tag{5.7}$$

The total indicatrix and the degree of polarization in the case of natural light will be as follows: /105

$$\gamma^{(1)} = \frac{a^2}{4} \frac{1}{2} I^0 (r_s + r_p), \tag{5.8}$$

$$p^{(1)} = \frac{r_s - r_p}{r_s + r_p}. \tag{5.9}$$

For the computations, it is advantageous to regard the indicatrix directly as a function of the scattering angle. By means of formulas (5.1) - (5.3), we may readily obtain the expression for r_s and r_p as a function of only the angle of incidence ϕ:

$$r_s = \left(\frac{\cos\varphi - \sqrt{n^2 - \sin^2\varphi}}{\cos\varphi + \sqrt{n^2 - \sin^2\varphi}}\right)^2; \quad r_p = \left(\frac{n^2\cos\varphi - \sqrt{n^2 - \sin^2\varphi}}{n^2\cos\varphi + \sqrt{n^2 - \sin^2\varphi}}\right)^2. \tag{5.10}$$

From (5.6), we thus have

$$\left.\begin{aligned} \gamma^{(1)}_s &= \frac{a^2}{4} I^0_s \left(\frac{\sin\frac{\beta^{(1)}}{2} - \sqrt{n^2 - \cos^2\frac{\beta^{(1)}}{2}}}{\sin\frac{\beta^{(1)}}{2} + \sqrt{n^2 - \cos^2\frac{\beta^{(1)}}{2}}}\right)^2; \\ \gamma^{(1)}_p &= \frac{a^2}{4} I^0_p \left(\frac{n^2\sin\frac{\beta^{(1)}}{2} - \sqrt{n^2 - \cos^2\frac{\beta^{(1)}}{2}}}{n^2\sin\frac{\beta^{(1)}}{2} + \sqrt{n^2 - \cos^2\frac{\beta^{(1)}}{2}}}\right)^2. \end{aligned}\right\} \tag{5.11}$$

The formulas for $\gamma^{(1)}$ and $p^{(1)}$[1] can be transformed in a similar manner.

---

[1] Formulas (5.11) are also suitable, because -- in contrast to formula (5.1) -- they do not lose any meaning in the case $\beta^{(1)} = \pi$ (for $\phi = 0$):

$$r_s(\pi) = r_p(\pi) = \left(\frac{n-1}{n+1}\right)^2.$$

In Tables 10 and 11 (pages 91 and 93), we have presented the values of r_s and r_p as functions of the scattering angle β (the second columns). Figure 19 shows the scattering indicatrix. The outer curve expresses the total scattering indicatrix $\gamma^{(1)}$. The inner curve expresses the scattering indicatrix of p-rays -- $\gamma_p^{(1)}$. We may see that our curve differs significantly from the indicatrix given (Ref. 35). Figure 20 presents a graph showing the degree of polarization of reflected light $p^{(1)}(\beta)$ (curve 1). The total polarization is obtained for a Brewster angle of incidence ϕ = arc tg n = 53°3'40.5".

This corresponds to the scattering angle $\beta_1^{(1)}$, for which the numerator /106
vanishes at $\gamma_p^{(1)}$ [formula (5.11)], $\beta_1^{(1)} = \arcsin \frac{1}{\sqrt{2n^2+1}}$. In our case, $\beta_1^{(1)}$ = 73°52'39". At this angle, the p-component vanishes.

Let us now investigate the intensity distribution of rays which are refracted twice. After two refractions, the angle of turn -- i.e., the scattering angle -- will be:

$$\beta^{(2)} = 2(\varphi - \psi). \tag{5.12}$$

We may readily see from formula (5.3) that the ray may turn by a maximum of 82.5° as the result of two refractions.

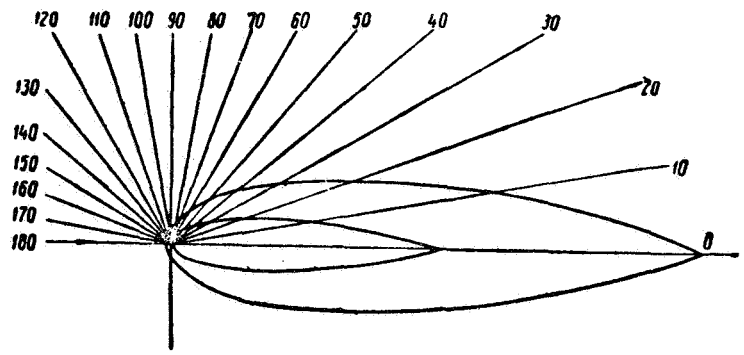

Figure 19. Indicatrix Taking only Reflected Light into Consideration.

Thus, light which is refracted twice is directed forward, and is located within the cone with the angle of turn 82.5°. The following flux, which falls on the circular band of the drop with the angular width $d\phi$, leaves the total flux dF^0 after two refractions

$$dF^{(2)} = d^2 \cdot dF^{(0)}.$$

All of this flux on the observational sphere R arrives on the surface

$$dS^{(2)} = R^2 2\pi \sin\beta^{(2)} d\beta^{(2)}.$$

Employing relationship (5.12), we obtain

$$dS^{(2)} = R^2 2\pi \sin\beta^{(2)} 2d\varphi\left(1 - \frac{1}{n}\frac{\cos\varphi}{\cos\psi}\right).$$

We have employed the following formula here /107

$$d\psi = \frac{1}{n}\frac{\cos\varphi}{\cos\psi}d\varphi,$$

which is obtained by differentiation of (5.3).

The intensity of light which is refracted twice will be:

$$I^{(2)} = \frac{dF^{(2)}}{dS^{(2)}} = \frac{a^2}{4R^2} I^0 \frac{d^2 \sin 2\varphi}{\sin\beta^{(2)}\left[1 - \frac{1}{n}\frac{\cos\varphi}{\cos\psi}\right]}. \tag{5.13}$$

Let us introduce the following notation

$$\theta^{(k)} = \frac{\sin 2\varphi}{\sin\beta^{(k)}\left[1 - \frac{k-1}{n}\frac{\cos\varphi}{\cos\psi}\right]}. \tag{5.14}$$

We obtain the following for the indicatrixes of s- and p-rays, having in mind only light which is refracted twice:

$$\gamma^{(2)}_{s,p} = \frac{a^2}{4} I^0_{s,p}\, d^2_{s,p}\, \theta^{(2)}. \tag{5.15}$$

Formulas (5.15) determine the indicatrix as a function of the angle of incidence ϕ. Employing (5.12), (5.3) - (5.1), we may calculate the indicatrix as a function of the scattering angle $\beta^{(2)}$. We here obtain:

$$\left.\begin{aligned} \gamma^{(2)}_s &= \frac{a^2}{4} I^0_s\, \alpha^4 \cdot \frac{(nq-1)^3(n-q)^3}{q(n^2+1-2nq)^2}; \\ \gamma^{(2)}_p &= \frac{a^2}{4} I^0_p\, \alpha^4 \cdot \frac{(nq-1)^3(n-q)^3}{q^5(n^2+1-2nq)^2}, \end{aligned}\right\} \tag{5.16}$$

where $q = \cos\frac{\beta^{(2)}}{2}$, $\alpha = \frac{2n}{n^2-1}$.

Table 10 presents the results of computations using these formulas for s-rays, and Table 11 presents the computation results for p-rays (third column).

The total indicatrix of light which is refracted twice will be

$$\gamma^{(2)} = \frac{a^2}{4}\cdot\frac{I^0}{2}\cdot\alpha^4\frac{(nq-1)^3(n-q)^3}{q(n^2+1-2nq)^2}\left(1+\frac{1}{q^4}\right), \tag{5.17}$$

and the degree of polarization for this light is determined by the following formula

$$p^{(2)} = \frac{\cos^4\frac{\beta^{(2)}}{2} - 1}{\cos^4\frac{\beta^{(2)}}{2} + 1}. \tag{5.18}$$

Thus, light which is refracted twice at all angles is polarized negatively. /108 A graph of $p^{(2)}(\beta)$ is shown in Figure 20 (curve 2).

When both reflection and refraction are taken into account, the scattering indicatrixes of s- and p-rays, respectively, will be

$$\left.\begin{aligned} \gamma_s &= \frac{a^2}{4} I^0_s\left\{\left(\frac{\sqrt{1-q^2}-\sqrt{n^2-q^2}}{\sqrt{1-q^2}+\sqrt{n^2-q^2}}\right)^2 + \alpha^4\frac{(nq-1)^3(n-q)^3}{q(n^2+1-2nq)^2}\right\}, \\ \gamma_p &= \frac{a^2}{4} I^0_p\left\{\left(\frac{n^2\sqrt{1-q^2}-\sqrt{n^2-q^2}}{n^2\sqrt{1-q^2}+\sqrt{n^2-q^2}}\right)^2 + \alpha^4\frac{(nq-1)^3(n-q)^3}{q^5(n^2+1-2nq)^2}\right\}. \end{aligned}\right\} \tag{5.19}$$

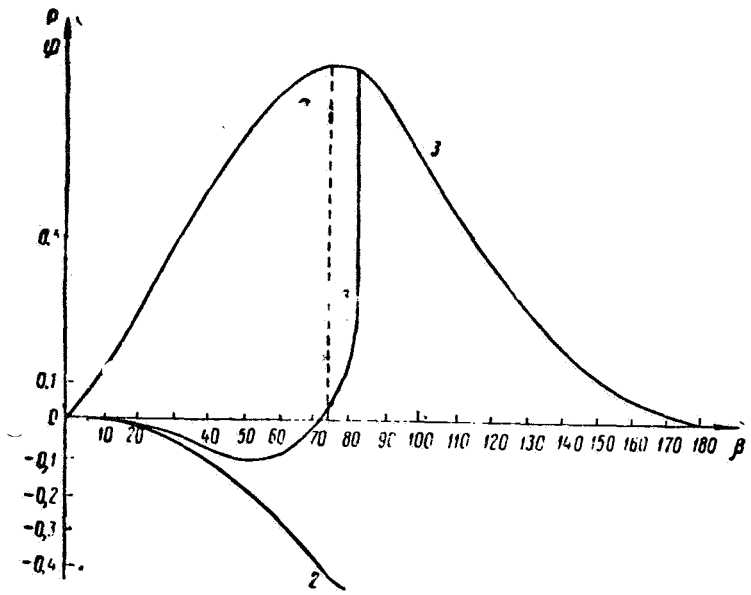

Figure 20. Polarization of Reflected and Refracted Bundles.

(1) - Polarization of a reflected bundle; (2) - Polarization of a refracted bundle; (3) - Polarization when both phenomena are taken into account.

Here $q = \cos\beta/2$, where β is the scattering angle.

Thus, in the second terms (in the parentheses) we may substitute only those angles β at which these terms will be positive $\left|0 \leqq \beta \leqq 2 \text{ arc cos } \frac{1}{n}\right|$. /109

The complete formulas for the indicatrix and the degree of polarization can be written, but due to their cumbersome nature we shall not write them here.

The graphs for $\gamma^{(2)}$ and $\gamma^{(2)} + \gamma^{(1)}$ are shown in Figure 21 ($\gamma^{(2)}$ is the inner curve, and $\gamma^{(2)} + \gamma^{(1)}$ is the outer curve).

§ 3. Light Undergoing Internal Reflections. Rainbows

Let us examine the intensity distribution of the third, fourth, and higher derivatives of rays. This pertains to rays undergoing one, two, and more internal reflections in a drop. The scattering angle for the kth derivative is determined according to the formula (5.4).

We should note that the angles $\beta^{(k)}$, computed according to this formula, are very large. This is simply related to the fact that, in the case of derivatives of higher orders, the ray turns several times within the drop before leaving for the outside. In actuality, the scattering angles $\beta^{(k)}$ must lie /110 within the limits $(0, \pi)$. This may always be achieved by subtracting the total

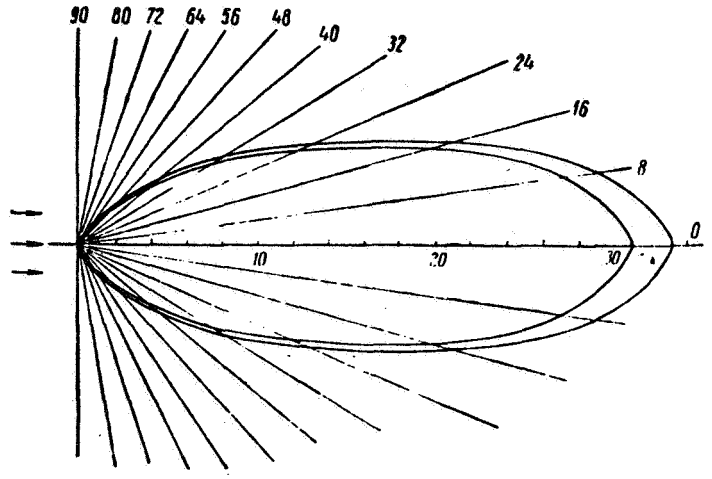

Figure 21. Indicatrix of Refracted and Reflected Light (Inner Curve -- Refracted Bundle; Outer Curve -- Composite).

number of turns and replacing the angle x by the angle 360 - x, which is equivalent to it (due to cylindrical symmetry).

Let us now calculate the intensities.

Just as previously, we find that, if $dF^{(0)}$ is the flux which initially falls on the band of a drop having the width $d\phi$, then the portion of it leaving the drop in the rays of $k^{\underline{th}}$ order will be

$$dF^{(0)} \cdot r^{k-2} d^2.$$

The three-dimensional intensity distribution of $k^{\underline{th}}$ derivatives of the rays may be determined by the following formula

$$I = \frac{dF^{(0)} \cdot r^{k-2} d^2}{dS^{(k)}}.$$

Here $dS^{(k)}$ is the area of that section of the observational sphere which is struck by the $k^{\underline{th}}$ derivatives of the waves which initially fall on the band $d\phi$. We apparently have:

$$dS^{(k)} = 2\pi R^2 \sin \beta^{(k)} d\beta^{(k)};$$

$$d\beta^{(k)} = \frac{d\beta^{(k)}}{d\varphi} d\varphi = 2\left[1 - \frac{(k-1)}{n} \frac{\cos\varphi}{\cos\psi}\right] d\varphi.$$

For high orders, $d\beta^{(k)}/d\phi$ vanishes at certain angles (shown in the second column of Table 8), changing the plus sign into a minus sign when ϕ changes from 90° to 0°. The extreme scattering angles for derivatives of the corresponding orders consequently correspond to these angles. They determine the position of the rainbow (this will be discussed in greater detail at a later point).

The change in the sign of $d\beta^{(k)}/d\phi$ is related to the fact that at high

orders some scattering angles which are adjacent to the rainbow direction pass two times in the forward and reverse directions when ϕ changes.

In addition, when the ray makes complete turns in the drop at high orders, the entire region of the scattering angle is traversed several times. Thus, for example, the region 22°27'36" - 16°50'52" is overlapped 5 times for derivatives of order ten. The entire remaining region (22°27'36" - 180°) is overlapped four times, etc.

We shall not direct our attention to the sign of $d\beta^{(k)}/d\phi$ in the calcula- /111 tions, and in the final result we shall take the fact into account that, for all scattering angles $\beta^{(k)}$ which appear several times, the corresponding intensities must be summed. For the intensity $I^{(k)}$, we obtain

$$I^{(k)} = \frac{dF^{(0)} \cdot r^{k-2} d^2}{2\pi \sin \beta^{(k)} \, |d\beta^{(k)}/d\varphi| \, d\varphi} = \frac{a^2}{4R^2} I^{(0)} r^{k-2} d^2 |\theta^{(k)}|. \tag{5.20}$$

The quantity $\frac{4R^2}{a^2|\theta(k)|}$ determines the geometric turn of rays in the $k^{\underline{th}}$ order.

This formula determines the three-dimensional intensity distribution of the $k^{\underline{th}}$ derivatives of rays. Thus, the intensity is determined as a function of the angles of incidence of initial rays ϕ.

The formula (5.20) pertains in equal measure both to s and to p-rays.

For certain scattering directions, it leads to infinite intensities. This pertains to those directions for which the denominator in $\theta^{(k)}$ vanishes.

Let us first investigate the case in which $\sin \beta^{(k)}$ vanishes. This occurs in the case $\beta^{(k)} = 0$ or π, i.e., in the forward and backward directions. We readily find from formula (5.4) that scattering forward and backward occurs for all k for $\phi = 0$ (forward -- in the case of even k, and backward in the case of odd k) and for $k \geq 5$ in the case of certain $\phi \neq 0$. In the first case ($\phi = 0$) $\theta^{(k)}$ has an indefinite value ($\sin 2\phi = 0$) is included in the numerator). These indeterminancies may be readily computed, and lead to the following formula

$$\lim_{\varphi \to 0} \theta^{(k)} = \frac{(-1)^k n^2}{[n-k+1]^2}.$$

Thus, this case does not yield infinity. On the other hand, the second case ($\phi \neq 0$) leads to infinite intensities. Within an accuracy of 1°, the corresponding values of ϕ for different k are as follows:

$k =$	5	6	7	8	9	10
$\beta^{(k)} =$	0	180	180 0	0 180	0 180 0	180 0 180
$\varphi =$	50	34	58 26	45 21	62 37 18	51 32 16

The occurrence of infinite intensities in our formulas indicates that geometric optics is a poor model in the corresponding directions, and the correct values /112 for the intensity may be obtained only by taking into account the wave properties of light (diffraction).[1]

(1) This statement pertains to the idealized case investigated in the book -- (continued on the following page).

We have already indicated previously the significant importance of diffraction for determining intensity in the case of small angles in the forward direction.

We would like to stress that a new phenomenon occurs here -- the significant importance of diffraction for determining the intensity distribution around the backward direction -- backward diffraction. We should note that this important fact occurs only in the sixth order.

Let us now investigate the physical consequences of the fact that the parentheses vanish in the denominator of $\theta^{(k)}$

It may be seen from the general formulas given above that, in the three-dimensional distribution of derivatives of rays of the third and higher orders, there is one feature which sharply distinguishes the distribution of these derivatives from the first two.

For each of these rays there is one direction for which the parenthesis in the denominator of $\theta^{(k)}$ vanishes, and consequently the scattering intensity becomes infinite.

These directions may be determined from the condition:

$$1-\frac{k-1}{n}\frac{\cos^2\varphi}{\cos\psi}=0,$$

which may be rewritten in the following form

$$\cos\varphi=\sqrt{\frac{n^2-1}{k^2-2k}}. \tag{5.21}$$

This coincides with the well known condition determining the position of rainbows. The scattering intensity becomes infinitely large for the rainbow direction.

The distribution of different rainbows in space, up to eight inclusively, /113 is shown in Table 8.

It may be seen from the table that, when the order of the rainbow increases, the angles of incidence of the initial angle ϕ, giving the rainbow in the given order, increase, striving to $\phi' = \frac{\pi}{2}$.

Thus, the refraction angles will also increase and strive to $\psi' = 48°45'08''$. This may be seen analytically.

For large k, we have

---

(1) continued: scattering of a plane flux. As Professor A. A. Gershun has noted, the infinities vanish if we take into account the finite angular dimensions of the source. The order of the infinities appearing here is determined by the inverse value of these angular dimensions.

$$\left.\begin{aligned} &\cos\varphi \doteq \frac{\sqrt{n^2-1}}{k-1}; \quad \varphi \doteq \varphi' - \frac{\sqrt{n^2-1}}{k-1}; \\ &\cos\psi \doteq \frac{\sqrt{n^2-1}}{n}\left(1+\frac{1}{2(k-1)^2}\right); \ \psi \doteq \psi' - \frac{\sqrt{n^2-1}}{2(k-1)^2}. \end{aligned}\right\} \tag{5.22}$$

TABLE 8

k	$\varphi_{rain.}$	$\beta^{(k)}_{rain.}$	$r_s^{k-2} d_s^2$	$r_p^{k-2} d_p^2$	$\frac{r_s^{k-2} d_s^2}{r_p^{k-2} d_p^2}$	p_k in %
3	59°35′06″	137°28′52″	0,08794	0,00377	23,08	91,78
4	71 56 22	129 53 58	0,03516	0,00381	9,23	80,45
5	76 54 52	42 52 40	0,01937	0,00247	7,82	77,34
6	79 41 20	42 17 40	0,00901	0,00163	5,52	69,33
7	81 28 35	126 31 10	0,00832	0,00119	6,99	74,99
8	82 43 44	149 46 26	0,00486	0,00088	5,51	69,12
9	83 39 26	66 21 56	0,00465	0,00072	6,42	73,04
10	84 22 26	16 50 52	0,00367	0,00058	6,27	72,35

Employing the general formula (5.4) for $\beta^{(k)}$, we find that the distribution of rainbows having higher orders in space is approximately determined by this formula, if we substitute the following expressions obtained above in this formula, instead of ϕ and ψ:

$$\beta^{(k)}_{rain.} = (k-1)\pi - 2(k-1)\psi' - \frac{\sqrt{n^2-1}}{k-1}. \tag{5.23}$$

In the case k = 10, this formula determines $\beta^{(k)}_{rain.}$ within an accuracy of 3'.

For odd rainbows ($k = 2\ell + 1$), we have:

$$\beta^{(2l+1)}_{rain.} = -4\psi' l - \frac{\sqrt{n^2-1}}{2l},$$

or, for large ℓ: /114

$$\beta^{(2l+1)}_{rain.} \doteq -4\psi' l.$$

For even rainbows [$k = 2(\ell + 1)$]:

$$\beta^{(2l+2)}_{rain.} = \pi - 2(2l-1)\psi' - \frac{\sqrt{n^2-1}}{2l+1},$$

or for large ℓ:

$$\beta^{(2l+2)}_{rain.} \doteq \pi + 2\psi' - 4\psi' l.$$

Thus, the directions of both odd and even order rainbows, for sufficiently large ℓ, rotate in space, turning by the angle $4\Psi'$ with an increase in the order ℓ. Thus, even order rainbows are displaced by the angle $\pi + 2\psi'$ with respect to odd order rainbows. We should note that it is impossible for the directions of rainbows to coincide precisely for different orders, due to the transcendent nature of the angle ψ'.

In the rainbow directions, the scattering indicatrix (in the approximation under consideration of geometric optics) will have infinite rays. Thus, the

intensity will be very small for derivatives of the corresponding order, if we deviate a little from the rainbow direction (see Tables 10 and 11), since the total flux included in the derivatives of any orders is finite. It rapidly decreases with an increase in the order, so that light is primarily scattered by drops at low orders (see Table 9).

Let us employ I' and I" to designate all the quantities, except for those which pertain to k-th rays, in the formula for the degree of polarization of scattered light p:

$$p = \frac{I' + \theta^{(k)}(r_s^{k-2} d_s^2 - r_p^{k-2} d_p^2)}{I'' + \theta^{(k)}(r_s^{k-2} d_s^2 + r_p^{k-2} d_p^2)}.$$

In the direction of a rainbow of the (k - 2)-order, the quantities I' and I" are finite, whereas $\theta^{(k)}$ is infinitely large. Disregarding the quantities I' and I", we consequently find that the degree of polarization of light in a rainbow of the (k - 2)-order is determined by the following formula

$$p_k = \frac{r_s^{k-2} d_s^2 - r_p^{k-2} d_p^2}{r_s^{k-2} d_s^2 + r_p^{k-2} d_p^2}. \tag{5.24}$$

Employing the relationship (5.21) and formulas (5.10), we readily find that /115
r_s and r_p for a ray leading to the rainbow will be:

$$r_s = \left(\frac{k-2}{k}\right)^2;$$

$$r_p = \left(\frac{k-1-n^2}{k-1+n^2}\right)^2.$$

This enables us to rewrite formula (5.24) for p_k as follows:

$$p_k = \frac{A-1}{A+1},$$

$$A(n, k) = \frac{d_s^2 r_s^{k-2}}{d_p^2 r_p^{k-2}} = \left(\frac{k-1+n^2}{nk}\right)^4 \left[\frac{(k-2)(k-1+n^2)}{k(k-1-n^2)}\right]^{2k-4}. \tag{5.24*}$$

Formula (5.24*) is much more suitable than (5.24), since it enables us to calculate p_k for particles of different substances and for rainbows of different orders directly in terms of n and k. The quantity A is the ratio of the transverse oscillation intensities in the rainbow to the longitudinal oscillation intensities.

Table 8 presents the values of the quantities p_k for rainbows of different orders. Attention should be called to the high degree of light polarization in the rainbows. The intensity of transverse oscillations exceeds the intensity of longitudinal oscillations by a factor of 5.5 (see Table 8, next to the last column).

P. N. Chirvinskiy (Ref. 54) has investigated the degree of light polarization in the first rainbow. After observing the rainbow through a Nicol prism

he established the fact that when the Nicol prism was at a certain position, the "rainbow completely disappeared. This indicates that its light is not polarized weakly, but very completely". Unfortunately, he did not make any quantitative measurements.

In conclusion, let us turn to the nature of the infinities occurring in the formulas of geometric optics. The infinities in the directions $\beta = 0$ and π are simply related to the fact that in these directions diffraction around the drop contours, diffraction forward or backward, is of essential importance. At first glance, the infinite intensities occurring in the rainbow directions are less understandable. However, the situation here is due to diffraction. Due to the purely geometric properties of a spherical surface, the scattering /116 angles of rays for orders of $k > 2$ are sharply limited by the rainbow directions (by the angles $\beta^{(k)}_{\text{rain.}}$). Every limitation upon the wave leads to diffraction around the limiting edge. In actuality, the intensity distribution in the rainbow is very similar to the intensity distribution in the case of diffraction at the edge of an infinite half-plane.

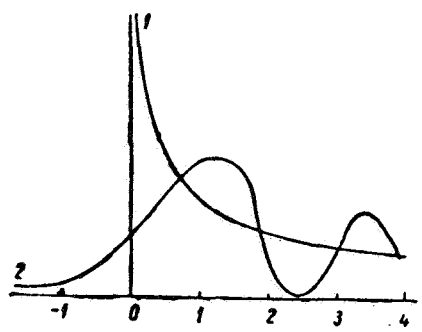

Figure 22. Intensity Distribution in the Rainbow.

(1) - According to geometric optics; (2) - According to wave theory. Quantities which are proportional to the angles of deviation from the rainbow direction are shown along the abscissa axis.

When one moves far into the geometric shade, the intensity of light in this case decreases monotonically, whereas in the illuminated region it -- while oscillating -- strives to a constant value.[1] Intensity is distributed in a similar manner according to the Airy theory in the case of rainbows. In the case of transition to angles which are less than the angle of minimum deviation, the intensity decreases monotonically, whereas for angles which are larger than the minimum angle, it oscillates, being damped. In Figure 22 we schematically present the intensity distribution around the rainbow directions according to geometric optics (curve 1) and according to the diffraction theory of Airy (curve 2).

§ 4. Energy Distribution Between Different Fluxes /117

Let us investigate the problem regarding what portion of the entire light flux falling on a drop is reflected from it, what portion penetrates it, being refracted twice or undergoing a certain number of internal reflections.

The total flux falling on a drop is $F^{(0)} = I^{(0)}\pi a^2$. The quantity $dF^{(0)}$ arrives at a circular band with the angular width $d\phi$ (see § 2).

---

(1) We should note that several excellent experimental investigations of this phenomenon have been made by V. K. Arkad'yev. They are included in all courses on optics.

The flux reflected by this band will be $rdF^{(0)}$; the flux which is refracted twice will be $d^2dF^{(0)}$; the flux undergoing one internal reflection will be $rd^2dF^{(0)}$, etc.

Consequently, the unknown portions of light flux in scattered rays of different orders may be expressed by the following formula

$$\left.\begin{aligned} R^{(1)}(n) &= \frac{1}{F^{(0)}}\int r\,dF^{(0)} = \int_0^{\pi/2} r(\varphi)\sin 2\varphi\,d\varphi, \\ R^{(k)}(n) &= \frac{1}{F^{(0)}}\int r^{k-2}d^2\,dF^{(0)} = \int_0^{\pi/2} r^{k-2}d^2\sin 2\varphi\,d\varphi \\ &\qquad (k=2,\ 3,\ \ldots). \end{aligned}\right\} \tag{5.25}$$

These formulas may be equally applied both to s- and p-rays.

For s-rays, the quantities $R_s^{(k)}$ may be readily calculated in general form.

Let us introduce the following quantities into the investigation

$$\psi_k = \int_0^{\pi/2} r_s^k \sin 2\varphi\,d\varphi.$$

We have the following from formulas (5.25)

$$\left.\begin{aligned} R_s^{(1)} &= \psi_1; \\ R_s^{(k)} &= \psi_{k-2} - 2\psi_{k-1} + \psi_k. \end{aligned}\right\} \tag{5.26}$$

In order to calculate ψ_k, we shall transform the integral to a new variable $y = \sqrt{r_s}$.

We readily obtain: /118

$$\begin{aligned} \psi_k &= \frac{n^2-1}{4}\int_0^1 y^{2(k-1)}(1-y^2)\,dy = \\ &= \frac{(n^2-1)}{4(2k-1)(2k+1)}\{2-\beta^{2k-1}[2k+1-\beta^2(2k-1)]\}, \end{aligned} \tag{5.27}$$

where

$$\beta = \frac{n-1}{n+1}\ (y=\beta \text{ for } \varphi=0).$$

For the quantity R_s, we now have

$$\left.\begin{aligned} R_s^{(1)} &= \frac{n^2-1}{12}\left\{2-\left(\frac{n-1}{n+1}\right)\left[3-\left(\frac{n-1}{n+1}\right)^2\right]\right\}; \\ R_s^{(2)} &= 1-\frac{n^2-1}{60}\left\{18-30\left(\frac{n-1}{n+1}\right)+15\left(\frac{n-1}{n+1}\right)^3-5\left(\frac{n-1}{n+1}\right)^5\right\} \end{aligned}\right\} \tag{5.28}$$

and so on.

For large k, we may disregard the term containing β^{3k-1} in the formula for

ψ_k, since β is a small quantity. Thus, for example, in our case $\beta = 0.1416$ and $\beta^7 = 1.432 \cdot 10^{-6}$. Consequently, if we wish to confine ourselves to an accuracy of 10^{-5}, beginning with $k = 3$, we may write

$$\psi_k = \frac{n^2-1}{2(4k^2-1)} \text{ and } R_s^{(k+2)} = \frac{12(n^2-1)}{(4k^2-1)(2k+3)(2k+5)}. \tag{5.29}$$

For large k, we have

$$R_s^{(k+2)} \sim \frac{3(n^2-1)}{4k^4}.$$

Thus, for large k, the fluxes of s-rays rapidly decrease ($\sim \frac{1}{k^4}$) with an increase in k.

A calculation of the quantities $R_p^{(k)}$ (for p-rays) even for the first orders leads to cumbersome expressions.

Employing seven-place logarithmic tables of Vega, we made a numerical tabulation of the integrals included in the expression for $R_p^{(k)}$, and also for $R_s^{(k)}$. The integration interval was divided into 90 sections, every 1°. A comparison of the results derived from numerical tabulation and the values computed according to precise formulas shows that five significant digits are reliable in the numerical tabulation. The results derived from these cal- /119
culations in percents for the first ten orders are given in Table 9 both for s-and p-rays and for the complete flux.

TABLE 9. TABLE SHOWING ENERGY DISTRIBUTION BETWEEN SCATTERING OF DIFFERENT ORDERS (IN PERCENTS)

k	1	2	3	4	5	6
s-rays...	10,111	82,324	6,117	0,962	0,264	0,102
p-rays...	3,074	94,643	1,877	0,255	0,076	0,029
Combined.	6,592	88,483	3,997	0,608	0,170	0,066
k	**7**	**8**	**9**	**10**	$\sum_k$	
s-rays...	0,048	0,025	0,015	0,009	99,977	
p-rays...	0,015	0,008	0,005	0,003	99,985	
Combined.	0,032	0,016	0,010	0,006	99,981	

We may see from Table 9 that in the orders under consideration, 99.98% of the total flux falling on the drop is included; 6.6% of the flux is reflected from the drop; 88.5% penetrates through it; 4% undergoes one internal reflection, etc. In all, less than 5% of the incident flux is concentrated in rainbows of different orders.

Important conclusions may be reached from Table 9 regarding the integral accuracy of our calculations, if we confine ourselves to considering scattering of a certain order. Confining ourselves, for example, to the first and second order, we may see that we have considered 95% of the flux falling on the particle.

§ 5. Scattering Indicatrix And Degree Of Polarization For Scattered Light

We shall give the results derived from calculations for the scattering intensities of s-and p-rays according to formulas of § 3. We have performed calculations for different rays of different orders up to the tenth, inclusively. All the computations were performed by means of the logarithmic tables of Vaga, in /120 order to provide sufficient accuracy even for the last orders to be studied.

The formulas given in § 3 give scattering indicatrixes of different orders as a function of the angle of incidence ϕ. Their transformation to the scattering angles $\beta^{(k)}$, similar to the procedure followed in the ratio of the derivatives of the first two orders, is not suitable for higher orders. For orders three, the expressions become very cumbersome, and for higher orders it is apparently impossible to express the intensity of scattered rays by means of trigonometric or other tabulated functions of the scattering angle. Therefore, we calculated the intensities of the scattered rays of different orders as a function of the angle of incidence of the primary ray ϕ. These intensities were compared, in accordance with formula (5.4), to the scattering angles $\beta^{(k)}$ which were fractions. The angles $\beta(k)$ were changed to whole values by interpolation.

Since the intervals in which the argument changed were completely different in different intervals of ϕ and at different orders, interpolation was performed according to the Newton interpolation method for unequal intervals. In practically every case, it was sufficient to take into account the first differences in order to obtain the requisite degree of accuracy.

Only for regions adjacent to the rainbow in the third order, and for the second order, did we also take into account the second differences.

A comparison of the results derived from calculations of the second order, obtained by interpolation, with the results derived from direct calculations based on formulas (5.16) showed that the fourth sign after the comma was reliable.

The results of these calculations are given in Table 10 (for s-rays) and Table 11 (for p-rays).

The Tables present the quantities $\tau^{(k)}_{s,p}$ which are proportional to the intensities of scattered rays

$$\tau^{(k)}_{s,p} = \frac{4R^2}{a^2} \cdot \frac{1}{I^0_{s,p}} \cdot I^{(k)}_{s,p} = r^k_{s,p} d^2_{s,p} \left| \theta^{(k)} \right|. \tag{5.30}$$

All $\tau^{(k)}_{s,p}$ (and $I^{(k)}_{s,k}$) have several branches (as a function of the number of

overlappings of the given interval of angles $\beta^{(k)}$). Two branches have a vertical asymptote in the direction of the rainbow of the corresponding order.[1] /121

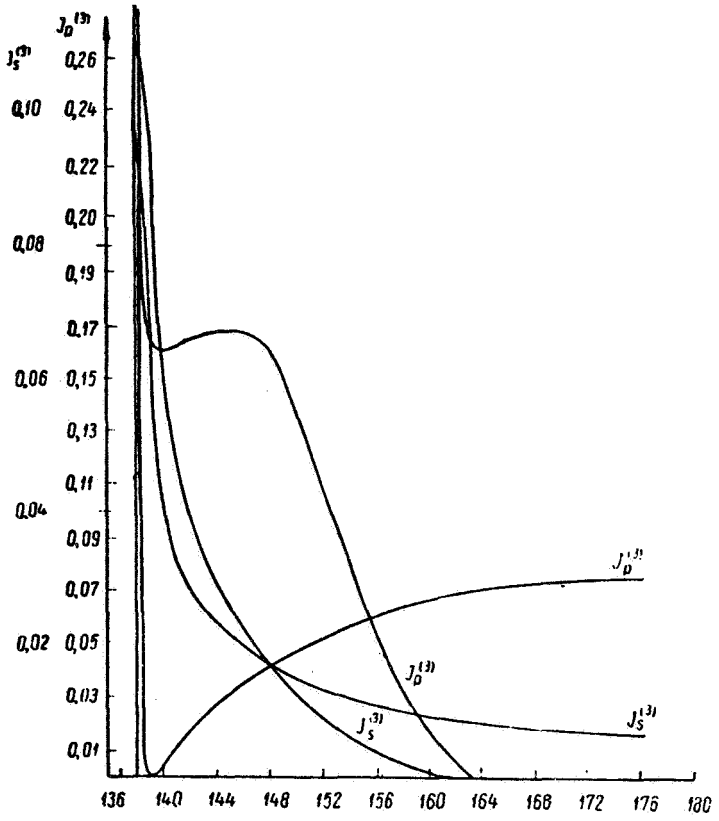

Figure 23. Angular Intensity Changes in a Bundle Forming the First Rainbow

All the $I_s^{(k)}$ may be expressed by monotonic curves. The curves of $I_s^{(3)}$ are shown in Figure 23 by way of an example.

In contrast to the s-rays, the curves $I_p^{(k)}$ for p-rays have maxima and minima, in addition to vertical asymptotes. These maxima and minima are most sharply expressed in the third order, and then gradually are smoothed out. /128

The reason for these intensity changes is the polarization in the case of internal reflections (the Brewster phenomenon). Figure 23 also shows the curves $I_p^{(3)}$.

The total scattering intensity is obtained by performing summation over

---

(1) Some of the numbers in the boxes in Tables 10 and 11 correspond to certain branches $I_{s,p}^{(k)}$. The lower number indicates the total value of $\tau_{s,p}^{(k)}$ for given β.

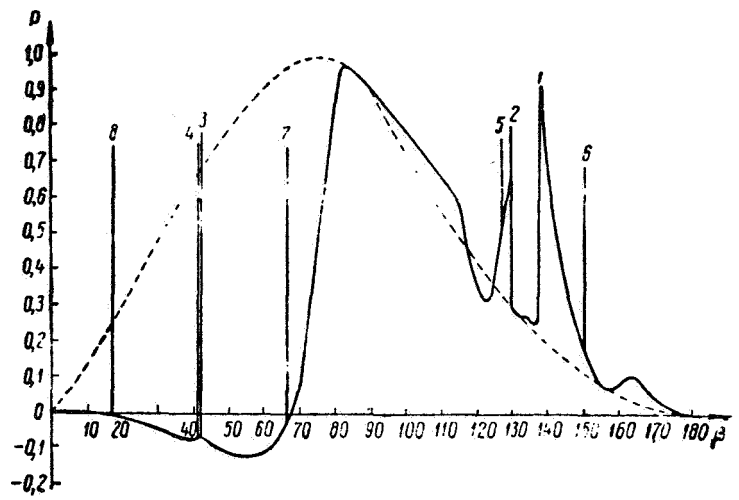

Figure 24. Total Polarization Curve with Allowance for the First Ten Bundles.
The Digits Indicate the Rainbow Number. Polarization in the Rainbows is Positive and Large.

different orders of the intensities of rays scattered at a given angle.

The data for the total τ_p, τ_s and τ are shown in Table 12:

$$\tau_p = \sum_k \tau_p^{(k)}; \quad \tau_s = \sum_k \tau_s^{(k)}; \quad \tau = \tau_s + \tau_p. \tag{5.31}$$

This table also presents the degree of polarization of scattered light p. For $\beta = 0, \pi$, we take into account only $k < 5$.

The solid curve in Figure 24 presents a graph of the quantity p.

The peaks on the curve are caused by the high degree of polarization in the rainbows (Table 8). The numbers around the peaks designate the order of the rainbows. With the exception of small angular intervals close to the rainbow and the angles 0 - 10° close to zero, the scattered light is polarized negatively at angles <68°. This fact is very important. The reason for this is negative polarization of refracted light, which is concentrated at the angles less than 80°, and contains 88.5% of the entire scattered light. /130

The superposition of high-order scattering upon simple reflection significantly changes the degree of polarization of scattered light, as follows from a comparison of the curve p for reflected light (it is shown by a dotted line in Figure 24) with the curve for the total light. The smallest polarization value occurs at the angle 55° and equals -12.35%. The largest value is displaced somewhat, as compared with its position in reflected light, to larger angles, and occurs at the angle 82°. It equals 97.2%.

The curve indicates certain maxima and minima which have a random

TABLE 10 /122

β	$\tau_\beta^{(1)}$	$\tau_\beta^{(2)}$	$\tau_\beta^{(3)}$	$\tau_\beta^{(4)}$	$\tau_\beta^{(5)}$	$\tau_\beta^{(6)}$	$\tau_\beta^{(7)}$	$\tau_\beta^{(8)}$	$\tau_\beta^{(9)}$	$\tau_\beta^{(10)}$
0	1,0000	15,5982		0,0002	∞		∞	∞	∞	∞
1	0,9610	15,5680		0,0002	0,0071 0,0037 0,0108					
2	0,9233	15,4783		0,0002	0,0057 0,0027 0,0084					
5	0,8195	14,8686		0,0002	0,0016 0,0027 0,0043					
10	0,6723	12,9519		0,0002	0,0018 0,0007 0,0025					
15	0,5525	10,4618		0,0003	0,0017 0,0003 0,0020					
20	0,4552	7,9784		0,0003	0,0019 0,0002 0,0021					0,0007 0,0008 0,0015
25	0,3762	5,8383		0,0003	0,0024 0,0001 0,0025					0,0001
30	0,3122	4,1467		0,0003	0,0037 0,0001 0,0038					
35	0,2601	2,8755		0,0003	0,0001 0,0043 0,0061 0,0105					
40	0,2180	1,9475		0,0003	0,0281 0,0157 0,0438					
45	0,1837	1,2822		0,0004		0,0105 0,0128 0,0233				
50	0,1557	0,8121		0,0004		0,0008 0,0030 0,0038				
55	0,1327	0,4861		0,0004		0,0010			0,0001	
60	0,1139	0,2670		0,0005		0,0004			0,0002	
65	0,0984	0,1278		0,0006		0,0002			0,0018 0,0013 0,0031	
70	0,0855	0,0480		0,0006		0,0001				
75	0,0749	0,0108		0,0008		0,0001				

/123

TABLE 10 (continued) /124

β	$\tau_s^{(1)}$	$\tau_s^{(2)}$	$\tau_s^{(3)}$	$\tau_s^{(4)}$	$\tau_s^{(5)}$	$\tau_s^{(6)}$	$\tau_s^{(7)}$	$\tau_s^{(8)}$	$\tau_s^{(9)}$	$\tau_s^{(10)}$
80	0,0660	0,0004		0,0009		0,0001				
85	0,0586			0,0011						
90	0,0523			0,0014						
95	0,0470			0,0018						
100	0,0426			0,0024						
105	0,0388			0,0032						
110	0,0356			0,0047						
115	0,0328			0,0010 0,0068 0,0078						
120	0,0305			0,0092 0,0115 0,0207						
125	0,0285			0,0433 0,0275 0,0708						
130	0,0268						0,0028 0,0018 0,0046			
135	0,0253						0,0005	0,0001		
140	0,0241		0,5160 0,3910 0,9070				0,0002	0,0002		
145	0,0231		0,2485 0,1980 0,4465				0,0001	0,0004 0,0007 0,0011		
150	0,0222		0,1221 0,1398 0,2619				0,0001			
155	0,0216		0,0499 0,1125 0,1624				0,0001			
160	0,0211		0,0070 0,0965 0,1035				0,0001			
165	0,0206		0,0877							
170	0,0203		0,0804							
175	0,0201		0,0771							
180	0,0201		0,0758			∞	∞	∞	∞	∞

/125

TABLE 11 /126

β	$\tau_p^{(1)}$	$\tau_p^{(2)}$	$\tau_p^{(3)}$	$\tau_p^{(4)}$	$\tau_p^{(5)}$	$\tau_p^{(6)}$	$\tau_p^{(7)}$	$\tau_p^{(8)}$	$\tau_p^{(9)}$	$\tau_p^{(10)}$
0	1,0000	15,5982		0,0002	∞		∞	∞	∞	∞
1	0,9321	15,5703		0,0002						
2	0,8686	15,4875		0,0002						
5	0,7030	14,9254		0,0002						
10	0,4931	13,1510		0,0002						
15	0,3443	10,8276		0,0002						
20	0,2386	8,4822		0,0002						0,0013
25	0,1637	6,4263		0,0002						
30	0,1107	4,7635		0,0002						
35	0,0734	3,4756		0,0002	0,0065					
40	0,0473	2,4977		0,0002	0,0165					
					0,0003					
					0,0168					
45	0,0294	1,7599		0,0002		0,0075				
						0,0001				
						0,0076				
50	0,0172	1,2036		0,0002		0,0014				
55	0,0093	0,7852		0,0002						
60	0,0044	0,4747		0,0002						
65	0,0016	0,2526		0,0001					0,0016	
70	0,0002	0,1066		0,0001						
75	0,0000	0,0272		0,0001						
80	0,0005	0,0012		0,0001						
85	0,0015			0,0001						
90	0,0027									
95	0,0042									
100	0,0057									
105	0,0073									
110	0,0088									
115	0,0103			0,0010						
120	0,0118			0,0141						
125	0,0130			0,0300						
				0,0001						
				0,0301						
130	0,0143						0,0030			
135	0,0153									
140	0,0163		0,1565							
			0,0080							
			0,1645							
145	0,0173		0,1692					0,0009		
			0,0325							
			0,2017							
150	0,0180		0,1395							
			0,0470							
			0,1865							
155	0,0185		0,0790							
			0,0580							
			0,1370							
160	0,0190		0,0215							
			0,0650							
			0,0865							
165	0,0195		0,0703							
170	0,0198		0,0732							
175	0,0200		0,0753							
180	0,0201		0,0758			∞	∞	∞	∞	∞

/127

TABLE 12. DEPENDENCE OF INTENSITY OF s- AND p-COMPONENTS, THE TOTAL INTENSITY, AND DEGREE OF POLARIZATION OF SCATTERED LIGHT UPON THE SCATTERING ANGLE

β	τ_s	τ_p	τ	p
0	16,5984	16,5984	33,1968	0,0000
1	16,5400	16,5026	33,0426	0,0011
2	16,4102	16,3563	32,7665	0,0016
5	15,6926	15,6286	31,3212	0,0020
10	13,6269	13,6443	27,2712	—0,0006
15	11,0166	11,1721	22,1887	—0,0070
20	8,4375	8,7223	17,1598	—0,0166
25	6,2174	6,5902	12,8076	—0,0291
30	4,4630	4,8744	9,3374	—0,0441
35	3,1463	3,5557	6,7020	—0,0611
40	2,2096	2,5620	4,7716	—0,0738
45	1,4896	1,7971	3,2867	—0,0935
50	0,9720	1,2224	2,1944	—0,1141
55	0,6203	0,7948	1,4151	—0,1235
60	0,3820	0,4793	0,8613	—0,1130
65	0,2301	0,2559	0,4860	—0,0530
70	0,1342	0,1069	0,2411	0,1132
75	0,0866	0,0273	0,1139	0,5206
80	0,0674	0,0018	0,0692	0,9480
85	0,0597	0,0016	0,0613	0,9478
90	0,0537	0,0027	0,0564	0,9043
95	0,0488	0,0042	0,0530	0,8415
100	0,0450	0,0057	0,0507	0,7751
105	0,0420	0,0073	0,0493	0,7038
110	0,0403	0,0088	0,0491	0,6415
115	0,0406	0,0113	0,0519	0,5645
120	0,0512	0,0259	0,0771	0,3281
125	0,0993	0,0431	0,1424	0,3947
130	0,0314	0,0173	0,0487	0,2895
135	0,0259	0,0153	0,0412	0,2572
140	0,9315	0,1808	1,1123	0,6749
145	0,4708	0,2199	0,6907	0,3632
150	0,2842	0,2045	0,4887	0,1631
155	0,1841	0,1555	0,3396	0,0842
160	0,1247	0,1055	0,2302	0,0834
165	0,1083	0,0898	0,1981	0,0934
170	0,1007	0,0930	0,1937	0,0398
175	0,0972	0,0953	0,1925	0,0098
180	0,0959	0,0959	0,1918	0,0000

distribution in general, in addition to the maxima in the directions of the rainbows.

Figure 25 presents a graph showing the total indicatrix. The inner curve gives the indicatrix for p-rays. The lines on the curve denote the directions of rainbows having different orders. Primarily all of the light is scattered /131 forward, and is concentrated within a solid angle with an opening of 65°.

The intensity of light scattered forward is 168 times greater than the intensity of light scattered backwards.

Let us calculate the amount of scattered light $F(\beta)$ which is directed within the cone, delimited by the scattering angle β. It is apparent that

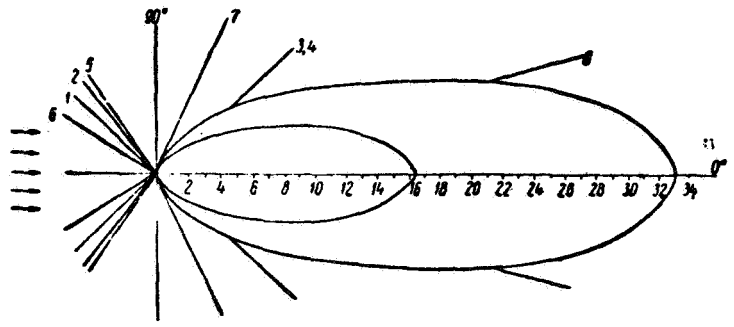

Figure 25. Indicatrix of a Transparent Drop in Terms of Geometric Optics (Lines -- Infinite Intensities in Directions of the Rainbows).

$F(0) = 0$ and $F(\pi) = \pi a^2$. The function $F(\beta)$ may be readily computed by means of Table 12. The results derived from these calculations (in fractions of the quantity πa^2) are given in Table 13, where $F' = \frac{1}{\pi a^2} F$.

TABLE 13*

β	F'	β	F'	β	F'	β	F'
0	0,000	50	0,864	100	0,946	150	0,989
10	0,118	60	0,914	110	0,948	160	0,996
20	0,365	70	0,934	120	0,951	170	0,999
30	0,597	80	0,940	130	0,957	180	1,000
40	0,763	90	0,944	140	0,969		

We may see from this table that all directions forward ($\beta = 90°$) represent 94.4% of the flux falling on the particle, and all the directions backward represent 5.6%.

Let us introduce the following notation:

$$\eta = \frac{F\left(\frac{\pi}{2}\right)}{F(\pi) - F\left(\frac{\pi}{2}\right)}. \tag{5.32}$$

We shall call the quantity η the coefficient of the indicatrix asymmetry. It is characterized by the indicatrix asymmetry and equals the ratio of the flux scattered forward to the flux scattered backward. For the Rayleigh indicatrix, $\eta = 1$; in our case, $\eta = 16.8$.

*Translator's Note: This was erroneously designated as Table 1 in the original.

When multiple scattering of light in a turbid medium is being investigated, sometimes the light field is approximately replaced by two radiation fluxes -- forward and backward.

In this case, elementary scattering may be schematized in the form of scattering only forward and backward. Asymmetry of the indicatrix η is then of /132 importance. Its magnitude roughly characterizes the form of the scattering indicatrix. For large η, for example, we may approximately assume that elementary scattering only takes place in the forward direction.

The fact that the wave effects have not been taken into account represents a significant limitation on the applicability of the results indicated above.

In certain directions, the intensity distribution essentially is determined by the wave properties of light. These represent the directions in which rainbows are observed, and also the directions forward and backward.

Since the number of rainbows is infinite, this means that the scattering indicatrix, calculated according to the formulas of geometric optics, represents a function which becomes infinite a countless number of times in the finite segment $(0, \pi)$.

In order to apply the computations performed here, it is important to note, however, that not only the total area included within all infinite branches is finite (for rainbows, it is less than 5% of the entire area circumscribed by the curve), but that with an increase in the number the size of the area located within the branch rapidly decreases. For s-rays, for example, it is $\sim \frac{1}{k^4}$. This means that, with an increase in the number, the corrections introduced into the geometric picture by the wave effects rapidly strive to zero.

In practice, in order to obtain a good degree of accuracy, it is necessary to correct the indicatrix calculated here to a certain extent in a small angular interval around the directions of the first and possibly the second rainbows. Except for the rainbow direction, geometric optics is not applicable in the region of small angles around the forward and backward directions. We shall see further on that a significant amount of light is concentrated in the forward direction. However, it is important to note that both in the directions of the rainbows, and in the forward and backward directions, the interval of angles subject to correction is very small. Thus, in the zero direction it is on the order of $6/\rho$ (see VI, 2). Therefore, for example, in the case of the scattering of visible light by drops of a cloud with $a = 10\mu$, where $\rho \simeq 120$, calculations based on geometric optics must be supplemented by allowance for the wave effects only in the region of angles which are on the order of several degrees around zero and of approximately the same order around the direction of the first and second rainbows[1]. The situation is somewhat better, for example, in the /133 problem of visible light propagation through rain, where the particles are significantly larger. Therefore, in spite of the fact that calculations based

(1) We shall discuss different methods of allowing for these effects at a later point (Chapters VI and VII).

on geometric optics cannot provide an accurate indicatrix in principle, they must yield a good approximation to actuality in practice for the case of rather large particles.

§ 6. Nontransparent Particles

Let us investigate the geometric optics of fully reflecting and absorbing particles.

In the first case, the situation may be described very simply.

In accordance with the formula (5.6), the scattering indicatrix of an absolutely reflecting sphere will be a sphere, since $r_s = r_p = 1$. The intensity of scattered radiation may be determined by the following formula

$$I_{s,p} = \frac{a^2}{4R^2} I^0_{s,p}. \tag{5.33}$$

We should note that this simple problem was discussed incorrectly in the book by Born (Ref. 38). He writes (page 392) that, in the case of an absolutely reflecting sphere, for $\lambda \ll a$, a scattered wave will be completely reflected

The picture of intensity distribution close to, and far from, a sphere is confused. Close to the sphere surface, the intensity distribution will be that indicated by Born. However, far from the sphere, the intensity distribution will be spherically symmetrical.

The total amount of scattered radiation coincides with the total flux of radiation penetrating the observational sphere having the radius R. It will equal $4\pi R^2 \cdot I_{s,p} = \pi a^2 I^0_{s,p}$, i.e., it coincides with the flux falling on a drop (intersected by the drop contours). Thus, the scattering coefficient equals πa^2.

Let us now turn to the geometric optics of an absorbing sphere.

Just as previously, the intensity of reflected light may be described by the formula (5.6). However, we must keep the fact in mind that since m is a complex number, the reflection coefficients for the fields will also be complex numbers. This indicates a shift of the phase in reflected light. In calculating the reflection coefficients for intensities (i.e., the quantities r_s and r_p), we must now take, not the squares of the expressions indicated in (5.10), but the squares of their moduli. With respect to refracted light, we have the following expression for the sine of real refraction ψ^*: /134

$$\left(\frac{\sin\varphi}{\sin\psi^*}\right)^2 = n^2\left[1 - x^2 + \frac{1}{2}(1 - x^2 - \alpha^2)(\sqrt{1+\beta^2} - 1)\right]. \tag{5.34}$$

Here ϕ is the angle of incidence, $\chi = \frac{\varkappa}{n}$ -- the absorption index, and for purposes of brevity we have indicated the following by α and β:

$$\alpha = \frac{\sin\varphi}{n} = \sin\alpha'; \quad \beta = \frac{2x}{1 - x^2 - \alpha^2}.$$

The field amplitude decreases in the direction which is normal to the boundary, and the amplitude decreases by a factor of $e^{-\Delta}$ at a depth of one wave length (in a vacuum). For Δ, we have

$$\Delta^2 = 2\pi^2 n^2 (1 - x^2 - \alpha^2)(\sqrt{1 + \beta^2} - 1). \tag{5.35}$$

In accordance with the data given in Table 7, we have $x < 0.3$ for water in the infrared region. Consequently, within an accuracy of 10% we have the following

$$\frac{\sin\varphi}{\sin\psi^*} = n, \tag{5.36}$$

i.e.,

$$\psi^* = \alpha'$$

and

$$\Delta = \frac{x}{\cos\psi^*}. \tag{5.37}$$

Thus, we can calculate the refraction angle in terms of the real part of the complex refraction coefficient. A decrease in the refracted wave amplitude may be determined by the factor $e^{-k_0 x \frac{z}{\cos\psi^*}}$. This yields the factor /135
$e^{-4\rho x \cos\psi^*}$ [1] for the intensity of the second derivative of the ray. In accordance with the data for n given in Table 7, and in accordance with the formula (5.36), $\cos\psi^*$ changes from 1 to approximately 1/2 for angles of incidence which change from 0 to $\pi/2$. Thus, if x is on the order of 5% and more, for ρ of an order of 30 we can disregard a bundle of refracted rays within an accuracy of $e^{-3} = 5\%$. In the absorption band for $\lambda = 3\mu$, this accuracy can be achieved in the case $\rho = 8.5$. For the intensity of the kth derivative of the ray, we obtain an expression which contains the intensity of the second derivative of order $(k - 1)$. This means that we can disregard these bundles, if we disregard the refracted bundle.

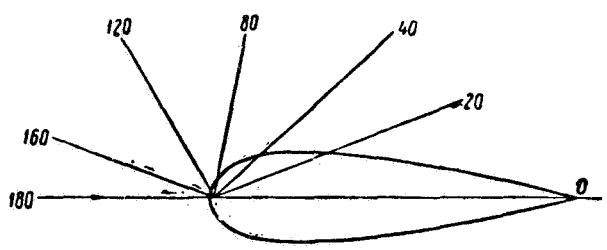

Figure 26. Indicatrix of Reflected Rays in the Band of Maximum Water Absorption.

In this connection, we should note that it is permissible to disregard absorption, which we have done for the visible region, not only for cloud drops, but also for rain drops. In actuality, as we have already noted, the absorption index for water in the visible region is on the order of 10^{-8}. Consequently, significant absorption occurs only in the case of ρ on the order of 10^8, i.e., for spheres having

(1) If ψ^* is the refraction angle, then the length of the ray path in the drop will be $2a \cos\psi^*$, and the path passing along the normal will be $z = 2a \cos^2\psi^*$.

a radius of about 10 m.

In accordance with the considerations presented above, we have computed the scattering indicatrix of a drop of water in a strong absorption band (for $\lambda = 3\ \mu$; $m = 1.409 - i\ 0.1747$).

We have taken into account only reflected light. This scattering indicatrix is shown in Figure 26. It barely differs from the scattering indicatrix in reflected light for a transparent drop (see Figure 19).

In conclusion, let us study the problem of the coefficients of attenuation/136 and scattering in terms of geometric optics. It is apparent that we have the following for a transparent and completely reflecting particle

$$k = k_p = \pi a^2.$$

For an absorbing particle, the attenuation coefficient also equals πa^2; $k_p = R^{(1)}\pi a^2$, a $k_t = \pi a^2(1 - R^{(1)})$ (in the spirit of the approximation method investigated here). We should recall that $R^{(1)}$ is determined by the formula (5.25). Calculating the integral included in this formula, we may find the absorption coefficient and the scattering coefficient. For an example to which Figure 26 pertains, we have found $R^{(1)} = 9\%$ and $k_a = 0.91\ \pi a^2$ (the exact value of k_a calculated directly from the formulas given in Chapter 2 is 2% less).

CHAPTER VI /137

ABSORBING AND FULLY REFLECTING PARTICLES HAVING ANY DIMENSIONS

§ 1. Coefficients of Attenuation and Scattering

The approximation method for large particles, developed in the preceding chapter, is very simple and suitable. However, there are several facts which cause some doubt. We have already noted that in general geometric optics does not enable us to determine the scattering indicatrix. However, a very important addition, which must be made to the preceding calculations, follows from an analysis of the data on the attenuation coefficient.

The attenuation coefficient for the case $m = \infty$ was tabulated by Götz (Ref. 55). Employing the tables of Bessel functions, Götz calculated the amplitudes of partial waves for different ρ, and then calculated the attenuation coefficient according to the formulas (2.52). The values he obtained are shown in Table 14.

The quantity $K(\rho)$ shown in this table is related to the attenuation /138 coefficient by the following relationship

$$k = \pi a^2 K(\rho). \tag{6.1}$$

In accordance with formula (2.52), $K(\rho)$ is determined by the following sum

$$K(\rho) = \frac{2}{\rho^2} \operatorname{Im} \sum_{l=0}^{\infty} l(l+1)(-1)^l (c_l - b_l). \tag{6.2}$$

TABLE 14

ρ	$\frac{a}{\lambda}$	$K(\rho)$	ρ	$\frac{a}{\lambda}$	$K(\rho)$	ρ	$\frac{a}{\lambda}$	$K(\rho)$
0,1	0,02	0,00034	1,2	0,19	2,290	4,00	0,64	2,140
0,2	0,03	0,00538	1,30	0,21	2,274	5,00	0,80	2,090
0,4	0,06	0,0882	1,50	0,24	2,154	6,00	0,95	2,100
0,5	0,08	0,22	1,70	0,27	2,130	8,00	1,27	2,076
0,6	0,10	0,446	1,80	0,29	2,150	10,00	1,59	2,064
0,8	0,13	1,238	1,90	0,30	2,184	12,00	1,91	2,080
1,0	0,16	2,036	2,00	0,32	2,210	20,00	3,18	2,032
1,1	0,18	2,230	3,00	0,48	2,172			

The handbook by Linke presents a more detailed table which is interpolated over the values of λ/a. We have given only the values which are tabulated directly. In order to provide a control for the Götz data, we have calculated the scattering coefficient by numerical integration of the Blümer indicatrix (Ref. 56). The data obtained by this method coincide with the data of Götz within an accuracy of 1.5%.[1]

For small particles ($\rho \ll 1$), in accordance with formula (4.21), $K(\rho)$ is proportional to ρ^4(the scattering coefficient is inversely proportional to λ^4). An increase in $K(\rho)$ with an increase in ρ gradually decreases, and $K(\rho)$ in the case $\rho = 1.23$ ($\frac{\lambda}{a} = 5.1$) passes through a maximum. The maximum value of $K(\rho)$ is 2.294. In addition, with an increase in ρ, the attenuation coefficient decreases, and $K(\rho)$ in the case $\rho = 1.66$ ($\frac{\lambda}{a} = 3.8$) passes through a minimum. Its value is 2.128 at the minimum. In the case $\rho = 2.25$ ($\frac{\lambda}{a} = 2.8$), $K(\rho)$ has a second maximum, after which it decreases monotonically, striving to unity.

However, we must note that more detailed computations show that a monotonic decrease in $K(\rho)$ after the second maximum does not occur. In actuality, the curve indicates damped oscillations (see Figure 27). The abscissa of the maxima $K(\rho)$ are approximately distributed in intervals around unity. This behavior of the curve was indicated in our study (Ref. 43) (1947). It was obtained from the values for the field E_θ scattered by an absolutely reflecting sphere in the forward direction, which were published in the same year by A. R. Vol'pert and A. I. Potekhin (Ref. 57).

We shall indicate the relationship which exists between the attenuation coefficient and the amplitude of the field scattered in the direction of incident rays. In order to derive the corresponding formula, we should note that $S_\ell = -Q_\ell = \frac{\ell(\ell+1)}{2}(-1)^\ell$ in the case $\beta = 0$. If we now write the field E_θ in /139

[1] Götz did not calculate $K(\rho)$ for $\rho = 0.5$. The value we have given was obtained from the Blümer indicatrix.

the following form

$$E_\theta = A_\theta \cos\varphi \frac{e^{-ikr}}{r} E_0, \tag{6.3}$$

then from (2.41) we readily obtain the following for A_θ, assuming that[1] $\phi = 0$:

$$A_\theta = \frac{1}{k_a} \sum_l \frac{l(l+1)}{2} (-1)^l (c_l - b_l). \tag{6.4}$$

Comparing this formula with the formula for k(2.52), we readily obtain

$$k = 2\lambda_a \operatorname{Im}(A_\theta). \tag{6.5}$$

Thus, the imaginary part of the amplitude in the forward direction determines the attenuation coefficient.

We should note that, if we select β and ϕ' as the fundamental angles, and not θ and ϕ (see the end of III, 2), then we must write formula (6.5) as follows

$$k = 2\lambda_a \operatorname{Im}(-A_\beta). \tag{6.5*}$$

The relationship (6.5) must not be regarded as a random consequence of the Mie formulas. In our opinion, this relationship is of fundamental importance. It establishes the deep relationship which exists between forward scattering and attenuation. In essence, this relationship is included in the concept of attenuation itself, and in this sense formula (6.5) is probably very general.

When a plane wave passes through a scattering center, it excites a scattered wave, whose interference with the incident wave yields a forward wave. The latter is attenuated, as compared with the incident wave, by the magnitude of the attenuation coefficient. It is thus apparent that the quantity k must be uniquely related to the amplitude and phase of a wave which is scattered directly forward, since the interference of this wave with the incident wave leads to attenuation of the forward wave. The attenuation of the wave may be determined experimentally by comparing the forward wave, at a sufficient distance behind the particle, with the incident wave in front of the particle. The formula (6.5) directly corresponds to this experimental meaning of the attenuation concept. Therefore, it must hold for a particle having any form, if we are only sufficiently far from it. This general property must hold only for the relationship between forward scattering and the attenuation coefficient. Naturally, it does not mean that the scattering indicatrixes of particles having different forms will be the same. /140

We should note that ordinarily the formula (6.5) does not simplify the calculations in any way. However, it can be suitable for calculating k when the problem of light scattering is investigated by other methods -- for example, by the methods which we shall present in Chapter VII or in those cases when the field which is scattered forward has already been computed. This case was presented to us in the study (Ref. 57). In this study, the field $E_\theta(0)$ is

[1] This means that we have arrived at the forward direction, displaced in the xz-plane (Chapter II). Apparently, the field cannot depend on the manner in which we have arrived at this direction.

designated as

$$A_\pi \frac{E_0}{r} e^{-i(kr-\alpha_\pi)}.$$

The authors present graphs for the quantities $\alpha_\pi(\rho)$ and $\frac{A_\pi}{2a} = f(\rho)$.

With the use of these quantities, k may be written as follows:

$$k = 2\pi a^2 \cdot \frac{4}{\rho} f(\rho) \cdot \sin \alpha_\pi.$$

For $\rho > 6$ with an error which is less than 1%, we have the following asymptotic formula

$$k = 2\pi a^2 \left(1 + \frac{0{,}4}{\rho}\right). \tag{6.6}$$

In Figure 27 we present a graph of $K(\rho)$ for an absolutely reflecting sphere. Up to the second maximum, we employed the data given by Götz, since the scale of curves for α_k and $f(\rho)$ is too small in (Ref. 57) in this section. The behavior of the curve given by Götz behind the second maximum is indicated by the dashed line.

The oscillatory nature of $K(\rho)$ follows formally from the fact that this /141 quantity may be expressed by rapidly oscillating Bessel functions. The physical cause of this phenomenon may be found in the interference nature of the problem. It is natural to also expect, as was noted by Professor Ya. I. Frenkel' in 1947 when discussing our study (Ref. 43), in more careful computations the large-scale oscillations which we have indicated in Figure 27 are furrowed by a small-scale "ripple" ("fine structure" of the attenuation spectrum).[1]

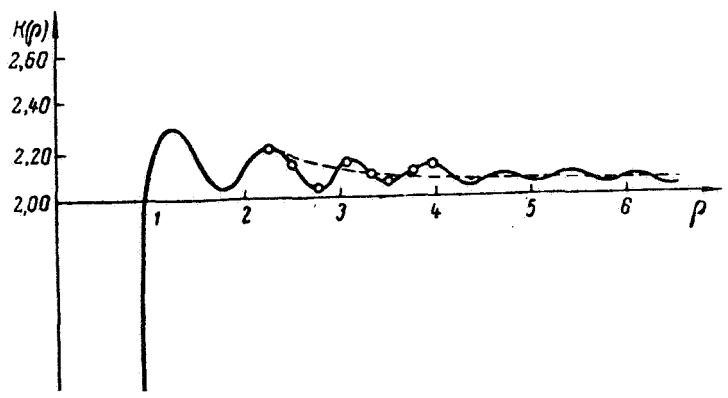

Figure 27. Attenuation Coefficient for m = ∞

The nature of the curves for $K(\rho)$ behind the first maximum is similar to the curves for damped oscillations.

(1) In actuality, this "fine structure" was discovered by Houghton and Chalker for drops of water (see VII, 1).

Up to the present time, however, we have not discussed the most essential aspect of the behavior of the curve $K(\rho)$ -- namely, its asymptotic behavior for large ρ. In this case, which occurs in the region where the validity of applying geometric optics is irrefutable, we find a value for k which is twice the value which follows from geometric optics. An analysis of this paradox will be given in the following section.

A study of the coefficients of attenuation and absorption for finite m, /142 with allowance for a change in the physical properties of matter in the spectral region under consideration, is of significant interest for several problems. For example, this is true of metals in the visible region (see Table 4). Fundamental studies in this region were performed by a school of scientific photography in the USSR , which was directed by Professor T. P. Kravets. Articles by Professor M. V. Savost'yanova, S. A. Artsybysheva, A. S. Toportsa, A. T. Asheulova, P. V. Meyklyara and others primarily deal with them.

The quantities $k(\lambda)$ and $k_p(\lambda)$ (in the visible region) for small particles of different substances -- primarily metals placed in different media -- were calculated and measured experimentally in these studies.

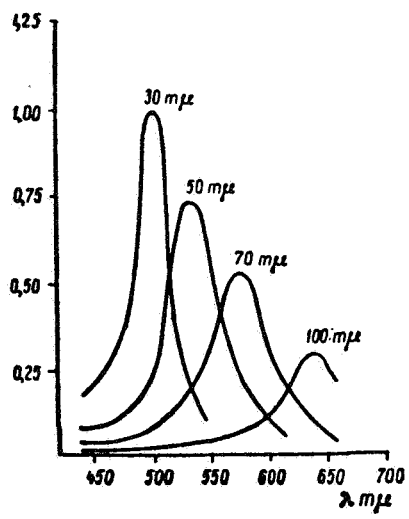

Figure 28. Absorption Coefficient for Particles of Na in Ether

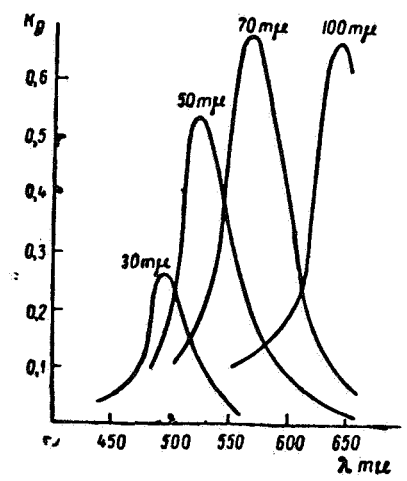

Figure 29. Scattering Coefficient for Particles of Na in Ether

The curves for the coefficients of attenuation and scattering have sharp maxima. In particular, metals for which a substantial portion of the refractive index is small (sodium, potassium, silver, and others) produce narrow bands. In Figure 28 we present the curves from (Ref. 58) showing the behavior of the /143 absorption coeficient for sodium particles of different diameters in ether. Figure 29 shows the behavior of the scattering coefficient for these same particles (the quantities which are proportional to these coefficients are plotted along the ordinate axes). In accordance with the ideas developed in Chapter V, the scattering coefficient decreases much more rapidly than the absorption coefficient when the particle dimensions decrease.

The location of the absorption maximum in the visible portion of the spectrum leads to bright coloration of a colloid solution. In the majority of cases, however, the absorption curves are primarily located in the ultraviolet and enter the visible region only slightly. In this case, one cannot expect a bright coloration. Actually, in these cases M. V. Savost'yanova detected only brown shades. With an increase in the particle dimensions, the absorption maximum is displaced toward long waves (see Figures 28 and 29). This important conclusion, which was reached at the beginning of the computations, was then experimentally corroborated.

However, we should note that this displacement of the maximum can be explained in qualitative terms by considerations which fall outside of the framework of this book. Regarding the smallest colloid particles as large molecules and applying to them the approximation methods of calculating the chromaticity of organic compounds, in 1946 F. Sh. Shifrin found that the absorption bands of such particles must be displaced toward large λ when their dimensions increase.

A conclusion may also be reached regarding the agreement between theory and experiment, based on the curves given in Figure 30. Curve 1 gives the theoretical behavior of absorption for Cu particles in NaCl. Curves 2-4 represent the experimental course of absorption in the Cu-NaCl system, based on measurements by S. A. Artsybysheva and A. S. Toportsa. As we may see, the experimental curves precisely transmit the nature of the theoretical curve.

The reader will find more detailed data on these investigations in the articles of M. V. Savost'yanova (Ref. 58, 59).

We should note that, in accordance with formulas (4.12) and (1.12), the absorption coefficient of a slightly conductive particle is proportional to the electrical conductivity σ. When considerations regarding the dependence of σ on a, developed in I, 2, are taken into account, this means that for the smallest particles $k \sim a^4$, whereas $k \sim a^3$ for larger particles. This apparently pertains to colloid systems, which are illustrated in Figures 29 and 30. /144

We shall discuss the data on spectral transmittance of the atmosphere before Chapter VII.

§ 2. Asymptotic Value of the Attenuation Coefficient for Large Particles[1]

As we have seen, precise formulas for the attenuation coefficient lead to an unexpected result. The asymptotic value of this coefficient for large particles equals $2\pi a^2$. Streton and Houghton (see Chapter VII for greater details on their work) found the same asymptotic value (in the case $\rho \to \infty$). They tabulated k for drops of water in the visible region. This value is opposed to the value obtained when the problem is investigated by the methods of geometric optics -- πa^2. The value of πa^2 is given in the study by Ruedy (Ref. 60) and many others.

This same erroneous value is given in the work by G. Gertner (Ref. 45).

(1) According to our study (Ref. 63).

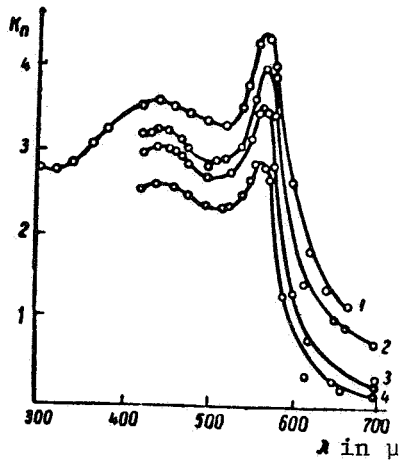

Figure 30. Theoretical and Experimental Curves for Particles of Cu in NaCl

We must take the fact into account/145 that Jobst (Ref. 61), who employed precise formulas to study analytically the attenuation coefficient for $m = \infty$, obtained the following formula for large ρ:

$$k = \pi a^2 \left(1 + \frac{1}{\rho} + \frac{f^2}{\rho^{4/3}} + \ldots\right), \qquad (6.7)$$

where $f^2 = 0.228 \ldots$

Thus, according to Jobst, the asymptotic value equals πa^2.

The result obtained by Jobst, however, is erroneous. The error may be immediately detected if we compare his initial formulas with the corresponding formulas in Chapter II. Jobst simply omitted the factor 2. He made this change in the precise formulas in order to obtain the asymptotic value in accordance with the requirements of geometric optics. However, the formulas given in Chapter II are absolutely precise, up to all the coefficients included in them. They were not subjected to any additional "normalization", since they were obtained from the general solutions of the Maxwell equations after satisfying a complete system of boundary conditions. Thus, the asymptotic value of the scattering coefficient obtained from the general formulas is $2\pi a^2$.

The error of Jobst must be kept in mind when employing his computations.

There are a few more inaccuracies in his work. For example, he indicates that the maximum of the curve for the attenuation coefficient occurs at $\rho \simeq 2.5$, whereas in actuality it occurs at $\rho \simeq 1.2$. The asymptotic formula (6.7) which he indicated does not coincide with the formula (6.6) which we obtain directly from numerical data in (Ref. 57).

We shall show further on that the paradoxical value for the coefficient of attenuation by large particles is in actuality due to diverse diffraction phenomena which occur here. However, we must stress the fact that the phenomenon which we have studied falls outside of the framework of our usual concepts regarding diffraction. They lead us to a certain significant change in these customary representations.

Actually, we can usually assume that diffraction phenomena disturb the geometric picture of the field at distances on the order of λ from the edge of the body. In our problem, this means that the portion of the flux disturbed /146 by diffraction phenomena will be on the order of $2\pi a\lambda$. The relative value of this diffraction disturbance in the case $\rho \to \infty$ will strive to zero as $1/\rho$ and, consequently, we arrive at the asymptotic value indicated by geometric optics.

The coefficient $2\pi a^2$ contradicts the geometric optics. In order to analyze this, we must study in greater detail the angular intensity distribution of light scattered by an extremely large particle ($\rho \to \infty$).

Based on the fundamental formulas, let us investigate the intensity distribution of scattering for the case of very small angles $\beta(\beta \sim \frac{1}{\rho})$, i.e., within a certain very narrow cone around the forward direction.

In Chapter III we saw that up to ℓ of the order ρ, the amplitudes have the order $1/\ell$, and the values of the angular functions do not exceed $\frac{\ell(\ell+1)}{2}$. This means that the oscillating terms of the sums have up to $\ell \sim \rho$ orders of ℓ. For ℓ which are larger than ρ, they become negligibly small. This means that for large ρ terms with large ℓ play the basic role in sums for the fields. For large ℓ, we may apply the approximation formula of V. A. Fok to the Legendre polynomials contained in the functions Q_ℓ and S_ℓ. Taking the properties of these functions into account, which are described in Chapter III, we obtain the following after simple transformations

$$Q_l(\beta) = (-1)^l \frac{l^2}{z'} \frac{dJ_0(z')}{dz'},$$

$$S_l(\beta) = (-1)^{l+1} l^2 \frac{d^2 J_0(z')}{dz'^2} = Q_l + (-1)^l l^2 J_0(z').$$

Here $z' = \ell\beta$.

These formulas may be written for $\ell \gg 1$ and $\beta \ll 1$. We have thus substituted $\sin\beta$ everywhere by β, and $\ell + \frac{1}{2}$ by ℓ.

Substituting this expression in the sum for E_ϕ, for the ℓth component of this sum, we obtain

$$(-1)^{l+1} l^2 \left\{ (c_l + b_l) \frac{J_1(z')}{z'} - b_l J_0(z') \right\}.$$

The ℓth component in the sum for E_θ will be

$$(-1)^{l+1} l^2 \left\{ (c_l + b_l) \frac{J_1(z')}{z'} - c_l J_0(z') \right\}.$$

We should now recall that in the case $\rho \to \infty$ the amplitudes c_ℓ and b_ℓ in /147 the case $\ell < \rho$ consist of the sum 1 and the rapidly oscillating component (within an accuracy of the factor) (3.26). The asymptotic contribution to the sum for the fields made by the oscillating portion (in the case $\rho \to \infty$ oscillation occurs with the frequency ρ) will be significantly less than that made by the constant component. Therefore, we can disregard the rapidly oscillating section in the amplitudes.[1]

Thus, for large ρ and (and small β), independently of the electric properties

(1) We shall see further on (see Chapter VII) that allowance for the oscillating part in (3.26) (for the fields) yields quantities whose order is lower than those we have obtained here by a factor of unity.

of the particles, we may assume that

$$c_l = (-1)^l i \frac{2l+1}{l(l+1)} \cdot \frac{1}{2} = (-1)^l \frac{i}{l},$$

$$b_l = -(-1)^l i \frac{2l+1}{l(l+1)} \cdot \frac{1}{2} = (-1)^{l+1} \cdot \frac{i}{l}.$$

The field E_ϕ will now be

$$E_\varphi = \frac{\sin\varphi}{k_a} E_0 \frac{e^{-ik_a r}}{r} i \sum_{l=1}^{\rho} l J_0(l\beta).$$

Replacing the sum with respect to ℓ by the integral, we readily obtain

$$\sum_{l=1}^{\rho} l J_0(l\beta) = \int_0^{\rho} t J_0(t\beta)\, dt = \rho^2 \frac{J_1(z)}{z}; \quad z = \rho\beta.$$

We have here employed the well known formula

$$\int_0^z t J_0(t)\, dt = z J_1(z).$$

The quantity E_ϕ will be

$$E_\varphi = \frac{\sin\varphi}{k_a} E_0 \frac{e^{-ik_a r}}{r} \left(i\rho^2 \frac{J_1(z)}{z} \right). \tag{6.8}$$

A similar expression is obtained for E_θ, only $\sin\phi$ will be replaced by $\cos\phi$.

Changing from the fields to the intensities, we obtain /148

$$I_1 = \sin^2\varphi I, \quad I_2 = \cos^2\varphi I, \tag{6.9}$$

where I designates the total intensity of scattered light (per unit of solid angle):

$$I = \frac{\rho^2 a^2}{4} \left(2 \frac{J_1(\rho\beta)}{\rho\beta} \right)^2. \tag{6.10}$$

We should note that in the scattering of natural light $I_1 = I_2$, i.e., the degree of polarization of scattered light equals zero. This is understandable, since in general for very small β the division into transverse and longitudinal components loses any meaning.

The formula which we obtained for the total I coincides exactly with the formula for intensity distribution in the case of light diffraction from a circular hole (in the case of small β) [see (Ref. 38), page 217]. A graph of the function

$$F(z) = \left(\frac{2J_1(z)}{z} \right)^2$$

is shown in Figure 31. In the case of $z = 0$ $F(z) = 1$, i.e., in the forward direction, the intensity of scattered light will be

$$I = \frac{a^2}{4} \rho^2 = \frac{\pi^2 a^4}{\lambda^2}. \tag{6.11}$$

The roots of the function F(z) and its derivative are shown in the first column of Table 15. The second column presents F(z).[1]

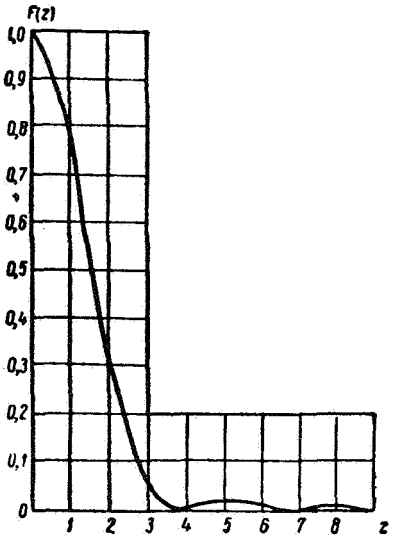

Figure 31. Graph of F(z)

The flux of energy contained within the cone, whose angle of opening is determined by the quantity z, will be

$$\Phi(z) = \frac{\pi a^2}{2}\int_0^z \left(2\frac{J_1(t)}{t}\right)^2 t\,dt.$$

TABLE 15 /149

z	$F(z)$	$\Phi(z)$	z	$F(z)$	$\Phi(z)$
0	1,0000	0	8,417	0,0042	0,923
3,832	0	0,838	10,17	0	0,938
5,136	0,0175	0,867	11,62	0,0016	0,945
7,016	0	0,910	13,32	0	0,952

This integral may be readily calculated, if we employ the following relationship

$$J_1(t)\frac{J_1(t)}{t} = [J_0(t) - J_1'(t)]J_1(t).$$

We thus find:

$$\Phi(z) = \pi a^2[1 - J_0^2(z) - J_1^2(z)]. \qquad (6.12)$$

The values of $\Phi(z)$ are shown in Table 15. It follows from this table and from Figure 31 that the entire diffracted light is concentrated in regions of small z. (This corresponds to small β[2]). Almost all of the light is concentrated, for example, in the regions $z < 6$,[3] i.e., in a cone with the angle of opening $\beta^* = \frac{6}{\rho}$. The total amount of light diffracted by the medium will be πa^2. All

(1) The distance between the roots of F(z) is approximately equal to π. This leads to the well known rule for determining the radius of coronas (Ref. 62).

(2) In formulas for diffraction from the opening, $2 \sin \frac{\beta}{2}$ is usually written instead of β. In view of the fact that (6.10) is only valid for large ρ (and small β), both expressions coincide.

(3) The position of the boundary for the diffraction region is arbitrary to a certain extent. In (Ref. 63) we assumed that it was horizontal when z = 3. In this case, about 80% of the diffracted light enters the diffraction region. In the case z = 6, about 90% of this light enters this region. The position of the boundary is determined by the experiment requirements.

of this light enters the cone with the angle of opening β^* and with the mean intensity

$$I_{mean} = \frac{a^2}{\beta^{*2}}.$$

Thus, within the directions lying in the very narrow angle $\beta^*(\beta^* \sim \frac{\lambda}{a})$, the intensity of light scattered by an extremely large particle is very great ($\sim a^4/\lambda^2$). The total amount of light scattered within this infinitely narrow /150 cone will be πa^2. The total scattering coefficient equals $2\pi a^2$. Consequently, in all the remaining directions, except for the narrow cone directed forward, the total amount of scattered light will equal πa^2.

The intensity distribution described by formula (6.10) may be observed experimentally in the form of coronas around the particle. It thus follows from our calculations that the coronas are one of the phenomena which accompany the scattering of light by large particles, and the theory of coronas must be regarded simply as part of a more general theory -- the theory of light scattering by particles.

Following is the essential meaning of the preceding calculations. The assertion that in the case of $\frac{\lambda}{a} \to 0$ the intensity distribution of scattered light must change into the intensity distribution corresponding to geometric optics is incorrect. This change actually occurs at all angles β, except for the angles $\beta \sim \frac{\lambda}{a}$. When there is an increase in the particle dimensions, the deviations from geometric optics will not vanish, and will be concentrated within a more narrow angle, so that the total amount of energy scattered into this small angle will equal the total amount of energy scattered in all directions according to the laws of geometric optics.

Thus, the scattering indicatrix for an extremely large particle will have a very narrow and long "tongue" in the forward direction.

The energy scattered contrary to the laws of geometric optics (6.10) goes directly forward. Therefore, if it enters a receiving device, it is not taken away from the flux in actuality and, in accordance with geometric optics, attenuation of the flux after the scattered particle has penetrated it will be πa^2.

Let us illustrate the results of the preceding computations by the following elementary considerations. The entire amount of light entering a particle is scattered, as a result of reflection and refraction. This yields πa^2 for the scattering coefficient.

However, light passing outside of the particle is also perturbed due to /151 the continuity of the electromagnetic field. In order to describe this perturbation and the intensity distribution on an infinitely long screen, which causes it, one customarily turns to the approximation diffraction theory -- to the Kirchhoff theory. In this theory, a real three-dimensional body is replaced by a two-dimensional screen which is assumed to be black, independently of the real electrical properties of the body (Ref. 30).

Our particle (for example, a transparent drop) is not a black disk . However, let us determine what the method usually employed in optics yields for our problem.

Since we are discussing diffraction in parallel rays, we may employ the Babinet principle here. According to this principle, the total amount of light diffracted by the contours of our disk will be the same as the amount of light diffracted by an additional screen, i.e., by a circular opening having the radius a in a nontransparent screen. The latter will be πa^2, and the angular intensity distribution, as we have already pointed out, will precisely coincide with that which we derived by the formula (6.10). Thus, the total amount of scattered light will be $2\pi a^2$.

However, we must emphasize the fact that these discussions employing the Babinet principle cannot be regarded as a conclusive answer to the problem. Since we are discussing a paradoxical conclusion, which is opposed to widely held concepts, only a rigorous analysis of the precise formulas can be regarded as conclusive. Naturally, the question arises as to whether the paradoxical nature of the result is due to inaccuracies in the discussions.

Discussions employing the Babinet principle are conclusive only after the formula for the coronas is derived by asymptotic analysis of the precise formulas. Thus, this analysis must be regarded as proof of the fact that in the case $\frac{\lambda}{a} \to 0$ and for $\beta \to 0$ the precise theory for diffraction by a sphere coincides with the Kirchhoff theory. The fact that the diffraction results around the contour do not depend on the electric properties of the particle, within the framework of the Kirchhoff theory, is substantiated in our precise analysis by the fact that m is not contained in the amplitudes c_ℓ and b_ℓ or /152
in the intensities (which we calculated) of scattered light at small angles. Thus, they are independent of the electric properties of the particle.

We should note that in our calculations we confined ourselves to investigating only the main term in the expansion of the desired quantity (intensity) with respect to λ/a. The scattering coefficient $2\pi a^2$ is obtained from the general formula in the same approximation. The correction term will be on the order of λ/a.

The concept of an absolutely black particle, which we have discussed here, does not coincide with the customary concept of a black particle which is assumed in meteorology [see, for example, (Ref. 64)]. There are no black particles in this customary meaning of the word -- i.e., particles which do not scatter anything. A particle from a strongly absorbing substance will always have scattered light. Roughly speaking, this scattered light will consist of diffracted light and reflected light. Thus, for drops of water in the strongest absorption band (around 3 μ), the scattering coefficient will be about 1.11 πa^2.

In Figure 32 we present the scattering indicatrix of a particle made of an "absolutely black" substance. The angles in the drawing are expanded. The correct form of the curve for a particle with a given ρ may be obtained from Figure 32, if the angles are decreased, if the curve is condensed by a factor

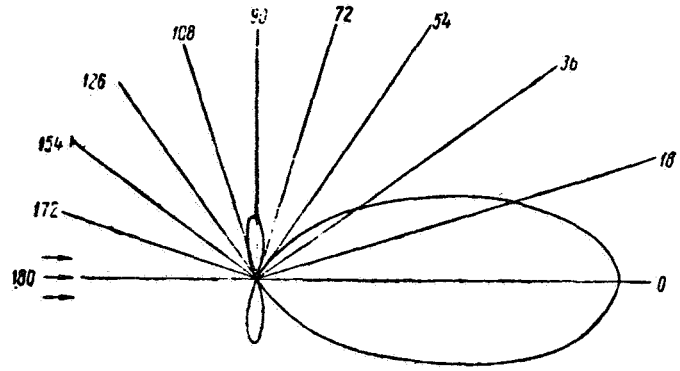

Figure 32. Indicatrix of "An Absolutely Black" Particle

of ρ/π, and if the radius vectors are correspondingly increased.

The discussion presented here shows that in the case being studied /153
perturbations caused by diffraction encompass not only a band having the width λ, as is usually assumed, but deeply penetrate the field at a distance on the order of $(\sqrt{2} - 1)\ a \simeq 0.4a$ from the edge of the particle.

We should also note that "doubling" of the attenuation coefficient must take place not only for spheres, but also for particles having any form which are randomly distributed. It must take place not only for electromagnetic waves, but also for sound waves, waves of matter, etc. if only the particle dimensions are significantly greater than λ and significantly less than the distance to the observer. This follows from the nature of each wave motion. In every case, the attenuation coefficient will equal the doubled area of the transverse cross section of the flux intersected by the geometric contours of the particle.

In experiments, we customarily use the integral attenuation coefficient to designate the flux attenuation when it penetrates a scattering center (in fractions of the incident flux). What value must this coefficient assume during scattering by an infinitely large particle? The answer to this problem depends on the fate of light scattered within the cone β^*. It cannot be given in general form, and is determined by the specific experiment conditions. For example, let us study the following experiment. A flux having the width d[1] falls on a particle with the radius a. We may observe an attenuated flux at the distance r from the particle.

Roughly speaking, attenuation of the flux, which is caused by the particle, may be divided into two sections: (1) radiation scattered at the angle β^*, and (2) the remaining section. They equal each other, and each of them equals πa^2.

If we are sufficiently close to the particle, the portion of the flux

(1) More precisely, d is the width of the flux recorded by the receiving device.

scattered at the angle β^* will not be taken away from the total flux, and the scattering coefficient will approximately equal πa^2. It is apparent that we here have

$$r < \frac{d}{2\beta^*}. \tag{6.13}$$

If $r > \frac{d}{2\beta^*}$, then the scattering coefficient will be greater than πa^2, and will /154 be close to $2\pi a^2$ in the case $r \gg \frac{d}{2\beta^*}$. This case customarily occurs.

Thus, the magnitude of the attenuation coefficient depends not only on $\rho = \frac{2\pi a}{\lambda}$, but also on the ratio of d/r, and may be determined in the case $\rho \gg 1$ by the number $\eta = \frac{d}{2\beta^*}$.

If a light flux passes through a system of particles (layer of sol), the observed scattering coefficient will be the average coefficient with respect to all particles. For very thin layers, generally speaking it will be small ($< \pi a^2$), since light which is refracted and reflected is also primarily directed forward. The scattering coefficient will increase up to $2\pi a^2$ as the layer thickness increases.

The statements developed above have been substantiated by the experiments of Sinclair (Ref. 72). He found experimentally that the attenuation coefficient changes in the way we described as the distance to the receiver changes.[1]

The statements developed above are of significant importance in different optical measurements, particularly for optical methods of determining the moisture of clouds and fogs. Measurement of the light extinction coefficient α is frequently used for this purpose in meteorology. This coefficient may be usually calculated either from the ratio of the light bundle intensity before (I_0) and after (I_ℓ) a layer of sol having the thickness ℓ has been penetrated (formula 6.14), or according to the meteorological range of visibility for the black body [formula (6.15)]:

$$\alpha = \frac{1}{l} \ln \frac{I_0}{I_l}, \tag{6.14}$$

$$\alpha = \frac{1}{S} \ln \left(\frac{1}{\varepsilon} + 1\right). \tag{6.15}$$

Here S is the meteorological range of visibility, ε -- threshhold of brightness contrast for the eye. The relationship between the extinction coefficient and /155 the radius of the drop a, their number per unit volume n for a monodispersed cloud or fog, is usually established by the formula (6.16):

---

(1) An article by Brilluin (Ref. 73) comprises the theoretical portion of this article. We should note it was submitted to the publisher one half year later than ours (Ref. 63), and that Brilluin only analyzed the special case of an absolutely reflecting sphere. We should also add that Professor M. I. Yudin, in a science seminar at the Main Geophysical Observatory, proposed using the same experimental arrangement as Sinclair when discussing our articles (Ref. 46) and (Ref. 63). This was more than half a year before the article by Sinclair was published.

$$\alpha = n\pi a^2. \tag{6.16}$$

If the mean radius of the particle is known, then the water content q may be readily determined, since

$$q = \frac{4}{3} a\alpha. \tag{6.17}$$

It is clear from the above that formula (6.17) is wrong. For q, it yields values which are twice as large as the correct values. The correct values can be obtained only when diffracted light is taken into account. Usually, we may simply assume

$$\alpha = 2n\pi a^2, \tag{6.16*}$$

$$q = \frac{2}{3} a\alpha \tag{6.17*}$$

instead of (6.16) and (6.17).

In the atmosphere, intense scattering of solar light at small angles by admixture particles is usually observed in the form of the so-called solar aureole.

The brightness of a clear sky at different points of the sky is different. The theory of this phenomenon must take into account both Rayleigh scattering by density fluctuations, and the Mie effect in the atmosphere.[1] As the Sun is approached, the brightness of the sky increases. The brightness is particularly great directly next to the Sun. N. N. Kalitin (Ref. 65, 66), Ye. V. Pyaskovskaya-Fesenkova (Ref. 67), V. A. Kratt (Ref. 68) and others have studied this phenomenon. In Figure 33 we present the results derived from measuring the aureole. These results were obtained by V. A. Kratt for three different wave lengths. The angles from the edge of the solar disk are plotted along the abscissa axis, and the relative brightness of sections of the sky (brightness of the center of the Sun for corresponding λ is assumed to be unity) is plotted along the ordinate axis. We can see that at 2° from the edge of the disk the brightness of the aureole amounts to 6-10% of brightness at the center of the sun. We should also note that at shorter wave lengths (larger than $\rho = \frac{2\pi a}{\lambda}$) the aureole is more intense.

Ye. V. Pyaskovskaya-Fesenkova (Ref. 67) proposed that observations of the /156 aureole be used as a method to determine the transmission coefficient of the atmosphere $p (p < 1)$. It is based on the formula of V. G. Fesenkov for the brightness of different points in the sky as a function of the number of "optical masses" m:

$$B(m) \sim mp^m.$$

The brightness maximum occurs for $m_{max} = -\frac{1}{\ln p}$. The meaning of this formula (which takes into account only scattering of the first order) is very simple: on the one hand, when m increases, the attenuation of the flux ($\sim p^m$) increases;

---

(1) The theory for the phenomenon, developed by Eksner, is not satisfactory, since it does not take into account scattering by admixtures [see (Ref. 64), page 64].

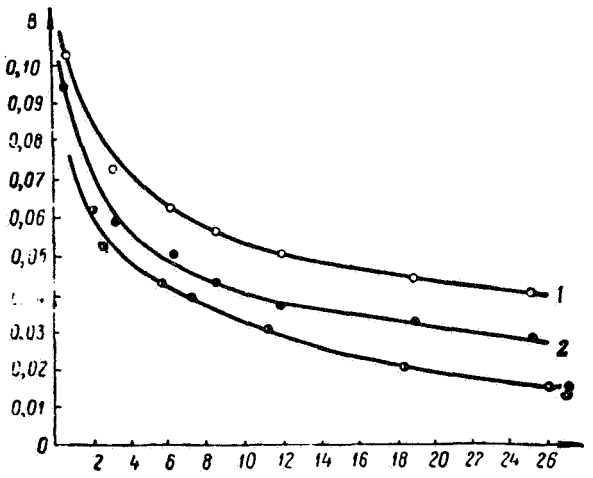

Figure 33. Solar Aureole.

(1) - $\lambda = 0.395\ \mu$; (2) - $\lambda = 0.48\ \mu$; (3) - $\lambda = 0.77\ \mu$.

on the other hand, the number of scattering centers ($\sim m$) increases. In (Ref. 125), Ye. V. Pyaskovskaya-Fesenkova showed that the brightness maximum may be observed for any points in the sky. It is particularly apparent for the aureole. We may readily determine m_{max} and, consequently, p.

The aureole brightness is primarily determined by the number of scattering centers per unit of volume. Therefore, /157 it is natural to expect that the atmosphere transmittance will decrease as the relative aureole brightness increases. N. N. Kalitin (Ref. 70) has established a correlated dependence of exactly this type.

§ 3. Scattering Indicatrix

For the case $m = \infty$, detailed computations were performed by Blümer (Ref. 56). He examined the following seven cases:

1) $\rho = 0{,}01$; 2) $\rho = 0{,}1$; 3) $\rho = 0{,}5$; 4) $\rho = 1$;
5) $\rho = 3$; 6) $\rho = 5$; 7) $\rho = 10$.

In Figures 34, 35, and 36 we present the graphs of Blümer for the quantities i_1 and i_2 [see formulas (2.45); the solid line is i_1] for cases (2), (7), (4), (5). In Figure 37 we give the complete indicatrixes for the cases (2), (4), (6), (7). (The scale of the curves is different.) The polarization distribution of scattered light is shown in Figure 38. Table 16 presents the values of i, which is related to the total intensity I by the following relationship

$$i = Ir^2 \frac{\rho^2}{a^2}. \tag{6.18}$$

It equals the half-sum of the quantities i_1 and i_2 tabulated by Blümer.

Case (1) was investigated incorrectly by Blümer. He performed calculations according to the Rayleigh formula (4.8), whereas formula (4.19) must be employed for the calculations.

We may see from Table 16 and from the figures that particles with $\rho = 0.1$ may be regarded as small particles with fairly good accuracy, in agreement with formulas given in § 2 of Chapter IV. Primarily all of the scattered light is directed backward. Complete polarization is observed at the 60° angle. Within an error of 5%, this holds for the case $\rho = 0.5$. In case (7), we may regard the particle as being large. Cases (4), (5), (6) are intermediate cases.

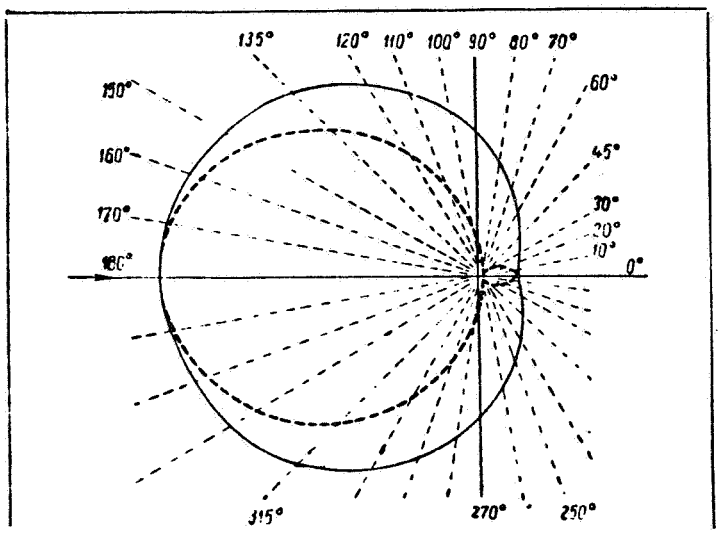

Figure 34. Indicatrix for m = ∞, ρ = 0.1

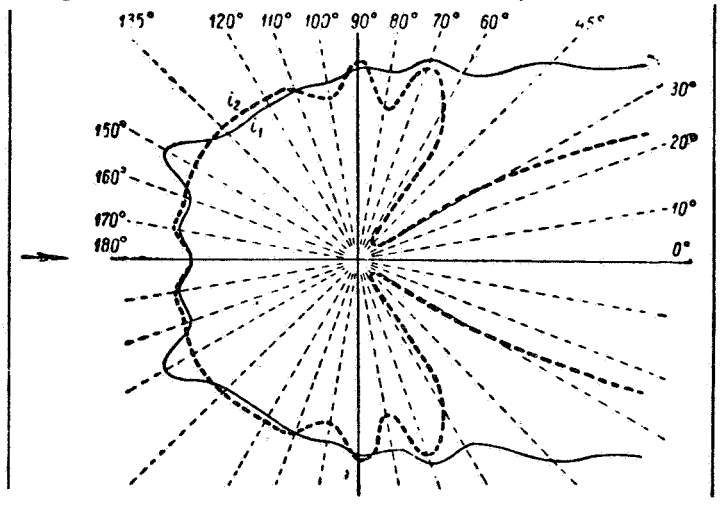

Figure 35. Indicatrix for m = ∞, ρ = 10

When ρ increases from 0 to 1, the polarization maximum decreases and is displaced from β = 60° toward larger angles. Thus, for ρ = 1 it occurs at the 82° angle, and equals 80%. We should also note that, if the polarization is positive for all angles for ρ = 1, then for ρ = 3 it is negative in two angular intervals. For ρ = 5 and 10, the polarization behavior is more complex. The /160 deformation of the polarization curve when ρ increases may be readily explained.

Let us first determine the manner in which the indicatrix is deformed. The scattering indicatrixes for ρ = 5 and 10 are greatly extended in the forward direction. In a conformance with the statements developed above, we have a characteristic diffraction "nose". The scattering can be obtained very simply here by performing summation of the reflection and diffraction effects. It follows from Chapter V that the intensity of scattered light will be constant;

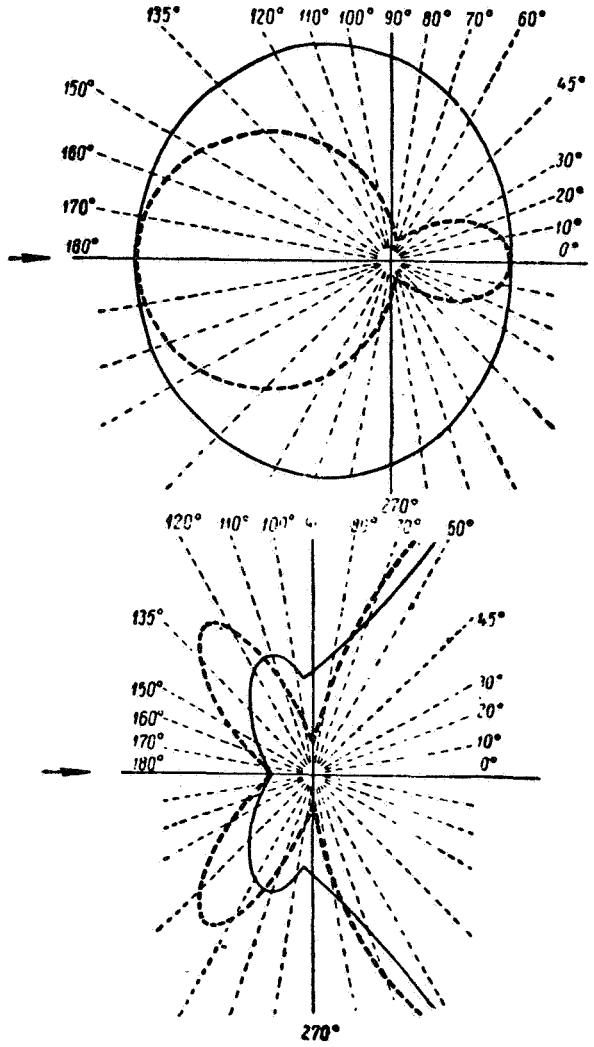

Figure 36. Indicatrix for m = ∞. Upper Curve Pertains to ρ = 1; Lower Curve Pertains to ρ = 3.

i will equal $\rho^2/4$ for reflected light. In actuality, we find that both for $\rho = 10$ and for $\rho = 5$ (for the angles $\beta \gtrsim 30°$ in the first case, and $\beta \gtrsim 45°$ in the second case) the expressions calculated by Blümer may be approximately described by this simple formula. Diffraction enters the picture for smaller angles. The formula for i will be:

$$i = \frac{\rho^2}{4} + \rho^4 \left(\frac{J_1(z)}{z}\right)^2, \tag{6.19}$$

where

$$z = \rho \sin \beta.$$

In order to illustrate the method employed here to calculate the indicatrixes, in the last column of Table 16 we give the values of i'_{10} calculated

according to formula (6.19) for $\rho = 10$. We should note that for $\beta = 0$ the approximate value differs from the precise value by 4%.

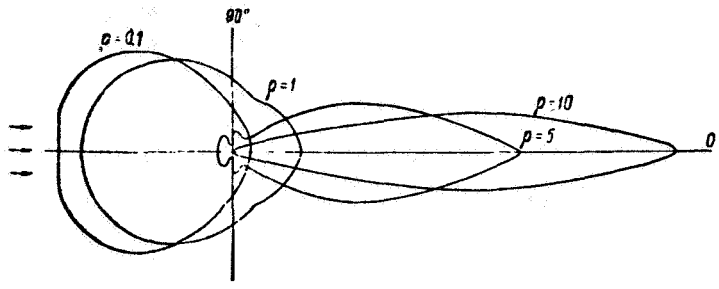

Figure 37. Complete Indicatrixes for Absolutely Reflecting Particles (Cases $\rho = 0.1$; 1; 5; 10).

The approximation method indicated here is rather rough. It can be readily improved if we combine the fields, instead of combining the intensities of diffracted and reflected light. Since both waves are coherent waves, their superposition leads to several interference phenomena. These interference phenomena will be most noticeable in the region of scattering angles where the intensities of both components will approximately be the same. For $\rho = 10$, this region of angles β is between 20 and 60°. /161

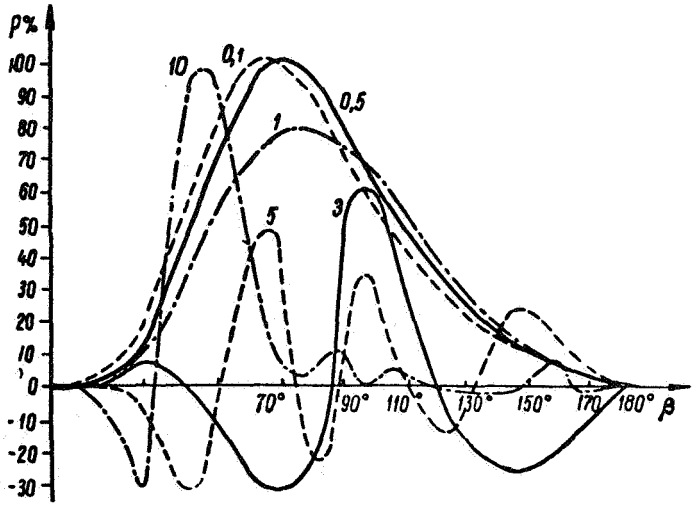

Figure 38. Polarization During Scattering by Absolutely Reflecting Particles.

Let us now turn to polarization. Since both reflection coefficients equal each other in the case under consideration, polarization will equal zero in the

reflected bundle. It will equal zero in the purely diffracted region. We may see from Figure 38 that, in accordance with the statements developed above, the polarization curve oscillates around the abscissa axis when ρ increases. It differs most strongly from zero in the interference region. When ρ increases, the region where polarization does not equal zero is condensed to β = 0.

TABLE 16 /162

β	$10^6 i_{0,1}$	i_1	i_5	i_{10}	i'_{10}
0	0,260	0,4232	175,653	2659,00	2525
10	0,255	0,4159	142,128	1167,66	1125
20	- 0,245	0,3960	79,897	104,426	52
30	0,235	0,3691	38,203	43,66	68,2
45	0,235	0,3330	9,996	20,63	25
60	0,285	0,3287	6,484	26,875	25
70	0,360	0,3426	10,161	29,294	25
80	0,470	0,3803	8,111	23,910	25
90	0,625	0,4352	5,018	27,379	25
100	0,820	0,5028	6,959	24,32	25
110	1,04	0,5772	7,746	25,351	25
120	1,28	0,6526	7,038	25,443	25
135	1,66	0,7564	5,229	26,077	25
150	1,95	0,8378	6,549	28,770	25
160	2,12	0,8756	7,491	25,202	25
170	2,22	0,8984	7,837	25,499	25
180	2,25	0,9066	7,892	23,221	25

In the work by A. R. Vol'pert and A. I. Potekhin (Ref. 57), which we mentioned above, the asymptotic amplitude and phase of a field which is scattered in the forward direction coincide with the diffracted field around an opaque disk, in accordance with the ideas developed in § 2.

They also studied a field which is reflected backwards. The phase of this field, which is measured from the plane which is tangent to the sphere from the side of the incident wave, oscillates, gradually striving toward its classical value π (the phase of the incident wave on the same plane equals zero). The field amplitude (pertaining to the sphere radius) oscillates around the value 1/2 corresponding to geometric optics. It must be pointed out that the most rigorous calculation of the reflected field employing the Kirchhoff formulas, which was done by A. I. Potekhin, does not significantly improve the results as compared with geometric optics.

In Figure 39 (according to [Ref. 71]) we present the behavior of the /163
amplitude obtained according to the Kirchhoff formula (curve A) and obtained according to the formulas of geometric optics (dashed line), in addition to a precise graph of the amplitude (curve B). We can see that the simple result yielded by the formulas of geometric optics is no worse than the computational results based on the Kirchhoff formula.

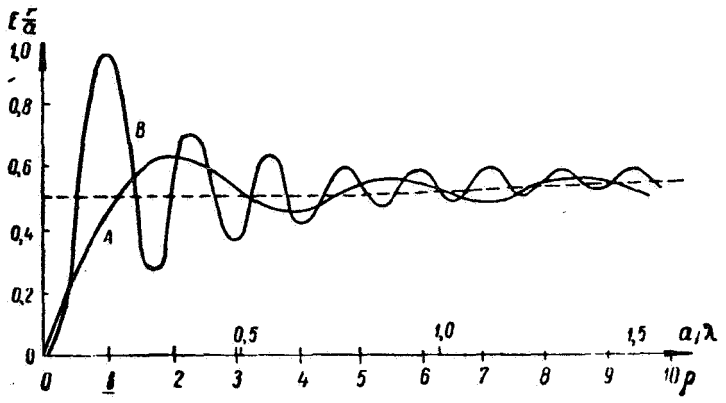

Figure 39. Field Reflected from the Sphere m = ∞.
Dashed Line - According to Geometric Optics;
A - According to the Kirchhoff formula; B - Precise Curve

The scattering indicatrixes for absorbing particles were recently published by Ruedy (Ref. 60). He investigated the scattering of visible light by angular pellets. He assumed that the complex refractive index is constant over the entire visible region, and equals $m = 2 - i\,\frac{2}{3}$. /164

The indicatrixes he obtained are shown in Figure 40. Curve (a) pertains to $\rho = \frac{\pi}{8}$, (b) $\rho = \frac{\pi}{4}$, (c) $\rho = \frac{\pi}{2}$ and (d) $\rho = \frac{3\pi}{4}$.

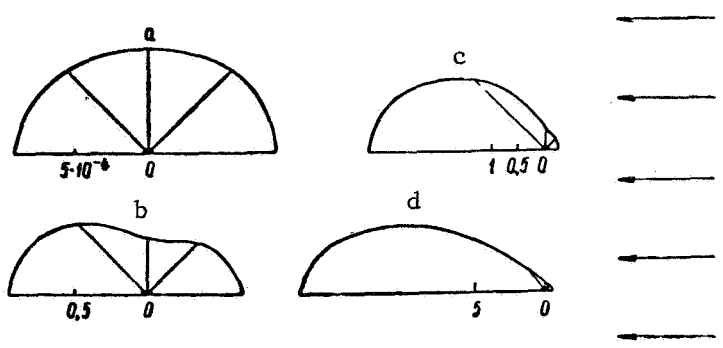

Figure 40. Scattering Indicatrix by Small Carbon Particles.

Let us now investigate the asymmetry of the indicatrixes η for completely reflecting particles (see the end of Chapter V). For an extremely small particle, from Chapter IV we readily find that η = 0.25. For an extremely large particle, the light which is reflected backwards will be 1/2, forward 1/2, and diffracted

1 (in units of πa^2). Consequently, $\eta = 3$. The intermediate values of the function $\eta(\rho)$ were determined by numerical integration of data given in Table 16. For ρ equal to 1, 3, 5, and 10, we obtain 0.55, 2.81, 3.05, and 2.90, respectively. The probable form of the function $\eta(\rho)$ is shown in Figure 41.

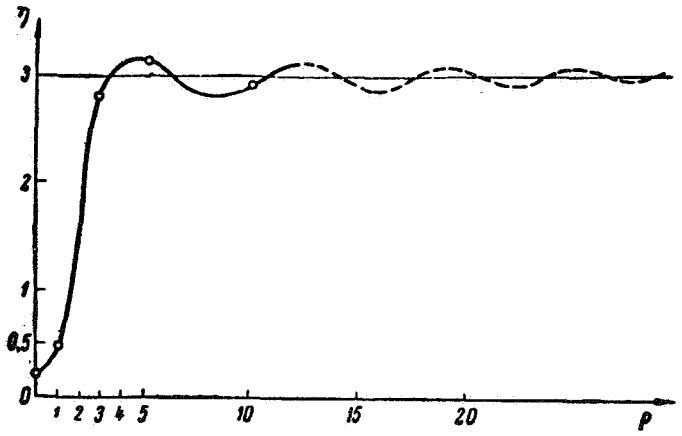

Figure 41. Coefficient of Indicatrix Asymmetry for $m = \infty$

§ 4. Radiation[1]

The absorption of radiation by particles is closely related to their emission. This problem is very important for geophysics, astrophysics, and physical chemistry.

Transforming the high frequency of solar radiation into the low frequency /165 of thermal radiation, the admixture particles noticeably participate in the thermal balance in the lower layers.

In the upper layers of the atmosphere, where the large number of dust particles is due to a meteor stream which is continuously trapped by the Earth, absorption and emission of radiation by particles is one of the most important mechanisms controlling the thermal processes.

In accordance with the Kirchhoff law, the radiation of particles is related to their absorption. In order to establish the appropriate formula, let us investigate an infinitely large sphere which is black on the inside (radius R), in the center of which our particle is located.

The energy flux which falls on the particle from an infinitely small area dS will be as follows (B_λ brightness of the area):

$$dF_\lambda = B_\lambda dS \frac{\pi a^2}{R^2}.$$

(1) Based on our article (Ref. 126).

The portion of it which is absorbed by the particle will be $\frac{k_a}{\pi a^2}$.[1] Thus, the particle decreases (by the quantity $\frac{k_a}{\pi a^2} dF_\lambda$) the amount of radiation which the area dS transmits to precisely the same area located at the other end of the diameter.

In the state of thermal equilibrium, this decrease in the flux will be compensated for by radiation of the particle on the same area. Thus, the particle brightness $b_\lambda(T)$ will be

$$b_\lambda(T)\frac{dS}{R^2} = \frac{k_a}{\pi a^2} B_\lambda dS \frac{\pi a^2}{R^2}, \qquad (6.20)$$
$$b_\lambda(T) = k_a B_\lambda(T).$$

The brightness of a unit area of the particle B^*_λ will be smaller by a factor of πa^2.

The particle radiation is isotropic. The total flux radiated by the particle per unit of time will be

$$f_\lambda = 4\pi k_a B_\lambda(T). \qquad (6.21)$$

For large black particles $k_a = \pi a^2$. We thus have

$$f_\lambda = 4\pi^2 a^2 B_\lambda(T) = 4\pi a^2 \cdot \pi B_\lambda. \qquad (6.22)$$

It is well known that the total radiation of a two-dimensional area dS equals dS · πB on the outside. In accordance with this, the latter formula thus yields the total radiation of a large black sphere. /166

If we take reflected light into account, then we must introduce the factor $(1 - R^{(1)})$ (see V, 6) in formula (6.22). When the radiation of large spheres is computed, it is not necessary to perform detailed numerical calculations of the integral for $R^{(1)}$. For example, the Gauss formula with three ordinates may be employed within an accuracy of 3-4%.

Let us now turn to small particles. The general formula (6.20) leads to several interesting results.

We saw above that attenuation is considerably greater than scattering for small particles. This means that attenuation is primarily due to absorption. In accordance with (4.12), the radiation brightness of a small particle may be determined by the following formula

$$b_\lambda = \frac{36\pi n x}{|m^2+2|^2} \cdot \frac{v}{\lambda_a} \cdot B_\lambda(T) \qquad (6.23)$$

The brightness of a unit area of a small particle will be /167

$$B^*_\lambda = \frac{24 n x}{|m^2+2|^2} \cdot \rho \cdot B_\lambda(T). \qquad (6.24)$$

---

[1] The quantity $\frac{dF_\lambda}{\pi a^2}$ is the radiation intensity.

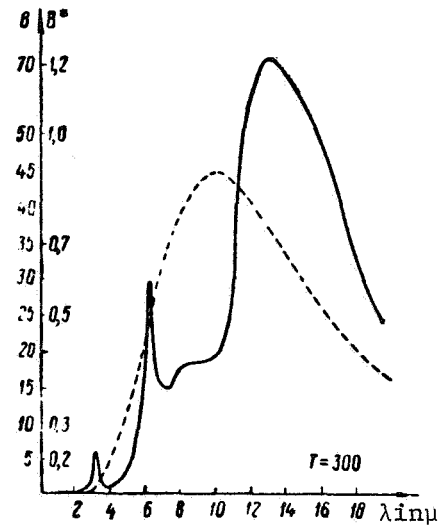

Figure 42. Thermal Radiation of Atmospheric Particles (Dashed Line Shows the Functions of Black Body Radiation).

If the spectral change m is small, and it may be approximately assumed that m is constant, then B^*_λ/B_λ for a small particle will be inversely proportional to the wave length λ. With allowance for the spectral behavior of m, the change in B^*_λ/B_λ will be more complex.

In order to illustrate the formula (6.24), we calculated the thermal radiation of mist particles -- small drops of water having a radius of 0.1 μ. Figure 42 shows the spectral changes in the radiation brightness of mist particles B* (at T = 300°) (solid line). For purposes of comparison, we present the same curve for radiation of a black body B (dashed curve). The scale of the second curve is ten times smaller.

Let us now find the integral radiation of a small particle. It may be determined by the general formula

$$b = \int_0^\infty k_\pi(\lambda) B_\lambda \, d\lambda.$$

For a small particle, a simple result may be obtained, if we assume that m is constant. By employing the Planck formula for radiation brightness, we obtain

$$b = \frac{36\pi n\varkappa}{|m^2+2|^2} \cdot v \cdot \frac{2h}{c^3}\left(\frac{kT}{h}\right)^5 \int_0^\infty \frac{x^4\,dx}{e^x-1}.$$

The integral thus included (we shall designate it by α) may be readily calculated;

$$\alpha = \int_0^\infty x^4\,dx\,(e^{-x}+e^{-2x}+\ldots) = \left(\sum_{k=1}^\infty \frac{1}{k^5}\right)\int_0^\infty e^{-t}\cdot t^4\cdot dt,$$

$$\int_0^\infty e^{-t} t^4 \, dt = \Gamma(5) = 24,$$

$$\sum_{k=1}^{\infty} \frac{1}{k^5} = 1{,}0369\ldots$$

Thus, $\alpha = 24.8856\ldots$

Consequently, the brightness of the particle b will be /168

$$b = \frac{b_0}{4\pi} \frac{n\varkappa}{|m^2+2|^2} v T^5; \; b_0 = \frac{72\pi\alpha k^5}{h^4 c^3}. \tag{6.25}$$

The constant b_0 is related to the Stefan-Boltzmann constant σ:

$$b_0 = \gamma \frac{k}{ch} \sigma; \quad b_0 = 21{,}808\ldots 10^{-5} \frac{\text{erg}}{\text{degree}^5 \cdot \text{cm}^3 \cdot \text{sec}} \tag{6.26}$$

(γ is the numerical factor; $\gamma = 5.7486\ldots$).

The total radiation of the particle is

$$f = b_0 \frac{n\varkappa}{|m^2+2|^2} v \cdot T^5. \tag{6.27}$$

We have obtained the following important result: the radiation of small particles is proportional to the fifth power of the temperature.

In the case of small conductive particles[1] [in accordance with (1.12)], the radiation will be $\sim \sigma v T^6$. Thus, the temperature dependence of the radiation is related to the temperature behavior of the resistance. Usually, $\sigma \sim \frac{1}{T}$ for metals, so that here $f \sim T^5$.

At low temperatures (as compared with the Debye temperature of the body), the behavior of σ is more complex. Theory leads to the dependence $\sigma \sim \frac{1}{T^5}$. This means that radiation of small metal particles will be $\sim T$ at low temperatures.

Based on their electric properties, dust particles are probably closest to semiconductors. For semiconductors which are highly conductive (electrons) $\sigma \sim e^{\Delta/T}$ [see, for example, (Ref. 88)]. Radiation of their small particles will be $\sim T^6 e^{\Delta/T}$.

For small particles (for constant m), the Wien displacement law will hold.

However, the constant in this law will differ from its customary value by the factor α/α^*. Here α and α^* are the roots of the transcendental equations:

$$1 = \frac{\alpha}{5} + e^{-\alpha}; \quad 1 = \frac{\alpha^*}{6} + e^{-\alpha^*}.$$

This factor is $\frac{\alpha}{\alpha^*} = 0.8296\ldots$

---

(1) If $|m^2 + 2|$ is assumed to be constant.

Particles suspended in air give up their heat due to thermal conductivity /169 and emission. It may be readily seen that the first flux is $\frac{k'}{4aT^3\sigma}$ times greater than the second (k' is the thermoconductivity coefficient of air, T -- temperature, σ -- Stefan-Boltzmann constant). This value is $\sim 10^4$ in the lower layers, and assumes the value ~ 1 only on the periphery of the atmosphere. In interstellar space, emission is the only cause of heat loss. Equilibrium between absorption and radiation determines the temperature of the particles located there.

An increase in the air temperature (per unit of time), causing it to be directly heated due to radiation absorption by admixture particles, is determined by the quantity $\Delta T = \frac{I_0 \pi a^2 n}{c}$ (n is the number of particles per cm^3, c -- specific heat of 1 cm^3). This yields about 0.05 - 0.1 degree/hour.

Both estimates pertain to large particles ($k_a = \pi a^2$). For small particles, the relative role of radiation will be significantly less. The same is true of heating of the air by particles.

In conclusion, we should note that the radiation of small particles determines the flame spectrum to a significant extent.

CHAPTER VII /170

TRANSPARENT PARTICLES HAVING ANY DIMENSIONS

§ 1. Attenuation Coefficient

Let us now analyze scattering by a large transparent sphere. We have already discussed this problem in Chapter V, but several new facts, which appeared in Chapter VI, compel us to return to this problem again. Let us begin by investigating data on tabulation of the attenuation coefficient.

For a transparent sphere, m is real. In this case, there is no absorption, and the attenuation coefficient must coincide with the scattering coefficient. We shall show that this fact actually follows from general formulas.

For real m, both arguments of the cylindrical functions are real. In this case, the formulas for amplitudes may be suitably transformed, so that in these formulas we may separate the real and imaginary parts in a general form. For this purpose, let us substitute the function $\zeta_\ell(\rho)$ by $\psi_\ell(\rho)$ and $\chi_\ell(\rho)$ in formulas (2.37), according to the formula (3.2). We may write the amplitudes in the following form

$$c_l = c_l' + ic_l''; \quad b_l = b_l' + ib_l''. \tag{7.1}$$

After simple transformations of the general expressions (2.39), we obtain the following formulas:

$$c_l' = q_l \frac{\varepsilon_l}{1+\varepsilon_l^2}, \quad c_l'' = q_l \frac{1}{1+\varepsilon_l^2}; \tag{7.2}$$

$$b_l' = -q_l \frac{\eta_l}{1+\eta_l^2}, \quad b_l'' = -q_l \frac{1}{1+\eta_l^2}. \tag{7.2*}$$

For purposes of brevity, we have introduced the following notation:

$$\left.\begin{aligned} q_l = (-1)^l \frac{2l+1}{l(l+1)}, \quad \varepsilon_l &= \frac{\chi_l(\rho)\psi_l'(m\rho) - m\chi_l'(\rho)\psi_l(m\rho)}{\psi_l(\rho)\psi_l'(m\rho) - m\psi_l'(\rho)\psi_l(m\rho)}, \\ \eta_l &= \frac{\chi_l'(\rho)\psi_l(m\rho) - m\chi_l(\rho)\psi_l'(m\rho)}{\psi_l'(\rho)\psi_l(m\rho) - m\psi_l(\rho)\psi_l'(m\rho)}. \end{aligned}\right\} \tag{7.3}$$

The following expressions are included in the formula for the scattering /171 coefficient:

$$\frac{l^2(l+1)^2}{2l+1}|c_l|^2 = \frac{2l+1}{1+\varepsilon_l^2}; \quad \frac{l^2(l+1)^2}{2l+1}|b_l|^2 = \frac{2l+1}{1+\eta_l^2}.$$

The corresponding terms in the expression for k will be:

$$\operatorname{Im}\left\{(2l+1)\left[\frac{\varepsilon_l}{1+\varepsilon_l^2} + i\frac{1}{1+\varepsilon_l^2}\right]\right\} = \frac{2l+1}{1+\varepsilon_l^2},$$

$$\operatorname{Im}\left\{(2l+1)\left[\frac{\eta_l}{1+\eta_l^2} + i\frac{1}{1+\eta_l^2}\right]\right\} = \frac{2l+1}{1+\eta_l^2}.$$

We can thus see that in actuality $k = k_p$ for real m.

The most detailed calculations of the attenuation coefficient have been published for drops of water suspended in air. They were performed by Stratton and Houghton (Ref. 74), who assumed that the drops were transparent, dielectric pellets with m = 1.33. These calculations were recently supplemented by Houghton and Chalker (Ref. 75).

The values given in Table 17 were obtained for the quantity $K(\rho)$ [$k = \pi a^2 K(\rho)$]. A graph showing the function $K(\rho)$ is shown in Figure 43.

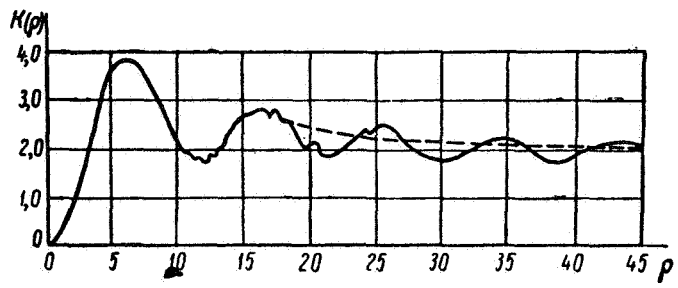

Figure 43. Scattering Coefficient for Drops of Water (m = 1.33).

The dashed line in Figure 43 shows the initial behavior of the curve [according to (Ref. 74)]. Along with large oscillations, which are similar to those which we noted for m = ∞, in the section ρ(12-25) the curve also has a small-scale ripple. Its occurrence may be simply explained by the fact that

more careful computations were performed in this section.

TABLE 17 /172

ρ	K(ρ)	ρ	K(ρ)	ρ	K(ρ)	ρ	K(ρ)
0,5	0,00676	9,0	2,738	12,250	1,892	17,125	2,704
0,6	0,0138	9,5	2,394	12,333	1,936	17,25	2,822
1,0	0,0938	10,0	2,152	12,5	1,938	17,375	2,820
1,2	0,171	10,25	2,052	12,6	1,822	17,5	2,738
1,5	0,322	10,5	1,886	12,75	1,850	18,0	2,598
1,8	0,522	10,625	1,918	13,0	2,012	18,5	2,432
2,0	0,710	10,75	1,930	13,5	2,192	19,0	2,218
2,4	1,126	10,875	1,832	14,0	2,474	19,25	2,090
2,5	1,212	11,0	1,740	14,5	2,528	19,5	1,998
3,0	1,754	11,125	1,728	15,0	2,744	19,75	1,976
3,6	2,376	11,333	1,734	15,5	2,740	20,0	2,092
4,8	3,490	11,4	1,768	16,0	2,870	20,25	2,180
5,0	3,592	11,5	1,858	16,25	2,872	20,5	2,078
6,0	3,888	11,75	1,758	16,5	2,850	21,0	1,834
7,0	3,722	12,0	1,670	16,75	2,810	22,0	1,922
8,0	3,282	12,125	1,776	17,0	2,632	24,0	2,438

We have already indicated, the reason for this "fine structure" may be found in the interference nature of scattering by drops. The oscillations $K(\rho)$ are gradually damped, and the limiting value for large particles is $2\pi a^2$.

Stratton and Houghton paid no attention to this fact (see Chapter VI). Their interest was directed toward the attenuation minimum which they discovered. They assumed that this minimum is caused by the transmittance maximum observed in artificial fogs in the case $\lambda = 0.490\ \mu$.

The large maxima and minima occur when ρ equals 6.15; 11.4; 16.2; 21.0; 25.5 approximately. At these points, $K(\rho)$ has the following values: 3.92; 1.67; 2.87; 1.83; 2.50.

Besides $m = 1.33$, the calculations of $K(\rho)$ were also performed for certain other m. Curves are presented in (Ref. 72) for m = 1.33; 1.44; 1.55 and 2.0.

We have shown these curves in Figure 44.

The first (large) maxima occur when ρ equals 6.15; 4.6; 3.6 and 2.0, respectively. Their values will be 3.9; 4.1; 4.4 and 4.8.[1] When m increases /173 (in the examined interval of m values), the position of the first large maximum is displaced to the left, and its value increases. We have discussed certain conclusions related to this fact in § 3.

We have already previously discussed the important consequences following

(1) There are no numerical data on the curves in Figure 44 in (Ref. 72).

from the doubling of the attenuation coefficient.

It is extremely difficult to calculate the scattering coefficient for large particles. The number of terms which must be taken into account will be on the order of ρ. For example, this means that for a cloud drop with $r = 10\ \mu$ we would have to calculate and combine about 120 terms in the visible region. Naturally, the question arises as to the analytical calculation of the sums determining k for $\rho \gg 1$. Jobst (Ref. 61) made an asymptotic investigation of k for this case. We have already presented the formula which he obtained for absolutely reflecting particles. We should point out that he also investigated the following cases:

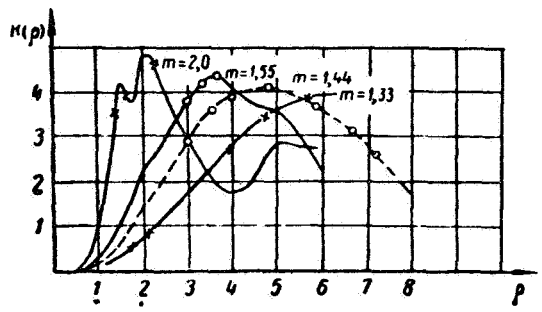

Figure 44. Scattering Coefficient for Different Transparent Particles.

a) $\rho(m-1) \ll \rho \ll 1$; b) $\rho(m-1) \ll 1 \ll \rho$; c) $1 \ll \rho(m-1) \ll \rho$.

Case (a) is the region in which the Rayleigh formula is applicable. The formula for k, which he obtains here, differs from the correct formula by the factor $1/2$ (see IV, 1). This is a result of incorrect "normalization" of the fundamental formulas, which we have already mentioned. In case (c), he /174 finds that $k = \pi a^2$. This is also incorrect. For case (b), which corresponds to scattering by a large transparent sphere, Jobst obtains the following after analyzing the general formulas

$$k = \pi a^2 \rho^2 (m-1)^2. \tag{7.4}$$

We shall discuss this result at a later point. We shall obtain it by a different method.

Due to the fact that the wave length is contained in the general formulas only in terms of ρ, we would like to point out that conclusions are frequently reached regarding the possible extension of the results derived from different calculations for given ρ to any λ, under the condition that the value of ρ will be maintained (with a corresponding change in a). These conclusions are invalid, since our formulas depend on λ also through m. We have seen, for example in (Chapter I), that in the case of water m changes greatly when a change is made from the visible region to the infrared region. Therefore, it is incorrect to extend the data given in Table 17, pertaining to the case $m = \frac{4}{3}$, to the infrared region.[1] However, we must stress the fact that spectral changes in m have considerably less influence upon the optical properties of fogs than upon the properties of solid bodies (see page 179).

The data presented in Table 17 give the dependence of the fog attenuation coefficient upon the size of its particles when there is a constant number of particles per unit volume. In certain cases, it is interesting to have the dependence of unit volume attenuation upon the particle values for a constant

(1) Several authors have made this mistake. In particular, this line of reasoning is widely employed by Gertner in his book [(Ref. 45), pages 44-47].

mass of suspended matter. Since the number of particles per unit volume is $n \sim \frac{1}{a^3}$, for small particles the attenuation coefficient in the medium $\alpha = kn$ will be $\sim a^3$, and for large particles it will be $\alpha \sim \frac{1}{a}$. This curve is shown in Figure 45.[1] The narrow scattering maximum occurring at $a \sim \lambda$ is of interest. This means that fog with particles of a corresponding size is the most transparent. This fact was first indicated in 1939 by G. I. Pokrovskiy, and in /175
1947 by Langmuir. These arguments were corroborated experimentally by K. I. Ivanov recently (Ref. 76). He studied the transmittance of kaolin and clay sediment suspensions in distilled water. He found that for a constant weight concentration of suspended substances, the attenuation coefficient has a maximum at $a \sim \lambda$, rapidly decreasing toward small a and decreasing more slowly toward large a.

Let us briefly investigate research on spectral transmittance of "pure" atmosphere, fogs, and clouds.

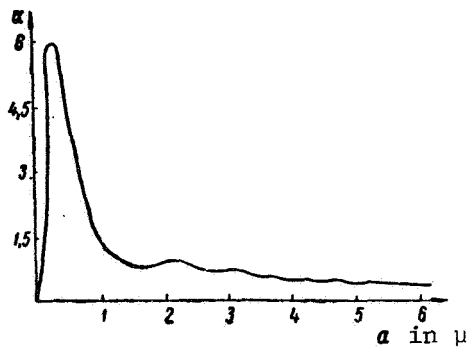

Figure 45. Attenuation of Visible Radiation in Fog with a Constant Amount of Deposited Water.

Research on the spectral transmittance of a "pure" atmosphere in the visible and close infrared region has indicated that the transmittance increases with an increase in λ. V. A. Faas (Ref. 78) assumes that for practical purposes the phenomenon may be described very well by the following simple formula with two terms

$$\alpha = \frac{a}{\lambda^4} + b. \qquad (7.5)$$

According to data given by M. M. Staude in (Ref. 79), which presents a detailed summary of observations on transmittance, the constants a and b will be [cited from (Ref. 78)]

$$a = 0{,}0014\ \frac{\mu^4}{\text{км}};\quad b = 0{,}018\ \frac{1}{\text{км}}.$$

When λ is substituted in μ, we obtain α in km^{-1}.

The data presented above refer to the total influence of absorption in /176
molecules scattered by density fluctuations and refer to attenuation by admixtures. In order to study the influence of admixtures, the first two phenomena must be eliminated. S. F. Rodionov and his co-workers (Ref. 80) made a detailed investigation of the influence of admixtures upon atmospheric transmittance.

In this study, which was performed at an altitude of 3-5 km in the mountains, it was shown that the assumption that the optical role of admixtures is negligibly small at altitudes of more than two kilometers is incorrect. It was found that

(1) In order to obtain α in cm^2/g, the digits on the ordinate axis in Figure 45 must be multiplied by 10^4.

attenuation, which depends on the admixtures at altitudes of 3-5 km, is of the same order as attenuation due to density fluctuations.

In contrast to the almost monotonic change in transmittance for total attenuation[1], attenuation by admixtures has a non-monotonic behavior. We present the data from one of the observations of S. F. Rodionov in Figure 46. This curve enables us to speak of an attenuation band which depends on the admixtures. We should note that similar bands were also discovered by Vassy (Ref. 81), who studied atmospheric transmittance in the lower layers with artificial light sources. The maxima of the Vassy bands are located at larger λ than are those of Rodionov. This shift in the maximum is naturally related to the fact that Vassy was dealing with larger particles. The Vassy bands were more diffused than the Rodionov bands. This may apparently be explained by the more diffused spectrum of the particle dimensions below. The dashed curve in Figure 46 shows the behavior of the attenuation coefficient calculated by Rodionov according to (Ref. 74). The maximum of k obtained in the experiment at $\lambda = 0.38\ \mu$ corresponds to drops of water with $a = 0.39\ \mu$, for which the dashed curve is compiled. The experimental band obtained by Rodionov is still theoretical. This fact, which seems to be incomprehensible at first glance, may be explained if we take the fact into account that the spectral changes of m are disregarded in the computations of Stratton and Houghton. When these changes are taken into account, the spectral curves become sharply constricted (see the data of Savost'yanova in Figure 29): they acquire the nature of narrow bands.

Data on the spectral transmittance of a "pure" atmosphere in the ultra- /177
violet region (0.30 - 0.36 μ) may be found by the reader in the work of Polyakova (Ref. 97). Along with admixtures and density fluctuations, absorption in ozone is of great importance for attenuation of solar radiation.

Several authors have performed experimental investigations of the transmittance of natural and artificial fogs and other aerosols. A survey of the old articles may be found in the book by Yu. I. Veytser and G. P. Luchinskiy, and the article by O. B. Orlov (Ref. 82) or in (Ref. 45). As a rule, when λ increases there is an increase in the transmittance. Houghton (Ref. 74), on the other hand, observed the reverse behavior, which is apparently related to the behavior of the theoretical curve $K(\rho)$.

P. Ya. Bokin, Ye. M. Brumberg, A. A. Lebedev, and V. I. Chernyayev (Ref. 83) performed a careful study of cloud transmittance. Great attention was paid to measuring the dimensions of drops in the cloud. The authors reached the conclusion that, in contrast to the case of mist, the use of infrared waves has no advantage over the use of visible waves in a fog. Figure 47 presents the data which they obtained for the ratio of passing light intensities I to /178
incident light intensity I_0 [according to Khvostikov (Ref. 23)]. Curve 1 pertains to a fog with the drops $a = 8\ \mu$ and curve 2 pertains to drops with $a = 9\ \mu$. In the case of almost identical drops, different spectral dependences were obtained (water content was almost the same in both cases). Similar

---

(1) A small distortion of the smooth behavior may be observed between 0.5 - 0.6 μ.

contradictions were also discovered when the experimental data of other authors were compared.

An analysis of the problem, which I. A. Khvostikov performed (Ref. 23), led him to the conclusion that in fogs, along with drops having a radius of 5 - 10 μ, there is a large number of submicroscopic drops (radius of about 0.1 μ), whose number and dimensions cannot be controlled by ordinary methods. A change in this uncontrollable component of the fog leads to an apparent contradiction in the data of different authors. It is apparently also the reason for the lack of agreement between observational data and theory in several cases.

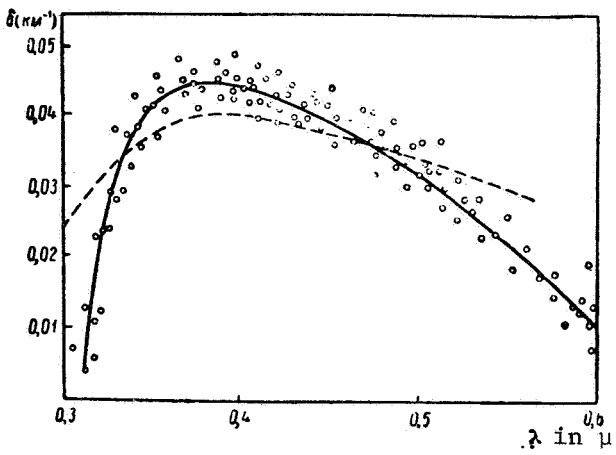

Figure 46. Band of Attenuation by Admixtures in Air.

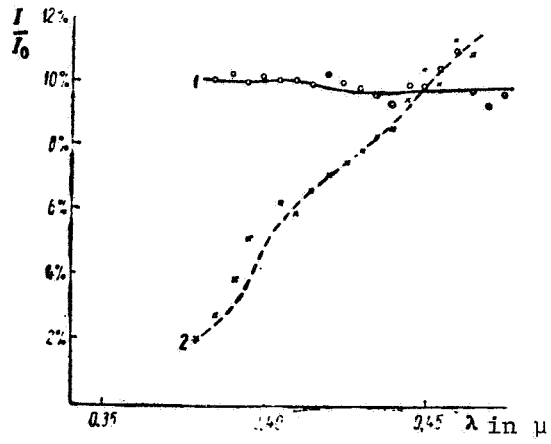

Figure 47. Spectral Transmittance of Fogs

In order to determine the transmittance of different hydrometeors, it is advantageous to introduce the magnitude of the ray path in the medium, over which its intensity decreases by a factor of e. We shall call this quantity the mean free path of radiation, and shall designate it by R. Let α be the attenuation coefficient in the medium, and n be the number of particles per unit volume. It is apparent that /179

$$R=\frac{1}{\alpha}=\frac{1}{kn}. \tag{7.6}$$

For clouds, fogs, and rain, in the visible region we have

$$R=\frac{1}{2\pi a^2 n}=\frac{2a\sigma\cdot 10^6}{3q}. \tag{7.6*}$$

Here n is given in $\frac{1}{cm^3}$, a -- particle radius in cm, σ -- density in g/cm^3, q -- water content in g/m^3, and R is given in cm. The values of R for clouds are about 5 - 10 m. The values of R are given below in meters for different hydrometeors:

Fog.....	510	Moderate Rain	1135
Thick Fog.....	590	Strong Rain.....	620
Fine Rain..... .	790	Very Strong Rain.....	380
Summer Rain	1075	Showers.....	180 - 65

We should note that, out of the hydrometeors investigated, moderate rain is the most transparent.

The mean free paths of radiation in the media are proportional to the meteorological range of visibility S in them (VI, 2):

$$S = R \ln\left(1 + \frac{1}{\varepsilon}\right).$$

The thickness of the medium layer, measured in R, is called its optical thickness.

When making a theoretical interpretation of the optical properties of fogs, one sometimes finds an analogy between the behavior of fogs and the behavior of sheets of water having a thickness coinciding with the thickness of a layer of "deposited water" in fog (Ref. 84). This analogy is incorrect. In actuality, due to the presence of a large number of phase boundary surfaces, on which reflection and diffraction occur, the optical properties of fogs and solid sheets are completely different. Thus, for example, it follows from Table 7 that a sheet of water having a thickness of 10 μ attenuates radiation at $\lambda = 3$ μ by a factor of $e^{7.33} = 1525$ whereas the equivalent layer of a cloud (equalling 10 m at $q = 1$ g/m^3, $R = 6.6$ m[1]) attenuates the flux by a factor of $e^{1.5} = 4.5$ in all, i.e., it is 340 times weaker. It is also important to note that the spectral changes of the sheet properties take place incomparably more intensely than the changes in fog.

As compared with the tremendous changes in the transmittance ($1/\alpha$) for sheets during a change from the visible region to the infrared region (by a factor of $\sim 10^6$), it can be assumed that the transmittance of fogs is practically unchanged (they can change by no more than a few times). /180

If we are dealing with a small fog layer, so that its optical thickness (τ) is small, the radiation intensity after penetrating the layer will be $I = I_0 e^{-\tau}$, and the relative attenuation will be $\frac{\Delta I}{I_0} = \tau$. If the fog mass in a column having the cross section 1 cm^2 is M, then $\tau = k \frac{M}{m_0} = k_0 M$, where k_0 is the ratio of the drop attenuation coefficient (k) to its mass (m_0). By employing the quantity $K = \frac{k}{\pi a^2}$, we may find the following:

$$k_0 = \frac{3}{4d_0}\frac{K}{a} = \frac{3\pi}{2d_0}\frac{1}{\lambda_a}\frac{K}{\rho}. \qquad (7.7)$$

Here d_0 is the density of the particles.

For large particles in any spectral region, $K = 2$ and $k_0 = \frac{3}{2d_0} \cdot \frac{1}{a}$. For example, this means that for fog with $a = 30\mu$ (for those λ for which we may assume that the particles are very large) we obtain $k_0 = 500$ cm^2/g. For a layer of this fog having a thickness of 10 m with a water content of 0.25 g/m^3, $M = 0.25 \cdot 10^{-3}$ g/cm^2 and $\tau = 0.375$.

---

(1) It is assumed that the drop radius equals 10μ.

For small absorbing particles we readily obtain the following from formula (4.2):

$$k_0 = \frac{36\pi n\varkappa}{|m^2+2|^2 d_0} \cdot \frac{1}{\lambda_a}. \qquad (7.7^*)$$

It is interesting to note that, in contrast to the case of small absorbing particles, k_0 does not depend on the particle dimensions. We may employ Table 7 to find the function $k_0(\lambda)$ for water. The curve obtained has maxima at 3 μ and 6 μ and rises beyond 11 μ, since its form is primarily determined by the form of the curve $x(\lambda)$. For thermal radiation (λ = 10μ), k_0 = 640 cm^2/g. In order to determine the value of k_0 in the region of average ρ -- i.e., in the region containing the attenuation maxima -- it is necessary to tabulate K(ρ). The behavior of the curve K(ρ) may be found, with an accuracy which is sufficient for several problems, by employing the rule of similarity (see § 3), if (m - 1) is small (< 1). For water, for λ = 10 μ, m = 1.208 - i 0.056. Omitting the /181 small imaginary part of m, by employing the rule of similarity we find that, for m = 1.21, the extremums K(ρ) occur when ρ equals 9.5; 17.6; 25.7 and 33.4. Approximate calculations of K(ρ) yield the following: 3.64; 1.65; 2.70 and 1.84. The values at the minimums practically coincide with the values in the case m = 1.33. The maxima are located somewhat lower.

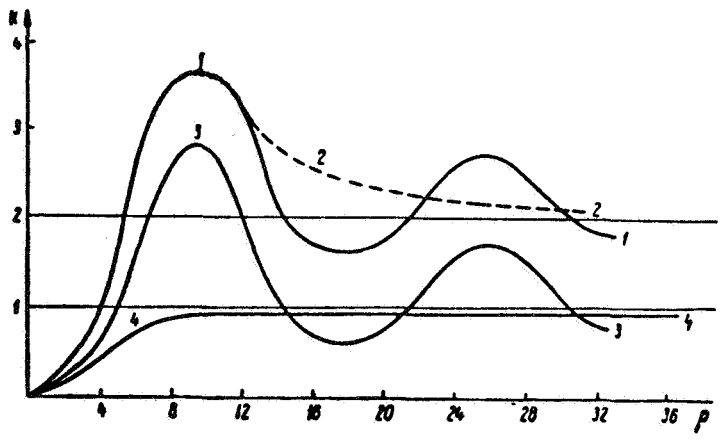

Figure 48. Coefficients of Attenuation, Scattering, and Absorption of Thermal Radiation by Drops of Water

Curve 1 in Figure 48 shows K(ρ); curve 2 -- the smoothed behavior of K(ρ); curve 3 -- the behavior of $K_p(\rho)$ (scattering coefficient in fractions of πa^2); curve 4 -- the behavior of $K_a(\rho)$ (absorption coefficient in fractions of πa^2). For k_0, in the case λ = 10 μ and d_0 = 1 g/cm^3, we find

$$k_0 = 4700 \frac{K}{\rho} \, cm^2/g.$$

If we smooth out the curve for K(ρ) behind the main maximum, we find the following values of radiation attenuation with λ = 10 μ in monodispersed fogs with particles having different radii:

a in μ....	0	4,8	9,6	14,4	19,2	24	32
k_0 in cm^2/g	640	700	1900	1900	1300	800	500

For a > 30 μ, the value is $k_0 \simeq \frac{3}{2a}$ cm^2/g.

The problem of the transmittance of fogs for thermal radiation is closely related to the problem of changes in the radiation balance of the Earth's surface when there are radiation fogs. It may be readily shown that the relative change in the balance R will be the following for small fog thicknesses /182

$$\frac{\Delta R}{R} = -(\alpha_a + r),$$

where α_a is the absorptive power of the fog, and r is its reflectivity. These values may be calculated by the data which we have given above for K(ρ) in the case λ = 10 μ. We thus find that the reflectivity r is 10 times smaller than the absorptive power of the fog α_a. The calculations show that for fogs with a < 14 μ (α_a + r) approximately equals -- 6W, where W is the amount of deposited water in a given layer of fog per g/m^2. We thus have the following simple formula

$$\frac{\Delta R}{R} = -6W.$$

It is of interest to note that this phenomenon is independent of the fog structure, if it only contains particles with a > 14 μ.

V. V. Shuleykin, A. A. Gershun and others studied scattered light in the sea. Even in 1921 (Ref. 85) V. V. Shuleykin had noted the significant influence of very large particles upon the behavior of a light flux in the sea. In a work published in 1923 (Ref. 86), V. V. Shuleykin presented the results derived from measuring scattering in seas. For two years he measured scattering at different depths (Ref. 87). It was thus found that the scattering coefficient decreases with depth. This may be explained by the higher contamination of the upper layers. V. V. Shuleykin also noted the value of the optical characteristics for studying sea currents and their transformation. We should point out that at a later time N. N. Kalitin developed a similar concept regarding optical methods of studying transformation of air masses [the method of "color temperature", and others (Ref. 90)].

A. A. Gershun studied the spectral behavior of the attenuation coefficient in sea water [(Ref. 91) and (Ref. 92)]. The experimental curves (1, 2, 3 in Figure 49) reveal a parallel behavior with the theoretical curves (curves I, II, III; they were calculated for three different particle dimensions, in /183 accordance with the differing, probable composition of samples 1, 2, 3).

Linke and Borne experimentally studied the spectral transmittance of haze from artificial fogs (NH_4Cl, ladanum, soot, tobacco smoke, and others) (Ref. 93). Assuming that $k \sim a^x \lambda^{-\alpha}$, they found that for the visible section in dusty air one can use the general curve for the dependence of x and α on a (Figure 50). This curve represents the averaging of their measurements for different smokes.

According to their data, fogs transmit in a neutral manner.

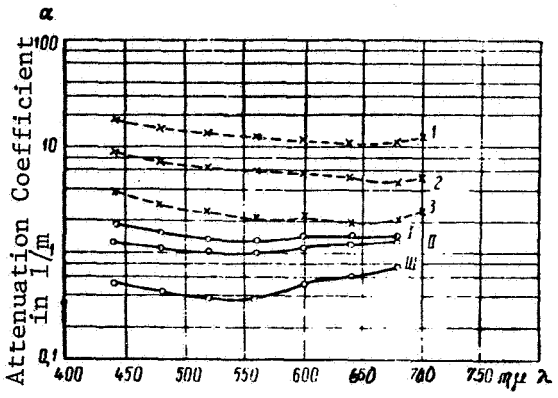

Figure 49. Spectral Transmittance for Admixtures in Sea Water.

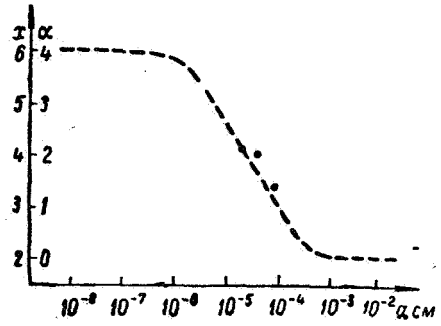

Figure 50.

We should point out that these data were cleverly employed by V. G. Fesenkov recently to determine the measurements of particles which remained in the atmosphere after the Tungusskiy meteorite burned up (Ref. 94). According to V. G. Fesenkov, the particle radius is $\sim 10^{-4}$ cm. /184

§ 2. Geometric Optics of a Sphere as the Limiting Case of Diffraction

In Chapter V we investigated scattering by a large sphere using the methods of geometric optics. This chapter differs from all of the chapters previously investigated in the fact that the formulas it contains were not separated from the general formulas of Chapter II, but were obtained directly from the laws of geometric optics.

However, in principle it is very important to show that these formulas are contained in the general formulas. This is the purpose of the present section. We shall show that geometric optics of a sphere comprises the limiting case (for $\rho \to \infty$) of the general diffraction theory. In contrast to the attenuation coefficient, where for $\rho \to \infty$ the passage to the limit of the precise value into a value corresponding to geometric optics does not occur, this passage to the limit occurs for the intensity of scattered light.[1]

Let us investigate the case of a large nonabsorbing particle -- a case which represents the primary difficulty in calculations, since it is necessary to take into account several bundles. Apart from its principal value, an asymptotic investigation of the formulas for intensity, which we shall give below, is important for understanding the structure and physical content of the general solution for large ρ.

---

(1) Except for the angles (and the sections close to them) where the formulas of geometric optics can be used.

The problem which we shall deal with has already been studied in one, comparatively little known work of Debye for the case of a cylinder (Ref. 95). In this study, Debye investigated the asymptotic form of the formulas for a diffracted field in the case of the cylinder.

In view of the linearity of the Maxwell equations (1.3), we must try to find their solution in the form of an integral whose kernel can be determined from the boundary conditions. This leads to the double Fourier integral, instead of the series (2.41).[1] By employing approximation representations for /185 the Bessel functions, Debye determined the asymptotic value of the double integral. He found that the quantity $\rho = \frac{2\pi a}{\lambda}$ strives to infinity for a cylinder, and the diffracted field around an absolutely reflecting or refractive cylinder strives to those values which follow from geometric optics. In certain directions -- namely in the directions of the rainbows -- the field amplitude strives to infinity.

Let us investigate a similar problem for the case of a sphere.[2] We shall follow our previous study in (Ref. 43) (1947).

Let us turn to formulas (3.26) for the amplitudes c_ℓ and b_ℓ in the case of large ρ. A very simple meaning may be attributed to these formulas, if we search for an analogy with geometric optics. In this sense, we shall regard the expression (3.26) as the angle at which a ray falls on a sphere. We should recall that τ_0, in accordance with the formula (3.23) and in accordance with the fact that $1 \leq \ell \leq \rho$, changes from $\pi 2$ to 0, and consequently the angle $\frac{\pi}{2} - \tau_0$ changes from 0 to $\pi 2$. In this case, $\frac{\pi}{2} - \tau_1$ is the refraction angle of the ray, since τ_1 and τ_0 are related by the following equation:

$$\cos\tau_0 = m\cos\tau_1, \tag{7.8}$$

which coincides with the refraction law. Different rays falling on the sphere correspond to different components in the sums. Components with small numbers ℓ correspond to rays with small angles of incidence which are close to zero. Rays which are tangent to the sphere correspond to components with the numbers ℓ around ρ. Viewed in this way, it is understandable that for large ρ our sums are truncated at $\ell \sim \rho$. Rays passing outside of the sphere correspond to terms of the sum with $\ell > \rho$. The physical meaning of the fact that our sums are truncated at $\ell \sim \rho$ in the case $\rho >> 1$ may be found in this fact.

The quantities ε_1 and ε_2 which were previously derived now acquire a simple meaning. By employing the refraction law, we may rewrite the formulas /186 for ε_1 and ε_2 as follows:

---

(1) For greater details, see our article (Ref. 43).

(2) This case is considerably more complex than the case investigated by Debye, since the angular dependences of partial waves are very simple for a cylinder.

$$\varepsilon_1 = \frac{\sin(\tau_0 - \tau_1)}{\sin(\tau_0 + \tau_1)}; \quad \varepsilon_2 = \frac{\operatorname{tg}(\tau_0 - \tau_1)}{\operatorname{tg}(\tau_0 + \tau_1)}. \tag{7.9}$$

Making a comparison with the formulas (5.1), we can see that the quantities ε_1 and ε_2 are the ordinary Fresnel reflection coefficients for fields with an oscillation normal to (ε_1) and along (ε_2) of the plane of incidence.[1]

It follows from formulas (7.9) that, in terms of absolute magnitude, the quantities ε_1 and ε_2 are less than unity over the entire interval considered for the numbers ℓ. Let us now represent our amplitudes c_ℓ and b_ℓ in the form of series in terms of the quantities $i\varepsilon_2 e^{-2im\rho f_1}$ and $i\varepsilon_1 e^{-2im\rho f_1}$. After simple transformations, we obtain

$$\begin{aligned} c_l &= (-1)^l \cdot i \cdot \frac{2l+1}{l(l+1)} \cdot \frac{1}{2} \cdot \{1 - i \cdot e^{2i\rho f_0}[-\varepsilon_2 + (1-\varepsilon_2^2)q + \\ &+ (1-\varepsilon_2^2)\varepsilon_2 q^2 + (1-\varepsilon_2^2)\varepsilon_2^2 q^3 + \ldots]\} = (-1)^l \cdot i \cdot \frac{2l+1}{l(l+1)} \times \\ &\times \frac{1}{2}\left\{1 - ie^{2i\rho f_0}\left[-\varepsilon_2 + (1-\varepsilon_2^2)q \sum_{k=2}^{\infty} (\varepsilon_2 q)^{k-2}\right]\right\}. \end{aligned} \tag{7.10}$$

For purposes of brevity, we have introduced the following notation here

$$q = \frac{1}{i} e^{-2im\rho f_1}.$$

In a similar way, we obtain

$$\begin{aligned} b_l = -(-1)^l i \frac{2l+1}{l(l+1)} \cdot \frac{1}{2}\Big\{1 - i \cdot e^{2i\rho f_0} \times \\ \times \left[-\varepsilon_1 + (1-\varepsilon_1^2)q \sum_{k=2}^{\infty} (\varepsilon_1 q)^{k-2}\right]\Big\}. \end{aligned} \tag{7.11}$$

In this form, the formulas for the amplitudes c_ℓ and b_ℓ in the case of large ρ acquire a simple and clear meaning.

A parallel bundle of light, falling on a drop, is scattered by it in different ways. Part of the light passing outside of the drop contours is diffracted by the drop contours. The other part is reflected from the /187 outer surface. Part of it penetrates right through, as though penetrating through a lens, undergoing two refractions; part of it undergoes refraction, internal reflection, refraction again, etc.

The structure of the partial wave amplitude according to formulas (7.10) and (7.11) exactly coincides with this physical picture. Unity in the parentheses corresponds to diffracted light. We have seen above (VI, 2) that in the forward direction it leads to a formula for coronas and to doubling of

---

(1) The formula for ε_1 is usually written with a minus sign. We have used this sign if we change from the angles τ_0 and τ_1 to the angles of incidence and refraction.

the attenuation coefficient. At a later point, we shall show that in the backward direction (direction to the source) it leads to an unusual diffraction phenomenon (diffraction backwards). The expressions contained in the brackets, as we shall show below, correspond to different bundles of geometric optics. The first term in the brackets is reflected light, the second term is refracted light, etc. Thus, for large particles a partial wave is composed of diffracted light and different bundles of geometric optics.

Let us now turn to the angular functions. We have already noted that for large ℓ we may disregard Q_ℓ, as compared with S_ℓ. The formula for S_ℓ in the case $\ell \to \infty$ may be readily obtained from the formula (3.40), if we assume that θ is not very close to 0 or to π. Assuming that $(\ell+\frac{1}{2})\,\theta=y \gg 1$ and employing the asymptotic formula for $J_0(y)$, we readily obtain

$$S_l(\theta)=\sqrt{\frac{2}{\pi\sin\theta}}\left(l+\frac{1}{2}\right)^{1/2}\cos\varphi, \tag{7.12}$$

where $\varphi=\left(l+\frac{1}{2}\right)\theta-\frac{\pi}{4}$.

Let us now turn to the formulas for intensity. Disregarding terms with Q_ℓ, and confining ourselves to summation over $\ell \sim \rho$ and changing from θ to the scattering angle β [see (3.41)], for the quantity i_1 we obtain

$$i_1=\left|\sum_{l=1}^{\rho} b_l^* S_l^*\right|^2=\frac{1}{2\pi\sin\beta}\left|\sum_{l=1}^{\rho}\left(l+\frac{1}{2}\right)^{1/2}(e^{i\varphi}+e^{-i\varphi})\,b_l^*\right|^2.$$

Let us now replace b_ℓ^* by its expression according to formulas (7.11) and (3.42). Taking the fact into account that $\ell \gg 1$, we readily obtain /188

$$i_1=\frac{1}{2\pi\sin\beta}\left|\sum_{l=1}^{\rho}\left(l+\frac{1}{2}\right)^{1/2}(e^{i\varphi}+e^{-i\varphi})\left\{1+i\varepsilon_1 e^{2i\rho f_0}-\right.\right.$$
$$\left.\left.-ie^{2i\rho f_0}(1-\varepsilon_1^2)\,q\sum_{k=3}^{\infty}(\varepsilon_1 q)^{k-3}\right\}\right|^2. \tag{7.13}$$

Let us now turn from the summation variable of ℓ to the variable τ_0, which is related to ℓ by the following equation

$$\cos\tau_0=\frac{l+\frac{1}{2}}{\rho}\doteq\frac{l}{\rho};\quad \varphi=\rho\beta\cos\tau_0-\frac{\pi}{4}. \tag{7.14}$$

At the same time, let us designate the expression contained in i_1 by the sign $|\ |^2$ by A. Let us represent it in the form of a sum over k in the following way:

$$A=a_{1,2}^{(0)}+a_{1,2}^{(1)}+\sum_{k=2}^{\infty}a_{1,2}^{(k)}. \tag{7.15}$$

Here $a_{1,2}^{(k)}$ correspond to different components within the parentheses and the index 1 indicates that a term is chosen which contains $e^{i\phi}$. The index 2 indicates that a term is chosen containing $e^{-i\phi}$:

$$\left.\begin{aligned} a_{1,2}^{(0)} &= \sum_{l=1}^{\rho} \sqrt{\rho\cos\tau_0}\, e^{\pm i\varphi}; \\ a_{1,2}^{(1)} &= \sum_{l=1}^{\rho} \sqrt{\rho\cos\tau_0}\, \varepsilon_1 e^{i\left(2\rho f_0 \pm \varphi + \frac{\pi}{2}\right)}; \\ a_{1,2}^{(k)} &= \sum_{l=1}^{\rho} \sqrt{\rho\cos\tau_0}\,(1-\varepsilon_1^2)\, q\,(\varepsilon_1 q)^{k-2} e^{i\left(2\rho f_0 \pm \varphi + \frac{3\pi}{2}\right)}. \end{aligned}\right\} \qquad (7.16)$$

In accordance with the above, the term $a_{1,2}^{(0)}$ corresponds to diffracted light, and the term $a_{1,2}^{(1)}$ corresponds to reflected light, etc.

Our subsequent problem consists of an asymptotic determination of the sums (7.16).

In order to avoid complicating the problem we shall first perform a simple, but approximate, examination of the problem, and then shall turn to a precise and rigorous analysis.

The approximate method consists of replacing our sums by their integrals. /189 The components contained in the sums for $a_{1,2}^{(k)}$ are complex numbers which fluctuate around each other. The asymptotic value of these sums will be very small, with the exception of those summation intervals where the terms have approximately the same phases. The integrals obtained from the sums (7.16) can be determined by the method of stationary phases. Thus, those integration intervals, where the phases rapidly change and where, consequently, the replacement of the sum by the integral could lead to errors, make a negligibly small contribution to the integral, and are not taken into account. In those intervals which make a real contribution to the integral -- intervals with approximately a constant phase -- the replacement of the sum by the integral cannot lead to significant errors.[1]

Let us now investigate the integrals obtained.

Noting that $dl = -\rho \sin\tau_0 d\tau_0$ and changing the order of integration ($\ell = 0$ corresponds to $\tau_0 = \frac{\pi}{2}$, and $\ell = \rho$ corresponds to $\tau_0 = 0$), we obtain integrals having the following form:

$$\left.\begin{aligned} a_{1,2}^{(0)} &= \rho^{3/2} \int_0^{\frac{\pi}{2}} \sqrt{\cos\tau_0}\,\sin\tau_0 \cdot e^{\pm i\left(\rho\beta\cos\tau_0 - \frac{\pi}{4}\right)} d\tau_0; \\ a_{1,2}^{(1)} &= \rho^{3/2} \int_0^{\frac{\pi}{2}} \sqrt{\cos\tau_0}\,\sin\tau_0 \cdot \varepsilon_1 \cdot e^{i\left(2\rho f_0 \pm \varphi + \frac{\pi}{2}\right)} d\tau_0; \end{aligned}\right\} \qquad (7.17)$$

---

(1) It follows from this that our approximate method cannot lead to significant errors. It is shown in (Ref. 43), by performing a comparison with the result of Debye, that for the case $m = \infty$ the replacement of the sums by the integrals is correct.

$$a_{1,2}^{(k)} = \rho^{3/2} \int_0^{\frac{\pi}{2}} \sqrt{\cos\tau_0} \sin\tau_0 \times$$
$$\times (1 - \varepsilon_1^2)\, \varepsilon_1^{k-2} \cdot e^{i\left(3\rho f_0 \pm \varphi + \frac{3\pi}{2}\right) - i(k-1)\left(2m\rho f_0 + \frac{\pi}{2}\right)} d\tau_0. \tag{7.17}$$

Several authors have made an asymptotic investigation of the integrals of /190 rapidly oscillating functions. The results derived from these studies are well known.

In the case $\rho \to \infty$, only those integration intervals where the phase is stationary make the largest contribution to the integral. If we write our integral in the following form

$$J = \int_a^b f(x)\, e^{i\rho\psi(x)} dx, \tag{7.18}$$

we obtain the following:

(a) If there are no points where $\psi'(x) = 0$ within the segment [a, b], we then have

$$J = f(x_1) \frac{1}{\psi'(x_1)} \cdot e^{i\left(\rho\psi(x_1) \pm \frac{\pi}{2}\right)} \cdot \frac{1}{\rho}. \tag{7.19}$$

Here x_1 is the segment boundary. The plus sign in the exponent corresponds to the lower boundary, and the minus sign corresponds to the upper boundary.

(b) At the points x_0 where $\psi'(x) = 0$, and $\psi''(x) \neq 0$, we have

$$J = \sqrt{\frac{2\pi}{\psi''(x_0)}} f(x_0) \frac{1}{\sqrt{\rho}} e^{i\left(\rho\psi(x_0) + \frac{\pi}{4}\right)}, \tag{7.20}$$

if x_0 lies within the segment [a, b]. J equals a quantity which is twice as small, if x_0 coincides with one of the segment boundaries, and has a higher order of smallness if x_0 is outside of [a, b].

(c) At the points x_0 where $\psi'(x) = \psi''(x) = 0$, a $\psi'''(x) \neq 0$, we have

$$J = \frac{\Gamma\left(\frac{1}{3}\right)}{\sqrt[3]{\frac{3^{3/2}\psi'''(x_0)}{6}}} f(x_0) \frac{1}{\sqrt[3]{\rho}} e^{i\rho\psi(x_0)}, \tag{7.21}$$

if x_0 lies within the segment [a, b]. If this point coincides with the lower segment boundary, then J acquires the factor $\frac{e^{i\frac{\pi}{6}}}{\sqrt{3}}$, and if this point coincides with the upper segment boundary, J acquires the factor $\frac{e^{-i\frac{\pi}{6}}}{\sqrt{3}}$.

Let us apply this rule for determining the different terms $a_{1,2}^{(k)}$. At $a_{1,2}^{(0)}$, the phase of the integrand will be stationary for all τ_0, where $\sin\tau_0 = 0$.

Here, however, the integrand equals zero, and consequently the asymptotic contribution to the diffracted light of the scattering angles, which are not close to 0 or π, equals zero. /191

The phase of the integrand for reflected light (at $a_{1,2}^{(1)}$) will be:

$$\psi_{1,2} = 2(\sin\tau_0 - \tau_0\cos\tau_0) \pm \beta\cos\tau_0. \tag{7.22}$$

Both functions (ψ_1 and ψ_2) have $\tau_0 = 0$ as a root of their first derivatives. This root is discarded, just as in the previous case: the integrand at this point equals zero.

In addition, the derivatives ψ_1 and ψ_2 also have roots in the case $\tau_0 = \pm\beta/2$ (plus for ψ_1, and minus for ψ_2).

The root ψ_2 lies outside of the integration interval, whereas the root ψ_1 lies within it. Consequently, only $a_1^{(1)}$ now remains for us.

Noting that

$$\psi_1''(\beta/2) = 2\sin\beta/2,$$

we readily find that the preexponential factor will be:

$$\rho\sqrt{\frac{\pi\sin\beta}{2}}\,\varepsilon_1(\beta/2),$$

where

$$\varepsilon_1(\beta/2) = \sin\beta/2.$$

Turning to i_1, we find that $i_1 = \frac{\rho^2}{4}|\varepsilon_1|^2$. We obtain the following for intensity of light:

$$I_1 = \frac{I^0}{2}\frac{a^2}{4R^2}\varepsilon_1^2. \tag{7.23}$$

If we take the fact into account that $\varepsilon_1^2 = r_s$, we immediately see that this expression exactly coincides with the expresssion for the intensity of reflected light I_s, which was given in Chapter V

$$\left[(5.6),\ I_s^{(0)} = \frac{I^0}{2}\right].$$

Repeating this line of reasoning for $i_2 = \left|\sum_{\ell=1}^{\rho} c_\ell^* S_\ell^*\right|^2$, we find in precisely the same way that the first term which differs from zero (for the intensity of scattered light) coincides with the intensity I_p for reflected light, given in Chapter V.

Let us now examine $a_{1,2}^{(k)}$. The phase $\psi_{1,2}^{(k)}$ of the integrand will be /192

$$\psi_{1,2}^{(k)} = 2(\sin\tau_0 - \tau_0\cos\tau_0) \pm \beta\cos\tau_0 - \\ - 2m(k-1)(\sin\tau_1 - \tau_1\cos\tau_1). \tag{7.24}$$

We readily find from formulas (3.23) (see III, 1) that

$$\frac{d\tau_1}{d\tau_0} = \frac{1}{m}\frac{\sin\tau_0}{\sin\tau_1}.$$

When this relationship is taken into account, we find that, except for $\tau_0 = 0$, the derivative $\psi_{1,2}^{(k)}$ has a certain root. It is determined from the following equation

$$2\tau_0 \pm \beta^{(k)} - 2(k-1)\tau_1 = 0. \tag{7.25}$$

If we now turn from the angle τ_0 to the angle of incidence $\phi(\tau_0 = \frac{\pi}{2} - \phi)$, and from the angle τ_1 - to the angle of refraction $\psi(\tau_1 = \frac{\pi}{2} - \psi)$, we find that the latter relationship may be rewritten as follows:

$$\beta^{(k)} = \pm\{(k-2)\pi + 2[\varphi - (k-1)\psi]\}. \tag{7.26}$$

It precisely coincides with the formula (5.4) given in Chapter V for the angle at which a ray (falling on a drop at the angle ϕ) leaves the drop. Consequently, the meaning of (7.26) may be found in the fact that it indicates the angle of incidence on the sphere of that ray which, for order k, makes the main contribution to the intensity of light scattered at the angle $\beta^{(k)}$.

Let us calculate the second derivative $\psi_{1,2}^{(k)}$ at that point where the first derivative has a root which is determined by the relationship (7.25). We readily find that

$$\psi_{1,2}^{(k)''} = 2\sin\tau_0\left[1 - \frac{(k-1)}{m}\frac{\sin\tau_0}{\sin\tau_1}\right]. \tag{7.27}$$

Substituting this in $a_{1,2}^{(k)}$, replacing τ_0 and τ_1 by ϕ and ψ, and turning to the intensity of light scattered for order k, we obtain

$$I_1^{(k)} = \frac{I_0}{2}\frac{a^2}{4R^2}(\varepsilon_1^2)^{k-2}(1-\varepsilon_1^2)^2\left|\frac{\sin 2\tau_0}{\sin\beta^{(k)}\cdot\left[1 - \frac{k-1}{m}\frac{\sin\tau_0}{\sin\tau_1}\right]}\right|. \tag{7.28}$$

The formula obtained exactly coincides with that which was indicated on the basis of the simple arguments of geometric optics [see (5.20) and (5.14)]. /193
We should recall that $\varepsilon_1^3 = r_s$, and $1 - \varepsilon_1^2 = d_s$). A similar conclusion may be reached for $I_2^{(k)}$.

In accordance with (7.13), along with the squares of individual component moduli at A, the intensity must also contain the product of the components.

These terms are due to interference of different bundles of geometric optics (see § 3).

In the directions of the rainbows, the second derivative $\psi_{1,2}^{(k)} = 0$. This means that we must perform the calculations in terms of the formula (7.21).

An analysis of the intensity distribution at angles which are close to

these directions leads us to a precise theory of rainbows, which must replace the approximate theory of Airy. The lack of space prohibits us from dwelling on this interesting problem in greater detail.

In conclusion, let us turn to a bundle which is diffracted backwards, which we discussed in Chapter V.

In formulas (3.39) and (3.40) for Q_ℓ and S_ℓ, we turn to small θ ($\sim \frac{1}{\rho}$) ($y = (\ell + \frac{1}{2})\,\theta \simeq 1$).

In addition, if we retain only unity in the parentheses in the expressions for c_ℓ and b_ℓ (in the case $\ell \to \infty$), we readily find that

$$i_1 = i_2 = \left|\sum_{l=1}^{\rho}(-1)^l \cdot l \cdot \left(J_0(y) - 2\frac{J_1(y)}{y}\right)\right|^2. \tag{7.29}$$

In view of the well known properties of Bessel functions, we have

$$J_0(y) - 2\frac{J_1(y)}{y} = -J_2(y).$$

Replacing the sum in $i_{1,3}$ by the integral and passing to the limits of integration, (0,1), we readily obtain the following expressions for it

$$-\rho^2\int_0^1 J_2(zt)\, te^{i\pi\rho t}\, dt.$$

Here $z = \theta\rho$.

In accordance with (7.19), the asymptotic value of the integral will be as follows in the case $\rho \to \infty$: /194

$$\frac{J_2(z)}{\pi\rho}\, e^{i\left(\pi\rho - \frac{\pi}{2}\right)}.$$

This means that for small angles around the direction to the source, the intensity of diffracted light may be determined by the following formulas

$$\left.\begin{aligned} I_1 = I_2 &= \frac{I_0}{2}\frac{a^2}{4r^2}\left[\frac{2}{\pi}J_2(\rho\theta)\right]^2; \\ I = I_1 + I_2 &= I_0\frac{a^2}{4r^2}\left[\frac{2}{\pi}J_2(\rho\theta)\right]^2. \end{aligned}\right\} \tag{7.30}$$

We may see that the angular change in diffracted intensity in the backward direction is determined by the function

$$F^*(z) = \frac{4}{\pi^2}J_2^2(z) \qquad (z = \rho\theta).$$

Table 18 gives $10 \cdot F^*(z)$. We present a graph for it in Figure 51.

The diffraction picture is just the opposite here from that which is obtained in the forward direction.

The intensity maxima lie at the points where $J_2'(z) = 0$. This is $z = 3.1$; 6.8; 10.0; ...; F^* will be: 0.096; 0.037; 0.026.

TABLE 18

z	$10 \cdot F^*(z)$
0,0	0
0,5	0,0038
1,0	0,0535
1,5	0,2183
2,0	0,5045
2,5	0,8064
3,0	0,9576
3,5	0,8525
4,0	0,5374
4,5	0,1924
5,0	0,0088
6,0	0,2391
7,0	0,3682
8,0	0,0517
9,0	0,0850
10,0	0,2628
11,0	0,0784
12,0	0,0292

Zeros lie at the points where $J_2(z) = 0$. This equation coincides with the equation $\frac{d}{dz}\left(\frac{J_1(z)}{z}\right) = 0$.

Thus, the position of the zeros in the case of backward diffraction coincides with the positions of the maxima in the case of forward diffraction. This is z = 0; 5.14; 8.42; 11.6; ...

The scattering intensities will not equal zero here, since, besides diffracted light, we have reflected light and other fluxes here. In essence, this distinguishes the angles $\theta \simeq 0$ from the angles $\beta \simeq 0$, and the intensity of a diffracted flux is of the same order as other fluxes. For example, for a cloud drop with a $\sim 6\ \mu$ ($\rho = 60$), the ratios of the /195 diffracted light intensities to other fluxes at the maxima (when θ equals 2.9°; 6.4°; 9.5°;...) will be 1; 0.38; 0.28;...

We should emphasize the fact that diffraction backwards must occur not only for transparent particles, but also for particles with any electric properties. Interfering with bundles of geometric optics, diffracted light can produce a characteristic oscillating intensity distribution at small angles θ, leading to the formation of so-called glories.

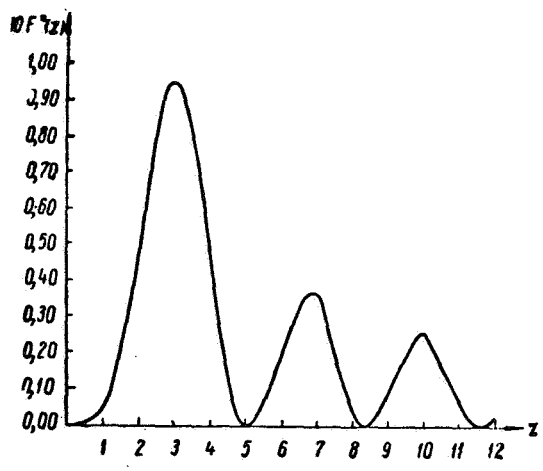

Figure 51. Graph of F*(z).

In this connection, we should note that the customary theory of glories, which attributes their occurrence to coronas in light which is scattered a second time [see (Ref. 64)] is incorrect. Several facts indicate that glories occur during single scattering.

In our opinion, the viewpoint of Ray is incorrect. He assumes that glories are coronas produced by a drop from the image of the light source in the drop (Ref. 44). It would be tempting to extend this clear explanation and state that it causes backward diffraction, but in actuality it is inadequate, since backward diffraction must occur for opaque particles.

The reason for backward diffraction is the same as for forward diffraction--the wave nature of the phenomenon.

The difference in light intensities in the two directions (Mie effect) /196 corresponds to the disappearance of the reverse wave during the transition (in wave optics) from elementary waves which are bent to light which is propagated rectilinearly [with the aid of the Huygens-Fresnel principle; see (Ref. 2) § 43].

Let us now perform a strict analysis of the problem. Let us turn to the sums (7.16), and let us employ the precise summation formula -- the Poussin formula -- for their transformation.[1]

The summation formula of Poisson and its derivation is given in the book by Courant and Hilbert (Ref. 96). The formula which appears in this book and also in other places gives the transformation of one infinite series into another one. It is not suitable for direct application to our problem, since we are interested in the formula for transforming a finite sum. We shall give the derivation of the corresponding formula, following the procedure of Courant and Hilbert. Let us investigate the following function of x:

$$F(x) = \sum_{n_1}^{n_2} \varphi(2\pi n + x).$$

Let us expand it in the interval $0 \leq x \leq 2\pi$ in Fourier series:

$$F(x) = \frac{1}{2\pi} \sum_{-\infty}^{+\infty} e^{i\nu x} \sum_{n_1}^{n_2} \int_0^{2\pi} \varphi(2\pi n + t) e^{-i\nu t} dt.$$

Under the inner summation sign in the integral, let us turn to the variable $\eta = 2\pi n + t$:

$$\sum_{n_1}^{n_2} \int_{2\pi n}^{2\pi(n+1)} \varphi(\eta) e^{-i\nu\eta} d\eta = \int_{2\pi n_1}^{2\pi(n_2+1)} \varphi(\eta) e^{-i\nu\eta} d\eta.$$

Assuming that x = 0, we obtain

$$\sum_{n_1}^{n_2} \varphi(2\pi n) = \frac{1}{2\pi} \sum_{-\infty}^{+\infty} \int_{2\pi n_1}^{2\pi(n_2+1)} \varphi(\eta) e^{-i\nu\eta} d\eta.$$

The latter formula may be rewritten as follows:

$$\sum_{n_1}^{n_2} \psi(n) = \sum_{-\infty}^{\infty} \int_{n_1}^{n_2+1} \psi(\mu) e^{-i2\pi\mu\nu} d\mu. \tag{7.31}$$

This relationship is the form of the Poisson formula which is necessary to us. /197
In the case in which we are interested, $n_1 = 0$, to n_2 is the whole number ($n_2 = [\rho]$) which is closest to ρ.

We can see from the precise formula (7.31) that simple substitution of the sum by the integral will be valid if it is found that, in view of the properties of the integrals contained in the right hand side of the equation, the sum on the right degenerates into only one term--the term with $\nu = 0$ (substitution of the limit n_2 by $n_2 + 1$ is not essential, in view of the fact that $n_2 \gg 1$).

Let us now analyze the sums (7.16) by means of the relationship (7.31).

Each of the sums may now be transformed into an infinite series of integrals:

$$a_{1,2}^{(0)} = \sum_{-\infty}^{+\infty}{}_{\nu}\, a_{1,2}^{(0),\nu}; \quad a_{1,2}^{(1)} = \sum_{-\infty}^{+\infty}{}_{\nu}\, a_{1,2}^{(1),\nu}; \quad a_{1,2}^{(k)} = \sum_{-\infty}^{+\infty}{}_{\nu}\, a_{1,2}^{(k),\nu}.$$

---

(1) The author is indebted to G.A. Grinberg, who devoted his attention to the formula of Poussin (1947).

The quantities $a_{1,2}^{(k)\nu}$ are the integrals contained in the right hand side of equation (7.31). Each of these integrals differs from the integrals which we investigated above by the factor $e^{-i2\pi\nu\ell}$ under the integral sign, or by the factor $e^{-i2\pi\nu\rho\cos\tau_0}$ in view of (7.14). For example, we thus obtain

$$a_{1,2}^{(0),\nu} = \rho^{2/3} \int_0^{\frac{\pi}{2}} \sqrt{\cos\tau_0}\sin\tau_0 e^{i\rho\cos\tau_0\left[\pm\beta-2\pi\nu\right]\mp i\frac{\pi}{4}}\, d\tau_0,$$

$$a_{1,2}^{(1),\nu} = \rho^{2/3} \int_0^{\frac{\pi}{2}} \sqrt{\cos\tau_0}\sin\tau_0 e_1 e^{i\rho\left[2f_0+\cos\tau_0\left(\pm\beta-2\pi\nu\right)\right]\mp i\frac{\pi}{4}+i\frac{\pi}{2}}\, d\tau_0$$

and so on.

If we formally replace $\pm\beta$ in the previous integrals (7.17) by $\pm\beta - 2\pi\nu$, we may transform the previous integrals into new ones which must be investigated. We can thus immediately calculate the quantities $a_{1,2}^{(k),\nu}$, if we replace $\pm\beta$ by $\pm\beta - 2\pi\nu$ in the previous results.

In accordance with this, the quantities $a_{1,2}^{(0),\nu}$ will be negligibly small. Just as previously, this means that the asymptotic contribution of diffracted light at angles which are not close to 0 or π is zero.

When analyzing $a_{1,2}^{(1),\nu}$, we find that the phase is stationary for /198
$\tau_0 = \frac{\pm\beta - 2\pi\nu}{2}$. Since the scattering angle β lies between zero and π, out of all the terms with different ν, only the term with $\nu = 0$ will have a stationary phase within the integration interval.

Thus, in this case the Poisson formula degenerates precisely into the simple replacement of the sum by the integral.

Let us now turn to $a_{1,2}^{(k),\nu}$. Condition (7.26) for the stationary nature of the phase will appear as follows:

$$\beta^{(k)} = \pm\left\{\left\{(k-2)\pi + 2\left[\varphi-(k-1)\psi\right]\right\} + 2\pi\nu\right\} \qquad (7.26^*)$$

The meaning of this relationship may be found in the fact that it indicates those values of the integration variable τ_0 (or ϕ) close to which the phase is stationary. These values will depend on the scattering angle β.

Let us investigate (7.26*) in greater detail. For this purpose, let us turn to Figure 52, where we have shown the values of the expression contained within the inner parenthesis in the case of different ϕ and k for the case of a water drop in the air ($\lambda \sim 0.5\mu$, $n = 1.3300$). We can see from this figure, for example, that for $k = 2$ (rays which pass through, just as through a lens), we must set $\nu = 0$, and must select the plus sign before the outer parenthesis in (7.26*). Other values of ν and terms with the minus sign drop out, since the β corresponding to them do not enter the region $(0, \pi)$. In the

case k = 3, we are left with only one term with $\nu = 0$ and with the plus sign in (7.26*). However, one significant new fact appears here. There will be two values for certain scattering angles β: τ_0 or ϕ, which will satisfy the relationship (7.26*). In Figure 52, the fact that the line, which is parallel to the ϕ-axis, intersects curve 3 at two points ocrresponds to this. When calculating the scattered light intensity, we must sum both intensities. In physical terms, this fact is related to the appearance of a rainbow in the third flux.

It may also be readily seen that, if the phase of the integrand is maximal for one of the rays scattered in a given direction, it will be minimal for the other one.

This means that the corresponding waves, which are scattered in one direction and interfere at infinity, will have different phases. In the case k = 4, in /199 order to enter the allowed region of β values (between 0 and π), we must select $\nu = -1$ and the minus sign. In the case k = 5, we must select $\nu = -1$ and the plus sign from $\phi=0$ to the point at which curve 5 in Figure 52 intersects the line 2π. In the subsequent interval of ϕ values, we must select $\nu = -1$ and the minus sign. We have already noted that these formulas differ from previous formulas only by the addition of the term $2\pi\nu$ in the expression for $\beta^{(k)}$. Thus, we obtain the same formulas for intensity (7.28) as we obtained previously. It /200 is important to note that the addition of the term $2\pi\nu$ makes it possible, for each scattering angle β, to find the angle of incidence of the rays ϕ which are scattered for any order k at the angle β. This fact results from a precise analysis of the problem by employing the Poisson formulas, and does not follow from the approximate analysis performed previously. The formula which was obtained then for $\beta^{(k)}$ in the case $k \geq 4$ leads to values of $\beta^{(k)}$ which are not contained in the region of allowed values of β. This means that in the case $k \geq 4$ scattered light would have to be absent [more precisely, its intensity would have to be described not by (7.28), but by another formula]. Naturally, this is not the case, and formula (7.28) is in actuality the correct formula for any k. The fact that the scattering angles β for any order enter the allowed region $(0, \pi)$ is due to the precise analysis of the problem based on the Poisson formula.

The application of the Poisson formula to the sum (7.29) leads to the same formula (7.30) for backward diffraction, which we obtained previously.

§ 3. Scattering Indicatrix

Several authors have calculated the intensities of the transverse and longitudinal components of scattered light for transparent particles.

The study by V. V. Shuleykin which was published in 1924 (Ref. 51) and then supplemented in 1933 (Ref. 52) is of great importance. V. V. Shuleykin not only performed calculations for three intermediate cases, but also investigated the limiting transition from an infinitely small particle to an infinitely large particle. The investigations of V. V. Shuleykin had an impact upon all subsequent studies on tabulation of the Mie formulas and on the use of these formulas for analyzing optical phenomena in the sea and the atmosphere.

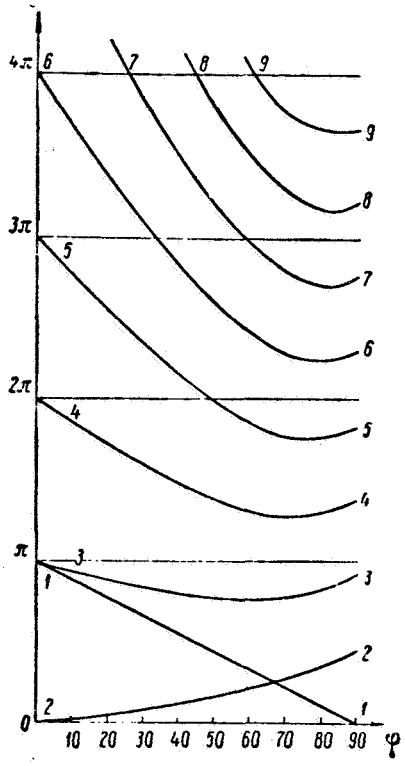

Figure 52. Rotation of Rays in a Drop

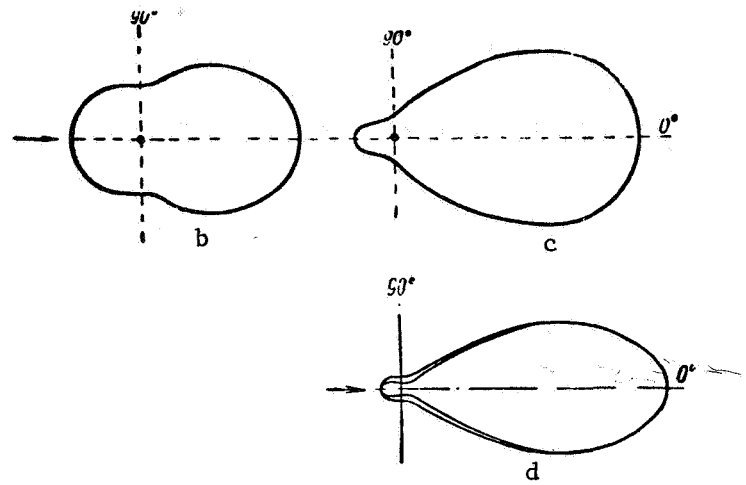

Figure 53. Indicatrix for m = 1.32 and and ρ = 1(b), ρ = 3, (c), ρ = 9 (d).

In the work by V.V. Shuleykin, the relative refraction coefficient is assumed to be 1.32. For example, this corresponds to the refraction of small drops of paraffin oil in water. He investigated the following values for ρ:

a) lim ρ=0 c) ρ=3
b) ρ=1 d) ρ=9 in (Ref. 52)
e) lim ρ=∞

Case (a) corresponds to Rayleigh scattering. In case (b), it is necessary /201 to take into account two electric oscillations and one magnetic oscillation. In case (c), V.V. Shuleykin considers three electric oscillations and three magnetic oscillations. The indicatrixes calculated by V.V. Shuleykin [for cases (b), (c), and (d)] are shown in Figure 53. We have already discussed his analysis of the case of an extremely large particle [case (e)].

The fundamental physical laws for the phenomenon are as follows:

1. When ρ increases, the Rayleigh scattering symmetry is disturbed. A large portion of the light is scattered in the region of angles β which are less than 90° , i.e., forward -- the Mie effect (see Figures 11 and Figure 53).

2. When ρ increases from 0 to approximately 2, the maximum of the degree of polarization for scattered light is displaced (for dielectric pellets) from β = 90° toward larger angles β, and becomes less than unity. With a further increase in ρ, the polarization changes irregularly.

Following V.V. Shuleykin, similar calculations were performed by Blümer (Ref 56). His studies provide numerical data pertaining to a great many different cases.

In order to illustrate the Mie effect, in Figure 54 we have presented the ratio of the intensities i_0/i_{180} (forward and backward) as a function of $\rho(m = 1.25)$ (logarithmic scale in Figure 54). In the section $\rho(0.5 - 5)$, the quantity i_0/i_{180} changes from a constant value (unity) to a rapid increase $(\sim \rho^2)$.[1] /202

An investigation of the scattering of visible light by drops of water $(m = \frac{4}{3})$ is of interest for geophysics. Blümer investigated the following cases: $\rho = 0.1; 1.5; 3$. We have presented his data in Table 19 [i according to (6.18)].

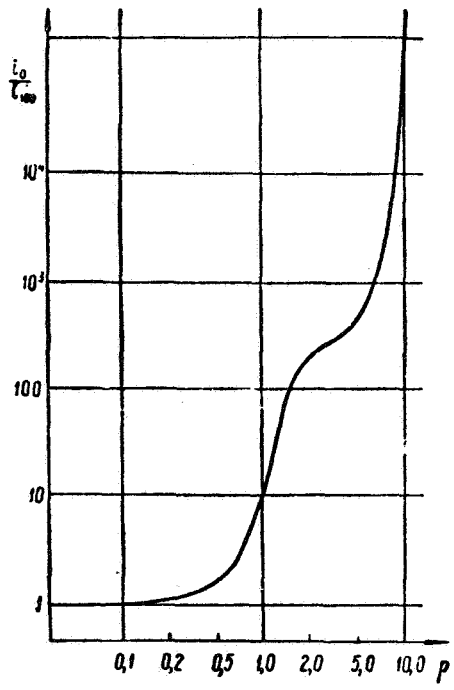

Figure 54. Ratio of Intensity Scattered Forward to Intensity Scattered Backward.

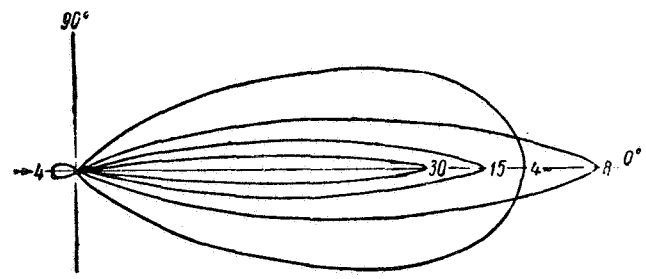

Figure 55. Indicatrixes for Drops of Water ($m = 1.33$ and $\rho = 4, 8, 15, 30$).

In addition, Blümer reduced the computational data of Ray (Ref. 44) for the case $\rho = 12$.

The study by Paranjpe, Naik, and Vaidya (Ref. 98) presents the results derived from calculating the indicatrixes for $\rho = 4, 5, 6, 7, 8, 9, 10, 12, 15, 20, 30$ $(m = 1.33)$. We have presented some of the data they obtained in Table 20 and Figure 55 (different scale of the curves). /203

In the case $\rho = 20$ and $\rho = 30$, the particle may be regarded as a large particle with a certain approximation. It is natural to search for an approximate representation of the indicatrix, just as in the case of reflected particles, as the simple sum of the geometric and diffraction pictures. It must be noted, /206

(1) The curve in Figure 54 was compiled on the basis of data by Blümer (Ref. 54). More detailed calculations revealed the interference nature of the curve: it has a sharply oscillating form. We have omitted these details in Figure 54.

TABLE 19

ρ	0,1		1,5		3	
β	$i \cdot 10^7$	p	i	p	i	p
0	0,4252	0,0000	0,6606	0,0000	42,519	0,0000
10	0,4188	0,0152	0,6426	0,0125	39,455	0,0070
20	0,4002	0,0614	0,5916	0,0507	31,459	0,0271
30	0,3719	0,1422	0,5664	0,1163	21,402	0,0568
45	0,3188	0,3326	0,3840	0,2711	8,618	0,0945
60	0,2654	0,5989	0,2606	0,4948	2,134	—0,0095
70	0,2372	0,7892	0,1950	0,6706	0,658	—0,3866
80	0,2187	0,9405	0,1451	0,8409	0,332	—0,4821
90	0,2120	1,0000	0,1098	0,9645	0,408	0,2095
100	0,2180	0,9426	0,0863	0,9974	0,497	0,5714
110	0,2363	0,7922	0,0714	0,9205	0,477	0,7161
120	0,2644	0,6015	0,0624	0,7552	0,363	0,7538
135	0,3171	0,3343	0,0551	0,4557	0,184	0,5934
150	0,3699	0,1437	0,0516	0,2032	0,169	0,0695
160	0,3982	0,0525	0,0504	0,0896	0,147	—0,0520
170	0,4164	0,0151	0,0498	0,0222	0,190	—0,0020
180	0,4227	0,0000	0,0496	0,0000	0,210	0,0000

however, that -- if the accuracy of this method (for $\rho = 30$) is about 5% for small angles ($\beta \sim \frac{1}{\rho}$) -- for larger angles the method is too rough.

The largest value of ρ for which precise calculations were made is $\rho = 60$. This corresponds to scattering of visible light by a cloud drop with a radius of about 6 μ. We carried out these calculations for m = 1.3300 (Ref. 127). When performing these complex calculations, we employed the tables of functions Q_ℓ and S_ℓ which we compiled. The calculation of the Bessel functions with large order were done according to the recursion formulas given in Chapter III. In order to obtain the requisite accuracy, we had to calculate all functions with the indices $\ell < 70$. For purpose of control, a "reference set" of cylindrical function values was calculated according to the approximate formulas of V. A. Fok (Ref. 42).

Tabulation of the partial wave amplitudes is usually complicated by the fact that the functions contained in the general formulas for amplitudes are complex even for real arguments. This fact greatly complicates the calculation. However, we can readily avoid this complication in the case of transparent particles. We must tabulate, not the general formulas for amplitudes, but the formulas (7.2) in which the real and imaginary parts of the amplitudes are separated from the very beginning, and where the amplitudes are determined in terms of the real functions ψ_ℓ and χ_ℓ.

The formulas of V. A. Fok yield the following approximate expressions for these functions (in the case $\ell \leqq x$):

$$\left.\begin{aligned}\psi_l(x) &= \sqrt{\frac{\pi x}{8}}\sqrt{\frac{q}{\operatorname{tg}\beta}}\left\{\sqrt{3}\,J_{1/3}(lq) - Y_{1/3}(lq)\right\},\\ \chi_l(x) &= -\sqrt{\frac{\pi x}{8}}\sqrt{\frac{q}{\operatorname{tg}\beta}}\left\{J_{1/3}(lq) + \sqrt{3}\,Y_{1/3}(lq)\right\}.\end{aligned}\right\} \tag{7.32}$$

Here $q = \operatorname{tg}\beta - \beta$, and the angle β is determined by the relationship

$$\cos\beta = \frac{l}{x} \qquad \left(0 \leqslant \beta \leqslant \frac{\pi}{2}\right). \tag{7.33}$$

TABLE 20

ρ	4		6		8		10	
β	*i*	*p*	*i*	*p*	*i*	*p*	*i*	*p*
0	125,240	0	1 237,15	0	2 922,05	0	2 768,31	0
10	114,645	— 0,08	908,35	0,4	1 499,30	— 5,6	635,98	— 2,2
20	80,273	— 1,30	343,15	— 3,1	358,81	— 8,0	237,20	—16,6
30	44,255	— 3,60	56,82	—25,8	145,22	9,4	164,26	— 6,2
40	18,853	—10,30	28,22	—11,6	66,48	—36,8	82,28	—28,9
50	6,549	—15,40	27,88	9,2	28,68	15,8	62,03	18,8
60	2,005	— 2,71	4,51	—64,2	59,81	—17,3	36,12	—41,4
70	2,522	—20,95	4,16	—45,4	15,71	—89,3	22,94	55,3
80	0,533	81,36	6,05	29,7	3,48	—20,4	31,75	—63,9
90	1,622	68,17	3,46	1,2	7,58	35,3	4,87	8,6
100	0,841	—15,18			3,03	—43,0	18,50	—94,6
110	1,277	—95,63	3,15	45,7	8,77	—75,4	8,78	—22,3
120	0,771	—13,95			12,77	—18,1	22,57	45,3
130	0,612	—13,42	0,20	71,7	14,53	—81,5	2,73	— 7,8
140	0,654	14,47			4,55	—18,0	44,95	35,3
150	1,429	34,02	5,24	26,9	8,31	46,2	33,28	—88,5
160	3,462	21,21			11,38	59,1	49,23	58,7
170	5,416	5,06	2,26	—15,1	5,63	—25,2	16,94	66,6
180	7,350	0			38,20	0	19,99	0

All the calculations were performed for constant x. Determining β by means of the table of cosines for given ℓ, we can find tg β, q and then ψ_ℓ and χ_ℓ. /207

TABLE 20 (continued)

15		20		30	
i	*p*	*i*	*p*	*i*	*p*
22 781,35	0	45 871,00	0	195 719	0
4 036,17	11,0	1 210,00	−26,5	9 560,58	7,1
228,66	31,2	685,04	− 6,3		
16,070	−14,6	226,03	−51,9	1034,20	− 0,8
227,08	−12,3	157,72	−72,7		
104,57	10,8	128,51	−82,7	333,09	−10,6
44,04	− 20,0	67,03	−76,2	97,90	−81,9
59,34	−92,4	22,76	−68,0		
27,54	−70,6	16,42	−85,8	34,30	−81,4
		29,92	−85,8	24,20	25,1
16,88	−42,4	23,88	−81,5	7,25	−37,1
12,64	−26,8	4,03	−27,1		
15,40	−11,0	18,07	33,2	23,75	25,1
8,82	−36,6	58,13	−16,2	39,25	−15,2
27,47	−99,2	48,48	−20,4		
13,14	75,4	34,50	88,6	97,91	43,7
24,44	−48,3	108,71	−10,6		
136,74	− 57,2	223,92	−90,6	173,30	58,4

The accuracy of this method is small for functions whose index is close to $x(\beta \to 0)$. We must directly calculate q according to the following formula

$$q = \left[\frac{2}{3^{3/2}}\left(1 - \frac{l}{x}\right)\right]^{2/3} \text{ and } \frac{q}{\operatorname{tg}\beta} = \frac{2}{3}\left(1 - \frac{l}{x}\right).$$

In the case $\ell \geqq x$, the formulas for ψ_ℓ and χ_ℓ will be

$$\left.\begin{aligned} \psi_l(x) &= \sqrt{\frac{x}{2\pi}}\sqrt{\frac{\eta}{\operatorname{th}\alpha}}\, K_{1/3}(l\eta), \\ \chi_l(x) &= \sqrt{\frac{x}{2\pi}}\sqrt{\frac{\eta}{\operatorname{th}\alpha}}\,\{2\pi I_{1/3}(l\eta) + \sqrt{3}\, K_{1/3}(l\eta)\}. \end{aligned}\right\} \qquad (7.34)$$

Here $\eta = \alpha - \operatorname{th}\alpha$, and the real quantity α is determined by the equation

$$\operatorname{ch}\alpha = \frac{l}{x}\,(0 \leqslant \alpha < \infty) \tag{7.35}$$

The quantities $I_{1/3}$ and $K_{1/3}$ are cylindrical functions with imaginary argument of order 1/3.

We should note that, if ℓq and $\ell\eta$ are considerably greater than unity, so that the first terms of the ordinary asymptotic expressions can be employed for the cylindrical functions, then the formulas of V. A. Fok change into the Debye formulas (see Chapter III).

By employing the table of ψ_ℓ and χ_ℓ, we calculated the amplitudes of c'_ℓ, c''_ℓ, b'_ℓ and b''_ℓ. Then employing the table of Q_ℓ and S_ℓ, we calculated all the components in the sums (2.45), and then the sums themselves.

The attenuation coefficient calculated according to these data [according to formula (6.5)] will be $1.9912\pi a^2$. The intensity of light (the quantity i) scattered at the angle β and the degree of its polarization, which we calculated, are given in Table 21.

The scattering indicatrix compiled according to these data is shown in Figures 56 and 57.

Curve 1 in Figure 57 shows the indicatrix for the section (0 - 10°); curve 2 gives the indicatrix for (10 - 40°), and curve 3 gives the indicatrix for (40 - 180°). The scale in the figure pertains to curve 3. Curve 2 has a scale which is ten times smaller, and curve 1 has a scale which is 2500 times smaller.

TABLE 21 /208

β	i	p	β	i	p
0	$3218 \cdot 10^3$	0,0000	90	36,90	—0,2594
1	$2368 \cdot 10^3$	0,0276	100	32,61	—0,6675
2	$793{,}2 \cdot 10^3$	0,0117	110	40,14	—0,4930
5	$110{,}4 \cdot 10^3$	—0,3184	120	58,62	0,4833
10	$14{,}50 \cdot 10^3$	0,0179	130	326,6	0,5295
20	5062	—0,0649	140	485,0	0,9532
30	2492	- 0,3000	150	649,0	0,7190
40	1307	—0,5850	160	271,2	—0,3252
50	602,0	—0,6356	170	167,3	—0,8798
60	297,3	—0,3582	175	483,1	0,8907
70	198,2	—0,3275	178	563,0	—0,8060
80	70,16	—0,3316	179	81,73	0,2527
			180	189,0	0,0000

This change in the scales clearly shows the order of intensity for light scattered at different angles. The scattered light is primarily concentrated at small angles.

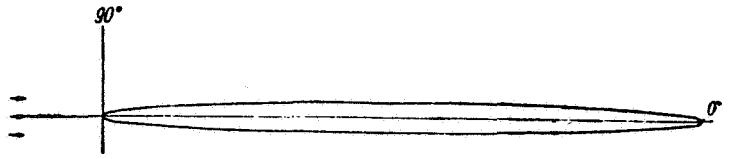

Figure 56. Indicatrix of Cloud Drop (m = 1.33; ρ = 60).

The maximum close to β = 140° belongs to the first rainbow. Based on the Airy formulas, the intensity maximum in the rainbow does not coincide with the rainbow direction in terms of geometric optics. For our drop, it is displaced by 5° toward larger angles. Its position may be noted in the figure by the point A.

The indicatrix shown in Figure 56 must be regarded as the characteristic curve for scattering in clouds. The fact that the scattering indicatrix in clouds is very greatly extended is extremely important. /209

It must be emphasized that such a strong anisotropy in the scattered light distribution will only occur in thin layers, where there is single scattering. In real clouds, whose optical thicknesses are usually considerably greater than unity, the spatial distribution of scattered light will be much more uniform, in spite of the fact that the scattering indicatrix will be very greatly extended. An almost symmetrical distribution of scattered light must be expected for sufficient cloud thickness. This fact is apparently substantiated in observations on the angular distribution of cloud brightnesses.[1]

The fact that the spatial distribution of scattered light is not only determined by the extension of the scattering indicatrix, but also by the layer thickness, pertains not only to clouds, but also to any turbid medium in general. /210

In order to change from monodisperse curves (the type shown in Figure 56) to real clouds, it is necessary to average over different particle dimensions in the cloud (see Figures 1 and 2). For this purpose, we must calculate the indicatrixes for an entire group of large transparent particles.

We have already noted that the case of large transparent particles is the most difficult to calculate. If superposition of the diffraction indicatrix and the geometric optics indicatrix in the case ρ = 10 yields fairly good results for m = ∞, for transparent particles -- even in the case ρ = 60 -- the agreement between the precise and approximate values is poor (small angles

---

(1) In the case of a spherically symmetrical distribution of scattered light within a cloud, the brightness of its surface must be described by the Lambert law.

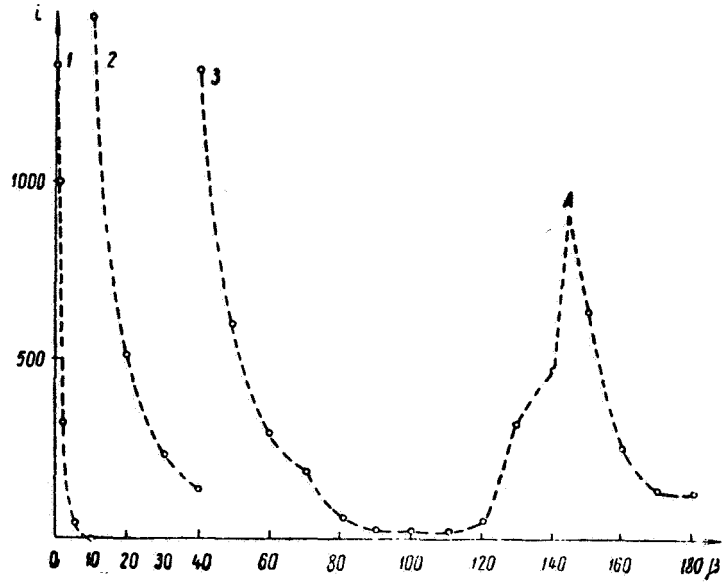

Figure 57. Indicatrix of a Cloud Drop in Rectangular Coordinates

represent an exception; in the case $\beta = 0$, for example, the approximate value is only 1% larger than the precise value). Two facts account for this:

1. A ray of geometric optics is the normal to the plane wave, which may be assumed to be infinite in directions which are perpendicular to the ray. A limitation upon it in the form of a "ray" (thin tube) must inevitably cause diffraction phenomena at the boundaries.

It may be readily seen that the smaller is ρ, the greater will be the error caused by this fact.

Rays having an infinitely small "thickness", which we employed in Chapter V, are far from being an idealization. Geometric optics does not eliminate the error occurring here by introducing any corrections to the geometric picture. It is only possible to perform a radical improvement by replacing the geometric investigation by a wave investigation.

2. Different fluxes which are scattered by a drop -- diffraction, reflected, etc. -- are coherent (they arise from different sections of one and the same wave surface). This means that we can introduce significant improvements in our geometric picture, if we allow for interference between these fluxes. This is the customary method for improving the geometric picture, which is applied in optics, and our problem is similar to the problem of bands having the same inclination. This causes the poor agreement between the approximate and /211
precise indicatrixes for transparent particles and for large ρ.[1]

---

(1) This is the same reason for the lack of agreement found by (continued)

The problem of allowing for interference between different fluxes is very important. Let us investigate it greater detail.[1]

When interference is taken into account, the intensity of scattered light will be

$$I_{p,s}(\beta)=\frac{a^2}{4R^2}I^0_{p,s}\left|\sum_{k=0}^{\infty}a^{(k)}_{p,s}(\beta)e^{i\Delta^{(k)}_{p,s}(\beta)}\right|^2. \tag{7.36}$$

Here $a^{(k)}_{p,s}$ are the absolute values for the amplitude of different fluxes, and $\Delta^{(k)}_{p,s}$ -- the phase displacements in waves of different fluxes.

The flux amplitudes investigated in Chapter V(k = 1, 2, 3...), may be readily determined by means of the quantity $\tau^{(k)}_{p,s}$, and are calculated as follows:

$$a^{(k)}_{p,s}=\sqrt{\tau^{(k)}_{p,s}}. \tag{7.37}$$

With respect to the phase displacement Δ, which we shall determine with respect to the central ray scattered in a given direction, we may write it as follows:

$$\Delta^{(k)}_{p,s}=\Delta^{(k),1}_{p,s}+\Delta^{(k),2}_{p,s}+\Delta^{(k),3}_{p,s}, \tag{7.38}$$

where $\Delta^{(k),1}_{p,s}$ is the phase displacement taking place in the case of external and internal reflections. It may be determined in the customary way [see (Ref. 38), page 44]; $\Delta^{(k),2}_{p,s}$ is the phase displacement due to the geometric difference in the behavior of different rays.

The difference between the paths which are traversed by the rays, calculated between the tangent planes to the sphere, will be

$$\Delta^{(k),2}_{p,s}=2\rho f_k(\varphi, m);\quad f_k(\varphi, m)=\cos\varphi-(k-1)m\cos\psi. \tag{7.39}$$

The third component $\Delta^{(k),3}_{p,s}$ is due to the special effect which arises /212 during an approximate investigation of wave phenomena. This is the so-called diffraction close to the focal points [see (Ref. 38), page 262].

The behavior of a plane wave is very complex right next to the focal point. However, far from the focal point the results derived from numerous studies of this phenomenon can be formulated quite simply: passage through the focal line

---

(footnote (1) continued from page 154): Blümer (Ref. 56). Such an agreement can only be expected (in view of 1 and others) for large ρ. An examination of the cases ρ = 0.1; 1.5 here is perplexing.

(1) We should note that Mecke [see (Ref. 69)] dealt with the problem of allowing for interference previously. However, he confined himself to only investigating very small angles around the forward direction, since his study was devoted to coronas. He thus committed errors in the formulas.

causes a phase shift of $\pi/2$. For light which is refracted twice, this yields a shift of π (focal point). For flux which causes the first rainbow, at the angles $\phi < \phi_{rain}$ we obtain π, and $\frac{3}{2}\pi$ for large angles, etc.

Let us now investigate a field which is diffracted in the forward direction. The Huygens principle (in the Kirchhoff formulation) leads to the following expression for the field (for diffraction in a circular hole):

$$E = i\left(\frac{1+\cos\beta}{2}\right)\cdot a\cdot\rho\cdot\left(\frac{J_1(z)}{z}\right)E_0\cdot\frac{e^{-ikr}}{r} \quad (z = \rho\sin\beta).$$

The field which is diffracted by the hole acquires a phase displacement of $\pi/2$, which leads to the factor + i. For diffraction around an opaque disk, in accordance with the Babinet principle, we must take the phase factor in the form of (- i), in order that the superposition of the disk and hole fields produce zero in the sum. Thus, the diffracted field will be

$$E = -i\left(\frac{1+\cos\beta}{2}\right)a\cdot\rho\cdot\left(\frac{J_1(z)}{z}\right)E_0\cdot\frac{e^{-ikr}}{r}. \tag{7.40}$$

The amplitude and phase of this expression form the zero component in the sums (7.36).

We should note that if we replace (in view of the smallness of β) $\cos\beta$ by 1, and $\sin\beta$ by β in formula (7.40), then this expression exactly coincides with the expression for the diffracted field obtained from an asymptotic study of the precise formulas. In (6.8), it is thus necessary to change the sign in accordance with the fact that we must change from the angles θ and ϕ to the angles β and ϕ' (see III, 2). In precisely the same way it may be readily shown that the phase displacements described above coincide with those which are obtained from the asymptotic expressions (in the case $\rho \to \infty$) for the precise values of the field.

Let us now turn to the numerical data. Let us compare the results derived from calculations with the precise formulas with the results derived from approximate calculations. The latter will be done in two different ways: (a) according to a simplified scheme, examining the superposition of the diffracted and geometric indicatrixes without allowance for interference; (b) according to a more precise scheme -- with allowance for interference. We shall employ the quantity i as follows: without an index, for precise values; as i_a and i_b respectively, for approximate values. /213

An analysis of the numerical data is very important in practice. In § 2 of this chapter, we showed that in the case $\rho \to \infty$ the precise formulas for the fields change into the superposition of the geometric optics fields. This means that in the case $\rho \to \infty$ the approximate and precise indicatrixes must coincide. This "matching" of both methods at infinity, is of great importance. However, the most important problem of the magnitude of the error which arises when the precise formulas are replaced by the approximate formulas for large, but finite, ρ, still remains open.

By modifying the discussion and methods given in § 2, we could try to

determine the accuracy of the approximate methods in the general form. However, the cumbersome nature and the immensity of the expressions thus obtained makes them practically unusable. A comparison of the numerical data yields reliable and simple conclusions. These conclusions and the accuracy of the approximate methods will depend not only on the magnitude of ρ, but also on m (substance of the particle) and on the region of scattering angles β under consideration. A given approximation accuracy for the total indicatrix will be achieved for larger ρ than the same accuracy which would be achieved for individual sections of the indicatrix.

Let us investigate the numerical data for drops of water in the visible region. This is very important for the geophysical case. Let us also confine ourselves to investigating scattering in the forward direction, i.e., scattering angles $\beta \leq 90°$. If we recall that the diffracted light also lies within the scattering angles, from Table 13 we then find that 97.2% of scattered light occurs in this region. Retaining the angular region $\beta \leq 70°$, we calculate 96.7%, and in the case $\beta \leq 50°$, we calculate 93.2%.

The quantity i_a was calculated according to formula (7.41), which was similar to the formula (6.19): /214

$$i_a(\beta) = \frac{\rho^2}{4}\left[\frac{\tau(\beta)}{2} + a^{(0)2}(\beta)\right]. \tag{7.41}$$

Here τ is the quantity given in formula given in (5.31), and

$$a_s^{(0)} = a_p^{(0)} = a^{(0)} = \rho(1+\cos\beta)\frac{J_1(\rho\sin\beta)}{\rho\sin\beta}.$$

When calculating i_b, we confined ourselves to taking into account only the first three bundles. They contain practically all of the light scattered in the forward direction. In addition, we employed the general formulas (7.36) - (7.40) given previously, keeping the following phases of the different bundles in mind

$$\Delta_{p,s}^{(0)} = -\frac{\pi}{2}; \quad \Delta_{p,s}^{(1)} = \pi + 2\rho f_1; \quad \Delta_{p,s}^{(2)} = \pi + 2\rho f_2.$$

This leads us to the following formula for i_b:

$$i_b(\beta) = i_a(\beta) + F(\beta); \tag{7.42}$$

$$F(\beta) = \frac{\rho^2}{4}\{a^{(0)}(\sqrt{\tau_s^{(1)}} + \sqrt{\tau_p^{(1)}})\sin(2\rho f_1) + a^{(0)}(\sqrt{\tau_s^{(2)}} + \sqrt{\tau_p^{(2)}})\sin(2\rho f_2) + (\sqrt{\tau_s^{(1)}\tau_s^{(2)}} + \sqrt{\tau_p^{(1)}\tau_p^{(2)}})\cos[2\rho(f_1 - f_2)]\}.$$

In order to perform calculations employing (7.42), we compiled tables of the amplitudes $\sqrt{\tau_{p,s}^{(k)}}$ and the quantities f_k for different β.

Let us now turn to Table 22, where we give the intensities for β calculated in (Ref. 98).

It follows from this table that, although both approximate methods yield

values which are of the same order as the precise methods, the agreement between the numerical data is poor.

The approximation of the results derived from approximate calculations to the results derived from precise calculations is oscillatory in nature: in certain cases, for large ρ the agreement between the approximate and precise values is worse than for small ρ.

In physical terms, it is apparent that allowance for interference must improve the computational results. The data given in Table 22 do not corroborate this conclusion (along with an improvement in certain cases, in other cases the allowance for interference makes the result worse).

TABLE 22 /215

β	$\rho = 15$			$\rho = 20$			$\rho = 30$		
	i	i_a	$i_б$	i	i_a	$i_б$	i	i_a	$i_б$
0	$22{,}8 \cdot 10^3$	$13{,}6 \cdot 10^3$	$17{,}0 \cdot 10^3$	$45{,}9 \cdot 10^3$	$41{,}7 \cdot 10^3$	$32{,}9 \cdot 10^3$	$196 \cdot 10^3$	$206 \cdot 10^3$	$164 \cdot 10^3$
10	$4{,}04 \cdot 10^3$	$2{,}39 \cdot 10^3$	$4{,}69 \cdot 10^3$	$1{,}21 \cdot 10^3$	$1{,}65 \cdot 10^3$	$0{,}410 \cdot 10^3$	$9{,}56 \cdot 10^3$	$6{,}54 \cdot 10^3$	$14{,}7 \cdot 10^3$
20	229	691	202	685	867	584			
30	16,1	277	142	226	513	759	$1{,}03 \cdot 10^3$	$1{,}18 \cdot 10^3$	$0{,}453 \cdot 10^3$
40	227	141	166	158	246	207			
50	105	75,1	50,3	129	126	130	333	248	212
60	44,0	25,1	23,9	67,0	49,3	43,3	97,9	97,0	83,0
70	59,3	9,0	7,8	22,8	15,8	6,20			
80	27,6	5,3	6,7	16,4	3,49	3,10	34,3	9,34	5,74
90				29,9	3,27	3,30	24,2	9,51	17,0

This fact is also caused by the oscillatory nature of the approximation of the precise formulas to the approximate formulas (the corresponding $\rho = \infty$). /216

It could be expected that $\rho \sim 10 - 15$ is large enough that in this case the asymptotic formulas could be employed. However, it follows from Table 22 that the convergence of the precise series given in Chapter II is so slow that in actuality even for $\rho = 30$ we cannot employ the asymptotic (approximate) formulas with sufficient accuracy.

However, it is very important to establish the fact that for any ρ the precise and asymptotic calculations coincide with the necessary accuracy. A desire to answer this question compels us to perform precise calculations for

$\rho = 60$ (Table 21) and to compare them with the approximate calculations. The numerical data obtained are given in Table 23. Several important conclusions may be drawn from this table. The basic conclusion consists of the fact that the approximation method which we developed for calculating the indicatrixes is sufficiently accurate for practical purposes for $\rho = 60$.

TABLE 23

β	i	i_a	$i_б$	β	i	i_a	$i_б$
0	$322 \cdot 10^4$	$325 \cdot 10^4$	$285 \cdot 10^4$	40	$1{,}31 \cdot 10^3$	$2{,}15 \cdot 10^3$	$1{,}35 \cdot 10^3$
1	$237 \cdot 10^4$	$246 \cdot 10^4$	$219 \cdot 10^4$	50	602	1040	569
2	$793 \cdot 10^3$	$970 \cdot 10^3$	$802 \cdot 10^3$	60	297	408	213
5	$110 \cdot 10^3$	$70 \cdot 10^3$	$120 \cdot 10^3$	70	198	123	34,5
10	$14{,}5 \cdot 10^3$	$12{,}7 \cdot 10^3$	$13{,}8 \cdot 10^3$	80	70,1	44,4	19,2
20	$5{,}06 \cdot 10^3$	$8{,}28 \cdot 10^3$	$5{,}25 \cdot 10^3$	90	36,9	27,3	27,0
30	$2{,}49 \cdot 10^3$	$4{,}38 \cdot 10^3$	$2{,}52 \cdot 10^3$				

In the region $\beta < 60°$, which contains 95.7% of the light which is scattered by a drop, the simple approximate formula (7.42) represents the indicatrix within an accuracy of 10 - 12%. This means that the total accuracy of our calculations will be about 14 - 15%. This accuracy is acceptable for our problems, and the tables thus mean that, for $\rho \geqq 60$, we can reliably employ the approximation method (b) for calculating the indicatrixes of individual particles.

It must be noted that usually we are not interested in the indicatrixes /217
of individual particles, but rather the scattering indicatrixes in real clouds. Since $\rho \sim 100$ for clouds, when averaging is performed over different ρ, the interference term practically disappears. This means that, when calculating the scattering indicatrixes of cloud systems, we cannot take into account interference between fluxes from the very beginning, but must employ a simple system of combining the intensities.

Employing the experimental data on the distribution functions of particles in clouds and rain, we have calculated the scattering indicatrixes in these systems. Figure 58 shows the indicatrixes for the clouds St and Ns. The indicatrixes are very greatly extended. They are very similar to the one we obtained for $\rho = 60$ (Figure 56). The significant difference between the forms of the indicatrixes for St and Ns is due to the difference in the particle sizes in both cloud forms. The drops are much larger in Ns.

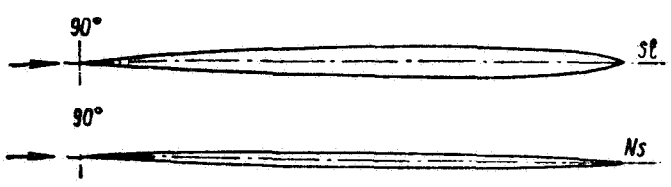

Figure 58. Scattering Indicatrixes in the Clouds St and Ns.

Employing the formula (6.5) for the attenuation coefficient and the considerations on the interference of bundles, which were developed above, we can obtain an interesting asymptotic formula for k for the case of large transparent particles.

Regarding the amplitude of

the field scattered forward, A_β, as the sum of the amplitudes of the first three bundles, we readily obtain

$$A_\beta = \frac{a\rho}{2} e^{-i\frac{\pi}{2}} + \frac{a}{2}\sqrt{\tau^{(1)}} \cdot e^{i(\pi + 2\rho f_1)} + \frac{a}{2}\sqrt{\tau^{(2)}} e^{i(\pi + 2\rho f_2)} \tag{7.43}$$

We may write τ without an index here (p or s), having in mind any of these indexes, since all $\tau^{(k)}_p = \tau^{(k)}_s$ in the direction $\beta = 0$. Taking the fact into account that $f_1(0) = 0$, $f_2(0) = -(m - 1)$ and that $\mathrm{Im}(e^{i\pi}) = 0$, we readily find that

$$k = 2\pi a^2 \left\{ 1 - \frac{\sqrt{\tau^{(2)}}}{\rho} \sin\left[2\rho(m-1)\right] \right\}. \tag{7.44}$$

A reflected bundle makes no contribution to k. If we employ the formula (5.16) for $\tau^{(2)}$, the latter expression for k can be rewritten in the following suitable form: /218

$$k = 2\pi a^2 \left\{ 1 - \frac{4m^2}{\rho(m+1)^2(m-1)} \sin\left[2\rho(m-1)\right] \right\}. \tag{7.44*}$$

Although formula (7.44*) correctly describes the behavior of $K(\rho)$ for large ρ, the agreement between the values of k calculated according to (7.44*) and those given in Table 17 is poor. Such an agreement must occur for values of ρ which are larger than those given in Table 17. We should note that in the case $m \sim 1$, the formula for k can be written very simply:

$$k = 2\pi a^2 \left\{ 1 - \frac{1}{\delta} \sin 2\delta \right\}; \quad \delta = \rho(m-1). \tag{7.45}$$

It is important to note that both main parameters of the problem m and ρ are only contained in the form of $\delta = \rho(m - 1)$.

The parameters ρ and m are the similarity criteria of our problem. This means that for indentical ρ and m the scattering pictures will be similar (the similarity coefficient -- square of the radius ratios).

In the general case, both parameters ρ and m are independent, and the number of independent parameters cannot be decreased. However, in the case $m \sim 1$, as we have seen, the behavior of $k(\rho)$ may be described by only one parameter δ.

The possibility of reducing the similarity to one parameter in the case $m \sim 1$ is not accidental. During the passage of a particle, the amplitude and phase of the wave change. The amplitude of a ray passing through the center acquires the factor $d_p = d_s = \frac{4m}{(m+1)^2}$ (see Chapter V), and the phase increases by a factor of 2δ. This means that in the case $m \sim 1$ the amplitude barely changes and the nature of the scattering is determined by the phase change, i.e., by the quantity δ.

Let us call the reduction of the problem to one independent parameter δ the similarity rule.

The curves shown in Figure 44 and, in particular, the position of the main maximum on these curves (the divergence of parts of the curves is not important) substantiate our similarity rule, not only for $\rho \gg 1$ -- as follows from (7.45) -- but also for $\rho \sim 1$ in the case $m \leq 2$. If the similarity rule holds, then the position of the first (main) maximum for any of the curves may be determined by /219 the following formula:

$$\rho_{max}^{(1)} = \frac{\delta_{max}^{(1)}}{m-1}, \tag{7.46}$$

where $\delta_{max}^{(1)}$ is the value of δ at the position of the maximum for one of the curves. In the case m = 1.33, we find that $\delta_{max}^{(1)} = 2.0$. Thus, for $m \leq 2$ we obtain the following formula

$$\rho_{max}^{(1)} = \frac{2}{m-1}. \tag{7.46*}$$

For m = 1.44; 1.55 and 2.00, this yields 4.5; 3.6 and 2.0. For the second and third case (within the limits of possible accuracy) the agreement is complete (see page 126). For m = 1.44 the divergence is within the unit of the last sign, i.e., about 2% in all.

We can thus see that the similarity rule provides us with a very simple and precise method for determining the general pattern of the curves $K(\rho)$ for different m in the case of small (m - 1). The curve for m = 1.33 (Figure 43) may be used, for example, as the "standard" curve.

All the statements given above pertain to determining the position of the first maximum. With respect to its magnitude, with an increase in (m - 1) from zero to 0.6, it increases approximately linearly, and from then on more slowly. The nature of the dependences of $\rho_{max}^{(1)}$ and $K(\rho)$ on (m - 1) is shown in Figure 59.

Based on these curves, we can readily determine the magnitude and position of the first maximum for any m < 2. The position of the subsequent extremums can be found, if we take the fact into account that $\delta_{min}^{(1)} = 3.8$; $\delta_{max}^{(2)} = 5.4$; $\delta_{min}^{(2)} = 7.0$ and $\delta_{max}^{(2)} = 8.5$ follow from the data for m = 1.33. The quantity $K(\rho)$ at these extremums can be approximately determined if we employ the data for m = 1.21, which we indicated previously, along with the data on m = 1.33. We should recall that we obtained values of $K(\rho)$ equal to 3.64; 1.65; 2.70 and 1.84, respectively, for ρ equalling 9.5; 17.6; 25.7 and 33.4. For small (m - 1), we can approximately assume linear changes in $K(\rho)$ with (m - 1) and for other extremums, in accordance with the rectilinear part of the curve for the first maximum (Figure 59).

We should add that we have already discussed the case $m \sim 1$ in Chapter VIII.

Interference between bundles leads to the occurrence of several maxima and minima in the indicatrixes. P. Ya. Bokin, Ye. M. Brumberg, A. A. Lebedev and /220 V. I. Chernyayev obtained these maxima in the form of wide rings (up to ten and more) around the projector ray [in the direction of the source (Ref. 83)]. Ordinarily, the indicatrixes do not have an interference nature: it is blurred

by the non-monochromatic nature of the source for light and fog.

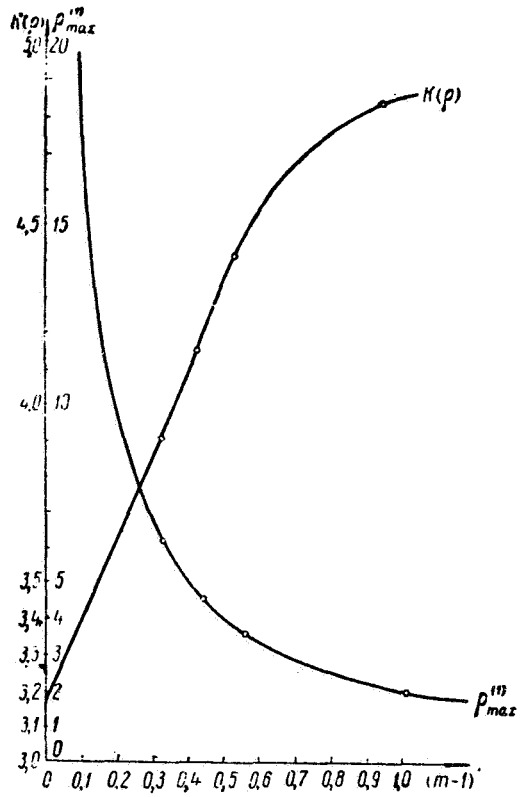

Figure 59. Graph for Interpolation of the Position and Magnitude of the Main Attenuation Maximum.

Let us now investigate the asymmetry of the indicatrix η for drops of water in the visible region. For an extremely /221 small particle, η = 1. For an extremely large particle, it follows from Table 13 that light which is scattered backwards will be 0.056 positive units, and light scattered forward will be 0.944 positive units (diffracted light; in fractions of πa^2). Consequently, η = 34.7.

We determined the intermediate values of the function η(ρ) by integration of the data provided by Blümer (Ref. 56), Paranjpe, Naik, and Vaidya (Ref. 98), and our data (Table 21). Table 24 presents the results derived from these calculations.

We sould like to note the very oscillatory nature of η(ρ) for drops of water; this essentially differs from the comparatively weak oscillations of η(ρ) in the case m = ∞ (see VI, 3).

Several authors have experimentally verified the theoretical scattering indicatrixes.

The basic difficulty encountered in these studies is that of obtaining stationary monodisperse sols and of determining the number and size of particles contained in them. Uniformity and constant size of the particles is very important, since a small change in the particles leads to a significant change in intensity.

TABLE 24

ρ	η	ρ	η	ρ	η	ρ	η
0	1,00	6	23,3	10	4,49	30	39,4
1,5	4,46	7	19,0	12	5,29	60	17,4
4	12,8	8	12,8	15	15,1		
5	14,2	9	23,8	20	9,53		

In the majority of studies, light which is scattered at right angles is investigated. G. I. Pokrovskiy (Ref. 99) was one of the first authors who systematically studied light which is scattered in different directions. He produced fog by condensing jets of water vapor in the air.

The drops were small in (Ref. 99). The values for ρ given in this study are about 0.5 - 0.7. In the article (Ref. 100) G. I. Pokrovskiy presented the results derived from scattering by larger drops ($a \sim 1\ 1 - 100\ \mu$). The results presented both in (Ref. 99) and in (Ref. 100) agree with the theoretical calculations. In several other investigations, G. I. Pokrovskiy studied a great many important problems entailed in the optics of turbid media [see (Ref. 101, 102, 103, 104) and others].

The most detailed quantitative investigation of the indicatrixes for large drops was performed in (Ref. 98).

The fog to be studied was created in a chamber F by quickly connecting it with a large vessel which was first evacuated up to a certain pressure (Figure 60). The authors stated that by controlling the degree of expansion, and also the composition of the dust particles, they were able to produce uniform drops having a given size. The size of the drops was determined and constantly controlled by measuring the corona observed at a great distance by means of a light source S_1, a lens L_1, and a measuring theodolite Th. The clearly defined rings of the corona, whose position did not change during the observational period, pointed to the uniformity of the fog and its stability. /222

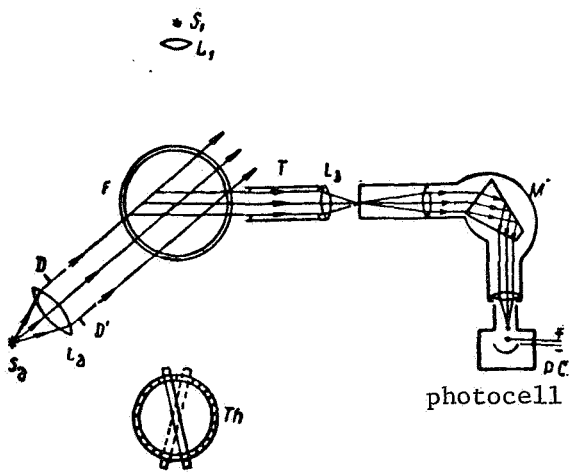

Figure 60. Diagram Showing the Apparatus for Determining Indicatrixes in Fog.

In accordance with VI, 2 clear coronas can only be observed for sufficiently large drops ($a > 2\mu$). The size of the drops with $a \leq 2\mu$ was determined according to the Stokes formula with corrections.[1]

A spectrometric stand, in the center of which a chamber F with fog was located, was employed to measure the intensity of light scattered by drops. One of the stand arms held a illuminating device, consisting of the light source S_2, a lens L_2 with a large aperture, and a diaphragm D'D. The other arm held a recording device consisting of a collimation tube T, a monochromator M, and a R. S. photocell. The photocell readings through the amplifier were recorded by the galvanometer. /223

It must be noted that the effective volume V, from which the scattered light enters the receiving device, changes as the scattering angle changes.

---

(1) A comparison of the results derived from optical measurements with measurements of the rate of decrease (in the measurement region where both methods could be used) showed that the divergence of the radii determined by both methods did not exceed 5%.

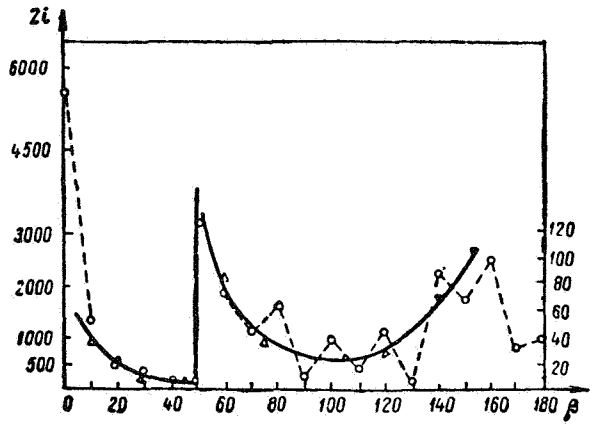

Figure 61. Comparison of Computational and Experimental Results for Drops of Water in the Visible Region.

0 - calculated points for ρ = 10;
Δ - experimental points for ρ = 10, 12; for the part β (0, 50), the scale is given on the left; for the remaining scattering angles, it is given on the right.

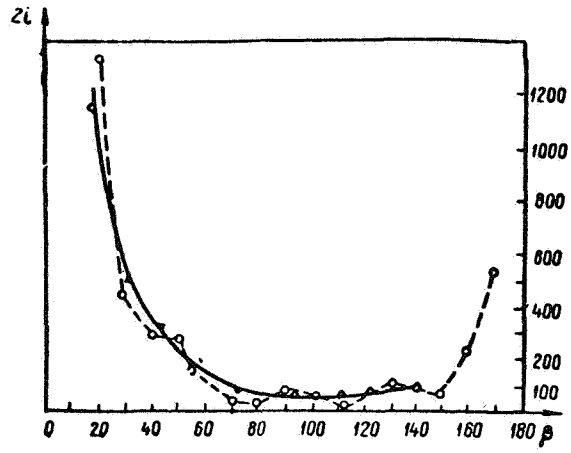

Figure 62. Comparison of Computational and Experimental Results for Drops of Water in the Visible Region.

0 - calculated points for ρ = 20;
Δ - experimental points for ρ = 20, 22.

It is apparent that

$$V = \frac{V_0}{\sin \beta},$$

where V_0 is the effective volume during perpendicular observations.

Thus, the galvanometer readings multiplied by sin β were compared with theory.

The results derived from the measurements coincided very well with theory.

We have illustrated this agreement in Figure 61 and 62, where the theoretical curves, are shown by the dashed line, and the experimental curves are shown by the solid line. It must also be noted that the values of ρ in the experiments did not exactly coincide with the rounded off values of ρ assumed in the calculations. The experimental curves are smooth; they do not have the flucutating change in intensity with the angle β which is characteristic for the theoretical curves. These (interference) fluctuations of the theoretical curves are due to the strictly monochromatic nature of the fog, assumed in the calculations.

The general pattern of both curves closely coincides in every case (the deviation at separate points does not exceed ± 17%). The authors connect a slight difference at small angles with inaccuracy with which the volume is corrected at small β.

The scattering indicatrix in "pure" atmosphere has been studied by many authors. The data obtained by different authors differ somewhat from each other, in accordance with the differing content of admixtures at the observational point. The general result is as follows: the scattering indicatrix is greatly extended.

In Figure 63 we present the indicatrix obtained by Ye. V. Pyaskovskaya-Fesenkova during observations with a blue Schott filter (Ref. 77, 195) (in the vicinity of the town of Ivanovo; summer). Curve I represents the total indicatrix (observed); curves III and II represent the Rayleigh and aerosol indicatrixes (calculated). V. G. Fesenkov assumes the following empirical formula for this indicatrix: /225

$$\gamma(\beta) = 1 + 1{,}652\cos^2\beta + 1{,}214\cos^3\beta. \tag{7.47}$$

We would like to note the indicatrix obtained by H. G. Boldyrev by analyzing the data on the brightness distribution over the sky (Ref. 89).

The empirical formula of Shenberg is frequently used to characterize the atmospheric scattering properties:

$$\gamma(\beta) = 1 + p\cos\beta + q\cos^2\beta. \tag{7.48}$$

The constants p and q are selected from observations (Shenberg assumes the following: p = 2.7; q = 3.0).

The indicatrix obtained by I. N. Yaroslavtsev (Ref. 106) (town of Tashkent, summer), who processed his observations based on the Shenberg formula [employing the calculations of A. N. Gordov (Ref. 107)], is shown in Figure 64 (in the λ region 0.525-3 μ.

V. A. Kratt (Ref. 68) assumes that the Shenberg formula must be corrected as follows for large values of the Mie effect:

$$\gamma(\beta) = 1 + pv(\beta) + q\cos^2\beta, \tag{7.49}$$

where $v(\beta) = e^{-3\beta} - e^{-3\frac{\pi}{2}}$ (β in radians).

The reader will find a description of the methods for determining p and q, their values for Tashkent, the dependence of these values on weather conditions, etc. in his study (Ref. 68).

The reader will find more detailed data on the scattering indicatrix in a "pure" atmosphere in the original works of V. G. Fesenkova, N. N. Kalitina, Ye. V. Pyaskovskoy-Fesenkovoy, I. N. Yaroslavtseva, N. G. Boldyreva, and others. According to V. V. Shuleykin (Ref. 35), the scattering indicatrix of sea water may be expressed by a curve like type a in Figure 65. It is close to the curve which was experimentally obtained by A. A. Gershun for two seas within the USSR (curve b in Figure 65 [Ref. 108]).

A. A. Gershun (together with M. M. Gurevich) developed a laboratory device for measuring indicatrixes in sea water tests (Ref. 92). It is shown in /227

Figure 66. The captions given on the figure explain the diagram. The measurements also require a correction of the volume.

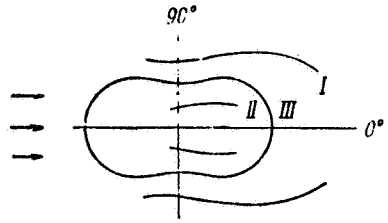

Figure 63. Indicatrix of Light Scattering in the Atmosphere.

I - complete curve; II - aerosol section; III - Rayleigh scattering in a "pure" atmosphere.

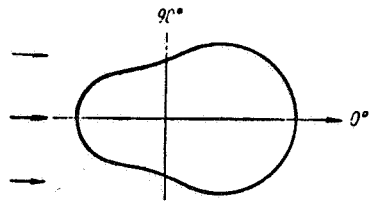

Figure 64. Typical Indicatrix for "pure" atmosphere.

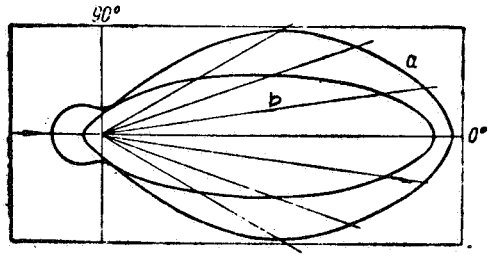

Figure 65. Indicatrix for Sea Water.

(a) - V. V. Shuleykina; (b) - experimental indicatrix of A. A. Gershun.

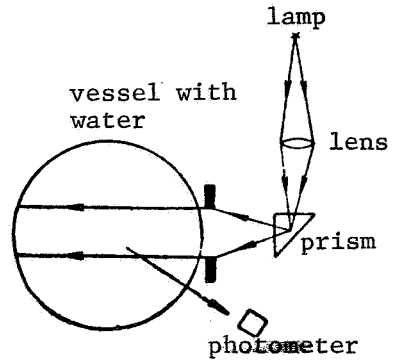

Figure 66. Diagram Showing the Device for Determining Indicatrixes in Sea Water Tests.

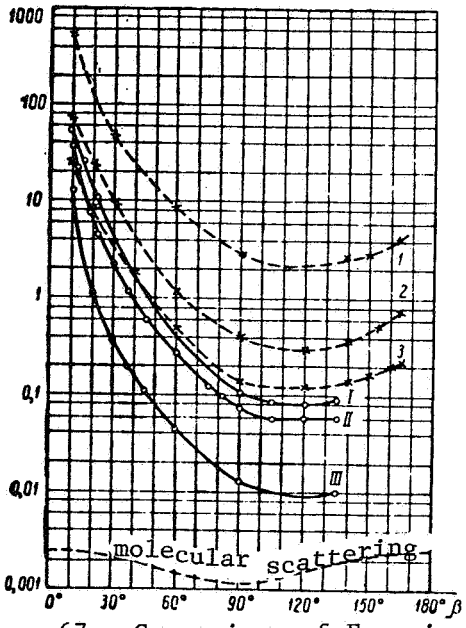

Figure 67. Comparison of Experimental Curves for the Indicatrix of Sea Water (1, 2, 3) with the Theoretical Curves (I, II, III).

Figure 67 presents the results derived from measurements for three different tests (1, 2, 3), compared with the theoretical curves for particles of different sizes (I, II, III). The experimental and theoretical curves have a parallel behavior (Ref. 92).

CHAPTER VIII /228

PARTICLES WITH ELECTRICAL PROPERTIES DEVIATING SLIGHTLY FROM THE SURROUNDING MEDIUM PROPERTIES

§ 1. Fundamental Equation

In the preceding chapters we presented a precise solution for the problem of diffraction by a sphere, and

presented different approximation methods for obtaining numerical data. The use of curvilinear coordinates, in which the boundary conditions of the problem can be described in the simplest way, lie at the basis of the method presented in Chapter II. It is important that this method is not extended to particles having an irregular form.[1] This is the main drawback of the method developed in Chapter II. Another drawback lies in the cumbersome nature of the final formulas, even for the case of small particles ($\rho \sim 1$).

In this chapter we shall present another method for investigating the problem of scattering of light by a particle -- the method of the integral differential equation. We shall follow our studies (Ref. 109, 110, 124).

We can apply this general method to particles whose electrical properties differ very little from the properties of the surrounding medium. This case is very important for admixtures in the atmosphere and the hydrosphere. As we shall see later, this method enables us to obtain a simple solution for spheres with $\rho \sim 1$ and for particles having a non-spherical form -- rods and tablets.

Let us turn to the Maxwell equation (1.3) to derive the fundamental integral equation.

Let us introduce the Hertz vector, which is related to the electric and magnetic fields by the following relationships /229

$$\mathbf{E} = \nabla \operatorname{div} \mathbf{Z} + \frac{\omega^2}{c^2}\mathbf{Z},$$

$$\mathbf{H} = \frac{i\omega}{c} \operatorname{rot} \mathbf{Z}.$$

From the Maxwell equation, we find that Z satisfies the following equation

$$\Delta \mathbf{Z} + \frac{\omega^2}{c^2}\mathbf{Z} = -4\pi \mathbf{I}.$$

Here

$$\mathbf{I} = \mu \mathbf{E}, \text{and} \mu = \frac{\varepsilon - 1}{4\pi} - i\frac{\sigma}{\omega} = \frac{m^2 - 1}{4\pi}.$$ [2]

The solution of the latter equation, which decreases rapidly towards infinity will be as follows, as is known:

---

(1) A formal solution of the problem in series was given by Moglich (Ref. 111) for ellipsoids. However, it was very complex and could not be used. Numerical data derived from his formulas have not been published.

(2) We would like to call the attention of the reader to the fact that the indices before i (imaginary unit) in this chapter are just the opposite of the indices in (Ref. 109) and (Ref. 110). This is due to the fact that in this chapter we have retained the same time factor $e^{i\omega t}$ as in all preceding chapters, whereas in (Ref. 109) and (Ref. 110) the time factor had the form $e^{-i\omega t}$. In order to change to the notation in (Ref. 109) and (110), it is sufficient to replace all complex expressions by the conjugate expressions.

$$Z(\mathbf{r}) = \int \frac{\mathbf{I}(\mathbf{r}')\, e^{-i\frac{\omega}{c}R}}{R}\, dv'.$$

Here $R = |\mathbf{r}' - \mathbf{r}|$ is the distance between the observational point and the point at which the source is located (element of the particle region polarized by an electromagnetic wave). Integration is performed over the entire region occupied by the sources (over the entire particle).

We have the following for an electric field produced by polarized elements of the region:

$$\mathbf{E}(\mathbf{r}) = \operatorname{rot}\operatorname{rot}\int \frac{\mathbf{I}(\mathbf{r}')\, e^{-ikR}}{R}\, dv' - 4\pi\mathbf{I}(\mathbf{r}).$$

For the total electric field both inside and outside the sphere, we obtain the following integral equation

$$\mathbf{E}(\mathbf{r}) = \mathbf{E}_0 e^{-i\mathbf{k}\mathbf{r}} + \\ + \operatorname{rot}\operatorname{rot}\int \frac{\mu(\mathbf{r}')\mathbf{E}(\mathbf{r}')\, e^{-ikR}}{R}\, dv' - 4\pi\mu(\mathbf{r})\mathbf{E}(\mathbf{r}). \qquad (8.1)$$

We shall determine the electric field as the solution of this integral equation. Its physical meaning is very simple. /230

It is known that the electric field produced by a dipole with the moment $\mathbf{p}$ at a point located at a distance of R from the dipole will be

$$\mathbf{E} = \operatorname{rot}\operatorname{rot}\frac{\mathbf{p}}{R};$$

where $\mu\mathbf{E}dv'$ is the dipole moment of an element of the region polarized by the electromagnetic wave. Thus, according to equation (8.1), the electric field at a certain point in space is the sum of the field produced by the external bodies (sources of light) $\mathbf{E}_0 e^{-i\mathbf{k}\mathbf{r}}$, the fields of the polarized elements of the particles

$$\int \operatorname{rot}\operatorname{rot}\frac{\mu\mathbf{E}e^{-ikR}}{R}\, dv'\ ^{1}$$

and the fields of the screening (fictitious) charges on the surface of the particle -- $4\pi\mu\mathbf{E}$.

When the differential equations are solved, it is necessary that the boundary conditions be satisfied, in addition to the equations.

When an integral equation is solved, the corresponding requirements are satisfied automatically. In our case, for example, we have already seen that the electric field is the superposition of the external field and the field of the dipoles which occupy the scattering particle. Since each term of this sum satisfies the Maxwell equation and the boundary conditions everywhere, the sum also satisfies them everywhere.

Based on considerations which will be clarified later, instead of the integral equation (for the mean electric field), it is more advantageous to study the integral equation which is obtained from (8.1) for the effective

(1) The occurrence of the factor e^{-ikR} here is due to delay.

electric field $\mathbf{E}_{eff}$. We may introduce the latter according to the following formula

$$\mathbf{E}_{eff} = \mathbf{E} + \frac{4\pi}{3}\mathbf{I}.$$

We also readily find that

$$\mathbf{I} = \alpha \mathbf{E}_{eff} \text{ where } \alpha = \frac{\mu}{1 + \frac{4\pi}{3}\mu} = \frac{3}{4\pi}\left(\frac{m^2 - 1}{m^2 + 2}\right) \tag{8.2}$$

and /231

$$\mathbf{E}_{eff}(\mathbf{r}) = \mathbf{E}_0 e^{-ikr} + \\ + \operatorname{rot}\operatorname{rot}\int \alpha \mathbf{E}_{eff}(\mathbf{r}')\frac{e^{-ikR}}{R}\,dv' - \frac{8\pi}{3}\alpha \mathbf{E}_{eff}(\mathbf{r}). \tag{8.3}$$

Equation (8.3) is the fundamental equation of our problem. We should note that outside of the particle the effective field coincides with the mean field.

The parameter α contained in the integral equation (8.3) is in actuality very small for all the cases which are of interest in practice. In Table 25 we present the value of the modulus $|\alpha|$ for different substances. Thus, both for the dielectric constant, and for electroconductivity, we select only their electron part.

The ion part of conductivity, and also the constant dipole moments of the molecules are excluded from the examination, since neither the ions nor the molecules will be able to oscillate due to the rapidly changing electric field of the light wave.

Solid dust particles are encountered in the atmosphere, in addition to water, ice, and small drops of different ion solutions (which Table 5 gives as HCl). The refraction coefficient of the latter is not usually known.

TABLE 25. ELECTRIC PROPERTIES OF ADMIXTURES

	$\varepsilon = n^2$	$\frac{\varepsilon - 1}{4\pi}$	σ	α
In the atmosphere:				
Water.....	1,77	0,061	0	0,048
Ice.....	1,71	0,056	0	0,045
HCl.....	1,56	0,044	0	0,037
In the hydrosphere:				
Air.....	0,56	0,35	0	0,030

If we assume that the following holds for them /232

$$\left|\frac{\varepsilon - 1}{4\pi}\right| \ll 1,$$

then α will be much smaller than unity for them, since their electron conductivity is usually smaller than 10 ohm^{-1} cm^{-1} (semiconductor) and

$$\frac{|\sigma}{\omega} < 10^{-2} \text{ for } \omega \sim 10^{15} \frac{1}{\text{sec}}.$$

We shall try to find the solution of the integral equation (8.3) in the form of series in terms of α.

Let us set

$$\mathbf{E}_{\text{eff}} = \mathbf{E}_{\text{eff}}^{(0)} + \alpha \mathbf{E}_{\text{eff}}^{(1)} + \alpha^3 \mathbf{E}_{\text{eff}}^{(2)} + \ldots \tag{8.4}$$

We thus obtain from equation (8.3):

$$\left.\begin{aligned} &\mathbf{E}_{\text{eff}}^{(0)} = \mathbf{E}_0 e^{-ikr}; \\ &\mathbf{E}_{\text{eff}}^{(1)} = \operatorname{rot}\operatorname{rot}\int \mathbf{E}_0 \frac{e^{-i(kR+kr')}}{R} dv' - \frac{8\pi}{3} \mathbf{E}_0 e^{-ikr} \end{aligned}\right\} \tag{8.5}$$

and so on.

If we know $\mathbf{E}_{\text{eff}}$, we can determine the mean electric field $\mathbf{E}$ and then the magnetic field $\mathbf{H}$.

The integral equation equation determines $\mathbf{E}_{\text{eff}}$ in the entire space, both inside of and outside of the sphere. In the latter case, the equation can be simplified, since the field outside of the sphere is usually measured at distances which are considerably greater than its radius ($r \gg a$).

We obtain the following for the field of a scattered wave:

$$\mathbf{E}_{\text{scat}} = \frac{-\alpha k^2}{r} \int \{\mathbf{R}_0 (\mathbf{R}_0 \mathbf{E}_{\text{eff}}) - \mathbf{E}_{\text{eff}}\} e^{-ikR} dv'. \tag{8.6}$$

Here $\mathbf{R}_0$ is the unit vector directed from the particle center to the observation point.

We have thus removed from the integral the slowly changing factor $1/R$ and substituted its mean value $1/r$ (r -- distance from the observational point to the center of the sphere).

The field of the scattered wave may also be represented in the form of a series in terms of α:

$$\mathbf{E}_{\text{scat}} = \mathbf{E}_{\text{scat}}^{(0)} + \alpha \mathbf{E}_{\text{scat}}^{(1)} + \alpha^2 \mathbf{E}_{\text{scat}}^{(2)} + \ldots \tag{8.7}$$

The zero term must be absent in the expansion of $\mathbf{E}_{\text{scat}}$, i.e., $\mathbf{E}_{\text{scat}}^{(0)} = 0$.[1] /233

We have the following in accordance with the formulas (8.7) and (8.4):

---

[1] More precisely, we measure $\mathbf{E}_{\text{scat}} - \mathbf{E}_{\text{scat}}^{(0)}$ in the form of a scattered wave field.

$$\mathbf{E}^{(1)}_{\text{scat}} = -\frac{k^2}{r}\int \{\mathbf{R}_0(\mathbf{R}_0, \mathbf{E}^0_{\text{eff}}) - \mathbf{E}^0_{\text{eff}}\} e^{-ikR}\, dv' \tag{8.8}$$

and so on.

In the last analysis, we are interested in the components of the scattered field with respect to the spherical axes θ and ϕ. Thus, the first term in the expressions $\mathbf{E}^{(i)}_{\text{scat.}}$, which contains $\mathbf{R}_0$, naturally drops out.

Let us employ $\mathbf{i}_\theta$ and $\mathbf{i}_\phi$ to designate the unit vectors of the axes θ and ϕ in the spherical coordinate system. We obtain the following for the projection of the scattered field over these axes:

$$\left.\begin{aligned} E_{\text{scat}_\theta} &= (\mathbf{E}_{\text{scat}}, \mathbf{i}_\theta) = \frac{\alpha k^2}{r}(\mathbf{A}, \mathbf{i}_\theta); \\ E_{\text{scat}_\varphi} &= (\mathbf{E}_{\text{scat}}, \mathbf{i}_\varphi) = \frac{\alpha k^2}{r}(\mathbf{A}, \mathbf{i}_\varphi). \end{aligned}\right\} \tag{8.9}$$

The following vector is indicated by **A**:

$$\mathbf{A} = \int \mathbf{E}_{\text{eff}} e^{-ikR} dv'. \tag{8.10}$$

The vector **A** can be represented in the form of series with respect to α, which will be similar to the series for $\mathbf{E}_{\text{eff}}$:

$$A = \mathbf{A}^{(0)} + \alpha\mathbf{A}^{(1)} + \alpha^2\mathbf{A}^{(2)} + \ldots \tag{8.11}$$

It is clear, without any calculations, that the smallness of α is insufficient for the convergence of the series described here. The smallness of α physically depends on the fact that the external field excites small electric moments in the molecules. However, the field produced by the molecules will only be small if the amount of molecules themselves is sufficiently small. Therefore, the series described can diverge for large spheres. The smaller is α, the later this divergence occurs. In view of the smallness of α, which was indicated above, it may be assumed that the region of application for the method advanced is quite wide.

§ 2. First Approximation for the Sphere /234

(a) Effective Field Within the Sphere. In order to calculate the first approximation in a scattered field, we must take the zero approximation for the effective field. Thus, we may set

$$\mathbf{E}_{\text{eff}} = \mathbf{E}_0 e^{-i(\mathbf{kr}-\omega t)},$$

i.e., we set $\mathbf{E}_{\text{eff}}$ equal to the field of the incident wave.

(b) Scattered Field. According to (8.8), we have

$$\mathbf{E}^{(1)}_{\text{scat}} = \frac{k^2}{r}\mathbf{E}_{0\perp} f'(\beta). \tag{8.12}$$

Here we have

$$\mathbf{E}_{0\perp} = \mathbf{E}_0 - \mathbf{R}_0(\mathbf{R}_0\mathbf{E}_0),$$

and

$$f'(\beta) = \int e^{-i(\mathbf{kr}' + kR)} dv'. \tag{8.13}$$

We should recall that the integral is extended over the sphere, $\mathbf{r}'$ is the radius vector of the variable point M within the sphere; R is the distance from this point to an infinitely removed observational point.

The vector **A** in this approximation will be

$$\mathbf{A}_0 = \mathbf{E}_{0\perp} f'(\beta).$$

The integrand in $f'(\beta)$ depends only on the two vectors **k** and $\mathbf{R}_0$. Let us draw the coordinate plane XZ through the plane of the vectors **k** and $\mathbf{R}_0$, and let us select the x-axis so that it bisects the angle $(\mathbf{k}, \mathbf{R}_0) = \beta$ (Figure 68). Recalling that r is the distance from the center of the sphere to the observational point, we readily obtain

$$\mathbf{kr}' + kR = k\left(r + x\cos\frac{\beta}{2} + z\sin\frac{\beta}{2} - x\cos\frac{\beta}{2} + \right.$$
$$\left. + z\sin\frac{\beta}{2}\right) = k\left(r + 2z\sin\frac{\beta}{2}\right).$$

Thus, we have replaced R by r - d, where $d = x\cos\frac{\beta}{2} - z\sin\frac{\beta}{2}$ is the distance from M to the plane passing through the center of the sphere perpendicularly to R_0 (the plane AA), and kr' has been replaced by $k\left(x\cos\frac{\beta}{2} + z\sin\frac{\beta}{2}\right)$.

We now obtain the following for $f'(\beta)$:

$$f'(\beta) = \int e^{-ik\left(r + 2z\sin\frac{\beta}{2}\right)} dx\,dy\,dz =$$
$$= \int_{-a}^{+a} \pi(a^2 - z^2) e^{-ikr} e^{-ik2z\cdot\sin\frac{\beta}{2}} dz = e^{-ikr} v \frac{3}{q^3}(\sin q - q\cos q).$$

Here $q = 2ak\sin\frac{\beta}{2}$, $v = \frac{4}{3}\pi a^3$ is the volume of the sphere.

Finally, the scattered field from the sphere will be as follows in the first approximation:

$$\mathbf{E}_{\text{scat}} = \alpha\frac{4\pi^2}{\lambda^2 r} v e^{-i(kr - \omega t)} \mathbf{E}_{0\perp} f(q), \tag{8.14}$$

where we have designated the following quantity by f(q)

$$\frac{3}{q^3}(\sin q - q\cos q). \tag{8.15}$$

For computational simplicity, we must keep the fact in mind that

$$f(q) = \frac{3}{q^{3/2}}\sqrt{\frac{\pi}{2}} J_{3/2}(q), \tag{8.16}$$

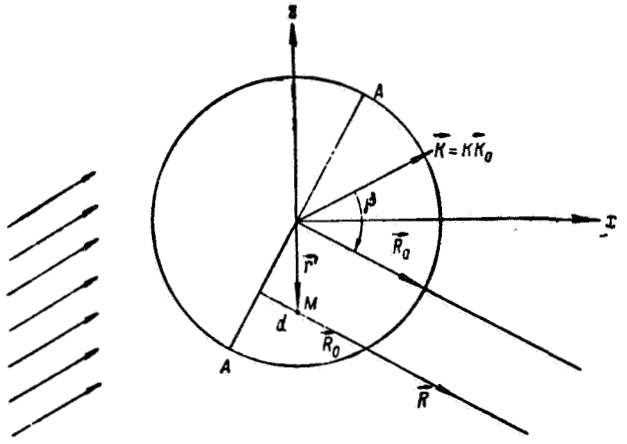

Figure 68. Position of the Vectors when Calculating (in the First Approximation) the Field Scattered by the Sphere.

where $J_{3/2}$ is the Bessel function of the order 3/2.

We have computed a similar table for the function f(q). It is given in (Ref. 110) (for q from 0 to 10 -- every 0.02; from 10 to 40 -- every 1). We shall present part of this table here.

TABLE 26

q	$f(q)$	q	$f(q)$	q	$f(q)$	q	$f(q)$
0,00	1,0000	3,20	0,2871	6,40	—0,0714	9,60	0,0314
0,20	0,9960	3,40	0,2314	6,60	—0,0622	9,80	0,0279
0,40	0,9842	3,60	0,1791	6,80	—0,0516	10,00	0,0235
0,60	0,9645	3,80	0,1308	7,00	—0,0404	12,00	—0,01852
0,80	0,9375	4,00	0,0871	7,20	—0,0288	14,00	—0,00101
1,00	0,9035	4,20	0,0481	7,40	—0,0174	16,00	0,01101
1,20	0,8627	4,40	0,0141	7,60	—0,0064	18,00	—0,00650
1,40	0,8169	4,60	—0,0147	7,80	—0,0036	20,00	—0,00259
1,60	0,7663	4,80	—0,0384	8,00	0,0126	22,00	0,00620
1,80	0,7111	5,00	—0,0570	8,20	0,0202	24,00	—0,00241
2,00	0,6531	5,20	—0,0708	8,40	0,0264	26,00	—0,00274
2,20	0,5924	5,40	—0,0799	8,60	0,0310	28,00	0,00372
2,40	0,5306	5,60	—0,0849	8,80	0,0340	30,00	—0,000624
2,60	0,4682	5,80	—0,0861	9,00	0,0354	32,00	—0,00239
2,80	0,4063	6,00	—0,0838	9,20	0,0353	34,00	0,00224
3,00	0,3456	6,20	—0,0787	9,40	0,0340	36,00	0,000232
						38,00	—0,00197
						40,00	0,00129

Figure 69 presents a graph showing the function f(q). The zeros of the

function coincide with the roots of the transcendental equation tg x = x.

For small q, we have:

$$f(q) = 1 - \frac{q^2}{10} + \frac{q^4}{280} - \frac{q^6}{15120} + \cdots \tag{8.17}$$

For large q (in addition to the vicinities of the points cos q = 0):

$$f(q) = -\frac{3}{q^3}\cos q. \tag{8.18}$$

If q is very small, then f(q) $\simeq$ 1, and formula (8.14) changes into the formula (4.5) -- the field of the oscillating dipole.

(c) Scattering indicatrix. From formula (8.14) we find that the scattering indicatrix differs from the Rayleigh indicatrix only by the factor $f^2(q)$. It is due to interference of the fields which are scattered by different elements of the sphere. We have the following for linearly polarized light: /237

$$I^{(1)} = I_0 |\alpha|^2 \frac{16\pi^4}{\lambda^4} v^2 (1 - \sin^2\beta \cos^2\varphi) f^2(q). \tag{8.19}$$

Here ϕ is the angle between the direction $\mathbf{E}_0$ and the projection $\mathbf{R}_0$ on the plane which is perpendicular to $\mathbf{k}$. For natural light, we have

$$I^{(1)} = I_0 |\alpha|^2 \frac{16\pi^4}{\lambda^4} v^2 \left(\frac{1 + \cos^2\beta}{2}\right) f^2(q). \tag{8.20}$$

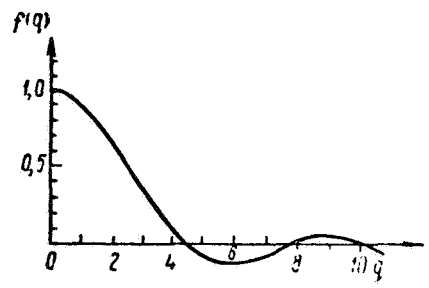

Figure 69. Graph Showing the Function f(q).

In order to illustrate the latter formula, we have used it to calculate the scattering indicatrixes of four particles with ρ = 0.4; 0.8; 1.6; 4. They are shown in Figure 70.

In the first approximation, the form of the indicatrixes for particles with different m will be the same. Thus, the curves presented in Figure 70 represent the indicatrixes for particles with a given ρ of any substances, provided that α is small enough.

(d) Polarization. Since there is no mutual influence of dipoles in the approximation under consideration, the degree of scattered light polarization will be Rayleigh polarization.

(e) Scattering Coefficient. In order to calculate the scattering coefficient, we must integrate the scattering indicatrix over all directions:

$$k_p = \frac{1}{I_0}\int_0^{2\pi} d\varphi \int_0^{\pi} I(\varphi, \beta) \sin\beta \, d\beta.$$

Substituting the expression for I from (8.19) or (8.20) -- it does not matter which one -- after integration we obtain /238

$$k_p^{(1)} = \pi a^2 |\alpha|^2 F^{(1)}(z). \tag{8.21}$$

Here we have

$$F^{(1)}(z) = \frac{2\pi^2}{z^2}\left\{\frac{z^4}{4} + 5z^2 + (4z^2 - 16)(\mathrm{ci}\, z - \ln z - c) - \right.$$
$$\left. - 2z \sin z + 14(\cos z - 1)\right\}; \tag{8.22}$$

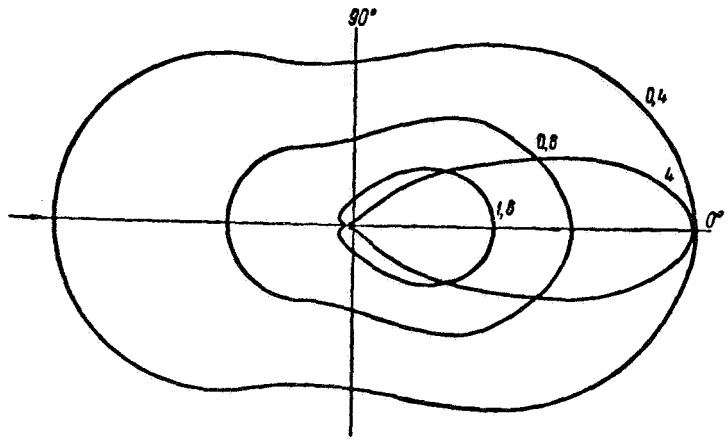

Figure 70. Indicatrixes of Weakly Refracted Particles With ρ = 0.4; 0.8; 1.6 and 4 (scale of the curves is equal).

where $z = \frac{8\pi a}{\lambda} = 4\rho$, c is the Euler constant equal to 0.577 ...; ci z is the integral cosine of z:

$$\mathrm{ci}\, z = -\int_z^\infty \frac{\cos t}{t} dt.$$

For small z (the Rayleigh case), we have

$$\left.\begin{aligned} F^{(1)}(z) &= 2\pi^2\left(\frac{z^4}{108} - 26 \cdot 10^{-5} z^6\right), \\ k_p^{(1)} &= 0{,}183 z^4 \pi a^2 |\alpha|^2. \end{aligned}\right\} \tag{8.23}$$

The scattering coefficient is proportional to $\frac{1}{\lambda^4}$. For large z, we have /239

$$\left.\begin{aligned} F^{(1)}(z) &= \frac{\pi^2}{2} z^2 \\ k_p^{(1)} &= 8\pi^2 \rho^2 |\alpha|^2 \cdot \pi a^2. \end{aligned}\right\} \tag{8.24}$$

Comparing this formula with formula (7.4), we can readily see that our formula differs by only a factor of 2 from the formula obtained by Jobst for the

same limiting case from the Mie solution. This difference is caused by the Jobst error which we pointed out above.

TABLE 27

z	$F^{(1)}(z)$	z	$F^{(1)}(z)$	z	$F^{(1)}(z)$	z	$F^{(1)}(z)$
0,00	0,000	2,8	9,277	3,8	26,944	7,0	158,012
1,00	0,173	3,0	11,883	3,9	29,372	8,0	217,111
1,20	0,375	3,1	13,363	4,0	31,938	9,0	285,508
1,40	0,651	3,14	14,015	4,5	46,545	10,0	365,570
1,60	1,145	3,2	14,920	5.0	64,093	11,0	463,141
1,80	1,757	3,3	16,640	5,9	102,407	12,0	571,884
2,00	2,665	3,4	18.456	6,0	106,927	13,0	691,089
2,20	3,810	3,5	20,391	6,1	111,368	14,0	818,506
2,4	5,290	3,6	22,463	6,2	116,224	15,0	956,147
2,6	7,106	3,7	24,654	6,28	120,054	20,0	1794,589
				6,4	125,956		

In the approximation under consideration, the scattering coefficient increases indefinitely ($\sim z^2$) with an increase in z.

We tabulated the function $F^{(1)}(z)$. Table 27 presents its values for z from 0 to 20. For larger values of z, we may employ the asymptotic formula (8.24).

Figure 71 (curve 1) presents a graph of the function $F^{(1)}(z)$.

For purposes of comparison, the graph also presents the Rayleigh dependence, i.e., the function $0.188\ z^4$ (curve 3).

The decrease in the rate at which $F_1(z)$ increases with an increase in the particle size is caused physically by the mutual cancelation of the fields from different parts of the sphere, which occurs due to the phase difference between them.

By employing tables 25 and 27, we can determine the region of applicability for the first approximation. If it is assumed that $k_p < 2\pi a^2$, we readily find that the first approximation is applicable up to $\rho \sim 5$ for a drop of water in the air, and is applicable up to $\rho \sim 5.5$[1] for a bubble of air in water. /240

(e) Relationship with the Kirchhoff diffraction theory. In conclusion, let us turn to the relationship between the first approximation and the /241

---

[1] This is the limit of applicability of the formulas for $k_p^{(1)}(\rho)$ and not for $I^{(1)}(\beta)$.

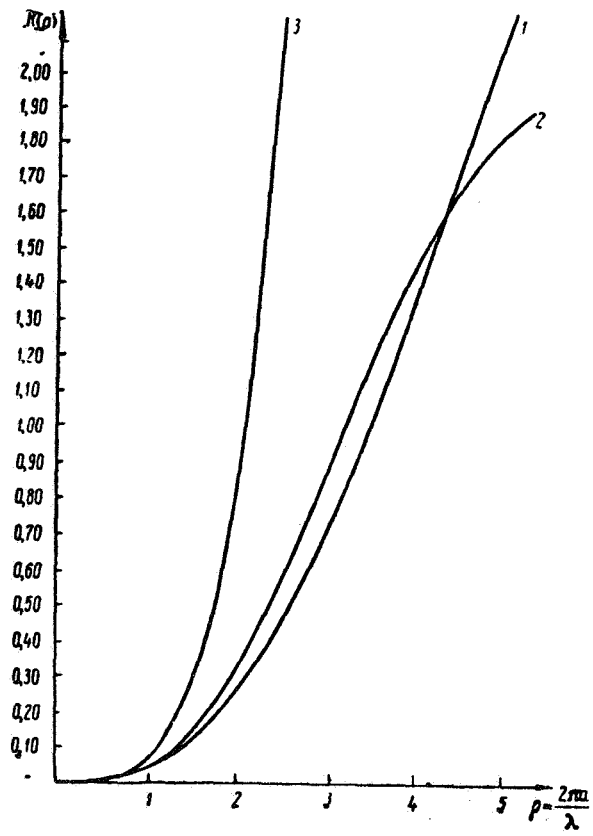

Figure 71. Scattering Coefficient $K(\rho)$ for m = 133.

1 -- in the first approximation; 2 -- exact curve; 3 -- according to Rayleigh.

Kirchhoff diffraction theory.

A calculation of the scattered field may be reduced, in the first approximation, to summation of the fields irradiated by dipoles which uniformly fill a sphere. This problem is similar to the customary diffraction problem. The only difference consists of the fact that here we have a volumetric "hole". Thus, since the intensity of dipole excitation is given by a plane wave, and the observational point is located at the distance $r \gg a$, the problem under consideration is similar to the diffraction problem in parallel rays in the Kirchhoff approximation [see (Ref. 2)].

It is well known that the diffraction theory developed by Kirchhoff is an approximation theory, taking into account terms of the first order with respect to λ/a (a -- dimensions of the body, the holes, etc.). Therefore, in order to establish the relationship between the formulas of the first approximation and the Kirchhoff theory, we must investigate the limiting form of these formulas in the case of large spheres.

Let us begin with deformation of the scattering indicatrix. We have already indicated that, as the radius of the sphere increases, its scattering indicatrix extends farther and farther forward. This extension leads to the fact that practically all of the scattered energy is only transmitted forward in the case of large particles. Waves in the lateral directions and in the backward direction are damped, resulting from mutual interference. The forward extension of the indicatrix must be in agreement with the well-known result of diffraction theory which proves the rectilinearity of light propagation. In diffraction theory, this result is obtained by compiling the Fresnel zones [see the end of § 2, Chapter VII].

The deviation of the indicatrix from a symmetrical form and its forward extension, as the particle size increases, is called the Mie effect. Thus, the physical essence of the Mie effect consists of the fact that the indicatrix is deformed as the particle size increases so as to produce the rectilinear propagation of light, in the case of an infinite medium.(1)

(1) These discussions pertain to a sphere which is assumed to be cut out of a uniform medium -- i.e., to the case $\alpha \to 0$ and $\rho \to \infty$, so that $|\alpha|\rho \to$ const (see the end of § 3).

Let us now examine the expression for the scattering coefficient [formula (8.21)]. We have already indicated that, in the case of large particles, our formula leads to a result which is paradoxical is physical terms -- the scattering coefficient increases in proportion to the fourth power of the radius (instead of the correct second power). /242

This result apparently arises due to an inaccurate calculation. It may be explained by the fact that we have considered the first approximation which, as we have already indicated above (see § 4), cannot be applied to the case $a \gg \lambda$. In the case $\frac{a}{\lambda} \gg 1$, in order to obtain the correct result we must take into account the mutual relationship between the radiative dipoles.

Formula (8.24) simply means that a system of non-interacting dipoles, which uniformly fill a sphere and which are excited according to the law $e^{i\,kr}$ (r -- dipole coordinates), radiates energy into space in proportion to the fourth power of the sphere radius.

This fact is related to the Kirchhoff theory. In order to prove this, we should recall that the intensity of light in the center of a diffracted spot during Fraunhofer diffraction from a circular hole is determined by the formula (6.11):

$$I = I_0 \frac{a^4\pi^2}{\lambda^2},$$

where $I_0 = \frac{cE_0^2}{4\pi}$ is the intensity of incident light.

Drawing an analogy between diffraction of light in a drop and its diffraction when penetrating a circular hole in an opaque screen, we should note that -- if the occurrence of the diffraction picture in the second case depends on the fact that $\mathbf{E}$ in the hole differs from zero -- the occurrence of the diffraction picture in the first case is caused by the fact that $\mathbf{E} = \varepsilon\mathbf{E}_0$ in the sphere, in contrast to $\mathbf{E}_0$ in the surrounding space. Therefore, if we write $I_0 = \frac{cE_0^2}{4\pi}$ for diffraction in a hole, we must write the following here:

$$I_0 = \frac{c(\varepsilon E_0 - E_0)^2}{4\pi} = \frac{cE_0^2}{4\pi}(\varepsilon - 1)^2 = \frac{cE_0^2}{4\pi}(4\pi)^2\alpha^2.$$

Luminous intensity in the direction of the wave vector will be: /243

$$I = I_0 \frac{a^4\pi^2}{\lambda^2} = \frac{cE_0^2}{4\pi}\,\alpha^2\pi a^2\left(\frac{4\pi a}{\lambda}\right)^2\pi.$$

We may obtain the total scattered flux if we multiply I by the solid angle in which scattering occurs. As we have already noted, light is primarily scattered in the forward direction (more precisely, in the region of scattering angles $0 \leqq \beta < \frac{\pi}{2}$).

The solid angle corresponding to these scattering angles is 2π. We thus

have:

$$\Pi = 2\pi I; \quad k = \frac{\Pi}{I_0} = \pi a^2 |\alpha|^2 z^2 \frac{\pi^2}{2},$$

i.e., exactly the formula (8.24) indicated above.(1)

Thus, a sphere consisting of non-interacting dipoles transmits in all directions within the angle 2π as much light as the "volumetric" hole transmits in only the forward direction, on the average. This leads to the fact that the scattering coefficient in the first approximation differs from the value $2\pi a^2$. We have already seen above (Chapters VI and VII) that the scattering coefficient for large spheres, no matter what the material they are made of may be, must equal $2\pi a^2$. This indicates the region of those ρ in which (for a given α) we may apply the method developed here (see the end of § 3).

§ 3. Second Approximation for a Sphere Whose Dimensions are Comparable with the Wavelength

In this section, we shall perform calculations in the second approximation, i.e., we shall take into account terms which are proportional to $|\alpha|^2$ in the field of the scattered wave. We thus confine ourselves to the case of a sphere whose dimensions will be comparable with the wavelength, i.e., $\rho \lesssim 1$.

(a) Effective Field within the sphere. In order to calculate the terms /244
$\sim|\alpha|^2$ in the scattered field, we must take into account the terms $\sim|\alpha|$ in the effective field. In the first approximation, the effective field within the sphere is determined from formula (8.5):

$$E^{(1)}_{\text{eff}} = \text{rot rot}\,\mathcal{J}\,\mathbf{E}_0 - \frac{8\pi}{3}\mathbf{E}_0 e^{-i\mathbf{kr}}. \tag{8.25}$$

Here

$$\mathcal{J} = \int \frac{e^{-i(kR+\mathbf{kr}')}}{R} dv' = a^2 \int \frac{e^{-i(\rho R+\rho\mathbf{r}')}}{R} dv',$$

where $\rho = ka$, $R = |\mathbf{r} - \mathbf{r}'|$ (both points -- the observational point $\mathbf{r}$ and the source $\mathbf{r}'$ -- are located within the sphere).

We can write the second expression for $\mathcal{J}$ in dimensionless coordinates. Integration may be performed over a sphere of unit radius.

Expanding the exponential function in series or employing the series for plane and spherical waves, contained in the integral in $\mathcal{J}$, we find [see

(1) Strictly speaking, we must introduce the factor $\beta 2\pi$, where $0 \leq \beta \leq 1$. However, systematic consideration of the hole "volume" (in contrast to the customary case, each direction is the direction of the disk axis, although it is not parallel to $\mathbf{k}$), which was done above, shows that $\beta = 1$.

(Ref. 110)]:

$$\left.\begin{aligned}
&\mathcal{J} = \sum_{i=1}^{\infty} \mathcal{J}_i \rho^i;\\
&\mathcal{J}_0 = 2\pi\left(1 - \frac{r^2}{3}\right);\\
&\mathcal{J}_1 = -i\frac{4\pi}{3}\left(1 + \cos\theta\,\frac{5r - 3r^3}{19}\right);\\
&\mathcal{J}_2 = -\frac{2\pi}{3}\left\{1 + r^2\frac{4 + 3\cos^2\theta}{10} - r^4\frac{2 + 15\cos^2\theta}{70}\right\};\\
&\mathcal{J}_3 = \frac{22\pi i}{45}\left\{1 - \frac{3}{11}r\cos\theta + \frac{3r^3}{77}\left(2\cos\theta + \frac{5}{2}\cos^3\theta\right) - \right.\\
&\qquad\qquad\left. - \frac{r^5}{11}\left(\frac{\cos\theta}{7} + \frac{5}{6}\cos^3\theta\right)\right\};\\
&\mathcal{J}_4 = \frac{4\pi}{45}\left\{1 - r\cos\theta + r^2\frac{36 - 3\cos^2\theta}{28} + \right.\\
&\quad + r^4\frac{48 + 24\cos^2\theta + 35\cos^4\theta}{336} - \\
&\qquad\qquad\left. - r^6\frac{16 + 60\cos^2\theta + 315\cos^4\theta}{3696}\right\}.
\end{aligned}\right\} \tag{8.26}$$

Let us now calculate the effective field. Let 1 be the unit vector in the direction E_0. In accordance with formula (8.25), we have /245

$$\mathbf{E}_{\text{eff}}^{(1)} = E_0\left\{\nabla(\mathbf{1}\nabla\mathcal{J}) - \mathbf{1}\Delta\mathcal{J} - \mathbf{1}\frac{8\pi}{3}e^{-i\mathbf{kr}}\right\}. \tag{8.27}$$

In the quasistatic case -- i.e., in the case $\lambda \gg a$ -- assuming that $\rho = 0$ and substituting $\mathcal{J}_0$ in (8.27) as $\mathcal{J}$, we find that $\mathbf{E}_{\text{eff}}^{(1)} = 0$. Thus, for very small spheres the effective field within the sphere exactly coincides with the external sphere, since -- if $\mathbf{E}_{\text{eff}}^{(1)} = 0$ -- then $\mathbf{E}_{\text{eff}}^{(2)} = \mathbf{E}_{\text{eff}}^{(3)} = \ldots = 0$. This fact holds only for the effective field, but not for the average field. Its physical meaning consists of the fact that, in the case of long waves, the field of screening charges on the surface exactly compensates for the field produced by polarized elements of the sphere volume. This compensation makes it easier to calculate the successive approximations for the effective field, rather than for the average field. In § 2, it caused us to cease studying the equation (8.1) and to study the solution of equation (8.3) (for the effective field).

By means of the values for $\mathcal{J}_i$ which we calculated, by using formula (8.27), we can readily determine $\mathbf{E}_{\text{eff}}^{(1)}$. Let **i** be the direction of the x-axis, and **k** be the direction of the z-axis. Omitting the factor E_0 (within an accuracy of the terms $\sim\rho^2$), we have

$$\left.\begin{aligned}
&E_{\text{eff}}^{(1)x} = \frac{-8\pi}{15}i\rho z + \frac{4\pi}{3}\rho^2\left(\frac{11}{10} - \frac{23x^2 + 31y^2 + 51z^2}{70}\right) + \ldots\\
&E_{\text{eff}}^{(1)y} = \frac{16\pi\rho^2}{105}xy + \ldots\\
&E_{\text{eff}}^{(1)z} = \frac{4\pi i\rho}{5}x + \frac{2\pi\rho^2}{105}38xz + \ldots
\end{aligned}\right\} \tag{8.28}$$

The terms containing ρ^3 and ρ^4 can be written in a similar way.

(b) Scattered field. In order to calculate E_θ and E_ϕ outside of the sphere, we must first determine the vector $A^{(1)}$:

$$\mathbf{A}^{(1)} = a^3 e^{-ikr} \int \mathbf{E}^{(1)}_{\text{eff}} e^{+ikd} dv'.$$

We have changed to dimensionless coordinates here, and we have replaced $R = |r - r'|$ by $r - d$, where r is the distance from the observational point to the center of the sphere, d -- distance from the source (element of the sphere volume) up to the plane passing through the sphere center and perpendicular to the scattering direction. Calculating $A^{(1)}$, we readily find E_θ and E_ϕ. /246

(c) Scattering Indicatrix. We obtain the following for the scattering intensities

$$\left.\begin{aligned} I_\theta^{(2)} &= \frac{|s|^2}{2}\cos^2\beta f^2(q)\left\{1 + 2\alpha\rho^2\left[\left(m_1 + \mu_1\cos\beta + \right.\right.\right. \\ &\quad \left.\left. + \mu_2\frac{\sin^2\beta}{\cos\beta}\right) - \rho^2\left(\lambda_1 + \lambda_2\cos\beta + \right.\right. \\ &\quad \left.\left.\left. + \lambda_3\sin^2\beta - \lambda_4\frac{\sin^2\beta}{\cos\beta}\right)\right]\right\}; \\ I_\varphi^{(2)} &= \frac{|s|^2}{2} f^2(q)\left\{1 + 2\alpha\rho^2\left[(m_1 + \mu_1\cos\beta) - \right.\right. \\ &\quad \left.\left. - \rho^2(\lambda_1 + \lambda_2\cos\beta - \lambda_3'\sin^2\beta)\right]\right\}. \end{aligned}\right\} \tag{8.29}$$

Here

$$s = \alpha\frac{4\pi^2}{\lambda^2 r} v E_0 e^{-ikr}.$$

The constants contained here have the following values:

$$m_1 = \frac{16\pi}{15} = 3{,}351\ldots;\ \mu_1 = \frac{8\pi}{75} = 0{,}335\ldots;\ \mu_2 = \frac{4\pi}{25} = 0{,}502\ldots$$
$$\lambda_1 = 1{,}428\ldots;\ \lambda_2 = 0{,}460\ldots;\ \lambda_3 = 0{,}0153\ldots$$
$$\lambda_4 = 0{,}0749\ldots;\ \lambda_3' = 0{,}0328\ldots$$

For the total scattering indicatrix (in the case of natural light scattering), we obtain

$$\begin{aligned} I^{(2)}(\beta) &= I^{(1)}(\beta)\left\{1 + 2\alpha\rho^2\left[(m_1 - \lambda_1\rho^2) + \right.\right. \\ &\quad \left.\left. + (\mu_1 - \lambda_2\rho^2)\cos\beta + \mu_2\frac{\sin^2\beta\cos\beta}{1 + \cos^2\beta}\right]\right\}. \end{aligned} \tag{8.30}$$

Here $I^{(1)}(\beta)$ is the indicatrix of the first approximation of (8.20).

We have thus omitted terms containing λ_3, λ_4, λ'_3, since they comprise no more than 2.5% of the terms containing λ_1 and λ_2 (and these latter terms are included in the correction -- the second approximation).

(d) Polarization. We obtain the following for the degree of polarization p:

$$p^{(2)} = p^{(1)}\left\{1 - \frac{4\rho^2 \cos\beta}{1+\cos^2\beta}\left[\mu_2 + \rho^2\left[\lambda_4 - (\lambda_3 + \lambda_3')\cos\beta\right]\right]\right\}. \tag{8.31}$$

Here $p^{(1)}$ is Rayleigh polarization. /247

We should point out that the polarization maximum in the second approximation occurs at $\beta = 90°$, and equals unity. At scattering angles which are less than 90°, the polarization is less than Rayleigh polarization; at larger scattering angles, it is larger than the Rayleigh polarization.

(e) Scattering coefficient. In the second approximation, we obtain the following for the scattering coefficient

$$k_p^{(2)} = \pi a^2 |\alpha|^2 F^{(2)}(z, \alpha), \tag{8.32}$$

where

$$F^{(2)}(z, \alpha) = F^{(1)}(z)\{1 + \alpha z^2 \gamma_1 (1 - \gamma_4 z^2)\}; \ (z = 4\rho).$$

Here $F^{(1)}(z)$ is determined by the formula (8.22), and the constants γ_1 and γ_4 have the following values: $\gamma_1 = 0.4183 \ldots$; $\gamma_4 = 0.02190 \ldots$.

A table of $F^{(2)}(z, \alpha)$ is given in (Ref. 110) (Table 4) for a drop of water in the air ($\alpha = 0.048$).

(f) Accuracy of the simple formulas obtained. In order to determine the accuracy of the formulas obtained, let us compare the computational results based upon these formulas (the calculations are very simple and straightforward) with the calculations based on the Mie formulas.

Blümer (Ref. 56) has tabulated the indicatrix for spheres of ice, assuming that $m = 1.25$, which yields $\alpha = 0.0377$. We have used our formulas to calculate the case $\rho = 0.4$ (case a) and $\rho = 0.8$ (case b).

The results are compared in Table 28, where we present the value of $i(\beta)$.

When compiling Table 28, we corrected the data of Blümer for the numerical error which they contained -- namely, we introduced the factor 1/2 which was erroneously omitted by Blümer (see III, 4).

In the second and fifth columns of Table 28, we have presented the data of Blümer. We have presented the results derived from our calculations for case (a) in the first approximation (i') and in the second approximation (i"), in the third and fourth columns. We have presented the same information for case (b) in the sixth and seventh columns.

In case (a), only two significant digits are given by Blümer for the angles > 20°. The third digit (5) which we give results from dividing by two at certain angles. In order to obtain an accuracy of 1%, in case (a) Blümer

had to take into account four partial oscillations -- two electric oscillations and two magnetic oscillations. Our calculations for this same case were based /248 on formula (8.30), which was simplified by the fact that we omitted the terms $\sim\rho$.[1] Comparing the second and third columns with the first column, we can see that in case (a) the first approximation provides an error of no more than 5%, whereas the simplified calculation of the second approximation leads to an error of no more than 0.8%. Since the divergence between our data and the data of Blümer is smaller than his computational accuracy, there is no point in performing computations with greater accuracy, and it may be assumed that this agreement is quite good.

TABLE 28

	a			b		
β	$10^3\ i_{Be}$	$10^3\ i'$	$10^3\ i''$	$10^2\ i_{Be}$	$10^2\ i'$	$10^2\ i''$
1	2	3	4	5	6	7
0	0,107	0,102	0,107	0,746	0,654	0,733
10	0,105	0,101	0,105	0,732	0,641	0,719
20	0,100	0,096	0,100	0,692	0,607	0,680
30	0,0925	0,089	0,0926	0,632	0,553	0,621
60	0,0645	0,062	0,0646	0,411	0,360	0,404
70	0,057	0,055	0,057	0,352	0,308	0,346
80	0,0515	0,050	0,0519	0,309	0,272	0,305
90	0,0495	0,048	0,0498	0,285	0,252	0,282
100	0,050	0,049	0,050	0,279	0,247	0,275
110	0,054	0,0525	0,054	0,287	0,256	0,285
120	0,060	0,058	0,060	0 308	0,275	0,304
150	0,082	0,080	0,082	0,390	0,349	0,388
160	0,0875	0,085	0,0879	0,412	0,367	0,410
170	0,0915	0,089	0,0917	0,426	0,380	0,424
180	0,093	0,090	0,093	0,431	0,384	0,428

In case (b), the first approximation yields values which are smaller than those of Blümer. The error does not exceed 12%, and its relative magnitude is almost constant. In the second approximation, the deviations from the Blümer calculations do not exceed 2%, and the error is also almost constant.

We should point out that, in order to obtain the requisite accuracy, in /249 this case Blümer had to take into account six partial oscillations.

The situation is the same with the formula for the degree of polarization of scattered light. A comparison of the numerical results shows that the maximum error which it yields in case (d) will be about 3%.

Let us now turn to Figure 71, in which we have compared the data calculated

(1) In the second approximation.

according to formula (8.21) for the scattering coefficient (1) with the curve of Stratton and Houghton (2), and with the Rayleigh curve for a drop of water (3). We can see that our formula for k_p in the first approximation represents k_p for a drop of water in the interval $0 < \rho < 5$, and even in the very worst interval, the relative error does not exceed 20%. This curve qualifies more precisely the considerations presented at the end of the preceding section, with respect to the region of applicability of the formula (8.21) for k_p ($\rho \lesssim 5$).

A comparison with the Rayleigh curve shows that consideration of the interference of the dipole waves, which distinguishes the first approximation from the simple Rayleigh formula, leads to a considerable expansion of the range of applicability of the formula for the scattering coefficient .

In the second approximation, the formula for k_p yields (for $m = \frac{4}{3}$) agreement with the accurate values up to $\rho = 1$ with an error which does not exceed 2%.

(f) Concluding remarks. The formula (8.20) for the indicatrix in the first approximation is usually called the Rocard formula, although it was first obtained by Rayleigh (Ref. 47). It was derived next by Gans (Ref. 112), and five years later (the third time) by Rocard (Ref. 113).

Rocard generalized this formula to polydisperse sol by introducing the following function for particle distribution by size:

$$f(a) = \mu a^2 e^{-\eta a}.$$

He obtained the following for the mean scattering indicatrix:

$$\bar{I} = I_0 |\alpha|^2 \left(\frac{4}{9}\right)^3 8\pi^4 \frac{1}{\lambda^4} \bar{v}^2 \left(\frac{1+\cos^2\beta}{2}\right)\left(\frac{3U^4+13U^2+118}{(1+U^2)^4}\right).$$

Here $\bar{v}$ is the volume of a particle having the mean radius $\bar{a}$ ($\bar{a} = \frac{3}{\eta}$) /250

$$U = \frac{2}{3}\frac{4\pi\bar{a}}{\lambda}\sin\frac{\beta}{2} = \frac{2}{3}\bar{q}.$$

For large particles, the monodisperse indicatrix has a sharply expressed interference nature (see Figure 72, 1). After averaging, the curve smooths out, and the lobes disappear (Figure 72, 2).

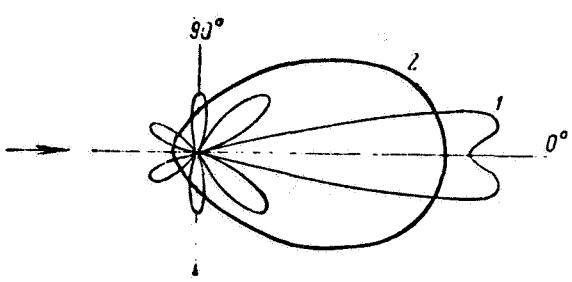

Figure 72. Indicatrix of a Large, Poorly Refracted Particle.
1 -- Monodisperse; 2 -- Average.

If we require an accuracy of 2 - 3% from the formulas, the region of applicability for the Rayleigh-Gans-Rocard formulas for drops of water and bubbles of air in water practically coincide with the region of applicability for the customary Rayleigh formula.

For particles with small values of α, the region of allowed ρ will be larger. It is connected with α by the condition $\frac{k_p}{2\pi a^2} \sim 1$, which yields

$\delta = 2\pi\rho\alpha \gtrsim 1$ or -- replacing $2\pi\alpha$ by $(m - 1)$ -- we find $\delta = (m - 1)\rho \gtrsim 1$.

The quantity δ has a simple physical meaning. It characterizes the change of the light ray phases after they have penetrated the scattering particle (one-half of the phase advance of the central ray).

We have noted previously that the smallness of α is insufficient for the convergence of the method applied here. The convergence of the method will be provided by the smallness of δ. This also follows from an analysis of the second approximation for large ρ. (The quantities $\mathcal{J}$ and A, which are thus encountered, may be calculated according to the stationary phase method). We /251 would like to emphasize the fact that the situation here is similar to the situation we encountered when analyzing the simple Rayleigh formula: the region of applicability for the formula is not determined by the particle dimensions, but by the perturbation which it introduces in the field $(\rho(m - 1))$.

Customarily, the intensity of diffracted light for large particles is considerably greater than the intensity of reflected and refracted light (by a factor of ρ^2). In the case $\delta \simeq 1$ and $\rho \gg 1$, they are both order of magnitude one. This can be readily seen if we set $\cos\frac{\beta}{2} = 1$ and $m \to 1$ in the formulas (5.16) for transmitted light (this is the main bundle here). In this case:

$$\gamma_s(0) = \gamma_p(0) = \frac{a^2}{4}\frac{\rho^0}{2}\frac{1}{(m-1)^2}.$$

In view of $\delta \sim 1$, this means that the factor ρ^2 is included in the intensity. Since both bundles are order of magnitude one, it is impossible to separate both bundles spatially, and the scattering indicatrix may be essentially determined by their interference. As a result, we obtained the picture for intensity distribution of type 1 in Figure 71.

In conclusion, we would like to note that, if the formulas of the first approximation (for geophysical problems) are of little value, the formulas of the second approximation are very useful. If we retain the simplicity inherent in the customary Rayleigh formula, they may be applied to particles which are 3 - 4 times larger than those to which this formula is applied. This is their essential advantage, and in this sense they must be regarded as a generalization of the simple Rayleigh formula.

§ 4. Nonspherical Particles

We have already indicated above that the essential advantage of the method which we have presented here for solving the problem of scattering is its adaptability to particles having an arbitrary form. After spherical particles, particles which are extended and contracted -- rods and disks -- are of the greatest importance. These may be ice prisms and lamellae, small particles of smoke or dust.

We would like to mention that the problem was investigated previously by Gans (Ref. 114) for infinitely small particles. S.V. Cherdyntsev (Ref. 115) /252 made interesting applications and important developments of the Gans formulas

to problems entailed in the theory of hidden images.

Let us investigate the problem in the first approximation, and we shall approximate the rod-like and disk-like particles by ellipsoids of revolution, which are extended and contracted, respectively.[1]

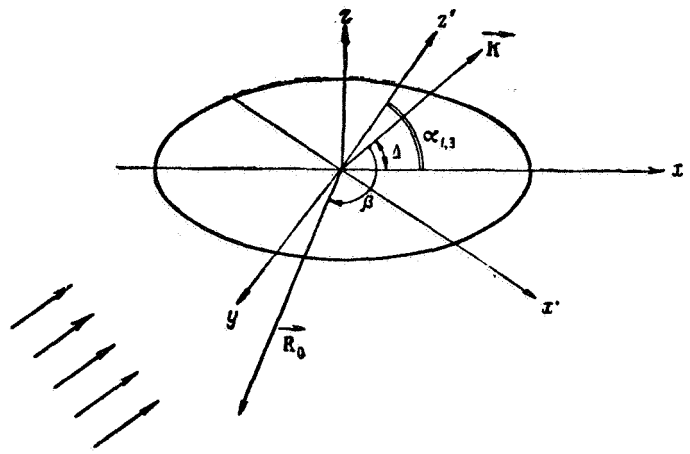

Figure 73. Incidence of a Plane Bundle on an Ellipsoid

(a) *The field scattered by an extended ellipsoid of rotation.* Let us assume that a monochromatic wave which is polarized linearly (Figure 73) falls on an ellipsoid of revolution at an angle Δ from its major axis:

$$\mathbf{E} = \mathbf{E}_0 e^{-i(\mathbf{kr}-\omega t)}.$$

In accordance with § 2, the field scattered by an ellipsoid in a certain direction $\mathbf{R}_0$ may be determined by the following formula

$$\mathbf{E}_{\text{scat}} = \alpha \frac{k^2}{r} \mathbf{E}_{0\perp} f'(\mathbf{R}_0, \Delta).$$

Here we have

$$f'(\mathbf{R}_0, \Delta) = \int e^{-i(\mathbf{kr}+\mathbf{kR})} dv'. \tag{8.33}$$

The latter integral is extended over the ellipsoid. The equation for the ellipsoid will be as follows in the coordinate system related to the axes of symmetry /253

$$\frac{x^2}{a^2} + \frac{y^2+z^2}{b^2} = 1. \tag{8.34}$$

Let a > b (a -- the semimajor axis). In this same coordinate system, the wave vector of an infinite wave **k** has the following components

$$k_x = k\cos\Delta; \quad k_y = 0; \quad k_z = k\sin\Delta,$$

(1) Based on our study (Ref. 124).

and the vector $\mathbf{R}_0$ has the components R_{0x}, R_{0y}, R_{0s}.

Let us change to a new coordinate system. We shall select the plane of the vectors $\mathbf{k}$ and $\mathbf{R}_0$ as the coordinate plane (x', z'). Let the x'-axis bisect the angle between $\mathbf{k}$ and $\mathbf{R}_0$ -- the scattering angle β. In the new coordinate system, the vectors $\mathbf{k}$ and $\mathbf{R}_0$ have the following components

$$k_{x'} = k\cos\frac{\beta}{2};\quad k_{y'} = 0;\quad k_{z'} = k\sin\frac{\beta}{2};$$

$$R_{0x'} = \cos\frac{\beta}{2};\quad R_{0y'} = 0;\quad R_{0z'} = -\sin\frac{\beta}{2}.$$

Let r be the distance from the observational point to the center of the particle. Noting that r >> a, we readily find

$$\mathbf{kr}' + kR = k\left(2z'\sin\frac{\beta}{2} + r\right).$$

We now have

$$f'(\mathbf{R}_0, \Delta) = \int_{z'_{\min}}^{z_{\max}} S(z'_0)\, e^{-ik\left(2z'_0\sin\frac{\beta}{2} + r\right)} dz'_0. \tag{8.35}$$

The quantity $S(z'_0)$ designates the area of an ellipse which is produced by the intersection of our ellipsoid with the plane which is perpendicular to the z'-axis at the point with the coordinate z'_0; $z'_{\min}$ and $z'_{\max}$ -- points at which the ellipsoid surface intersects the axis z'. Let $\alpha_{i,\,k}$ be the matrix of transformation from the new coordinate to the old coordinates:

$$x_i = \alpha_{ik} x'_k.$$

We may readily determine its components, if we compare the value for the components of the vector $\mathbf{k}$ or $\mathbf{R}_0$ in the old and new systems.

From this point on, we only need $\alpha_{1,\,3}$. It can be readily seen that in the case $\beta \neq 0$, we have /254

$$\alpha_{1,3} = \frac{\cos\Delta - R_{0x}}{2\sin\frac{\beta}{2}}. \tag{8.36}$$

We may write the equation for the ellipsoid (8.34) in the following form

$$c^2r^2 - b^2x^2 = c^2b^2.$$

Here

$$r^2 = x^2 + y^2 + z^2, \text{ and } \quad c^2 = \frac{a^2b^2}{a^2 - b^2}.$$

In the new coordinates, the ellipsoid equation will be

$$x'^2e^2 + y'^2g^2 + z'^2f^2 - 2mx'y' - 2nx'z' - 2ly'z' = 1, \tag{8.37}$$

where e, g, f, m, n, ℓ are the constants which may be readily determined. For

example, we have

$$f^2 = \frac{c^2 - \alpha_{1,3} b^2}{c^2 b^2}.$$

Assuming in (8.37)

$$x = y = 0,$$

we obtain

$$z'_{\min} = -\frac{1}{f}, \quad z'_{\max} = \frac{1}{f}.$$

Assuming $z' = z'_0$ in the equation for the ellipsoid (8.37), we obtain the equation for an ellipse whose area $S(z_0)$ must be determined. This equation will be

$$x'^2 e^2 + y'^2 g^2 - 2mx'y' - 2nz'_0 x' - 2lz'_0 y' + z'^2_0 f^2 - 1 = 0.$$

After simple transformations, we obtain

$$S(z'_0) = \frac{\pi}{(e^2 g^2 - m^2)^{3/2}} \{[f^2 (e^2 g^2 - m^2) - n(ng^2 + me) - \\ - l(e^2 l + mn)] z'^2_0 - (e^2 g^2 - m^2)\}.$$

Substituting the corresponding values of the coefficients e, g, f, m, ℓ and n, we readily obtain

$$S(z'_0) = \pi M^2 \{1 - L^2 z'^2_0\}.$$

Here we have /255

$$M^2 = \frac{cb^2}{\sqrt{c^2 - b^2(1 - \alpha^2_{1,3})}}; \quad L^2 = \frac{c^2 - b^2}{b^2[c^2 - b^2(1 - \alpha^2_{1,3})]}.$$

The integral (8.35) may be now readily calculated.

Substituting it in (8.33) and eliminating all the time notation, we obtain

$$\mathbf{E}_p = \alpha \mathbf{E}_{0\perp} \frac{k^2}{r} e^{-ikr} \cdot v \cdot F(\Delta, \beta). \tag{8.38}$$

Here $v = \frac{4}{3}\pi ab^2$ is the volume of the ellipsoid.

$$F = \frac{3}{q^3}\left[\frac{1 - \varepsilon^2}{1 - \varepsilon^2 + \alpha^2_{1,3}(1 - \alpha^2_{1,3})\varepsilon^4}\right]^{3/2} \times \\ \times \left\{\left[1 + q^2 \frac{\alpha^2_{1,3}(1 - \alpha^2_{1,3})\varepsilon^4}{2(1 - \varepsilon^2)}\right] \sin q - q \cos q\right\}; \tag{8.39}$$

where ε is the eccentricity of the ellipsoid, and

$$q = \frac{4\pi b}{\lambda} \frac{1}{\sqrt{1 - \alpha^2_{1,3}\varepsilon^2}} \sin\frac{\beta}{2} \tag{8.40}$$

In the case $\varepsilon \to 0$, our field changes into a field which is scattered by a

sphere (8.14). For finite ε, the amplitude of the scattered field depends not only on the scattering angle β, but also on the orientation of the ellipsoid in space. We should recall that $\alpha_{1,3}$ depends on Δ:

$$\alpha_{1,3} = \frac{\cos\Delta - \cos\gamma}{2\sin\frac{\beta}{2}}.$$

Here we have

$$\cos\gamma = R_{0\omega}.$$

We would like to point that for given β and Δ the angle γ cannot assume any values. It may be readily seen that we always have

$$\beta - \Delta \leqslant \gamma \leqslant \beta + \Delta.$$

This coincides with the fact that $\alpha_{1,3} \leqq 1$.

Let us investigate the limiting form of formulas (8.38) and (8.39) in the case of particles which are almost spherical, i.e., assuming that $\varepsilon \ll 1$.

Retaining the terms $\sim \varepsilon^2$ in F, we have the following in this case /256

$$F = \frac{3}{q^3}(\sin q - q\cos q).$$

Outwardly, the formula coincides with the corresponding formula for the sphere. However, q depends not only on β, but also on Δ.

Namely, we have

$$q = q_0(1 + S\varepsilon^2), \tag{8.41}$$

where

$$S = \frac{3\alpha_{1,3}^2 - 1}{6}, \quad q_0 = \frac{4\pi a^*}{\lambda}\sin\frac{\beta}{2}; \quad a^* = \sqrt[3]{\frac{3v}{4\pi}}.$$

Here a* is the radius of the equivalent sphere.[1]

Taking into account (8.40), we have the following for F

$$F = F_0(1 + S\varphi\varepsilon^2), \tag{8.42}$$

where

$$F_0 = \frac{3}{q_0^3}(\sin q_0 - q_0\cos q_0) = f(q_0);$$

$$\varphi = \frac{q_0^2\sin q_0}{\sin q_0 - q_0\cos q_0} - 3q_0.$$

Let us now examine another limiting case of our formulas (8.39) and (8.40) -- the case of a greatly extended rod.

Let the major axis of our ellipsoid be m times greater than the minor axis.

---

[1] A sphere with a volume which equals the volume of the ellipsoid under consideration.

We may readily assume that in the case m >> 1 we have

$$\left.\begin{aligned} F &= \frac{3}{q^3}\left[\frac{1}{1+m^2\alpha_{1,3}^2(1-\alpha_{1,3}^2)}\right]^{3/2}\left\{\left[1+m^2q^2\frac{\alpha_{1,3}^2(1-\alpha_{1,3}^2)}{2}\right]\times\right. \\ &\qquad \left.\times\sin q - q\cos q\right\}; \\ q &= q_0\frac{1}{\sqrt{m}\cdot\sqrt{1-\alpha_{1,3}^2}}. \end{aligned}\right\} \tag{8.43}$$

For $\alpha_{1,3}$ which is not close to zero or one, and for q which equals zero, we obtain

$$F = \frac{3}{2m^{3/2}q_0\cdot\alpha_{1,3}}\sin\frac{q_0}{\sqrt{m}\cdot\sqrt{1-\alpha_{1,3}^2}}. \tag{8.44}$$

In order to illustrate the formulas which we have derived, we have calculated the scattering indicatrix for an ellipsoid in which the major axis is ten times greater than the minor axis, and $\frac{2\pi q^*}{\lambda} = 1$. The light falls along the major axis. In this case we have /257

$$\alpha_{1,3} = \sin\frac{\beta}{2}; \quad q = \frac{2}{\sqrt[3]{10}}\operatorname{tg}\frac{\beta}{2}.$$

The dependence of the intensity of light scattered at the angle β on the quantity β is shown in Figure 74 a. We may see that our ellipsoid primarily scatters light forward.

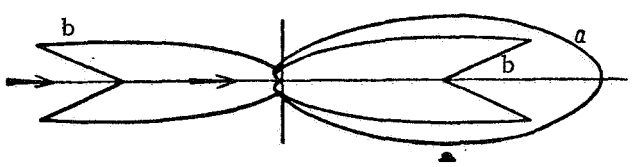

Figure 74. Indicatrixes of Non-Spherical Particles.

Figure 74 b shows the indicatrix of the same ellipsoid in the plane passing through the major axis of the ellipsoid, and the incident ray, when light falls across the axis. In this case, we have

$$\alpha_{1,3} = \cos\frac{\beta}{2} \text{ and } q = \frac{2}{\sqrt[3]{10}}.$$

(There is no axis of symmetry here, and therefore we must consider the plane in which the indicatrix is calculated.)

In the first approximation which is considered here, polarization of scattered light is determined by the Rayleigh formula. This is valid for particles having an aribtrary form.

(b) *Case of a small, extended particle.* Let us make a detailed investigation of a small particle, i.e., the case where

$$\frac{2\pi a^*}{\lambda} \ll 1.$$

In this case, we have

$$F = \left[\frac{1-\varepsilon^2}{1-\varepsilon^2+\alpha_{1,3}^2(1-\alpha_{1,3}^2)\varepsilon^4}\right]^{3/2}\left\{1+\frac{3}{2}\frac{\alpha_{1,3}^2(1-\alpha_{1,3}^2)\varepsilon^4}{1-\varepsilon^2}\right\}. \tag{8.45}$$

Thus, the dependence on the scattering angle is only given here in terms of $\alpha_{1,3}$. /258

Let us illustrate this case by means of an example. Let us set $\varepsilon = 0.9$, which corresponds to a particle in which the long axis is 2.3 times larger than the short axis. Let the light fall along the long axis ($\Delta = 0$). In this case, the scattering indicatrix of natural light will have an axis of symmetry. This is the axis of the ellipsoid. Thus, $\alpha_{1\ 3} = \sin\frac{\beta}{2}$. The scattering indicatrix is shown in Figure 75 (curve 2).

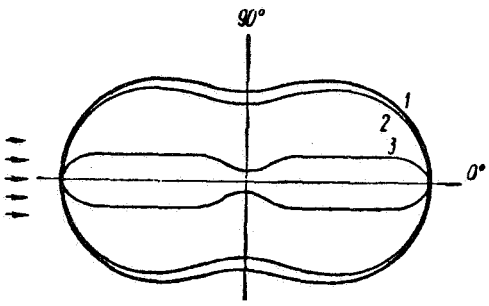

Figure 75. "Stability" of the Rayleigh Indicatrix.

For purposes of comparison, the same figure gives the Rayleigh indicatrix (curve 1). We can see that there is a certain difference only for β which are close to 90°. The stability of the Rayleigh scattering indicatrix toward changes in the form of the scattering particle is a very important fact. In the case of contractions by a factor of 2-3, the scattering indicatrix of a small particle barely changes.

If the light is oblique to the axis, the indicatrix will not have an axis of symmetry. Let us select the vector **k** as the polar axis, and we shall direct the ellipsoid axis along the x-axis. It may be readily seen that

$$\alpha_{1,3} = \cos\varphi \cdot \cos\frac{\beta}{2}, \tag{8.46}$$

where ϕ is the angle formed by the planes (x, k) and ($\mathbf{R}_0$, **k**) -- (longitude). In the case $\phi = 0$ -- i.e., if $\mathbf{R}_0$ lies in the plane (x, **K**) -- the indicatrix exactly coincides with that investigated previously.

It is thus found that in this plane the ellipsoid of rotation by 90° does not change the intensity distribution. This will not be the case in other planes. The corresponding indicatrix may be readily calculated according to formula (8.45), with allowance for the values for $\alpha_{1,3}$ in the plane under consideration [determined according to formula (8.46)]. /259

If we contract our ellipsoid, its indicatrix will also be extended, and for greatly extended particles it will differ considerably from the Rayleigh indicatrix.

Curve 3 in Figure 75 corresponds to the case when the major axis is 10 times longer than the minor axis, and $\Delta = 0$.

(c) *The "average" indicatrix for different orientations.* In the atmosphere, we are dealing with a scattering indicatrix which is averaged over a large number of particles which have random distribution.

Let the dimensions and form of our particles be absolutely the same. We shall also assume that the distribution of the particles in space is absolutely random. The following important problem then arises: can we attribute such an averaged indicatrix to a spherical partical having a certain radius, and what must this radius be.

In order to solve this problem, we must average the indicatrix over all possible orientations of the ellipsoid in space, assuming that the direction of the initial bundle and the scattering direction are fixed.

Let us examine the case of a particle which is almost spherical.

In accordance with (8.42), we find that for $\varepsilon \ll 1$, the scattering indicatrix will be

$$I = I_0(1 + 2\,S\varphi\varepsilon^2),$$

where I_0 is the scattering indicatrix of the sphere.

Let us assume that our ellipsoid occupies arbitrary positions in space, i.e., the apex of its major axis is uniformly displaced over the sphere. Our $\mathbf{k}$ and $\mathbf{R}_0$ directions are fixed. Therefore, the direction OZ', lying in the plane of the vectors $\mathbf{k}$ and $\mathbf{R}_0$ and perpendicular to the bissectrix of the angle between them, will also be fixed. We shall choose it as the polar axis. In this case, $\alpha_{1,\,3} = \cos\theta$, where θ is the angle between the ellipsoid axis and OZ'.

We thus have /260

$$\overline{\alpha_{1,3}^2} = \frac{1}{4\pi}\int_0^{2\pi} d\varphi \int_0^{\pi} \cos^2\theta \sin\theta\, d\theta = \frac{1}{3}.$$

Consequently,

$$\bar{S} = 0 \text{ and } q = q_0,\ F = F_0.$$

Thus, for small ε, the ellipsoid indicatrix, averaged over its different spatial orientations, coincides with the indicatrix of a sphere having the same volume.[1]

Let us now study the averaged indicatrix for small particles, but with any ε. In accordance with (8.45), we must average the expression

$$F^2(\varepsilon) = \frac{\left(1 + \frac{3}{2}\,\frac{\alpha_{1,3}^2(1-\alpha_{1,3}^2)\,\varepsilon^4}{1-\varepsilon^2}\right)^2}{\left(1 + \frac{\alpha_{1,3}^2(1-\alpha_{1,3}^2)\,\varepsilon^4}{1-\varepsilon^2}\right)^3}.$$

(1) Within an accuracy of terms $\sim \varepsilon^4$.

Just as previously, selecting the oz'-axis as the polar axis, we readily find that

$$\overline{F^2} = \frac{1}{2}\int_{-\pi}^{\pi} \frac{\left(1+\frac{3}{2}\lambda\cos^2\theta\sin^2\theta\right)^2}{(1+\lambda\cos^2\theta\sin^2\theta)^3}\sin\theta\, d\theta = \varphi(\lambda);$$

$$\lambda = \frac{\varepsilon^4}{1-\varepsilon^2}.$$

This integral may be readily calculated

$$\varphi(\lambda) = \frac{1}{32(\lambda+4)^2}\Big\{-(43\lambda+148)+ \\ +\frac{1}{2\sqrt{\lambda^2+4\lambda}}(A_\lambda - c_2^2 B_\lambda)\cdot\frac{2}{c_2}\operatorname{arc\,tg}\frac{1}{c_2}+ \\ +(A_\lambda + c_1^2 B_\lambda)\frac{1}{c_1}\ln\frac{c_1+1}{c_1-1}\Big]\Big\}, \tag{8.47}$$

where

$$A_\lambda = 41\lambda^3 + 363\lambda + 660; \quad B_\lambda = 21\lambda^2 + 72\lambda;$$

$$c_1^2 = \frac{\sqrt{\lambda+4}+\sqrt{\lambda}}{2\sqrt{\lambda}}; \; c_2^2 = \frac{\sqrt{\lambda+4}-\sqrt{\lambda}}{2\sqrt{\lambda}}.$$

Thus, for a small rod-like particle, the indicatrix averaged over its different orientations coincides with the indicatrix of a sphere whose volume is /261

$$v^* = \sqrt{\varphi(\varepsilon)}\, v, \tag{8.48}$$

where v is the volume of the particle. In the case $\lambda \to 0$, in accordance with the result obtained previously for particles with small ε, $\phi \to 1$.

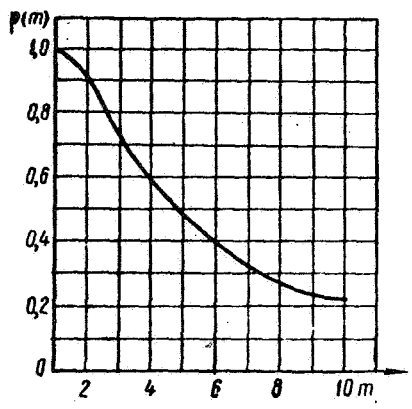

Figure 76. Graph of $\phi(m)$.

TABLE 29

λ	m	ε	$\varphi(\lambda)$
0	1.00	0.00	1,00
1	1,62	0,79	0,98
2	1,93	0,85	0,94
3	2,19	0,89	0,90
4	2,41	0,91	0,84
5	2,62	0,93	0,80
8	3,14	0,95	0,72
12	3,73	0,96	0,61
16	4,24	0,97	0,56
20	4,68	0,98	0,51
30	5,66	0,98	0,42
40	6,48	0,99	0,36
50	7,21	0,99	0,31
100	10,10	1,00	0,23

The formula for $\phi(\lambda)$ is very cumbersome. We have compiled a table of $\phi(\lambda)$ (Table 29). Let us introduce the quantity m -- the ratio between the ellipsoid major axis and its minor axis:

$$m = \frac{a}{b} = \frac{\sqrt{\lambda+4}+\sqrt{\lambda}}{2}.$$

Figure 76 shows the dependence of the effect under consideration on m.

(d) *Scattering of disk-like particles.* Let us now study the scattering of light by very oblate particles, such as tablets.

We shall approximately represent such particles as ellipsoids of revolution whose transverse axis is greater than the axis of rotation. The calculations in section (a) are fully applicable. We now have a < b, and we must introduce the eccentricity of the tablet ε^* in the final formulas (8.39) and (8.40), instead of the ε introduced previously. We may determine the eccentricity ε^* /262
according to the formula

$$\varepsilon^{*2} = \frac{b^2 - a^2}{b^2}, \tag{8.49}$$

The quantity ε may be expressed by means of ε^*:

$$\varepsilon^2 = \frac{-\varepsilon^{*2}}{1-\varepsilon^{*2}}.$$

Consequently, we have

$$\frac{\varepsilon^4}{1-\varepsilon^2} = \frac{\varepsilon^{*4}}{1-\varepsilon^{*2}}$$

and

$$q = \frac{4\pi a}{\lambda} \frac{\sin\frac{\beta}{2}}{\sqrt{1-\varepsilon^{*2}(1-\alpha_{1,3}^2)}}. \tag{8.50}$$

Here $\alpha_{1,\ 3}$, just as previously, depende on Δ, where Δ is the angle between the direction of the primary bundle and the axis of symmetry a. The minor axis of the ellipsoid is again contained in q -- this time this is the axis of symmetry a. The quantity F may be determined by the same formula, if ε is replaced by ε^*.

For the case of particles which are almost spherical -- i.e., for $\varepsilon^* \ll 1$ -- we obtain the same formulas (8.41) and (8.42) as previously. The quantity S which is contained in the formula (8.42) must now be replaced by the quantity S*:

$$S^* = \frac{1-3\alpha_{1,3}^2}{6},$$

i.e., S = -S*. The quantity q_0 may be determined as follows:

$$q_0 = \frac{4\pi}{\lambda}\sqrt{\frac{3v}{4\pi}}\sin\frac{\beta}{2}.$$

For very oblate particles, assuming that $m = \frac{b}{a} \gg 1$, we find that F may be expressed by the same formula (8.43), but

$$q = q_0 \frac{1}{\sqrt{m}\cdot\alpha_{1,3}}.$$

In order to illustrate the formulas derived here, let us investigate the scattering indicatrix of light for a particle whose transverse axis is 10 times greater than the axis of symmetry (m = 10).

Let us set /263

$$\frac{2\pi}{\lambda} a^* = 1 \quad \left(a^* = \sqrt[3]{\frac{3v}{4\pi}}\right)$$

and let the light fall along the axis of symmetry.

In this case, we have

$$\alpha_{1,3} = \sin\frac{\beta}{2}$$

and

$$q = \frac{4\pi a}{\lambda} = \frac{2}{\sqrt[3]{10}}.$$

Figure 74 b presents the graphs of the indicatrix.

If light now falls across the axis of symmetry on the same particle, we have the following for the directions lying in the plane of the incident ray and the axis of symmetry

$$\alpha_{1,3} = \cos\frac{\beta}{2} \text{ and } q = \frac{4\pi a}{\lambda}\operatorname{tg}\frac{\beta}{2} = \frac{2}{\sqrt[3]{10}}\operatorname{tg}\frac{\beta}{2}.$$

A graph of this indicatrix is presented in Figure 74 a.

We can see that a greatly contracted particle has a behavior which is just the opposite of that for a greatly extended rod (Figure 74 b corresponds to a scattering indicatrix of light oblique to the axis of symmetry, and Figure 74 a corresponds to light falling along it). We should point out that this contradictions occurs for very large particles. Small oblate particles, i.e., those for which

$$\frac{2\pi}{\lambda} a^* \ll 1,$$

scatter in exactly the same way as small extended rods. Formula (8.45) and also all the statements in (b) are fully applicable to them.

Everything that was stated in (c) regarding the average indicatrix of rods having a random distribution also holds when averaging oblate particles having a random distribution. For small eccentricities, the averaged indicatrix of a slightly oblate particle coincides with the indicatrix for a sphere having the same volume.

The averaged indicatrix of a small, but arbitrarily oblate, particle coincides with the indicatrix of a sphere whose volume is $\sqrt{\phi(\varepsilon)}$ times greater than the particle volume.

F. P. Polatbekov (Ref. 116) recently made an experimental investigation /264
of light scattering by particles having a non-spherical form (hydrosols of clay). The particles which he examined had an effective size which was considerably larger than the Rayleigh size. The reader may find the numerical data and curves in his work.

§ 5. Scattering Coherence

When studying light which is scattered by a transparent colloid system, one usually assumes that the intensity of light observed at a certain point I is the sum of the intensities produced here by each element of turbidity in the illuminated volume (I_j):

$$I = \sum_j I_j.$$

If the distance to the observational point is considerably greater than the linear dimensions of the illuminated volume, this sum changes simply into NI_0, where N is the number of particles, and I_0 is the intensity scattered in a given direction by one particle. It is apparent that, if the mean distances ℓ between the particles are small as compared with the length of the scattered wave λ, the interference of light scattered by individual particles can be of great importance. The interference part in the scattered bundle, for sufficiently small ℓ/λ, can even be considerably greater than the non-interference part.

Considerable difficulties are entailed in a general examination of the problem. As we have already noted in the introduction, L. I. Mandel'shtam (Ref. 1) has advanced the principal concepts pertaining to the circle of problems under consideration. Together with the problem of elementary scattering, consideration of the "plurality" of scattering makes up the total content of the optics of turbid media in general. Fortunately, in the cases which are important in practice we have only had to search for corrections in the case of large ℓ/λ (see 1.3). In one case, however, it was possible to study any ratios of ℓ/λ. This is the case of transparent systems.

The problem of this section (Ref. 128) is to investigate the coherence during scattering by a transparent system, employing the approximation method developed in § 1. In transparent systems, we can confine ourselves to the first approximation; we shall thus assume that the field within the system coincides with the external fields. Let us derive the inequalities determining the /265 conditions under which non-coherent or coherent scattering will prevail.

The total electromagnetic field produced by all the particles at the observational point, which is located rather far from the volume being illuminated, will be

$$\mathbf{E} = \mathbf{E}_0 \sum_j e^{ik(\mathbf{k}_0 - \mathbf{R}_0, \mathbf{r}_j)}.$$

Here $\mathbf{E}_0$ is the field produced by a particle located at the origin of the coordinate system; $k\mathbf{K}_0$ -- the wave vector of the incident radiation; $\mathbf{r}_j$ -- the radius vector of the $j^{\underline{th}}$ particle ; $\mathbf{R}_0$ -- unit vector directed to the observational point.

We thus obtain the following for the intensity:

$$I = I_0 \sum_{j,l} e^{ik(\mathbf{k}_0 - \mathbf{R}_0, \mathbf{r}_j - \mathbf{r}_l)}.$$

Separating the terms with j = ℓ in this double sum, we have

$$I = NI_0\left\{1 + \frac{1}{N}\sum_{j \neq l} e^{ik(\mathbf{k}_0 - \mathbf{R}_0, \mathbf{r}_j - \mathbf{r}_l)}\right\}. \tag{8.51}$$

The double sum with J ≠ ℓ is a quantitative measure of the interference part in the scattered bundle. It is usually assumed that the sum equals zero, due to the fact that the particles have a completely random distribution in the volume. However, if the closest neighbors of the given particle are located at distances which are considerably less than λ, the phases of the waves emitted by several particles will differ very little from each other. The problem may be reduced to summing the emissions of the volume elements of a quasi-solid body, along which the phases of the emitted waves will change uniformly. Consequently, the sum of the corresponding expressions in (8.51) will not equal zero.

The total intensity, which can be recorded by an instrument, is the result of averaging the expression (8.51) over all possible arrangements of the particles in the system.

Since the mean value of a term in the sum is the same for different pairs of (j, ℓ), we have

$$\overline{\sum_{j \neq l} e^{ik(\mathbf{k}_0 - \mathbf{R}_0, \mathbf{r}_j - \mathbf{r}_l)}} = N(N-1)\overline{e^{ik(\mathbf{k}_0 - \mathbf{R}_0, \mathbf{r}_j - \mathbf{r}_l)}}.$$

Designating the mean exponential term by τ, we readily find that /266

$$\tau = \int_v \frac{dv_j}{v} \int_{v'} \frac{dv_l}{v} e^{ik(\mathbf{k}_0 - \mathbf{R}_0, \mathbf{r}_j - \mathbf{r}_l)}. \tag{8.52}$$

Here v is the entire volume to be illuminated, and v' is this same volume from which a sphere having the radius 2a is cut out (a -- radius of the particles). This sphere lies around the center of the j<u>th</u> particle, within which the center of the ℓ<u>th</u> particle cannot penetrate. When writing formula (8.52), we also assumed that all positions of the two particles within a given volume are equally probable, and that the probability for the j<u>th</u> particle to be located in an element of the volume dv_j, and for a ℓ<u>th</u> particle to be located at dv_ℓ at the same time, is simply

$$\frac{dv_j}{v} \cdot \frac{dv_l}{v}.$$

We shall assume that the volume occupied by the particles has the form of a sphere with the radius R. We shall represent the double integral in (8.52) in the form of the difference of the two integrals. In this first case, integration is performed twice over the entire volume v, and in the second case, inner integration is extended over the sphere having the radius 2a. Outer integration is extended over the volume v. We now readily obtain the following (see VIII, 1):

$$\tau = f^2(q) - 8\frac{v_0}{v} f(q'). \tag{8.53}$$

Here

$$q = \frac{4\pi R}{\lambda} \sin\frac{\beta}{2}; \quad q' = 2 \cdot \frac{4\pi a}{\lambda} \sin\frac{\beta}{2},$$

where $\beta = (\widehat{\mathbf{k}_0, \mathbf{R}_0})$ is the scattering angle, and v_0 is the volume of the particle:

$$f(x) = \frac{3}{x^3}(\sin x - x\cos x).$$

For the scattered intensity, we now obtain

$$I = NI_0\left\{1 - \frac{8Nv_0}{v} f(q')\left[1 - \frac{v}{8v_0}\frac{f^2(q)}{f(q')}\right]\right\}. \tag{8.54}$$

This formula provides a solution of the problem which we formulated regarding the derivation of a relationship describing both types of scattering. The first component in the parentheses (unity) corresponds to non-coherent scattering, and the second component corresponds to coherent scattering.

Formula (8.54) pertains to the case of transparent systems. /267

In order to analyze formula (8.54), we shoule note that $f(x) \to 1$ in the case $x \to 0$. Since we have $\lambda > \ell$, and ℓ is always greater than a, this means that $q' \ll 1$ and $f(q') \simeq 1$.

Let us set $\frac{Nv_0}{v} = \delta$. This is the relative portion of the volume occupied by the substance. We now obtain

$$I = NI_0\left\{1 - 8\delta\left[1 - \frac{N}{8\delta} f^2(q)\right]\right\}. \tag{8.55}$$

We should note that usually $\delta \ll 1$. In this case, we obtain

$$I = NI_0\{1 + Nf^2(q)\}. \tag{8.56}$$

Let us study the formula (8.56) in greater detail.

Let us first turn to the case $\beta = 0$, i.e., to scattering in the forward direction. For $\beta = 0$, $q = 0$ and $f(q) = 1$. Here

$$I = NI_0\{1 + N\}.$$

Since $N \gg 1$ always holds, then

$$I = N^2 I_0. \tag{8.57}$$

In the forward direction, the phases of the fields for all particles are the same, and the total scattered field has a factor N and the intensity has the factor N^2. The combination of the fields in the forward direction causes the Mie effect. We can see that strong forward scattering occurs not only for a solid body, but also for a system of particles.

Let us now study the case $\beta \neq 0$.

We should note that customarily $R \gg \lambda$, i.e., $q \gg 1$. We thus have

$$f^2(q) \sim \frac{9}{q^4}\cos^2 q.$$

For large q, relatively insignificant changes in q lead to great changes in $\cos^2 q$. Therefore, the values observed experimentally actually represent the result of averaging $\cos^2 q$ over relatively small changes in q. Since $\overline{\cos^2 q} = \frac{1}{2}$, then $f^2(q) \sim \frac{9}{2q^4}$. Let us designate the component in (8.56) by η:

$$\eta = Nf^2(q).$$

Assuming that $\sin \frac{\beta}{2} \simeq 1$, we readily find that the quantity η has the following order: /268

$$\eta \simeq 0{,}75 \cdot 10^{-8} \frac{\lambda^4}{R l^3}. \tag{8.58}$$

The numerical value of η, which may be determined by the specific experimental conditions, yields the ratio of the coherent part of the scattered intensity to the non-coherent part of the scattered intensity. If $\frac{\lambda}{\ell} \leq 1$, then $\eta \ll 1$. Here $I = NI_0$ is non-coherent scattering. If $\eta \simeq 1$, we must retain both terms in formula (8.56). If $\frac{\lambda}{\ell} \gg 1$, ($\eta \gg 1$), the scattering will be coherent, and its intensity may be determined by the formula

$$I = N^2 f^2(q) I_0. \tag{8.59}$$

Another form may be attributed to the latter formula. In the case which we are considering, due to $\ell > a$, $\lambda > \ell$, we can always apply the Rayleigh formula for scattering by an individual rod, since here $\lambda \gg a$. We thus have

$$I_0 = \frac{16\pi^4}{\lambda^4} \left| \frac{m^2 - 1}{m^2 + 2} \right|^2 a^6 \frac{(1 + \cos^2 \beta)}{2}.$$

Here m is the relative (complex) index of refraction of a suspended rod. Substituting I_0 in (8.59), and noting that

$$\frac{N}{v} a^3 \left(\frac{m^2 - 1}{m^2 + 2} \right) = \mu \simeq \alpha$$

is the dipole moment of a unit volume of the suspended particles, we readily obtain

$$I = |\alpha|^2 \frac{16\pi^4}{\lambda^4} v^2 f^2(q) \frac{(1 + \cos^2 \beta)}{2}. \tag{8.60}$$

This formula coincides with the formula for intensity which we obtained previously (8.20). This means that scattering of waves with $\lambda \gg \ell$ from a system can be simply regarded as scattering from a solid, macroscopic body, whose dielectric constant is determined by the suspended particles. Since we are considering the case of transparent systems, the formula which we obtained for intensity coincides with the formula for intensity during light scattering, /269 which was obtained in § 2.[1]

---

(1) If we wish to consider the influence of the basic substance, we must substitute $(\mu_1 + \mu_2)$ in (8.60), instead of μ, where μ_1 pertains to suspended particles, and μ_2 pertains to the basic substance.

The quantity η is small in the case of scattering of infrared radiation by particles of an admixture. Thus, the correction for coherence is unimportant here.

The effect considered is important for transparent colloid systems.

Let us discuss two points: (a) distribution of light which is scattered by a system at small angles forward ($\beta \sim \frac{\lambda}{2\pi R}$); (b) deformation of the scattering indicatrix, caused by the scattering coherence.

Let us assume that we have a conglomeration of very small particles ($a \ll \lambda$), forming a particle with the radius R -- for example, a conglomeration of such a type was studied experimentally by L. M. Moroz and Ya. I. Frenkel' (Ref. 20).

(a) We readily see from formula (8.56) that the intensity of light scattered by the system (conglomeration with the radius R) at the angles $\beta \sim \frac{\lambda}{2\pi R}$ will be $I = I_0 N^2 f^2(q)$, where $q = \frac{2\pi R}{\lambda}\beta$ is a quantity on the order of unity. If our system is a solid particle with the radius R -- more precisely, if we are considering the deviation of its inner field from the incident wave field, then the intensity distribution may be determined by the diffraction formula (see VI, 2). Figure 77 shows this curve by a solid line; our curve is shown by a dashed line. In the direction

$$\beta_i = \frac{q_i}{\frac{2\pi R}{\lambda}},$$

where q_i are zeros of the function $f(q)$, the scattering intensity vanishes. We find from (8.15) that q_i coincides with the roots of the equation $\operatorname{tg} x = x$. It is known that these roots are $x_1 = 4.49 \ldots$, $x_2 = 7.72 \ldots$, $x_3 = 10.90 \ldots$, while the zeros of the diffraction picture lie at $x_1 = 3.83 \ldots$, $x_2 = 7.02 \ldots$, $x_3 = 10.17 \ldots$, i.e., they are somewhat displaced.

(b) When the effect which we are considering (scattering coherence) is significant, the scattering indicatrix will be a Rayleigh indicatrix. Thus, /270
for a conglomeration with $R = 5\lambda$ and $N = 10$ we find ($\lambda = 0.5\mu$) that the deviation from the Rayleigh curve will be 3% for an angle of 10°. For smaller angles, the deviations from the Rayleigh curve rapidly increase. The relative error in the forward direction amounts to N. For angles which are greater than 10°, the deviations from the Rayleigh curve will be small.

Thus, the theory which we have developed is important for describing the picture of scattering by a colloid system (a conglomeration of particles) at small angles in the forward direction. We must emphasize the fact that the phenomena we have noted increase with an increase in the ratio λ/ℓ.

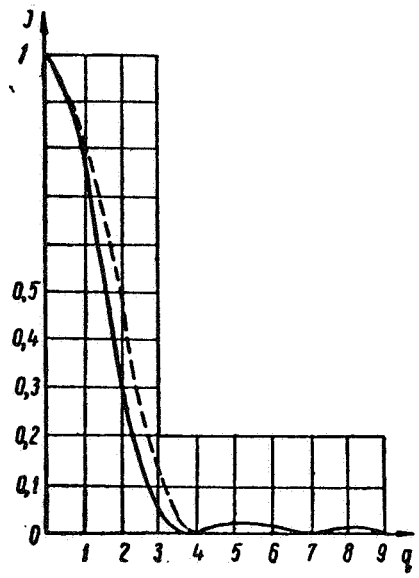

Figure 77.

Let us formulate the basic analysis result. The general formula (8.54) which we have obtained for the intensity of the scattered field correctly describes both limiting cases $\frac{\ell}{\lambda} \to \infty$ and $\frac{\ell}{\lambda} \to 0$ for a transparent system. It also enables us to calculate the scattering intensity in the intermediate region of values for $\ell/\lambda \left(\frac{\ell}{\lambda} \sim 1\right)$, and to study the change from one limiting case to another.

A dispersed system, such as a solid body, whose complex index of refraction is determined by suspended particles, was studied previously in the works of T. P. Kravets (Ref. 117) and Maxwell-Garnett (Ref. 118). T. P. Kravets investigated the customary solutions, and Maxwell-Garnett investigated colloid systems. In colloid optics, the work of Mie is sometimes compared to the work of Maxwell-Garnett. Such a comparison is incorrect. We have investigated different aspects of the scattering phenomenon.

The method of the "solid body" is the correct limiting case which is valid for small ℓ/λ (and, consequently, for small particles). Our analysis has constructed a bridge between both methods, and has established a region of applicability for non-coherent scattering, assumed in the calculations of Mie, and /271 for the coherent scattering of T. P. Kravets and Maxwell-Garnett (for the case of transparent systems).

Let us now turn to the second approximation, and let us study the field change when it is extended within the system, in the sense of a "solid body" system.

The electric field within the sol differs from the external field by the field which is produced by the sol particles which are electrically excited.

The dipole moment which one particle acquires will be (4.3):

$$\mathbf{p} = \frac{c_1}{k_a^3} \mathbf{E}'.$$

Here E' is the field which influences the particle.(1) If the number of particles per unit volume is n, we obtain the following in the customary way for the dielectric constant:

(1) Strictly speaking, we must select the effective field as E'. In the approximation under consideration, it does not differ from the mean field.

$$\varepsilon = \varepsilon_0\left(1 + 4\pi c_1 \frac{n}{k_a^3}\right).$$

Let us introduce the complex index of refraction of a turbid medium m and the index of absorption in this medium κ. The complex refractive index for a pure "solvent" is assumed to equal unity.

Since the coefficient c_1 is a complex number, this means that our medium is an "absorbing"medium.

We should recall that the refractive index is $\kappa = -\operatorname{Im}\sqrt{\varepsilon}$. The quantity c_1/k_a^3 has the order a^3, whereas $n = \frac{1}{\ell^3}$, where ℓ is the mean distance between particles. Ordinarily, $(\frac{a}{\ell}) << 1$. Thus, $4\pi \frac{n}{k_a^3} c_1 << 1$.

Retaining terms of the first order with respect to (a/ℓ), we obtain

$$\varkappa = \frac{2\pi}{k_a^3} n \operatorname{Im}(-c_1).$$

Thus, the absorption coefficient for the field will be /272

$$\alpha' = \frac{2\pi}{k_a^2} n \operatorname{Im}(-c_1).$$

The intensity decreases twice as fast, and if we relate it to one particle, we obtain precisely the same formula for the attenuation coefficient as we presented in Chapter IV [formula (4.11)]. Thus, both systems reduce to one and the same result. The field attenuation is caused by Rayleigh scattering, along with real absorption; the Rayleigh scattering leads to the occurrence of the imaginary part of the refractive index. We must emphasize the fact that the conclusion drawn here is valid for dilute systems ($a << \ell$).

In addition to the case $\ell \sim \lambda$, there is another case when the simple combination of intensities is incorrect. This is the case $\ell \sim a$. The particles may have an influence upon each other here. This influence will be considerable only if the particles are quite large (large perturbation, which they introduce in the field), or if there is a great number of them (the system has a large volume). Allowance for the mutual influence of the particles requires a change to the second approximation.

In the simplest case of a system of two particles, the significant influence of one particle upon another may be expected only if the particles are quite large. We indicated above (VI, 2) that large particles distort the field outside of themselves at a distance of $\sim a$. This means that the influence of particles upon each other must be expected at distances of $\sim 4a$ between the centers of the particles. In very thick systems, the customary combination of intensities is not valid. Trinks (Ref. 119) reached this conclusion by a very cumbersome method; he investigated the scattering of a plane wave by two spheres.

CONCLUSION

In this book, we have discussed the theory of scattering and absorption of electromagnetic waves in a translucent body. If the distances between particles are not very small, the problem may be primarily reduced to scattering by a single particle. /273

Simple analytical formulas hold for small spheres. They were presented in Chapters IV and VIII.

For large spheres, one can confine oneself to the superposition of a diffracted field and the fields of geometric optics (Chapters VI and VII).

The intermediate cases must be tabulated.

In Chapter VIII we also presented simple formulas for non-spherical particles.

We would now like to say a few words regarding the use of scattered light for studying suspended particles. This method has several advantages, as compared with all other methods used for these purposes. The most significant advantage lies in the fact that practically no distortions in the object to be studied are introduced. This makes it possible to trace the different processes occurring in the system.

Thus, for example, F. F. Yudalevich studied the kinetics of the particle enlargement by observing the scattering intensity at different angles (Ref. 120). L. V. Smirnov and G. A. Zhirov studied the same process by continuously recording the transparency in two spectral regions (Ref. 121).

Optical methods can be applied not only for studying suspended particles, but also for studying the condition of the medium in which the particles are suspended. Thus, for example, in a study by the author, and I. Z. Gordon, M. G. Faynshteyn (Ref. 122) the intensity of turbulent mixing within a large closed vessel was measured by an optical method.

In principle, the optical methods may be reduced to three types of measurements: /274

(a) Measurement of transparency;

(b) Measurement of the scattering indicatrix;

(c) Measurement of the degree of polarization for scattered light.

It is desirable to perform all measurements with monochromatic light. Different methods may be applied to particles having different dimensions:

1. $\rho \ll 1$. It is only possible to measure transparency here. We thus obtain $\overline{a^6}$.

2. For larger particles, we may employ all three methods. Methods (b) and (c) (if the measurements are performed at different angles), in principle make it possible to determine the distribution function of particles by size.

When ρ increases from zero to unity, the displacement of the angle of maximum polarization occurs uniformly (see Chapters VI and VII). This provides us with a simple method for studying suspended particles. It was employed by V. A. Gavrilov (Ref. 123).

A very effective research method for large particles (determination of the distribution function, etc.) consists of studying the scattering at small angles.

3. For extremely large particles, in addition to the methods presented in Section 2, it is also effective to measure the coronas and the first rainbow. On the other hand, if the particles are accessible, we can employ optical microscopes.

APPENDIX

TABLES OF ANGULAR FUNCTIONS

A. TABLE OF FUNCTIONS Q_ℓ (θ)

ℓ \ θ	0	1	2	5	10	20	30	40	50	60	70	80	90
1	1	1	1	1	1	1	1	1	1	1	1	1	1,0000
2	3	2,9995	2,9982	2,9886	2,9544	2,8191	2,5981	2,2981	1,9284	1,5000	1,0261	0,5209	0,0000
3	6	5,9977	5,9909	5,9430	5,7738	5,1227	4,1250	2,9012	1,5988	0,3750	—0,6226	—1,2739	—1,5000
4	10	9,9931	9,9726	9,8295	9,3284	7,4732	4,8714	2,1215	—0,1732	—1,5625	—1.8649	—1,2107	0,0000
5	15	14,984	14,936	14,604	13,453	9,3974	4,3359	0,0301	—2,2490	—2,2266	—0,6568	1,1193	1,8750
6	21	20,968	20,872	20,210	17,952	10,460	2,4154	—2,4950	—2,9726	—0,5742	1,7437	1,8804	0,0000
7	28	27,942	27,770	26,584	22,611	10,332	—0,5264	—4,1763	—1,5161	1,9756	2,0584	—0,5985	—2,1875
8	36	35,904	35,618	33,653	27,198	8,8510	—3,7373	—4,0040	1,3090	2,7730	—0.4843	—2,3718	0,0000
9	45	44,850	44,394	41,333	31,482	6,0507	—6,2855	—1,8196	3,4935	0,7237	—2,6677	—0,2019	2,4609
10	55	54,774	54,100	49,534	35,232	2,1689	—7,3391	1,5063	3,2863	—2,3171	—1,3880	2,5613	0,0000
11	66	65,674	64,702	58,159	38,232	—2,3757	—6,4332	4,4247	0,5932	—3,2291	1,9376	1,1562	—2,7070
12	78	77,544	76,184	67,106	40,292	—7,0340	—3,6428	5,4439	—2,7879	—0,8481	2,8997	—2,3743	0,0000
13	91	90,378	88,528	76,266	41,247	—11,197	0,3968	3,8947	—4,3759	2,6147	—0,0330	—2,1115	2,9326
14	105	104,17	101,71	85,528	40,974	—14,277	4,6368	0,3338	—2,8396	3,6286	—3,1461	1,7955	0,0000
15	120	118,92	115,70	94,778	39,393	—15,794	7,8928	—3,6432	0,9075	0,9568	—2,1937	2,9081	—3,1421
16	136	134,61	130,48	103,90	36,469	—15,444	9,1806	—6,1238	4,2346	—2,8819	1 8052	—0,8715	0,0000
17	153	151,24	146,02	112,78	32,220	—13,150	8,0120	—5,8045	4,6497	—3,9885	3,6042	—3,4019	3,3385
18	171	168,80	162,29	121,29	26,713	—9,0894	4,5648	—2,6706	1,6697	—1,0544	0,6267	—0,2938	0,0000
19	190	187,28	179,26	129,33	20,066	—3,6762	—3,3311	1,9218	—2,7019	3,1264	—3,3640	3,4862	—3,5239
20	210	206,68	196,91	136,78	12,443	2,4771	—5,3936	5,8329	—5,3225	4,3186	—3,0212	1,5517	0,0000
21	231	226,99	215,18	143,54	4,0522	8,6318	—9,2278	7,1421	—4,1765	1,1438	1,4140	—3,1081	3,7001
22	253	248,19	234,06	149,50	—4,8647	14,014	—10,713	5,0923	0,0789	—3,3532	4,1552	—2,7308	0,0000
23	276	270,28	253,51	154,57	—14,036	17,911	—9,3313	0,5123	4,4700	—4,6252	1,4288	2,2792	—3,8683
24	300	293,25	273,48	158,66	—23,170	19,771	—5,3346	—4,5117	5,7891	—1,2268	—3,3374	3,6582	0,0000
25	325	317,08	293,95	161,68	—31,965	19,274	0,2879	—7,5900	2,9412	3,5656	—3,8189	—1,0774	4,0295
26	351	341,77	314,87	163,58	—40,122	16,386	6,0566	—7,1690	—2,1640	4,9127	0,8064	—4,1861	0,0000
27	378	367,30	336,20	164,27	—47,350	11,372	10,393	—3,3128	—5,8897	1,3045	4,5281	—0,3630	—4,1845
28	406	393,66	357,91	163,72	—53,381	4,7756	12,054	2,2651	—5,4678	—3,7661	2,3185	4,2142	0,0000
29	435	420,84	379,95	161,88	—57,976	—2,6427	10,486	6,9633	—1,0547	—5,1844	—3,0754	1,8657	4,3339
30	465	448,83	402,28	158,72	—60,936	—9,9926	6,0067	8,5091	4,2771	—1,3778	—4,5384	—3,7004	0,0000
31	496	477,60	424,85	154,23	—62,114	—16,362	—0,2587	6,0586	6,6799	3,9564	0,0218	—3,2344	—4,4784
32	528	507,17	447,63	148,40	—61,412	—20,932	—6,6558	0,6484	4,3110	5,4425	4,7001	2,6785	0,0000
33	561	537,50	470,56	141,24	—58,793	—23,080	—11,441	—5,2390	—1,2600	1,4475	3,2426	4,2803	4,6183
34	595	568,56	493,60	132,78	—54,281	—22,468	—13,260	—8,8162	—6,0860	—4,1380	—2,5908	—1,2504	0,0000
35	630	600,40	516,71	123,04	—47,963	—19,087	—11,527	—8,3129	—6,6420	—5,6889	—5,1362	—4,8468	—4,7542
36	666	632,94	539,84	112,07	—39,986	—13,275	—6,6112	—3,8498	—2,4009	—1,5140	—0,8986	—0,4214	0,0000
37	703	666,19	562,94	99,930	—30,556	—5,6783	0,2369	2,5636	3,6971	4,3119	4,6558	4,8332	4,8862
38	741	700,13	585,96	86,694	—19,930	2,8181	7,2058	7,9346	7,2829	5,9251	4,1507	2,1341	0,0000
39	780	734,75	608,88	72,440	—8,4105	11,194	12,402	9,6854	5,6915	1,5776	—1,9018	—4,2093	—5,0148
40	820	770,03	631,63	57,263	3,6630	18,417	14,365	6,8911	—0,0589	—4,4791	—5,5745	—3,6691	0,0000

l \ θ	0	1	2	5	10	20	30	40	50	60	70	80	90
41	861	805,59	654,17	41,264	15,926	23,571	12,480	0,7622	—5,9105	—6,1522	—1,9115	3,0245	5,1402
42	903	842,50	676,46	24,558	27,998	25,974	7,1647	—5,8772	—7,6307	—1,6389	4,3870	4,8217	0,0000
43	946	879,66	698,45	7,2647	39,496	25,263	—0,2201	—9,8920	—3,8754	4,6403	4,9937	—1,4021	—5,2626
44	990	917,40	720,08	—10,487	50,048	21,454	—7,7171	—9,3177	2,7681	6,3713	—1,0336	—5,4266	0,0000
45	1035	955,72	741,33	—28,561	59,301	14,940	—13,293	—4,3210	7,5626	1,6980	—5,8221	—0,4719	5,3822
46	1081	994,60	762,14	—46,817	66,939	6,4602	—15,392	2,8310	7,0006	—4,7960	—2,9700	5,3814	0,0000
47	1128	1034,0	782,46	—65,110	72,686	—2,9918	—13,367	8,7995	1,3707	—6,5830	3,8947	2,3715	—5,4992
48	1176	1074,0	802,25	—83,291	76,324	—12,280	—7,6790	10,734	—5,3687	—1,7550	5,7257	—4,6636	0,0000
49	1225	1114,4	821,46	—101,21	77,695	—20,266	0,2062	7,6335	—8,3730	4,9469	—0,0187	—4,0573	5,6137
50	1275	1155,3	840,06	—118,72	76,709	—25,945	8,1965	0,8617	—5,3956	6,7882	—5,8554	3,3354	0,0000
51	1326	1196,7	858,00	—135,66	73,349	—28,577	14,128	—6,4528	1,5346	1,8102	—4,0264	5,3085	—5,7260
52	1378	1238,5	875,23	—151,90	67,673	—27,780	16,354	—10,862	7,4937	—5,0934	3,1897	—1,5391	0,0000
53	1431	1280,7	891,72	—167,27	59,812	—23,584	14,198	—10,224	8,1622	—6,9874	6,3065	—5,9500	5,8361
54	1485	1323,4	907,42	—181,66	49,967	—16,439	8,1608	—4,7456	2,9570	—1,8639	1,1046	—0,5179	0,0000
55	1540	1366,4	922,29	—194,91	38,408	—7,1597	—0,1948	3,0757	—4,4767	5,2357	—5,6605	5,8785	—5,9442
56	1596	1409,8	936,31	—206,91	25,462	3,1595	—8,6497	9,5869	—8,8182	7,1810	—5,0321	2,5877	0,0000
57	1653	1453,5	949,42	—217,54	11,503	13,278	—14,917	11,688	—6,8811	1,9160	2,2887	—5,0770	6,0504
58	1711	1498,0	961,59	—226,68	—3,0532	21,959	—17,262	8,3098	0,0491	—5,3742	6,6994	—4,4115	0,0000
59	1770	1542,8	972,79	—234,24	—17,767	28,119	—14,983	0,9510	7,0634	—7,3695	2,2938	3,6190	—6,1547
60	1830	1587,8	982,99	—240,12	—32,185	30,962	—8,6159	—6,9812	9,1076	—1,9666	—5,2303	5,7534	0,0000
61	1891	1633,2	992,14	—244,27	—45,858	30,087	0,1850	—11,752	4,6249	5,5093	—5,9394	—1,6646	6,2572
62	1953	1678,7	1000,2	—246,61	—58,350	25,539	9,0802	—11,057	—3,2625	7,5824	1,2203	—6,4305	0,0000
63	2016	1724,5	1007,2	—247,10	—69,256	17,813	15,666	—5,1351	—8,9270	2,0453	6,8764	—0,5599	—6,3582
64	2080	1770,5	1013,1	—245,69	—78,214	7,7980	18,126	3,3024	—8,2532	—5,6412	3,5016	6,3367	0,0000
65	2145	1816,6	1017,8	—242,38	—84,917	—3,3210	15,729	10,314	—1,6265	—7,7625	—4,5697	2,7865	6,4575
66	2211	1862,9	1021,3	—237,17	—89,123	—14,207	9,0482	12,571	6,2730	—2,0943	—6,7054	—5,4589	0,0000
67	2278	1909,3	1023,6	—230,05	—90,665	—23,532	—0,1764	8,9349	9,7766	5,7700	0,0178	—4,7389	—6,5554
68	2346	1955,8	1024,7	—221,06	—89,455	—30,136	—9,4912	1,0327	6,2958	7,9386	6,8176	3,8821	0,0000
69	2415	2002,4	1024,6	—210,25	—85,488	—33,176	—16,381	—7,4725	1,7672	2,1420	4,6799	6,1665	6,6518
70	2485	2049,0	1023,2	—197,67	—78,848	—32,230	—18,950	—12,579	—8,6753	—5,8960	—3,6920	—1,7813	0,0000
71	2556	2095,7	1020,5	—183,39	—69,700	—27,354	—16,441	—11,831	—9,4400	—8,1108	—7,2902	—6,8778	6,7468
72	2628	2142,4	1016,5	—167,50	—58,291	—19,088	—9,4610	—5,4970	—3,4238	—2,1888	—1,2782	—0,5987	0,0000
73	2701	2189,1	1011,2	—150,12	—44,940	—8,3883	0,1689	3,5146	5,1390	6,0194	6,5111	6,7640	6,8405
74	2775	2235,7	1004,6	—131,34	—30,031	3,4765	9,8851	10,994	10,122	8,2794	5,7799	2,9723	0,0000
75	2850	2282,2	996,65	—111,31	—14,002	15,079	17,066	13,395	7,8927	2,2347	—2,6190	—5,8162	—6,9329
76	2926	2328,7	987,39	—90,153	2,6692	25,006	19,739	9,5192	—0,0431	—6,1402	—7,6602	5,0452	0,0000
77	3003	2375,1	976,79	—68,029	19,478	32,027	17,124	1,1086	—8,0524	—8,4447	—2,6205	4,1292	7,0242
78	3081	2421,3	964,85	—45,097	35,910	35,252	9,8562	—7,9334	—10,376	—2,2796	5,9556	6,5539	0,0000
79	3160	2467,4	951,58	—21,525	51,454	34,238	—0,1624	—13,355	—5,2685	6,2587	6,7539	—1,8915	—7,1142
80	3240	2513,3	937,02	2,5095	65,621	29,056	—10,264	—12,557	3,6910	8,6068	—1,3818	—7,2982	0,0000

B. TABLE OF FUNCTIONS S_ℓ (θ)

ℓ \ θ	0	1	2	5	10	20	30	40	50	60	70	80	90
1	1	0,9998	0,9994	0,9962	0,9848	0,9397	0,8660	0,7660	0,6428	0,5000	0,3420	0,1736	0,0000
2	3	2,9982	2,9927	2,9544	2,8191	2,2981	1,5000	0,5209	−0,5209	−1,5000	−2,2981	−2,8191	−3,0000
3	6	5,9922	5,9690	5,8069	5,2407	3,1649	0,3247	−2,5253	−4,6303	−5,4375	−4,7431	−2,7473	0,0000
4	10	9,9779	9,9118	9,4533	7,8775	2,4769	−3,7500	−8,0053	−8,4394	−5,0000	0,5618	5,5283	7,5000
5	15	14,950	14,800	13,762	10,271	−0,6860	−10,453	−12,614	−6,1891	3,8086	10,066	8,2361	0,0000
6	21	20,901	20,605	18,574	11,907	−6,8090	−17,801	−11,678	4,2785	13,863	8,1764	−5,8758	−13,125
7	28	27,823	27,295	23,702	12,253	−15,714	−22,514	−2,4345	16,959	11,508	−9,0215	−15,771	0,0000
8	36	35,707	34,834	28,936	10,788	−26,450	−21,155	13,049	20,376	−6,6884	−19,851	2,0003	19,688
9	45	44,542	43,177	34,049	7,0472	−37,338	−11,618	27,495	7,1207	−24,473	−3,3703	23,402	0,0000
10	55	54,315	52,277	38,791	0,6615	−46,178	5,5817	31,554	−17,305	−19,547	24,598	6,6699	−27,070
11	66	65,014	62,083	42,911	−8,6125	−50,584	26,785	19,209	−35,242	10,045	23,945	−28,527	0,0000
12	78	76,620	72,537	46,135	−20,870	−48,432	45,774	−7,4775	−29,215	36,889	−13,288	−19,978	35,191
13	91	89,118	83,572	48,203	−36,017	−38,302	55,467	−37,430	2,4639	28,869	−40,742	28,474	0,0000
14	105	102,50	95,127	48,848	−53 777	−19,876	50,265	−54,840	40,085	−13,820	−14,570	36,037	−43,989
15	120	116,74	107,13	47,810	−73,674	5,8104	28,342	−47,204	54,184	−50,882	39,083	−21,153	0,0000
16	136	131,82	119,51	44,837	−95,037	36,303	−6,9682	−13,124	28,122	−39,320	47,171	−51,858	53,415
17	153	147,72	132,19	39,699	−117,03	67,910	−47,294	34,637	−25,413	17,972	−11,536	5,6416	0,0000
18	171	164,41	145,09	32,188	−138,65	96,113	−81,070	73,462	−69,026	66,292	−64,623	63,719	−63,431
19	190	181,88	158,11	22,111	−158,80	116,15	−96,743	81,383	−66,392	50,789	−34,393	17,376	0,0000
20	210	200,09	171,17	9,3132	−176,30	123,75	−86,466	49,009	−11,684	−22,469	49,979	−67,821	74,002
21	231	219,02	184,16	−6,3255	−189,95	115,84	−49,164	−13,429	60,718	−82,999	76,621	−45,472	0,0000
22	253	238,63	197,01	−24,888	−198,60	91,175	8,1149	−78,450	97,174	−63,193	−1,2548	61,052	−85,103
23	271	258,91	209,59	−46,432	−201,16	50,789	71,251	−113,19	64,192	27,287	−88,487	74,641	0,0000
24	300	279,83	221,86	−70,960	−196,73	−1,8931	122,41	−95,756	−22,442	100,91	−63,116	−41,736	96,708
25	325	301,34	233,71	−98,405	−184,59	−61,259	144,93	−28,053	−103,25	76,466	54,119	−99,789	0,0000
26	351	323,42	245,00	−128,70	−164,27	−120,06	128,60	62,145	−115,58	−32,406	110,28	10,189	−108,80
27	378	346,04	255,64	−161,69	−135,61	−170,27	73,434	132,21	−41,626	−119,95	19,236	115,52	0,0000
28	405	369,16	265,51	−197,19	−98,790	−204,14	−9,1093	144,65	72,393	−90,555	−109,11	31,017	121,35
29	435	392,74	274,51	−234,97	−54,319	−215,28	−98,251	86,739	144,37	37,808	−100,06	−117,03	0,0000
30	465	416,75	282,53	−274,72	−3,0825	−199,77	−169,02	−20,311	115,17	140,05	48,772	−77,113	−134,35
31	496	441,15	289,46	−316,13	53,687	−156,87	−199,16	−128,42	−3,7592	105,42	145,46	101,00	0,0000
32	528	465,91	295,20	−358,80	114,44	−89,472	−175,91	−184,04	−131,76	−43,481	50,718	121,62	147,79
33	561	490,97	299,63	−402,34	177,32	−4,0312	−100,69	−154,48	−173,30	−161,16	−123,20	−66,538	0,0000
34	595	516,31	302,64	−446,26	240,23	89,974	10,013	−46,260	−88,908	−121,01	−143,62	−157,19	−161,64
35	630	541,87	304,14	−490,07	300,91	181,07	127,97	94,505	69,666	49,412	31,787	15,554	0,0000
36	666	567,62	304,01	−533,26	356,99	257,14	220,37	201,41	190,20	183,24	178,98	176,70	175,90
37	703	593,52	302,16	−575,24	406,08	307,03	258,82	218,96	179,16	137,30	93,065	47,068	0,0000
38	741	619,52	298,59	−615,46	445,86	322,08	227,89	130,99	33,706	−55,588	−127,63	174,41	−190,56
39	780	645,58	293,20	−653,33	474,17	297 50	130,63	−28,026	−148,64	−206,24	−191,39	113,86	0,0000
40	820	671,64	285,82	−688,26	489,12	233,30	−10,848	−185,95	−234,87	−154,27	1,7102	147,10	205,61

l \ θ	0	1	2	5	10	20	30	40	50	60	70	80	90
41	861	697,67	276,34	—719,63	489,18	134,634	**—160,19**	—265,49	—153,29	62,003	207,32	175,63	0,0000
42	903	723,62	264,67	—746,86	473,23	11,542	**—276,05**	—221,87	48,145	230,13	145,21	—94,890	—221,03
43	946	749,43	250,72	—769,36	440,63	—122,04	**—323,45**	—67,243	228,64	171,88	—119,59	—222,63	0,0000
44	990	775,07	234,41	—786,57	391,32	—249,82	**—284,15**	131,08	252,68	—68,645	—240,27	21,637	236,82
45	1035	800,47	215,66	—797,96	325,82	—355,10	**—163,06**	279,66	91,417	—254,88	—42,057	245,93	0,0000
46	1081	825,59	194,39	—803,02	245,25	—422,94	**11,621**	302,85	—148,44	—190,11	226,90	65,167	—252,96
47	1128	850,39	170,54	—801,30	151,30	—442,23	**194,73**	180,93	—294,62	75,508	205,17	—238,95	0,0000
48	1176	874,80	144,04	—792,38	46,279	—407,31	**335,76**	—36,495	—232,81	280,45	—96,848	—155,07	269,45
49	1225	898,78	114,82	—775,89	—66,997	—319,11	**392,70**	—250,16	4,7158	208,95	—286,60	198,66	0,0000
50	1275	922,28	82,843	—751,54	—185,26	—185,45	**344,40**	—356,30	253,61	—82,588	—99,182	235,88	—286,30
51	1326	945,54	48,043	—719,09	—304,89	—20,392	**197,79**	—296,91	330,88	—306,82	234,27	—126,43	0,0000
52	1378	968,22	10,382	—678,42	—421,97	157,14	**—12,343**	—90,673	169,14	—228,37	270,12	—295,24	303,48
53	1431	989,97	—30,178	—629,46	—532,49	325,50	**—231,44**	171,43	—126,59	89,875	—57,928	28,348	0,0000
54	1485	1011,0	—73,668	—572,16	—632,40	462,98	**—399,23**	366,03	—346,28	333,98	—326,45	322,39	—320,99
55	1540	1031,1	—120,12	—506,60	—717,80	550,54	**—466,28**	395,34	—323,86	143,04	—168,34	85,152	0,0000
56	1596	1050,8	—169,54	—432,97	—785,09	574,36	**—408,38**	235,95	—62,251	—97,364	226,27	—309,92	338,82
57	1653	1082,2	—221,96	—351,50	—831,06	527,98	**—234,68**	—45,667	259,34	—361,89	336,47	—200,33	0,0000
58	1711	1113,3	—277,36	—262,56	—853,06	413,41	**13,028**	—320,41	407,82	—268,89	—2,1421	255,11	—356,97
59	1770	1130,5	—335,76	—166,64	—849,12	241,38	**270,19**	—455,60	264,93	105,05	—355,67	—301,76	0,0000
60	1830	1146,7	—397,13	—64,294	—818,00	30,443	**466,26**	—378,89	—79,616	390,54	—247,25	—160,82	375,44
61	1891	1161,8	—461,46	43,949	—759,35	—195,01	**543,96**	—116,31	—383,33	290,84	200,37	—374,34	0,0000
62	1953	1175,8	—528,74	157,38	—673,69	—407,55	**475,89**	215,23	—421,37	—112,03	400,05	35,636	—394,21
63	2016	1188,6	—592,49	275,23	—562,46	—579,98	**273,61**	459,81	—152,70	—420,84	70,075	405,43	0,0000
64	2080	1200,2	—672,95	396,64	—428,02	—688,84	**—13,678**	495,69	240,73	—313,46	—370,31	106,82	413,28
65	2145	1210,4	—747,81	520,68	—273,63	—717,51	**—310,89**	295,62	476,75	120,04	—332,70	—386,77	0,0000
66	2211	1219,3	—826,43	646,35	—103,33	—658,63	**—536,66**	—55,494	375,10	450,98	154,82	—249,26	—432,65
67	2278	1226,9	—907,74	772,62	78,110	—515,46	**—625,52**	—396,24	—5,5152	335,70	456,37	316,06	0,0000
68	2346	1232,9	—991,67	898,39	265,40	—301,98	**—546,76**	—562,71	—399,40	—128,22	157,34	372,82	452,32
69	2415	1237,5	—1078,2	1022,5	452,75	—41,564	**—314,48**	—467,26	—519,08	—481,80	—366,79	—197,86	0,0000
70	2485	1240,4	—1167,1	1143,7	634,13	235,56	**14,289**	—143,98	—264,88	—358,44	—420,66	—459,48	—472,28
71	2556	1241,8	—1258,4	1260,9	803,51	495,50	**353,44**	262,24	193,80	136,58	88,783	43,470	0,0000
72	2628	1241,5	—1351,9	1372,9	954,93	705,36	**610,28**	560,45	530,66	513,29	500,71	491,60	492,52
73	2701	1239,5	—1447,6	1478,4	1082,8	837,08	**710,79**	603,32	494,50	381,68	257,15	130,05	0,0000
74	2775	1235,7	—1545,4	1576,5	1182,0	870,86	**620,83**	359,62	96,070	—145,11	—342,06	—469,11	—513,04
75	2850	1230,1	—1645,0	1665,7	1248,2	798,54	**357,20**	—65,930	—388,81	—545,44	—506,45	—301,64	0,0000
76	2926	1222,6	—1746,4	1745,1	1277,9	624,73	**—14,885**	—477,24	—609,85	—405,40	2,5624	381,27	533,84
77	3003	1213,2	—1848,6	1813,6	1268,8	366,91	**—397,78**	—677,11	—395,19	153,81	528,49	448,73	0,0000
78	3081	1201,6	—1953,6	1870,1	1219,6	53,647	**—686,99**	—561,61	115,93	578,23	365,89	—237,44	—554,91
79	3160	1188,4	—2057,4	1913,7	1130,3	—278,44	**—799,61**	—173,56	562,51	429,59	—293,96	—550,27	0,0000

REFERENCES

1. Mandel'shtam, L.I. Annalen d. Physik, 23, 626, 1907; Polnoye sobraniye trudov (Collected Works), Vol. 1, 100, Moscow, 1948. /284
2. Landsberg, G. S. Optika (Optics), Moscow, 1940.
3. Landsberg, G. S. Tekhn. Entsiklopediya, 19, 129, Moscow, 1934.
4. Landsberg, G. S. Yub. Sbornik (Anniversary Collection), AN SSSR, Part 1, 333, Moscow, 1947.
5. Vavilov, S. I. Trudy Noyabr'sk. Yub. Sessii AN SSSR (Transactions of the November Anniversary Session of the USSR Academy of Sciences), Leningrad, 1933.
6. Brounov, P. I. Atmosfernaya optika. Svetovyye yavleniya neba v svyazi s predskazaniyem pogody (Atmospheric Optics. Light Phenomena in the Sky in Connection with Weather Prediction). Moscow, 1924.
7. Kalitin, N. N. Geofizicheskiy Sbornik, 4, No. 2, 1924.
8. Cornu. Congr. Meteor. Internat. 2, p. 95, 1889.
9. Veksler, V., Groshev, L., Dobrotin, N. Eksperimental'nyye metody yadernoy fiziki (Experimental Methods of Nuclear Physics). Izdatel'stvo AN SSSR, 1940.
10. Kosonogov, I. I. Zhurnal Russkogo Fiziko-khimicheskogo obshchestva (ZhRFKhO), 35, 307, 1903; Physik. Zeitschrift, 4, p. 208, 258, 516, 1903.
11. Fok, V. A. Diffraktsiiya radiovoln vokrug zemli (Diffraction of Radio Waves Around the Earth). Izdatel'stvo AN SSSR, 1946.
12. Fok, V. A. Uspekhi Fizicheskikh Nauk (UFN), 36, No. 3, 1948.
13. Vavilov, S. I. Izvestiya AN SSSR, Seriya Geogr. i Geofiziki, p. 63, 1942.
14. Khvostikov, I. A. UFN, 24, 165, 1940.
15. Arkad'yev, V. K. ZhRFKhO, 44, 165, 1912; 45, 103, 1913.
16. Frenkel', Ya. I. Elektrodinamika (Electrodynamics), Vol. I, Ob'yedineniye Nauchno-Tekhnicheskikh Izdatel'stvo (ONTI), 1934.
17. Kupradze, V. D. Doklady Akademii Nauk (DAN), 1, 52, 1934.
18. Kravets, T. P. UFN, 36, 338, 1948.
19. Frenkel', Ya. I. Elektrodinamika (Electrodynamics), Vol. II, ONTI, 1935.
20. Moroz, L. M., Frenkel', Ya. I. Kolloidnyy Zhurnal, 11, 178, 1949.
21. Selezneva, Ye. S. Meteorologiya i Gidr., No. 2, 1948.
22. Borovikov, A. M. Trudy Tsentral'naya Aerologicheskaya Observatoriya (TsAO), No. 3, Istoricheskiye Zapiski Gosudarstvennogo Instituta Meteorologii (GIMIZ, 1948.
23. Khvostikov, I. A. Izvestiya AN SSSR, Seriya Geogr. i Geofiz., p. 82, 1942.
24. Spravochnik Fizicheskikh, khimicheskikh, i tekhnologicheskikh velichin (Handbook on Physical, Chemical, and Technological Quantities). Moscow, 1932.
25. Veyigerov, M. L. Zeit für Physik, 70, 104, 1931. /285
26. Gol'dgammer, D. A. Dispersion und absorption des lichtes (Dispersion and Absorption of Light). Leipzig, 1915.
27. Sharonov, V. V. Izmereniye i raschet vidimosti dalekikh predmetov (Measurement and Calculation of Visibility of Far-Removed Objects). Gosudarstvennoye Teoreticheskoye i Tekhnicheskoye Izdatel'stvo (GTTI), 1947.
28. Gershun, A. A. Zhurnal Tekhnicheskoy Fiziki (ZhTF), 14, 117, 1944.
29. Khvostikov, I. A. Izvestiya AN SSSR, Seriya Geogr. i Geofiz, p. 441, 1945.
30. Frank, F., Mizes, R. Differentsial'nyye i integral'nyye uravneniya matematicheskoy fiziki (Differential and Integral Equations of Mathematical Physics). ONTI, 1937.

31. Love, A. E. H. Proc. Lond. Math. Soc., 30, 308, 1899.
32. Mie, G. Ann. d. Phys., 25, 377, 1908.
33. Debye, P. Ann. d. Phys., 30, 57, 1909.
34. Rayleigh. Proc. Roy. Soc. A, 84, 25, 1910.
35. Shuleykin, V. V. Fizika morya (Physics of the Sea), Vol. I, ONTI, 1933.
36. Shtaude, N. M. Fotometricheskiye nablyudeniya sumerek kak metod izucheniya verkhney stratosfery (Photometric Observations of Twilight as a Method of Studying the Upper Stratosphere). Moscow, 1936.
37. Kupradze, V. D. Osnovnyye zadachi matematicheskoy teorii diffraktsii (Fundamental Problems of the Mathematical Theory of Diffraction). ONTI, 1935.
38. Born, M. Optika (Optics). Edited by Professor I. V. Obreimov. Khar'kov, 1937.
39. Wolfson, G. Handbuch der Physik (Handbook of Physics), Vol. 20, 1928.
40. Smirnov, V. I. Kurs vysshey matematiki (Course on Higher Mathematics), Vol. III, GTTI, 1934.
41. Steibing. Annalen der Physik, 26, 3299, 1908.
42. Fok, V. A. DAN, 1, 97, 1934.
43. Shifrin, K. S. Trudy Glavnoy Geofizicheskoy Observatorii (GGO), No. 26, 1951.
44. Ray, B. Proc. Ind. Ass. for Cultiv. Science, 8, 23, 1923.
45. Gertner, G. Prozrachnost' zamutnennoy atmosfery dlya infrakrasnykh voln (Transparence of a Turbid Atmosphere for Infrared Waves). Gosudarstvennoye Energeticheskoye Izdatel'stvo (GEI), 1949.
46. Shifrin, K. S. Izvestiya AN SSSR, Seriya Geogr. i. Geofiz., No. 2, 1949.
47. Rayleigh. Phil. Mag (4), 41, 107, 274, 447, 1871; (5), 12, 81, 1881; (5), 47, 375, 1899.
48. Rzhanov, A. V. UFN, 38, 461, 1949.
49. Thomson, I. I. Recent Researches in Electricity and Magnetism , p. 437, 1893.
50. Schwarzschild, K. Sitzungsberichte der math-phys. Classe d. K. Bayer. Akad. d. Wis., 31, 1902.
51. Shuleykin, V. V. Philosoph. Magaz., 48, 307, 1924.
52. Shuleykin, V. V. Zhurnal Geofiziki, 3, 145, 1933.
53. Shifrin, K. S. Izvestiya AN SSSR, Seriya Geogr. i Geofiz., No. 2, 1950.
54. Chirvinskiy, P. N. Meteorologiya i Gidr., No. 6, p. 68, 1941.
55. Götz, F. P. Astronomische Nachrichten, 225, 63, 1935.
56. Blümer, H. Zeit. für Physik, 32, 115, 1925; 38, 304, 1926; 38, 920, 1926.
57. Vol'pert, A. R., Potekhin, A. I. Zhurnal Eksperimental'noy i Teoreticheskoy Fiziki (ZhETF), 17, 807, 1947. /286
58. Savost'yanova, M. V. UFN, 22, 1, 1939.
59. Savost'yanova, M. V. UFN, 22, 129, 1939.
60. Ruedy, R. Canadian Journal of Research (A), 19, 117, 1941; 20, 25, 1942.
61. Jobst, G. Ann. d. Physik, 76, 863, 1925; 78, 157, 1925.
62. Tverskoy, P. N. Kurs Geofiziki (Course on Geophysics). p. 302, 1939.
63. Shifrin, K. S. Izvestiya AN SSSR, Seriya Geogr. i Geofiz., 14, 65, 1950.
64. Obolenskiy, V. N. Meteorologiya, Vol. II, GIMIZ, p. 184, 1939.
65. Kalitin, N. N. Meteorologicheskiy Vestnik, 1923.
66. Kalitin, N. N. Byulleten' PAK, No. 15, 1930; Meteorologicheskiy Vestnik, 1932.
67. Pyaskovskaya-Fesenkova, Ye. V. Astronomicheskiy Zhurnal, 22, No. 6, 1945; DAN, No. 3, 1946.

68. Kratt, V. A. Izvestiya GAO, 17, No. 1, 1946.
69. Mecke, R. Ann. d. Phys. 62, 1920.
70. Potekhin, A. I. Nekotoryye zadachi diffraktsii elektromagnitnykh voln (Certain Problems in the Diffraction of Electromagnetic Waves). Moscow, 1948.
71. Potekhin, A.I. Nekotoryye zadachi diffraktsii elektromagnitnykh voln (Problems of Electromagnetic Wave Diffraction). Moscow, 1948.
72. Sinclair, D. IOSA, 37, 9, 475, 1947.
73. Brilluin, L. Journ. of Appl. Phys. 20, 1110, 1949.
74. Stratton, I., Houghton,H. G.Phys. Rev., 38, 159, 1931.
75. Houghton, H. G., Chalker, W. R. IOSA, 39, 955, 1949.
76. Ivanov, K. I. DAN, 74, 925, 1950.
77. Pyaskovskaya-Fesenkova, Ye. V. DAN, 61, 1035, 1948.
78. Faas, V. A. Izvestiya AN SSSR, Seriya Geogr. i Geofiz., No. 4, 1942.
79. Shtaude, N. M. Izvestiya Nauchnoy Instituta imenii Lesgaft, XV, No. 1, 2, 1929.
80. Rodionov, S. F., Pavlova, Ye. N., Rdutlovskaya, Ye. V., Reynov, N. M. Izvestiya AN SSSR, Seriya Geogr. i. Geofiz., p. 135, 1942.
81. Vassy, A., and E. Journ. de Phys., 10, 75, 403, 459, 1939.
82. Orlova, O.B. ZhTF, 6, No. 3, 1936.
83. Bokin, P. Ya., Brumberg, Ye. M., Lebedev, A. A., Chernyasv, V. I. Trudy El'brusskoy Ekspeditsii AN SSSR (Reports of the Elbrus Expedition of the USSR Academy of Sciences), 1934-1935, Izdatel'stvo AN SSSR, 1936.
84. Brent, D. Fizicheskaya i Dinamicheskaya Meteorologiya (Physical and Dynamic Meteorology). GIMIZ, p. 109, 1938.
85. Shuleykin, V. V. Izvestiya Fizicheskogo Instituta pri MGU, 2, 119, 1922.
86. Shuleykin, V. V. Trudy Plovuchego Morskogo Nauchno-issledovatel'skogo Insituta, No. 5, Saratov, 1923.
87. Shuleykin, V. V. Ibid, No. 10, Moscow, 1925.
88. Shifrin, K. S. ZhTF, 14, 63, 1944.
89. Boldyrev, N. G. Svetotekhnika, 6, 1935. /287
90. Kalitin, N. N. Meteorologiya i Gidr., No. 4, 1941.
91. Gershun, A. A. Trudy GOI, 11, No. 99, 1936.
92. Berezkin, Vs. A., Gershun, A. A., Yanishevskiy, Yu. D. Prazrachnost' i tsvet morya (Transparence and Color of the Sea), Leningrad, 1940.
93. Linke, F., Borne, V. Gerlands Beitrage zur Geophysik, 37, No. 1, 1932.
94. Fesenkov, V. G. Meteoritika, No. 6, 1949.
95. Debye, P. Phys. Zeits. 9, 775, 1908.
96. Kurant, R., Gil'bert, D. Metody matematicheskoy fiziki (Methods of Mathematical Physics), Vol. 1, p. 70, 1933.
97. Polyakova, Ye. A. Trudy GGO, No. 19, 1950.
98. Paranjpe, G. R., Naik, Y. G., Vaidya, P. B. Proc. Ind. Acad. Of Sciences, 9, 333, 1939.
99. Pokrovskiy, G. I. Zeit. für Physik, 43, 394, 1927.
100. Pokrovskiy, G. I. Zeit. für Physik, 43, 769, 1927.
101. Polrovskiy, G. I. Zeit. für Physik, 31, p. 14, p. 514, 1925; 32, 563, 713, 1925; 33, 860, 1925; 34, 49, 1925.
102. Pokrovskiy, G. I. Zeit für Physik, 35, 34, 464, 633, 776, 1926.
103. Pokrovskiy, G. I. Zeit. für Physik, 41, 493, 688, 1927.
104. Pokrovskiy, G. I. Zeit. für Phys., 36, 548, 1926; 65, 130, 1930.
105. Pyaskovskaya-Fesenkova, Ye. V. Astronomicheskiy Zhurnal, 24, No. 2, 1947.

106. Yaroslavtsev, I. N. Izvestiya AN SSSR, Seriya Geogr. i Geofiz., 8, 111, 1944.
107. Gordov, A. N. Zhurnal Geofiziki, 6, No. 4, 1936; 7, No. 2 - 3, 1937.
108. Gershun, A. A. Morskoy Sbornik, No. 13 - 14, 1939.
109. Shifin, K. S. DAN, 9, 483, 1948.
110. Shifrin, K. S. Trudy GGO, No. 19, 1950.
111. Möglich, F. Ann. d. Phys., 83, 609, 1927.
112. Gans, R. Ann. d. Phys., 76, 29, 1925.
113. Rocard, I. Rev. d'Optique, 9, 97, 1930.
114. Gans, R. Ann. d. Phys., 37, 881, 1912; 47, 270, 1918; 61, 465, 1920.
115. Cherdyntsev, S. V. Acta Physicochimica URSS 3, 1, 1935; Zhurnal Fizicheskogo Khimii, 7, 265, 1936.
116. Polatbekov, F. P. Izvestiya Kazakh AN, No. 32, Seriya Astronomicheskiya i Fizicheskiya, No. 2, Alma Ata, 1946.
117. Kravets, T. P. Izvestiya Imp. Moskogo Inzhenernoy Uchilishcha, Moscow, 1912.
118. Maxwell-Garnett. Phil. Trans (A); 203, 385, 1904; 205, 237, 1906.
119. Trinks, W. Ann. D. Physik, 22, 561, 1935.
120. Yudalevich, F. F. DAN, 2, 368, 1935.
121. Smirnov, L. V., Zhirov, G. A. Kolloidnyy Zhurnal, 2, 641, Voronezh, 1936.
122. Shifrin, K. S., Gordon, I. Z., Faynshteyn, M. G. Izvestiya AN SSSR, Seriya Geograf. i Geofiz., No. 3, 1949.
123. Gavrilov, V. A. Priroda, No. 9, p. 8, 1949.
124. Shifrin, K. S. Trudy GGO, No. 6, 1947.
125. Pyaskovskaya-Fesenkova, Ye. V. Astronomicheskiy Zhurnal, 27, No. 4, 1950.
126. Shifrin, K. S. DAN 77, No. 3, 1951.
127. Shifrin, K. S. DAN 77, No. 4, 1951.
128. Shifrin, K. S. Kolloidnyy Zhurnal, 13, 129, 1951.

Scientific Translation Service
4849 Tocaloma Lane
La Canada, California
NASw-1496

NASA-Langley, 1968 —— 13 F-477

National Aeronautics and Space Administration
WASHINGTON, D. C.

OFFICIAL BUSINESS

FIRST CLASS MAIL

POSTAGE AND FEES PAID
NATIONAL AERONAUTICS AN
SPACE ADMINISTRATION

POSTMASTER: If Undeliverable (Section 15
Postal Manual) Do Not Retu

"The aeronautical and space activities of the United States shall be conducted so as to contribute . . . to the expansion of human knowledge of phenomena in the atmosphere and space. The Administration shall provide for the widest practicable and appropriate dissemination of information concerning its activities and the results thereof."

—NATIONAL AERONAUTICS AND SPACE ACT OF 1958

NASA SCIENTIFIC AND TECHNICAL PUBLICATIONS

TECHNICAL REPORTS: Scientific and technical information considered important, complete, and a lasting contribution to existing knowledge.

TECHNICAL NOTES: Information less broad in scope but nevertheless of importance as a contribution to existing knowledge.

TECHNICAL MEMORANDUMS: Information receiving limited distribution because of preliminary data, security classification, or other reasons.

CONTRACTOR REPORTS: Scientific and technical information generated under a NASA contract or grant and considered an important contribution to existing knowledge.

TECHNICAL TRANSLATIONS: Information published in a foreign language considered to merit NASA distribution in English.

SPECIAL PUBLICATIONS: Information derived from or of value to NASA activities. Publications include conference proceedings, monographs, data compilations, handbooks, sourcebooks, and special bibliographies.

TECHNOLOGY UTILIZATION PUBLICATIONS: Information on technology used by NASA that may be of particular interest in commercial and other non-aerospace applications. Publications include Tech Briefs, Technology Utilization Reports and Notes, and Technology Surveys.

Details on the availability of these publications may be obtained from:

SCIENTIFIC AND TECHNICAL INFORMATION DIVISION

NATIONAL AERONAUTICS AND SPACE ADMINISTRATION

Washington, D.C. 20546